INVESTIGATING THE ROLE OF THE ANAPHASE PROMOTING COMPLEX/CYCLOSOME SUBUNIT APC5 IN MITOSIS

By

Maria Teresa Tilotta

A thesis submitted to the University of Birmingham for the degree of DOCTOR OF PHILOSOPHY

Institute of Cancer and Genomic Sciences

College of Medical and Dental Sciences

University of Birmingham

September 2019

ABSTRACT

The Anaphase-Promoting Complex/Cyclosome (APC/C) is a multi-subunit E3 ubiquitin ligase that targets key cell cycle regulators for 26S proteasome-mediated degradation during mitosis and G1 phases of the cell cycle. APC/C activity is regulated through protein-protein interactions and post-translational modifications (PTMs). The precise role of individual APC/C subunits and their PTMs in the control of APC/C activity is not fully understood. Here we show that APC5 knockdown by RNA interference promotes either mitotic arrest or a delay in the ability of cells to progress through mitosis; a small but significant proportion of cells that progress through mitosis also display defects in cytokinesis. We also show that almost the entire cellular pool of the APC/C subunit, APC5 is phosphorylated during mitosis at S195 and that this phosphorylation event might play a crucial role in the control of APC/C during mitosis. We determined that the phosphorylated APC5 S195 species localized at centrosomes from prophase to anaphase whereupon it re-localized to midbodies during the late stages of mitosis and co-localized with known APC/C substrates. As such, our findings provide new insights into how phosphorylation regulates APC5 and the APC/C during mitosis and defines potential new roles for the APC/C in cytokinesis.

To my family,

"You can do anything as long as you have the passion,
the drive, the focus, and the support"
Sabrina Bryan

ACKNOWLEDGEMENTS

I would like to thank the MIBTP and the BBSRC for funding my research and for providing me with an extensive training that have enriched me personally and professionally.

I want to thank my supervisor Dr Andy Turnell, for his help, support, guidance and trust. He made me feel home since the first day and have inspired and encouraged me during the entire course of my PhD, sharing his knowledge and nourishing my enthusiasm, for which I am extremely grateful. I also would like to thank Dr Phil Byrd, for his help and kindness, and Dr Chris Weston, for his support with the live cell imaging experiments.

Indeed, I want to thank all my colleagues from Turnell's group and all the people in the lab, whose friendship made this journey pleasant and funny. Thanks to Reshma, Jess F, Ahmed, Fadi, Abeer, Jess B, Ellie, Fabio and to all the people in my office, for everything they have done for me.

I am grateful to my family, especially my my mum, Erina, for her unconditional love, endless support and for believing in me. Thanks to my brother, Antonio, and to my sister in law Floriana, whose love and admiration has supported me constantly. Thanks also to my mother in law, Rosa, and my sister in law Valentina, who have shared with me the enthusiasm of this path.

Finally, I am eternally grateful to my beloved husband, Francesco, who builds his dreams with me and whose endless support, patience and encouragement makes my life wonderful.

TABLE OF CONTENTS

LIST OF FIGURES

LIST OF TABLES

LIST OF ABBREVIATIONS

5-FU	5-Fluoro Uracil
53BP1	p53-binding protein 1
AI	Auto-Inhibitory
APC/C	Anaphase Promoting Complex/Cyclosome
Apcin	APC/C inhibitor
AS	Asynchronous
ATCC	American Type Culture Collection
BRCA1	Breast Cancer Type 1 Supsceptibility Protein
BRCT	BRC1 C-terminal
BSA	Bovine Serum Albumin
Bub1	Budding uninhibited by benzimidazole-1
Bub3	Budding uninhibited by benzimidazole-3
BubR1	Budding uninhibited by benzimidazole-related 1
CBP/p300	CREB-Binding Protein/Histone Acetyltransferase p300
Cdc	Cell division cycle
Cdc20	Cell division-cycle protein 20
Cdh1	Cdc20 homolog 1
Cdk	Cyclin dependent kinase
Cdk1	Cyclin-dependent kinase 1
Chk	Checkpoint Kinase
CPC	Chromosome Passenger Complex
DAPI	4’,6-diamidino-2-phenylindole
DMEM	Dulbecco’s Modified Eagle Medium
DNA	Deoxyribonucleic Acid
Dox	Doxycycline

EC	Error Correction
Ect2	Epithelial cell transforming 2
EM	Electron Microscopy
Emi1	Early mitotic inhibitor 1
FCS	Foetal Calf Serum
FRT	FLP Recombination Target
GC	Guanylyl-Cyclase
GEF	Guanine Nucleotide Exchange Factor
GST	Glutathione S-transferase
HECT	Homologous to the E6AP Carboxyl Terminus
HINGS	Heat Inactivated Normal Goat Serum
HRP	Horseradish Peroxidase
ida	imaginal discs arrested
IgG	Immunoglobulin G
INCENP	Inner Centromeric Protein
IP	Immunoprecipitation
IPTG	isopropyl-β-D-1-thiogalactopyranoside
IRES	Internal Ribosome Entry Site
KD	Kinase Domain
KIF	Kinesin-like protein
KLH	Keyhole Limpet Hemocyanin
LB	Luria Broth
mAb	monoclonal antibody
Mad1	Mitotic checkpoint deficient protein 1
Mad2	Mitotic arrest deficient 2
MCAK	Mitotic Centromere Activated Kinesin

MCC	Mitotic Checkpoint Complex
MDC1	Mediator of DNA Damage Checkpoint protein 1
MKLP2	Mitotic Kinesin-Like Protein 2
Mps1	Monopolar spindle 1
mRNA	Messenger Ribonucleic Acid
NEBD	Nuclear Envelope Breakdown
Nek	NIMA-related kinase
NIMA	Never in Mitosis Gene A
Noco	Nocodazole
NSCLC	Non-Small Cell Lung Cancer
NudC	Nuclear distribution protein c
p	phosphorylated
PABP	Poly-A Binding Protein
PBD	Polo-box Domain
PBS	Phosphate Buffer Saline
PC	Phase Contrast
PCR	Polymerase Chain Reaction
PDB	Protein Data Bank
PDB	Protein Data Bank
pH3	Phospho-Histone H3
Plk1	Polo like kinase 1
PMP	Protein Metallo Protease
PRC1	Protein Regulator of Cytokinesis 1
PTM	Post-Translational Modification
PTMs	Post-Translational Modifications
Rho	Ras homologous
RING	Really Interesting New Gene

RNAi	RNA interference
SAC	Spindle Assembly Checkpoint
SCF	Skp-Cullin-F box
SDS-PAGE	Sodium Dodecyl Sulphate - Polyacrylamide Gel Electrophoresis
SGO1	Shugoshin
siRNA	Small Interfering Ribonucleic Acid
Skp2	S-phase kinase associated kinase 2
TAME	Tosyl -1-Arginine Methyl Ester
TBE	Tris-Boric Acid-EDTA
TBST	Tris-Buffered Saline-Tween 20
TEMED	N, N, N', N;-tetramethylethylenediamine
TIF1γ	Transcriptional Intermediary Factor 1 gamma
TPR	Tetratricopeptide Repeat
TRIP13	Thyrod hormone Receptor Interactor 13
UPS	Ubiquitin Proteasome System
UTB	Urea-Tris-β-Mercaptoethanol
UV	Ultra Violet
WT	Wild Type
ZBR	Zinc-Binding Region
λPPase	Lambda Phosphatase

CHAPTER 1: INTRODUCTION

1.1 The Anaphase-Promoting Complex/Cyclosome (APC/C): a master regulator of cell cycle progression

The safeguarding of genome integrity during cellular growth and division is paramount for the maintenance of physiological homeostasis in multicellular organisms. The Anaphase-Promoting Complex/Cyclosome (APC/C), a multi-subunit protein complex that operates as an E3 ubiquitin ligase, is considered a master regulator of these processes, as it dictates the timing of chromosome segregation, controls the series of events underlying mitotic exit and regulates replication licensing through the poly-ubiquitylation of several key cell cycle regulators (Peters, 2006, Sivakumar and Gorbsky, 2015, Zhou et al., 2016, Pray et al., 2002).

Poly-ubiquitylation is a post-translational modification (PTM) generated by the Ubiquitin Proteasome System (UPS), a cellular pathway that controls the covalent attachment of multiple ubiquitin molecules to protein substrates, which ultimately targets these proteins for proteolytic degradation by the 26S proteasome (King et al., 1995, Hershko, 1998, Pickart and Eddins, 2004). The UPS regulates many diverse cellular processes, including the unidirectional progression of cells through the cell cycle. It is defined by a three-step reaction requiring an E1-activating enzyme, an E2-conjugating enzyme and an E3-ubiquitin ligase. In this reaction the ubiquitin molecule, a small 76 amino acid protein, is first activated by the E1-activating enzyme in an ATP-dependent manner. Following this step, the ubiquitin is transferred to the E2-conjugating enzyme, to which it temporally associates before being transferred to specific lysine (K) acceptor residues within the target substrate, in a reaction catalysed by the E3-ubiquitin ligase. The mechanism of this last step truly depends on the class of E3-ubiquitin ligase that catalyses the transfer. In fact, some E3-ubiquitin ligases,

such as the Homologous to the E6AP Carboxyl Terminus (HECT), associates directly with ubiquitin and catalyses its direct transfer to the target substrates. In contrast, Really Interesting New Gene (RING) E3-ubiquitin ligases, such as the APC/C, act as molecular adaptors bringing together the E2-conjugating enzyme and the target substrate and facilitating the transfer of ubiquitin from the E2 to the target proteins (Fig. 1.1) (Metzger et al., 2012, King et al., 1995, Hershko, 1998, Pickart and Eddins, 2004).

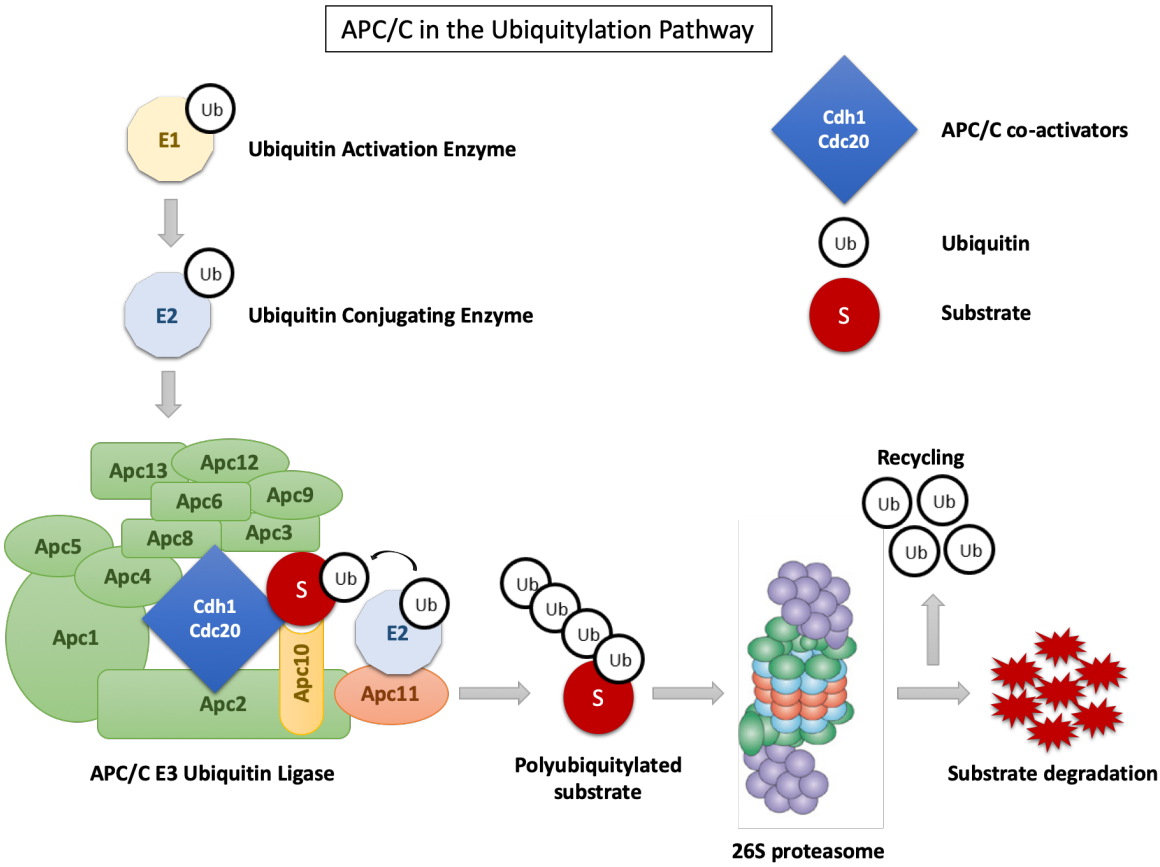

Figure 1. 1: **The APC/C and the Ubiquitin Proteasome System.** Ubiquitin is first activated by an E1-activating enzyme and then transferred to an E2-conjugating enzyme. The E2 carrying the ubiquitin then contacts the APC/C bound to one of its activators, which recognises the target protein and promotes ubiquitin transfer from the E2 to the substrate. The reaction is repeated to construct K11 and K48 polyubiquitin chains on protein substrates that act as a signal for substrate degradation through the 26S proteasome. By author.

Multiple cycles of ubiquitylation generates a poly-ubiquitylated substrate, with additional ubiquitin moieties added during each cycle to one of the seven K residues present within ubiquitin itself. K11 and K48 ubiquitin linkages typically target substrates for proteasomal degradation. Indeed, the types of ubiquitin linkages and the topology of the poly-ubiquitin chains attached to the target proteins determines the cellular fate of the protein. Thus, ubiquitylation can affect several aspects of protein function, including their localization and interaction with partner proteins, as well as their stability (Pickart and Eddins, 2004).

The APC/C is a cullin-based, E3-ubiquitin ligase and catalyses the formation of K11-linked poly-ubiquitin chains on its substrates, which are recognized by the 26S Proteasome as substrates for degradation. It has been suggested that the stability of more than 170 substrates is regulated by the APC/C. Many of these substrates are targeted for degradation during mitosis and G1, that guarantees the fidelity of chromosome segregation, and promotes an orderly mitotic exit and progression through G1 phase by preventing the premature entrance into the next stage of the cell cycle (Fig. 1.2) (Brown et al., 2016, Mocciaro and Rape, 2012, Sivakumar and Gorbsky, 2015, van Zon and Wolthuis, 2010, Zhang et al., 2016, Watson et al., 2018, Yamano, 2019, Komander and Rape, 2012).

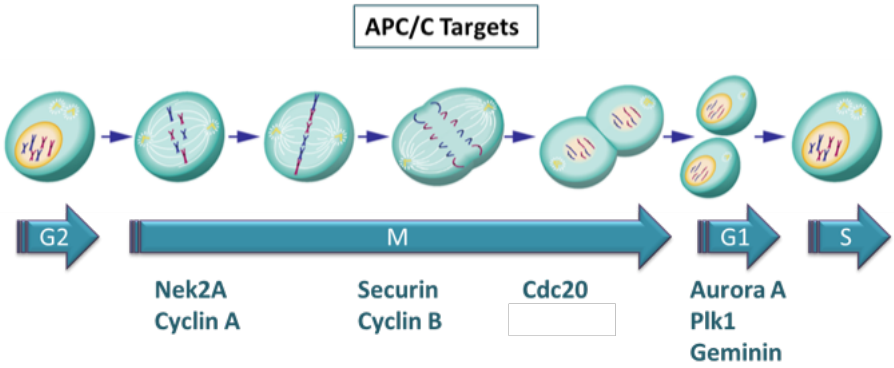

Figure 1. 2: **Cell cycle progression through the ordered degradation of APC/C substrates.** The timing of mitotic degradation for a limited number of APC/C substrates is shown for clarity. Adapted from Zhou et al. (2016)

In addition to its role in the regulation of cell cycle progression, several other roles for the APC/C have been reported. As such, the APC/C is implicated in regulating: the DNA damage response; transcription; translation; cellular metabolism; and post-mitotic functions in neuronal cells, establishing the APC/C as a regulator of multiple cellular processes (Sivakumar and Gorbsky, 2015, Zhou et al., 2016).

Given its central role in coordinating key stages of cell cycle progression APC/C activity is tightly regulated and several mechanisms have evolved to fine-tune APC/C activity and ensure the spatio-temporal events it controls occur at the correct time and location, and in the appropriate order. Dysregulation of APC/C activity is associated with inherited disease and cancer, making it not only an extremely fascinating object of study, but also a potential target for the development of new therapeutic treatments (Zhou et al., 2016, Ajeawung et al., 2019).

1.2 APC/C structure

The human APC/C holoenzyme is a 1.2 MDa complex composed of 14 distinct subunits, four of which are present within the structure as homodimers (Table 1.1).

Subunit	Length (aa)	Stoichiometry	Location
APC1	1944	1	Platform domain
APC2	822	1	Catalytic domain (Cullin)
APC3	824	2	TPR lobe
APC4	808	1	Platform domain
APC5	755	1	Platform domain
APC6	620	2	TPR lobe
APC7	599	2	TPR lobe
APC8	597	2	TPR lobe
APC10	185	1	Catalytic domain (Degron recognition)
APC11	84	1	Catalytic domain (RING)
APC12	85	2	TPR lobe
APC13	74	1	TPR lobe
APC15	121	1	Platform domain
APC16	110	1	TPR lobe
Cdc20	499	1	activator (Degron recognition)
Cdh1	496	1	activator (Degron recognition)

Table 1. 1: **APC/C subunits and stoichiometry in the APC/C holoenzyme.** Adapted from Alfieri et al. (2017)

Despite its composition of multiple subunits, to become catalytically active the APC/C associates, in a cell-cycle dependent manner, with one of two activators, identified as Cell division-cycle protein 20 (Cdc20) and Cdc20 homolog 1 (Cdh1), which also participate in the target recognition process with the APC/C catalytic subunit, APC10 (Table 1.1) (Sivakumar and Gorbsky, 2015, Kataria and Yamano, 2019, Alfieri et al., 2017).

The atomic structure of the APC/C has recently been elucidated by cryo-Electron Microscopy (EM) at a resolution of 3.2Å (Chang et al., 2015). It is organized into three main functional zones: the catalytic domain, the Tetratricopeptide Repeat (TPR) lobe and the platform domain, and is represented as a pyramid with a central cavity where the E2 conjugating enzymes – UbcH10 or UbE2S – the substrates and the activators, Cdc20 and

Cdh1, all associate to allow for the catalytic transfer of ubiquitin to the substrate (Fig. 1.3 A, B and C) (Alfieri et al., 2017, Kataria and Yamano, 2019, Sivakumar and Gorbsky, 2015, Yamano, 2019).

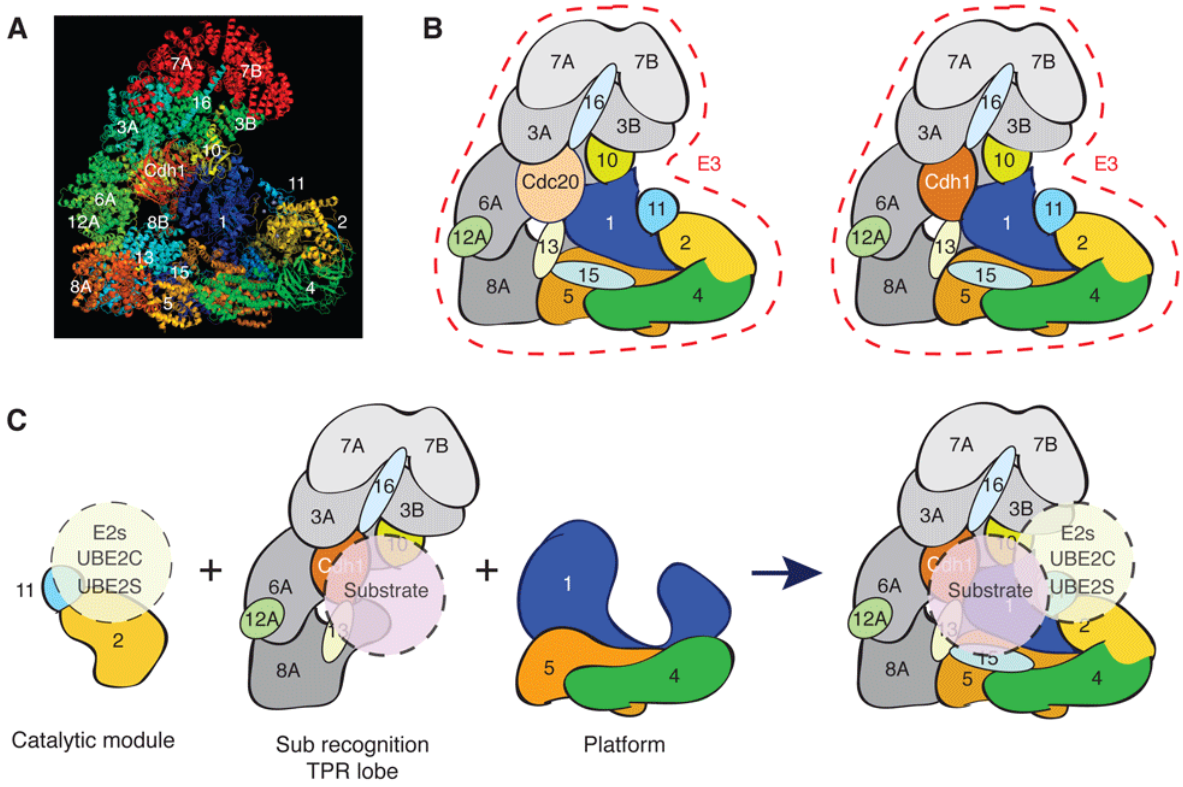

Figure 1.3: **APC/C Structure and organization. (A)** APC/C structure – Protein Data Bank (PDB) 4UI9 – with numbers showing APC/C individual subunits. (**B**) Schematic representation of the APC/C holoenzyme. (**C**) Schematic representation of the APC/C domains and their catalytic reaction in association with the activator (Cdh1), with the E2 conjugating enzymes (UBE2C and UBE2S) and with protein substrate. Taken from Yamano (2019).

The catalytic core is located in close proximity to the central cavity of the APC/C and it is composed of the Cullin subunit- APC2, the RING subunit- APC11, and the catalytic subunit, APC10. Whilst APC2 and APC11 are directly responsible for the E3-ubiquitin ligase catalytic activity of the APC/C, APC10 has a major role in the target recognition process and participates with Cdc20 and Cdh1 to create a target recognition receptor (Fig. 1.3, Table 1.1) (Alfieri et al., 2017, Watson et al., 2018).

The vast majority of the APC/C subunits lie within the TPR lobe which is comprised of APC3, APC6, APC7, APC8, APC12, APC13 and APC16. Constituting the top and the back of the APC/C pyramidal structure, this domain functions as a scaffold for extensive protein-protein interactions, which are mediated by the TPR domain, which is shared by many of the APC/C subunits in this region. As such, the TPR lobe is employed strategically by the APC/C holoenzyme to interact with its substrates, as well as its activators, Cdc20 and Cdh1. In this regard, the APC/C subunits within the TPR lobe region operate as a regulatory hub for extensive PTMs that coordinate the conformational changes undertaken by the holoenzyme during the cell cycle, that affects activator and substrate binding to the APC/C. As such, the TPR lobe ultimately regulates APC/C E3-ubiquitin ligase activity. Additionally, some subunits within the TPR lobe, including APC12, APC13 and APC16, which lack the typical TPR protein-protein interaction motif, have been found to have an integral role in the structural stabilization of the TPR lobe (Fig. 1.3, Table 1.1) (Kataria and Yamano, 2019, Alfieri et al., 2017, Watson et al., 2018, Sivakumar and Gorbsky, 2015).

The platform domain, formed by the subunits APC1, APC4, APC5 and APC15 occupies the base of the APC/C structure, where it acts as a bridge to link together the TPR-lobe and the catalytic domain, and is responsible for defining the overall structure of the APC/C (Fig. 1.3, Table 1.1) (Vodermaier et al., 2003). In addition to its structural role, the platform domain also acts a regulatory centre for the APC/C, such that the cell cycle-dependent PTMs on individual APC/C subunits within this region, affect the overall structure of the APC/C holoenzyme, and modulate its E3-ubiquitin ligase activity (Pines, 2011, Sivakumar and Gorbsky, 2015, Zhou et al., 2016, Kataria and Yamano, 2019, Alfieri et al., 2017, Watson et al., 2018, Yamano, 2019, Chang et al., 2014).

1.3 The APC/C E2 conjugating enzymes: UbcH10 and UBE2S

To poly-ubiquitylate its substrates, the APC/C makes use of two different E2-conjugating enzymes: the "initiating enzyme", UBE2C, also known as UbcH10, and the "elongating enzyme", UBE2S (Meyer and Rape, 2011, Garnett et al., 2009, Brown et al., 2016).

It has been postulated that UbcH10 is responsible for the initiation of poly-ubiquitin chain formation on the substrate, which occurs through a direct association of its C-terminal region with the RING-containing subunit, APC11, which also associates with the acceptor substrate. Through this series of interactions the APC/C acts as an adaptor, bringing together E2-conjugated ubiquitin, activator and protein substrate for the APC/C-dependent catalytic transfer of the first ubiquitin molecule onto the target protein (Kataria and Yamano, 2019, Brown et al., 2016, Sivakumar and Gorbsky, 2015). This catalytic reaction is coordinated by a small amino acid cluster known as the TEK-box, which is shared by many of the APC/C substrates and by ubiquitin itself. The TEK-box is recognised by the E2, which ultimately nucleates the APC/C, substrate and activator both during the priming and the elongation of the poly-ubiquitin chain (Meyer and Rape, 2011, Jin et al., 2008, Williamson et al., 2009).

Following the priming of the substrate, it has been suggested that the elongation of the poly-ubiquitin chain occurs through the APC/C E2 conjugating enzyme, UBE2S. In contrast to UbcH10, UBE2S does not bind to the RING subunit APC11, but associates instead with the Cullin-containing subunit APC2, and catalyses the highly processive formation of K11 linkages exclusive to the APC/C, leading to the degradation of APC/C targets (Williamson et al., 2009, Garnett et al., 2009).

1.4 Role of the APC/C activators, Cdc20 and Cdh1, in the regulation of mitotic progression

To become active, the APC/C associates with one of two activators, Cdc20 and Cdh1, that are responsible for stimulating the APC/C enzymatic activity by aiding the target-recognition process and enhancing the APC/C binding affinity for the E2-conjugating enzyme, UbcH10 (Sivakumar and Gorbsky, 2015, Kataria and Yamano, 2019, Van Voorhis and Morgan, 2014, Kimata et al., 2008, Min et al., 2013, Meyer and Rape, 2011).

Cdc20 and Cdh1 are closely related members of the same protein family, and share similar overall structural architecture, characterized by the presence of two highly conserved regions: the WD40 domain, and the IR-tail, both of which are located in the C-terminal region of these proteins. The beta-propeller secondary structure adopted by the WD40 domain of Cdc20 and Cdh1 creates a suitable interface for protein-protein interactions, which, together with the APC/C catalytic subunit APC10, contributes to the creation of a target-recognition motif used by both APC/C-Cdc20 and APC/C-Cdh1 complexes to associate with substrates. Moreover, the IR-tail located at the C-terminus of both Cdc20 and Cdh1 anchors these proteins to the TPR lobe subunit, APC3, whilst a newly characterized functional motif known as the C-box, present within the N-terminal region of Cdc20 and Cdh1, is also used to facilitate activator association with the APC/C through interaction with APC8 (Kataria and Yamano, 2019, Zur and Brandeis, 2001, Alfieri et al., 2017, Watson et al., 2018).

Cdc20 and Cdh1 association with the APC/C is cell cycle-dependent and defines the temporal regulation of APC/C E3-ubiquitin ligase activity. Indeed, it has been shown that APC/C-Cdc20 complex formation occurs during the early stages of mitosis during nuclear

envelope breakdown (NEBD), making it responsible for the degradation of substrates that ultimately leads to metaphase-to-anaphase transition, whilst the APC/C-Cdh1 complex regulates mitotic exit and progression through G1 (Fig. 1.4) (Sivakumar and Gorbsky, 2015).

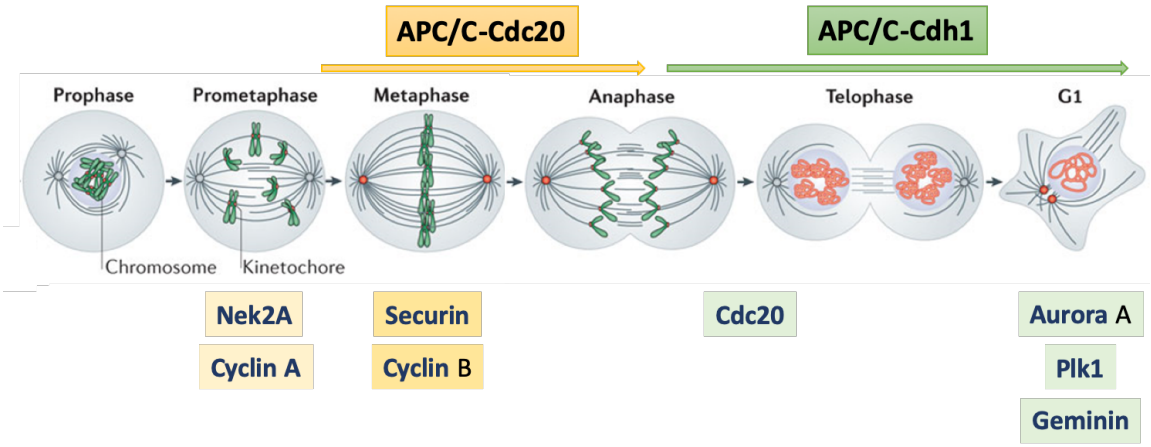

Figure 1. 4: **APC/C cell cycle-dependent association with the activators Cdc20 and Cdh1.** Figure shows the different stages in mitosis when Cdc20 and Cdh1 associate with the APC/C. Adapted from Sivakumar and Gorbsky (2015).

The temporal association of Cdc20 and Cdh1 activators with the APC/C holoenzyme is critical in controlling the timely and ordered degradation of APC/C substrates. Indeed, although Cdc20 and Cdh1 are highly similar they have differing specificities for the various APC/C substrates, which is essential in ensuring an orderly progression through mitosis. It is interesting to note that although the APC/C-Cdh1 can recognize and degrade all of the APC/C substrates targeted by Cdc20, APC/C-Cdc20 activity promotes the degradation of a limited number of APC/C targets. This selectivity is crucial in promoting early mitotic progression and preventing the premature degradation of proteins, such as Polo like kinase 1 (Plk1) and Aurora kinases that are required for cytokinesis (Zhao and Fang, 2005, Zhou et al., 2016, Sivakumar and Gorbsky, 2015, Alfieri et al., 2017, Davey and Morgan, 2016, Mocciaro and Rape, 2012, Kataria and Yamano, 2019, Visintin et al., 1997).

The main role of the APC/C-Cdc20 complex is to promote metaphase-to-anaphase transition by inducing the 26S proteasomal degradation of two key cellular proteins that regulate this process: Securin and Cyclin B1 (Pines, 2011). Securin is a small protein responsible for preventing premature separation of sister chromatids after DNA replication. In this regard, Securin associates with the protease, Separase, impeding the cleavage of the Cohesin ring that holds sister chromatids together, thus retarding chromosome segregation until they are properly attached through kinetochores to the mitotic spindle and aligned on the metaphase plate (Choi et al., 2009, Waizenegger et al., 2002). Once chromosomes are attached correctly on the metaphase plate, APC/C-Cdc20 catalyses the degradation of Securin, which consequently releases Separase, which cleaves Cohesin and allows for chromosome segregation and hence, metaphase-to-anaphase transition (Hagting et al., 2002, Zur and Brandeis, 2001). Remarkably, APC/C-Cdc20 activation during prometaphase is caused by the rise in the levels of Cyclin B1 and by the consequent activation of the Cyclin-dependent kinase 1 (Cdk1), which positively affects Cdc20 association with the APC/C holoenzyme, allowing for critical conformational changes that promote the formation of an active APC/C-Cdc20 complex (Kraft et al., 2003, Zhang et al., 2016, Peters, 2006, Primorac and Musacchio, 2013). As well as degrading Securin, the APC/C-Cdc20 complex is responsible for the degradation of Cyclin B1 and for the drastic drop in its levels prior to anaphase onset. As such, the APC/C-Cdc20-dependent degradation of Cyclin B1 leads to Cdk1 mitotic kinase inactivation, and a negative regulatory feedback mechanism that leads to the inactivation of APC/C-Cdc20 complexes as Cdc20 does not bind to the APC/C when it is dephosphorylated (King et al., 1995, Peters, 2006, Clute and Pines, 1999, Gavet and Pines, 2010, Sivakumar and Gorbsky, 2015).

Whilst the Cdk1-Cyclin B1-dependent phosphorylation of the APC/C has a positive effect on the formation of active APC/C-Cdc20 complexes, phosphorylation of the activator Cdh1 impedes its association with the holoenzyme (Kataria and Yamano, 2019, Sivakumar and Gorbsky, 2015, Pines, 2011, Alfieri et al., 2017, Primorac and Musacchio, 2013). Thus, following Cdk1 inactivation during anaphase, unphosphorylated Cdh1 can associate with the APC/C and drive the degradation of a new spectrum of substrates, which allows for mitotic exit and for the movement of cells into G1. As well as sustaining the degradation of Cyclin B1 and Securin, active APC/C-Cdh1 complexes induce the degradation of the mitotic kinases Plk1, Aurora A and Aurora B, whose clearance is necessary to terminate mitosis. APC/C-Cdh1 also promotes the degradation of Cdc20 and UbcH10, allowing for the complete inactivation of the APC/C and readying cells to enter a new cycle of replication (Pines, 2011, Sivakumar and Gorbsky, 2015, Davey and Morgan, 2016). APC/C-Cdh1 enzymatic activity stays high during G1 and the degradation of substrates during this phase prevent cells from entering S phase. As such, APC/C-Cdh1 promotes the degradation of the S-phase kinase associated kinase 2 (Skp2), a component of the E3 ubiquitin ligase Skp-Cullin-F box (SCF) complex, which is an important regulator of entry into S phase. By reducing the levels of Skp2, APC/C-Cdh1 participates in the inactivation of the SCF E3 ubiquitin ligase and allows for the accumulation of proteins required during G1 (Chang et al., 2014, Penas et al., 2012, Bashir et al., 2004, Wei et al., 2004, Reed, 2008). APC/C-Cdh1 activity in G1 is also required for the maintenance of low levels of Cyclins, including Cyclin A and Cyclin D1, whose accumulation is necessary to sustain S-phase entry(Chang et al., 2014, Penas et al., 2012). Moreover, APC/C-Cdh1 also plays a role in the control of DNA replication directly, as it targets Geminin, a protein required for pre-replication complex formation, for degradation. Reduction in the levels of Geminin during G1 allows the

formation of new replication origins that facilitate DNA replication during S-phase (Wirth et al., 2004, Diffley, 2004, McGarry and Kirschner, 1998).

1.5 APC/C targets degradation recognition motifs (degrons) within protein substrates

The orderly degradation of APC/C substrates is key towards maintaining genomic stability and ploidy status during mitotic progression and mitotic exit. Simplistically, APC/C substrates are defined by the presence of one, or more, degradation motifs, known as degrons, within their primary sequence which facilitate substrate recruitment to the APC/C. Characteristic APC/C degrons are D-boxes (RXXLXXI/VXN), KEN boxes (KENXXXN/D), and the more recently identified ABBA motif (FX[ILV][FHY]X[DE]) (He et al., 2013, Glotzer et al., 1991, Pfleger and Kirschner, 2000, Lischetti et al., 2014, Lu et al., 2014). These degrons, are in the most part, recognised specifically by the degron-recognition receptor generated by the association of the Cdc20 and Cdh1 WD40 domain with the APC/C subunit, APC10 (Fig. 1.5) (Di Fiore et al., 2015, Buschhorn et al., 2011, da Fonseca et al., 2011, Li et al., 2008, Davey and Morgan, 2016, Sivakumar and Gorbsky, 2015).

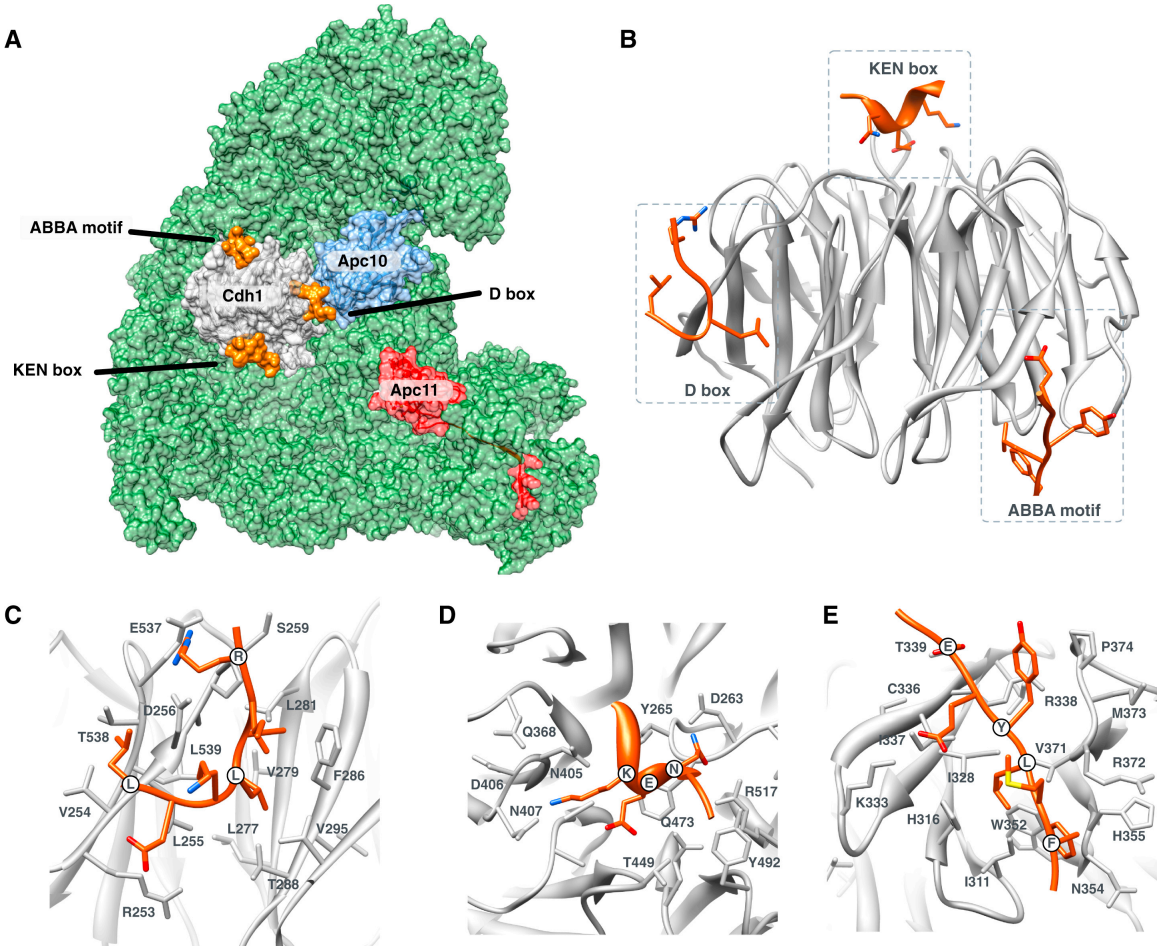

Figure 1. 5: **APC/C degradation motifs.** (**A**) Structure of the Cdh1 activator subunit WD40 domain (grey) bound to APC/C (green). The APC10 subunit (blue), the APC11 RING subunit (red), and the positions of the motif-binding pockets (with degrons in orange) are also shown. (**B**) The WD40 domain of Cdh1 with the three degron-binding pockets occupied by the D box, KEN box and ABBA motif. (**C**) The D box-binding pocket. (**D**) The KEN box-binding pocket. (**E**) The ABBA motif-binding pocket. Taken from Davey and Morgan (2016).

Although the ability of Cdc20 and Cdh1 to recognise APC/C substrates during the different mitotic phases contributes towards the timing of substrate degradation, such that APC/C-Cdc20 recognize D-box-containing substrates and, Cdh1 is capable of recognizing both D-boxes and KEN-boxes, other mechanisms also contribute to the establishment of a precise substrate hierarchy (Komander and Rape, 2012, Sivakumar and Gorbsky, 2015, Pines, 2011, Davey and Morgan, 2016). Indeed, the inherent structural characteristics of the substrates can greatly contribute towards the timing of their degradation, by affecting both their binding

affinity for the APC/C degron receptor and the processivity of the poly-ubiquitylation reaction. For instance, some APC/C substrates possess multiple degrons within their primary sequence, and this increases their binding affinity for the APC/C, which allows for more efficient degradation (Davey and Morgan, 2016). Furthermore, amino acids proximal to D-boxes and KEN-boxes can contribute towards the creation of extended degrons, which can bind more avidly to the APC/C, which ultimately increases the rate of substrate degradation (Davey and Morgan, 2016). The order of APC/C substrate degradation is also regulated by PTMs that occur in proximity to degrons, and can positively or negatively influence APC/C-dependent degradation. For instance, some substrates such as Aurora A and the NIMA-related kinase Nek2A, are characterized by the presence of a S residue immediately before the acceptor K residue of their KEN boxes, such that phosphorylation promotes substrate binding to the APC/C (Min et al., 2013). Another example of phosphorylation-dependent regulation is the Cdk1-Cyclin B1-dependent phosphorylation of Securin, which increases its association with, and degradation by, the APC/C (Sivakumar and Gorbsky, 2015, Pines, 2011). In contrast, phosphorylation has a negative effect upon the ability of Skp2 and Geminin to be recruited to the APC/C-Cdh1 complex, which leads to stabilization of these substrates and, ultimately, cellular progression from G1 to S-phase (Rodier et al., 2008, Tsunematsu et al., 2013). Akin to phosphorylation, other PTMs can also contribute towards the degradation hierarchy of APC/C substrates. For instance, acetylation of Budding uninhibited by benzimidazole-related 1 (BubR1) proximal to its KEN box is responsible for masking the activity of this degron motif of this protein, which prevents its degradation such that it can contribute towards the Spindle Assembly Checkpoint (SAC)-mediated inhibition of the APC/C (Diaz-Martinez et al., 2015, Sivakumar and Gorbsky, 2015, Lu et al., 2015). Other mechanisms also contribute towards the timing of APC/C substrate degradation. For

instance, differential localization of substrates can prevent their contact with the holoenzyme, increasing therefore their stability within a particular cellular compartment (Sivakumar and Gorbsky, 2015, Pines, 2011, Davey and Morgan, 2016). Moreover, accessibility of the acceptor K residue within the substrate is critical in determining the timing of poly-ubiquitylation, such that substrate association with a partner protein can effectively hide the K acceptor site and prevent its ubiquitylation (Davey and Morgan, 2016).

The mechanisms outlined above all contribute towards "substrate competition" for binding to the APC/C that defines the complex nature of APC/C-mediated degradation. In this regard, it is recognised that high affinity substrates have a highly processive behaviour during the ubiquitylation reaction and are subjected to a more efficient poly-ubiquitylation, with more than one ubiquitin molecule added to a poly-ubiquitin chain during each step of contact with the APC/C. In contrast, substrates with a lower affinity for the APC/C are poly-ubiquitylated at a lower rate, as they might require multiple association/dissociation steps before receiving the appropriate number of ubiquitin molecules necessary for their targeted degradation by the 26S proteasome. The complexity of APC/C regulation and substrate recruitment all contribute towards an orderly progression through mitosis, the retention of chromosomal fidelity and ploidy status, cytokinesis, mitotic exit and progression in to and through the successive G1 phase (Davey and Morgan, 2016).

1.6 APC/C regulation

Given its defining role in the regulation of mitosis APC/C activity is tightly regulated (Lara-Gonzalez et al., 2012, Zhou et al., 2016). Whilst APC/C activation depends upon its interaction with the activators Cdc20 and Cdh1, other mechanisms exist to restrain APC/C activity during the cell cycle. For instance, from NEBD until anaphase onset APC/C-Cdc20

activity is inhibited by the Spindle Assembly Checkpoint (SAC), a surveillance mechanism aimed at preventing metaphase-to-anaphase transition until all chromosomes are associated with the mitotic spindle (Lara-Gonzalez et al., 2012, Alfieri et al., 2016, Musacchio, 2015, Musacchio and Salmon, 2007). Similarly, at the end of G1 APC/C-Cdh1 needs to be inactivated to allow cells to enter S-phase and begin a new cycle of replication and division; Early mitotic inhibitor 1 (Emi1) association with APC/C-Cdh1 inhibits APC/C activity in these circumstances (Reimann et al., 2001, Cappell et al., 2018, Frye et al., 2013). Additionally, transient interactions with other cellular proteins serve to modulate APC/C activity during the different phases of the cell cycle and contribute to the fine-tuning of APC/C activity during the various mitotic phases (Townsend et al., 2009, Sedgwick et al., 2013, Turnell et al., 2005, Kucharski et al., 2017). Furthermore, PTM of individual APC/C subunits is critical in regulating APC/C conformation and activation status (Kraft et al., 2003, Kataria and Yamano, 2019, Alfieri et al., 2017).

1.6.1 The SAC

The SAC is regulated principally by the Mitotic Checkpoint Complex (MCC), a trimeric complex comprising Mitotic arrest deficient 2 (Mad2), BubR1 and Budding uninhibited by benzimidazole-3 (Bub3). The MCC complex binds to, and sequesters 'free' Cdc20, thus impeding the Cdc20-dependent recruitment of substrates to the APC/C, and furthermore, limiting APC/C E3 activity. An active SAC ensures that the levels of APC/C substrates Securin and Cyclin B1 remain high and consequently, that metaphase-to-anaphase transition is inhibited (Diaz-Martinez et al., 2015, Fang, 2002, Lara-Gonzalez et al., 2012).

At the beginning of mitosis the kinase, Monopolar spindle 1 (Mps1) is recruited to unattached kinetochores where it initiates a phosphorylation cascade, that results in the

phosphorylation of the Mitotic checkpoint deficient protein 1 (Mad1) (Pachis et al., 2019, Musacchio and Salmon, 2007, Musacchio, 2015, Lara-Gonzalez et al., 2012). Phosphorylated Mad1 then associates with Mad2 causing a conformational change and switch from an open conformation (o-Mad2), incapable of binding Cdc20, to a closed conformation (c-Mad2), that can bind Cdc20. The heterodimer, c-Mad2-Cdc20 facilitates the recruitment of BubR1 and Mad3 to Cdc20 to form an active MCC. The MCC complex can also associate directly with APC/C-Cdc20 active complexes to further strengthen the SAC-dependent inhibition of the APC/C. Structural analyses by the Barford group, have revealed that the substrate recognition receptor normally created by APC10 and Cdc20 is obstructed upon MCC binding to APC/C-Cdc20 complexes (Fig. 1.6 A) (Alfieri et al., 2016). In this regard, BubR1 acts as a pseudo-substrate, and occupies the APC/C catalytic pocket, disrupting the target recognition site and preventing UbcH10 binding (Fig. 1.6 B) (Alfieri et al., 2016, Kulukian et al., 2009, De Antoni et al., 2005, Fang, 2002, Sudakin et al., 2001).

Upon SAC satisfaction, Mps1 is inactivated and Cdc20 released from the MCC, which allows for the formation of active APC/C-Cdc20 complexes (Pachis et al., 2019). Dissociation of the MCC from the APC/C also contributes towards silencing of the SAC; auto-ubiquitylation of Cdc20 associated with the MCC promotes MCC dissociation from the APC/C (Reddy et al., 2007, Uzunova et al., 2012, Foster and Morgan, 2012, Mansfeld et al., 2011). Cryo-EM analyses have revealed that structural rearrangements in APC15 regulates MCC association with, and MCC dissociation from, the APC/C. During an active SAC APC15 conformational changes facilitate MCC association with the APC/C and inhibit UbcH10 association. When the SAC is satisfied MCC dissociation from the APC/C allows for the re-organization of APC15, which leads to the restoration of the UbcH10 binding site

on the APC/C and to the APC/C-dependent poly-ubiquitylation of Cdc20 associated with the MCC (Fig. 1.6 C) (Alfieri et al., 2016).

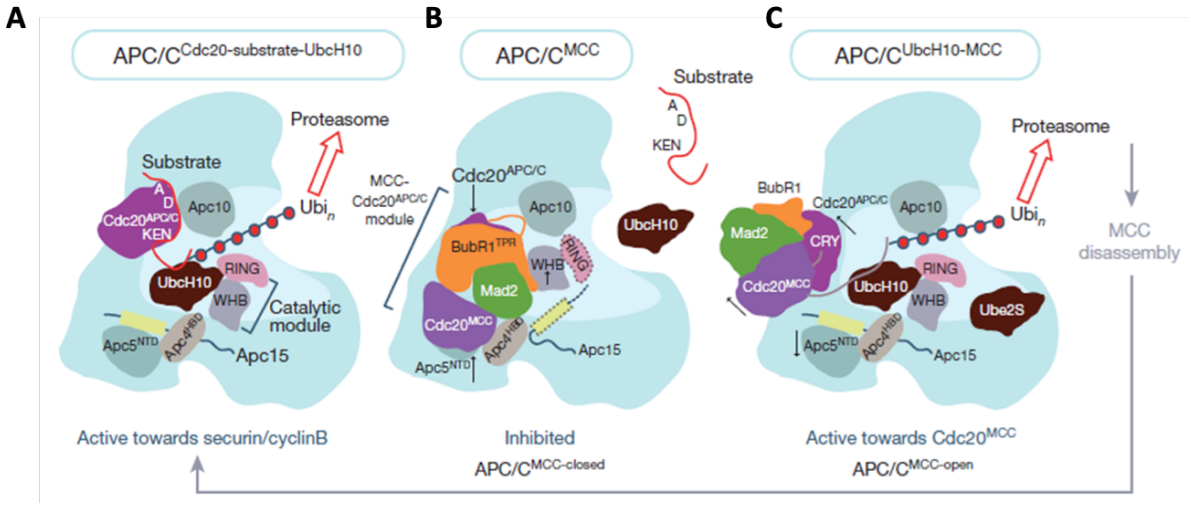

Figure 1. 6: **SAC-dependent inhibition of the APC/C mediated by MCC association.** (**A**) Active APC/C in complex with Cdc20, UbcH10 and substrate. (**B**) Inhibited APC/C in complex in association with the MCC. (**C**) APC/C is re-activated after SAC satisfaction. Taken from Alfieri et al. (2016).

Intriguingly, some substrates, including Nek2A and Cyclin A, are able to overcome the SAC-dependent inhibition of the APC/C and are degraded early in mitosis in an APC/C-dependent, SAC-insensitive, manner. The mitotic kinase, Nek2A, which plays a central role in the process of centrosome separation and the formation of the mitotic spindle is degraded at the beginning of mitosis. As such, Nek2A utilises a C-terminal MR motif, similar to the IR-tail used by Cdc20 and Cdh1 and competes, during an active SAC, with the MCC to associate with the APC/C, thus triggering its degradation (Faragher and Fry, 2003, van Zon and Wolthuis, 2010). Similarly, the SAC-insensitive substrate Cyclin A is degraded during prometaphase through its ability to compete effectively with BubR1 and associate directly with the APC/C through interaction with the WD40 domain of Cdc20 (Di Fiore and Pines, 2010, Yam et al., 2002, van Zon and Wolthuis, 2010). Another example of SAC-insensitive

substrate is represented by the more recently identified tumour suppressor p53-binding protein 1 (53BP1), which by means of its KEN box and of a BRC1 C-terminal (tBRCT) domain can contact Cdc20 directly and drive its own degradation in the presence of an active SAC (Kucharski et al., 2017).

Overall, these mechanisms contribute to the fine tuning of APC/C activity and prevent its premature activation, contributing to the maintenance of genome stability (Lara-Gonzalez et al., 2012, Pines, 2011).

1.6.2 EMI1

Akin to the SAC-dependent inhibition of APC/C-Cdc20, the inhibition of APC/C-Cdh1 by Emi1 in G1 phase allows for cells to commit to another cycle of replication and division (Cappell et al., 2016). Emi1 acts as a pseudo-substrate inhibitor of APC/C-Cdh1 activity (Frye et al., 2013, Davey and Morgan, 2016, Yamano, 2019, Watson et al., 2018). Emi1 possesses a C-terminal D-box that associates with Cdh1 and APC10 to block the substrate recognition receptor whilst its zinc-binding region (ZBR) inhibits UbcH10 association with APC11 and inhibits the UbcH10-dependent priming of ubiquitin chains on substrates. The C-terminal LRRL-tail of Emi1 occupies the UBE2S binding site on the catalytic subunit APC2 and inhibits UBE2S elongation (Chang et al., 2015, Cappell et al., 2018, Frye et al., 2013, He et al., 2013, Watson et al., 2018). Interestingly, the stability of Emi1 is regulated by an SCF E3 ubiquitin ligase, whose activity during G2 contributes to a reduction in Emi1 levels and the reactivation of the APC/C (Margottin-Goguet et al., 2003).

1.6.3 Other APC/C regulators

Mass spectrometric studies from our laboratory and others have identified numerous APC/C substrates and APC/C-interacting partners that regulate APC/C activity through the

integration of signals from other cellular pathways to ultimately regulate cell division. For instance, Mediator of DNA Damage Checkpoint protein 1 (MDC1), a scaffold protein integral to the DNA damage response pathway, acts as a positive regulator of the APC/C in mitosis through its ability to bind to the APC/C and promote Cdc20 association with the APC/C (Townsend et al., 2009). The tumour suppressor protein, Transcriptional Intermediary Factor 1 gamma (TIF1γ), interacts with the APC/C through APC7 and stimulates the activity of the APC/C-Cdc20 complex (Sedgwick et al., 2013), whilst CBP and p300 transcriptional co-activators interact with APC5 and APC7 to stimulate APC/C holoenzyme activity directly and promote the progression of cells through mitosis and G1 (Turnell et al., 2005). Consistent with the role of these proteins to regulate APC/C activity, siRNA-mediated knockdown of these positive regulators causes mitotic arrest (Townsend et al., 2009, Sedgwick et al., 2013, Turnell et al., 2005). APC/C activity can also be regulated negatively by its transient interaction with cellular proteins. For instance, 53BP1, a SAC-insensitive APC/C substrate, can also inhibit APC/C activity in response to mitotic stress caused by mitotic poisons, coupling the process of mitotic progression to the stress response pathway (Kucharski et al., 2017).

1.6.4 PTMs in the control of APC/C activity

PTMs on APC/C subunits are critical modulators of APC/C function, having extraordinary effects on APC/C structure, activity and interactome (Davey and Morgan, 2016, Sivakumar and Gorbsky, 2015). Phosphorylation of APC/C subunits is a critical PTM in the regulation of the APC/C, as it is responsible for the conformational changes required for Cdc20 association with the APC/C and, moreover, accelerates the rate and efficiency of the ubiquitylation reaction (Kraft et al., 2003, Qiao et al., 2016, Zhang et al., 2016, Golan et al., 2002, Fujimitsu et al., 2016). The majority of the APC/C phosphorylation events occur on

TPR domains, particularly on APC3 whose hyper-phosphorylation is considered a hallmark for APC/C activation in mitosis (Kraft et al., 2003, Pines, 2011). Remarkably, a total of 150 phosphorylation sites have been identified by mass spectrometry screening on APC/C subunits, 70 of which have been shown to occur specifically during mitosis on APC1, APC2, APC3, APC4, APC5, APC6, APC7, APC8, APC10 and APC12 (Kraft et al., 2003, Herzog et al., 2005, Hegemann et al., 2011, Steen et al., 2008, Zhang et al., 2016). The functional relevance of many of these phosphorylation sites have yet to be identified, mostly because they occur within unstructured 'loop' regions that are not visible in the cryo-EM structures, making it difficult to model and predict the effect of these phosphorylation events on APC/C structure and interactions with activators and regulators. Moreover, many of these phosphorylation events might act synergistically, and cooperate to trigger conformational changes that affect APC/C activity, such that single, site-directed mutagenesis approaches might not be appropriate to study function (Qiao et al., 2016).

To account for such complexities a study conducted in the Peter's laboratory, mutated simultaneously, 68 of the mitotic phosphorylation sites found on different APC/C subunits, to create a phospho-inhibited APC/C-pA complex and a phospho-mimetic APC/C-pE complex, which gave rise to APC/C species where all the selected phosphorylation sites were either inhibited, or, constitutively phosphorylated. By studying the behaviour of these reconstituted APC/C mutants, they were able to demonstrate that association of Cdc20 with the APC/C is dependent upon its phosphorylation status, as the phospho-inhibited APC/C-pA complex failed to associate with Cdc20, whilst its binding to Cdh1 was not compromised (Qiao et al., 2016). This study also demonstrated that mimicking the mitotic phosphorylation status of APC1, was sufficient to trigger Cdc20 association and activation of the APC/C, although they did not exclude that other phosphorylation events on the APC/C platform

domain could also positively contribute to Cdc20 association (Qiao et al., 2016). These data were confirmed by the Barford group, who conducted Cryo-EM analyses and showed that phosphorylation of an auto-inhibitory (AI) segment within the N-terminal loop of APC1 allows for Cdc20 binding to APC8 (Zhang et al., 2016). A similar study conducted by the Yamano lab was able to elucidate the mechanism that regulates APC1 mitotic phosphorylation (Fujimitsu et al., 2016). Using reconstructed APC/C complexes in *Xenopus* extracts their study showed the existence of extensive phosphorylation-dependent cross-talk between APC/C subunits. In this regard, they reported that Cdk1-dependent phosphorylation of APC3, which occurs within an unstructured, regulatory loop domain, is responsible for the subsequent Cdk1-dependent phosphorylation of the APC1 regulatory loop, which ultimately causes the dislocation of the AI helix of APC1 from APC8, and allows Cdc20 binding to APC8 (Fig. 1.7) (Fujimitsu et al., 2016).

Taken together these studies determined that phosphorylation promotes extensive conformational changes within the APC/C during mitosis, highlighting the importance of these PTM events on the fine-tuning of the APC/C function.

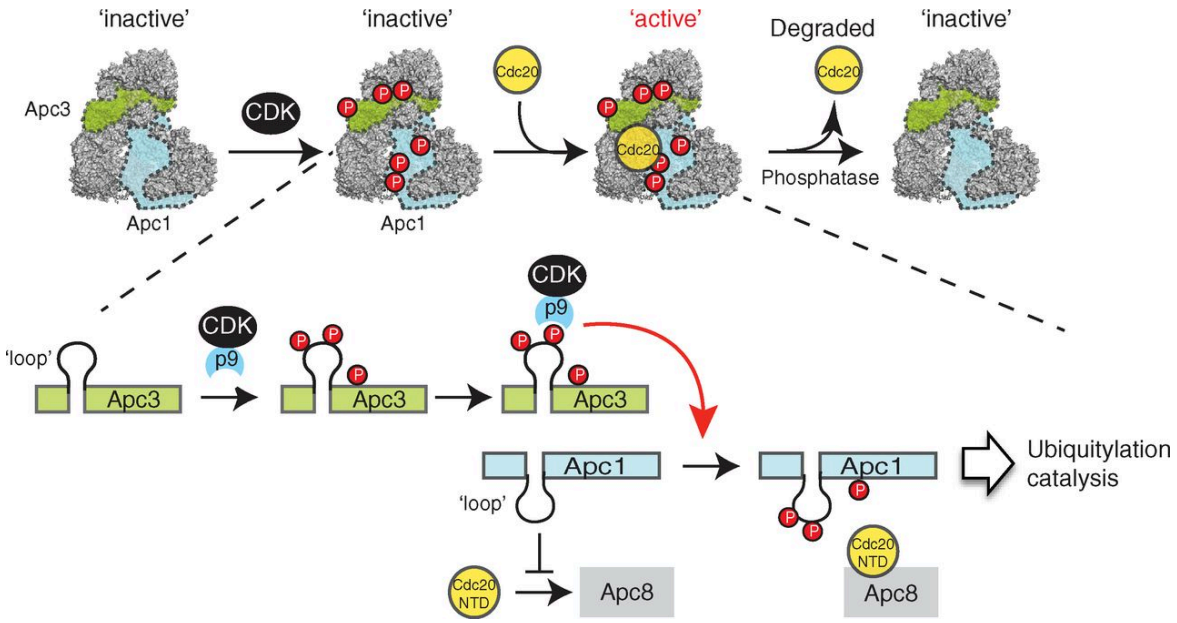

Figure 1. 7: **Proposed mechanism for APC/C activation through mitotic phosphorylation during mitosis.** See text for details. Taken from Fujimitsu et al. (2016).

Other PTMs have also been shown to be critical in controlling APC/C activity. Key amongst these is SUMOylation; APC4 SUMOylation at residues 772 and 798 serve to recruit the APC/C substrate, Kinesin-like protein KIF18B to the APC/C, strengthening the concept that transient alterations in the PTM status of APC/C individual subunits can impact the ability of the APC/C to recognize its target (Eifler et al., 2018). Mass spectrometric screening has revealed that APC1, APC4 and APC8 are methylated, whilst APC3, APC7, APC8, APC10 and APC12 are acetylated (Cuijpers and Vertegaal, 2018, Lundby et al., 2012). Although the functional relevance of these PTMs have yet to be characterized, it is likely that they affect APC/C structure and its ability to recruit substrates for degradation. As key role for acetylation in the regulation of APC/C has been determined. CBP/p300 acetyltransferases interact with the APC/C and promote mitotic progression, although a specific acetylation site was not determined during that study (Turnell et al., 2005). As yet, unpublished studies revealed that APC3, was the major target for CBP/p300-dependent acetylation (P. E.

Minshall, PhD thesis, The University of Birmingham, 2015) and the consequence of this PTM on APC/C activity is currently being studied in our laboratory.

The PTM studies detailed herein have revealed the critical role played by individual APC/C subunits in the regulation of APC/C structure and E3 ubiquitin ligase activity.

1.7 APC/C dysregulation in cancer

Given its pivotal role as a master regulator of the cell cycle, dysregulation of APC/C activity, through modulation of its regulatory pathways, are often associated with the loss of genome integrity and tumourigenesis (Penas et al., 2012, Kataria and Yamano, 2019, Zhou et al., 2016). Multiple mutations in many APC/C subunits have been identified in different cancer types, but their functional significance has yet to be established (Wang et al., 2003, Pray et al., 2002). For instance, heterozygous, somatic mutations in TPR APC/C subunits APC3, APC6 and APC8 have been identified in human colon cancer, and is accompanied by increases in APC/C substrates such as Cyclin B1 (Wang et al., 2003). Other reports indicate that APC3 is overexpressed in gastric and colorectal cancers, and its dysregulation has been proposed to contribute towards enhanced cellular proliferation, invasion and metastasis (Xin et al., 2018, Qiu et al., 2017, Qiu et al., 2016). Microarray analysis of multiple cancer cell lines has determined that APC2 and APC7 are overexpressed in cell lines derived from ovarian, breast, lung, bladder and oral cancers, though the biological significance of these findings has yet to be determined (Rahimi et al., 2015). In contrast, another study identified APC7 as being under-expressed in fibroadenomas and breast tumours, where it purportedly contributes to cellular transformation by increasing chromosomal instability (Kang et al., 2009). The potential impact of APC/C subunit alterations in cancer have also been characterized by functional genomic screening of colon, head and neck, lung, bladder and

breast cancers (Sansregret et al., 2017). In this regard, 132 missense mutations in the APC/C subunits APC1, APC3, APC4, APC5, APC6, APC8 and APC10 were evaluated with predictive software to calculate the potential effect of these mutations on APC/C structure and function. Intriguingly, the results of this study revealed a positive correlation between mutations in APC/C subunits, potential structural aberrations and the cancer phenotype (Sansregret et al., 2017). Although it is difficult to ascribe particular APC/C mutations to cancer initiation, or cancer maintenance, modelling the effect of APC/C mutations on APC/C holoenzyme structure and function could be important in this regard. Indeed, it is highly likely that APC/C mutations will be important in tumourigenesis, as the APC/C activator, Cdc20, and the APC/C E2-conjugating enzyme, UbcH10, are both well characterized oncogene products, and are overexpressed in a number of human cancers and are often used as prognostic markers (Wu et al., 2013, Wu et al., 2019, Van Ree et al., 2010).

The oncogenic properties of Cdc20 are associated with its ability to overcome the SAC by inducing the hyperactivation of the APC/C, which promotes chromosome missegregation and aneuploidy (Lehman et al., 2007, Kataria and Yamano, 2019, Musacchio and Salmon, 2007). As such, Cdc20 is overexpressed in colorectal cancer, non-small cell lung cancer (NSCLC), lung adenocarcinomas, gastric cancer, osteosarcoma and pancreatic ductal adenocarcinomas (Wu et al., 2013, Kato et al., 2012, Singhal et al., 2003, Kim et al., 2005, Wu et al., 2019, Dong et al., 2019). A meta-analysis aimed at evaluating the impact of Cdc20 overexpression in solid tumours confirmed that high expression levels of Cdc20, correlated positively with poor prognosis, and identified Cdc20 as a potential therapeutic target (Wang et al., 2018). Indeed, APC/C-Cdc20 complexes are targeted indirectly by the chemotherapeutic agents Paclitaxel (Taxol) and Vinka alkaloids, which stabilise microtubules and activate the SAC, which leads to a prolonged mitotic arrest and apoptosis

(Jordan and Wilson, 2004, Kataria and Yamano, 2019, Wang et al., 2000b). Unfortunately, however, APC/C-Cdc20 active complexes that exist even in the presence of an activated SAC can induce mitotic slippage by promoting the sustained degradation of Cyclin B1 (Brito and Rieder, 2006). As such, being able to target the APC/C-Cdc20 complexes more directly might represent a great advantage for cancer treatment. APC/C inhibitors Tosyl -1-Arginine Methyl Ester (TAME) and Apcin target APC/C-Cdc20 directly, through their ability to block Cdc20 C-box and IR-tail to bind APC8 and APC3, respectively, and associating directly with Cdc20's degron recognition receptor; TAME and Apcin inactivate completely APC/C-Cdc20 complexes and promote apoptosis (Zhang et al., 2016, Sackton et al., 2014, Brito and Rieder, 2006, Kataria and Yamano, 2019).

Akin to Cdc20, UbcH10 is overexpressed in multiple cancer types, and is similarly associated with poor prognostic outcome; UbcH10 is thus considered a therapeutic target as well as biomarker for multiple cancers (Van Ree et al., 2010, Summers et al., 2008, Xie et al., 2014). Gene expression profiling of various tumours, including glioblastoma, lung, ovary, breast and bladder tissue have shown that UbcH10 overexpression is often due to duplication of its gene locus, revealing a causal relationship between UbcH10 overexpression and tumourigenesis (Wagner et al., 2004). Moreover, studies conducted in mice, aimed at evaluating the correlation between UbcH10 overexpression levels with the cancer phenotype, clearly established that overexpression of UbcH10 correlated positively to increase in chromosomal instability and aneuploidy. As such, UbcH10 overexpression induced APC/C hyperactivation and the premature degradation of Cyclin B1, leading to the development numerous spontaneous tumours, including lung adenomas, hepatic adenomas, lymphomas, skin tumours and adenocarcinomas (Van Ree et al., 2010) Interestingly, UbcH10 overexpression in cancer is often associated with Cdc20 overexpression. Although

the exact correlation between overexpression of these APC/C-related oncogenes has not been clarified, one study reported that Cdc20 stimulates UcbH10 overexpression transcriptionally through its association with the CBP/p300 acetyltransferase transcriptional co-activators (Nath et al., 2011).

As the SAC inhibits APC/C-Cdc20 it is not surprising that the SAC functions as a tumour suppressor; SAC components are often inactivated in cancer (Kops et al., 2005). In this regard, studies in mice have indicated that homozygous mutations in Cdc20 that inhibit its association with Mad2 are lethal, whilst mice which are heterozygous for the same Cdc20 mutation are viable but showed a marked susceptibility to spontaneous tumours (Li et al., 2009). Mutations in SAC components, Budding uninhibited by benzimidazole-1 (Bub1) and BubR1 have been observed in colon cancers and are characterized by extensive chromosomal instability and aneuploidy, whilst Mad2, Bub1 and Bub3 mutations have been found in breast, gastrointestinal and colorectal cancers (Cahill et al., 1998, Rio Frio et al., 2010, Mur et al., 2018, Wang et al., 2015).

In contrast to Cdc20 and UbcH10, Cdh1 possesses tumour suppressor properties. Although *Cdh1* knockout mice die during the early stages of embryo development, the deletion of one copy of the *Cdh1* gene promotes tumour formation at the later stages of life (García-Higuera et al., 2008, Li et al., 2008, Kataria and Yamano, 2019). In contrast, stable expression of the *Cdh1* murine homologue in B-lymphoma cell lines inhibits tumour growth (Wang et al., 2000a). It has been suggested that the tumour suppressor properties of Cdh1 are due to its ability to maintain low levels of various APC/C substrates, including Skp2, Aurora A, Plk1 and Cyclins in G1, as all of these proteins have oncogenic properties (Lehman et al., 2007, Engelbert et al., 2008, Zhou et al., 2016). Consistent with this idea, the oncogenic

overexpression of Skp2 in breast cancer correlated positively with a reduction in the levels of Cdh1 (Fujita et al., 2008). Similarly, overexpression of the APC/C-Cdh1 substrate, Aurora A in pancreatic cancer cell lines was found to be due to augmented stability of the protein that contributed to the chromosomal instability and aneuploidy of these cell lines (Li et al., 2003). Moreover, overexpression of the APC/C-Cdh1 inhibitor, Emi1 has been postulated to promote tumourigenesis through its ability to inhibit the degradation of APC/C-Cdh1 oncogenic substrates (Lehman et al., 2007, Pray et al., 2002). APC/C-Cdh1 is also involved in the DNA damage response in G2; reduction in Cdh1 levels can affect the cell's ability to repair DNA leading to replication errors that contribute towards increased genome instability (Penas et al., 2012, Bassermann et al., 2008).

Together, these studies highlight the pivotal role of the APC/C in the maintenance of cellular homeostasis and emphasize that the dysregulation of APC/C activity can promote tumourigenesis; an understanding of APC/C function is therefore important in the rational design of new cancer therapies.

1.8 Mitotic kinases and their crosstalk in the control of mitotic progression

Given the central role of the APC/C in regulating mitosis it is not surprising that the mitotic kinases, which control the cytological changes that occur during mitosis, namely NEBD, DNA compaction, cytoskeletal re-organization, chromosome segregation and cytokinesis, are also APC/C substrates (Kataria and Yamano, 2019, Carmena et al., 2009, Malumbres and Barbacid, 2007, Taylor and Peters, 2008, Archambault et al., 2015, Qian et al., 2015). Cdk1, Plk1 and Aurora B kinases, amongst others, are responsible for the phosphorylation of multiple cellular proteins, including APC/C subunits, and control almost all aspects of cell cycle progression from G2 through mitosis to G1 (Kataria and Yamano, 2019, Carmena

et al., 2009, Malumbres and Barbacid, 2007, Taylor and Peters, 2008, Golan et al., 2002). Intriguingly, although Cdk1, Plk1 and Aurora B have discrete roles in mitosis, they also modulate each other's activities, either directly or indirectly, and work together to regulate mitosis (Cuijpers and Vertegaal, 2018). For instance, both Cdk1 and Plk1 phosphorylate APC/C on multiple subunits to allow for full activation of the APC/C E3 ubiquitin ligase activity during mitosis (Golan et al., 2002, Kraft et al., 2003, Fujimitsu et al., 2016, Petronczki et al., 2008). Moreover, Cdk1 can, through targeted phosphorylation, modulate both the activity and localization of both Plk1 and Aurora B kinases during mitosis (Ma and Poon, 2011). Mitotic kinases are essential components of the machinery that controls mitotic progression and understanding their function help shed light on their role in regulating APC/C activity and function during mitosis.

1.8.1 Cdk1-Cyclin B1

Cdk1 is a proline-directed serine-threonine mitotic kinase highly conserved during evolution, first discovered in yeast by Hartwell in a genetic screen aimed at the identification of the principal regulators of cell cycle progression (Hartwell et al., 1973). Cdk1 is responsible for the phosphorylation of numerous mitotic substrates on the conserved consensuses S/T-P-X-K/R (where X corresponds to any amino acid) or S/T-P, and drives the initial stages of mitosis including NEBD, chromosome condensation and the formation of the mitotic spindle, as well as controlling Cdc20 association with the APC/C (Fig. 1.8) (Enserink and Kolodner, 2010, Qian et al., 2015, Fujimitsu et al., 2016, Malumbres and Barbacid, 2005, Holt et al., 2009).

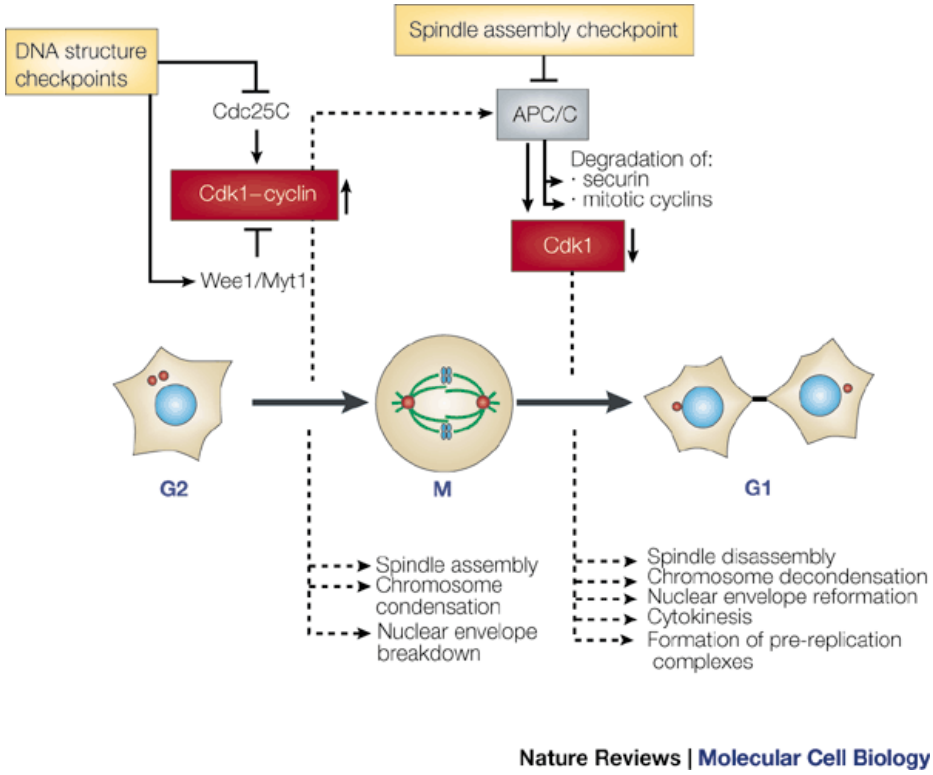

Figure 1. 8: **Role of Cdk1 and its regulation during mitotic progression.** (**G2**) During G2 Cdk1-Cyclin B1 activity is inhibited by the checkpoint kinases Wee1 and Myt2. Plk1-dependent phosphorylation in G2 activates Cdc25 phosphatase, which reactivates Cdk1-Cyclin B1. (**M**) Active Cdk1-Cyclin B1 triggers multiple events during the early stages of mitosis. (**M-G1**) APC/C-dependent degradation of Cyclin B1 inactivates Cdk1 ensuring mitotic exit and passage into G1. See text for further details. Taken from Nigg (2001).

Cdk1-Cyclin B1 complexes are active from the beginning of mitosis until anaphase onset whence APC/C-dependent degradation of Cyclin B1 inhibits its activity to allow for mitotic exit (Clute and Pines, 1999, Enserink and Kolodner, 2010, Ma and Poon, 2011). Activation of Cdk1-Cyclin B1 is achieved through a complex regulatory network: checkpoint kinases Wee1 and Myt2 phosphorylate, and inhibit, Cdk1 activity during G2 to prevent cells from entering into mitosis prematurely (Ma and Poon, 2011, Kataria and Yamano, 2019). Once the G2 DNA damage checkpoint is satisfied, Cdk1-Cyclin B1 complexes translocate from the cytoplasm to the nucleus where Plk1 phosphorylates, and activates the protein phosphatase Cdc25C, so that it can remove the inhibitory phosphorylation signals on Cdk1,

generated by Wee1 and Myt2. The Cdk1-activating kinase is then responsible for activating Cdk1 through phosphorylation (Ma and Poon, 2011, Boutros et al., 2006, Lindqvist et al., 2005, Mailand et al., 2002, Takizawa and Morgan, 2000, Van Vugt et al., 2004, Barr et al., 2004).

Active Cdk1-Cyclin B1 complexes trigger the series of events necessary for the disassembly of the nuclear envelope, for instance, through phosphorylation of the nuclear laminins. Cdk1 activity also contributes to cellular rounding, Golgi fragmentation and DNA condensation, which is achieved through the phosphorylation of the Condensin II complex (Abe et al., 2011, Gavet and Pines, 2010, Nigg, 2001, Litvak et al., 2004). Following its activation, Cdk1-Cyclin B1 complexes accumulate at centrosomes, through Plk1-directed phosphorylation of Cyclin B1; Cdk1-Cyclin B1 participate in spindle formation through the targeted phosphorylation of several proteins, including β-tubulin, which is necessary for the dynamic re-organization of the cytoskeleton (Jackman et al., 2003, Takizawa and Morgan, 2000, Fourest-Lieuvin et al., 2006). Cdk1-Cyclin B1 also localize at kinetochores, where it regulates the attachment of chromosomes to the metaphase plate, as Cdk1-Cyclin B1 depletion at kinetochores has a negative effect on this process (Chen et al., 2008).

1.8.2 Plk1

Initially identified in *Drosophila*, Plk1 is an evolutionary conserved serine-threonine kinase involved in the regulation of multiple mitotic processes, including Cdk1-Cyclin B1 and APC/C activation, centrosome maturation, spindle assembly, kinetochore-microtubule attachment, central spindle organization and cytokinesis (Fig. 1.9) (Sunkel and Glover, 1988, Petronczki et al., 2008, Barr et al., 2004).

Plk1 is activated in G2 by Aurora A and Bora-mediated phosphorylation of Plk1 residue, T210 in its N-terminal Kinase Domain (KD) (Macůrek et al., 2008). Plk1 substrates are characterized by the presence of a common consensus D/E-X-S/T-Φ-X-D/E (Φ-hydrophobic amino acid) (Nakajima et al., 2003). The ability of Plk1 to phosphorylate its substrates depends upon a Polo-box Domain (PBD) present within its C-terminal domain, which functions as a phospho-peptide binding motif (Taylor and Peters, 2008, Jang et al., 2002). As such, Plk1 substrates are primed for Plk1-directed phosphorylation through prior phosphorylation, typically by Cdk1-Cyclin B1, which serves to recruit Plk1 to its substrate (Cuijpers and Vertegaal, 2018, Elia et al., 2003a, Elia et al., 2003b, Neef et al., 2003, Neef et al., 2007, Jang et al., 2002). In this regard Cdk1-Cyclin B1 also has the ability to restrain Plk1 from phosphorylating some substrates until later in mitosis (Elia et al., 2003a, Elia et al., 2003b, Neef et al., 2003, Neef et al., 2007, Jang et al., 2002).

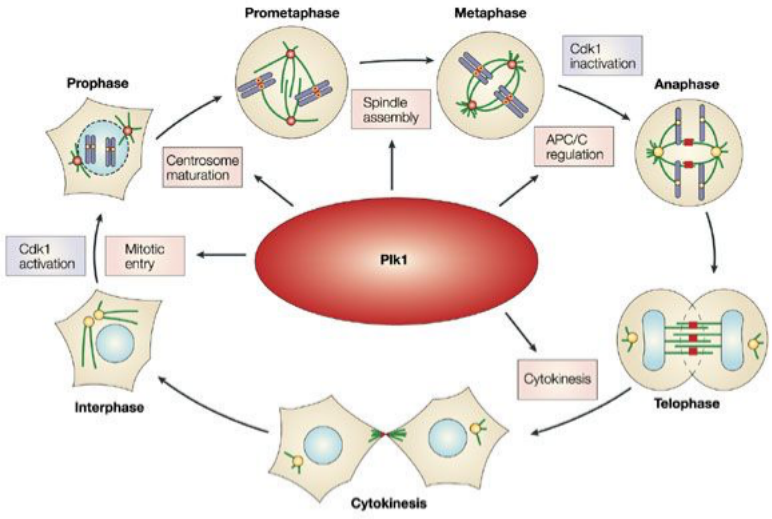

Figure 1. 9: **Role of Plk1 during mitotic progression.** Plk1 accumulates at during early mitosis and contributes to Cdk1 activation during *Prophase*. During *Prometaphase* and *Metaphase* Plk1 accumulates at centrosomes where it participates in Spindle Assembly. Following metaphase-to-anaphase transition it participates in APC/C regulation. From *Anaphase* onwards Plk1 moves in the midzone, where it participates to the regulation of the early stages of *Cytokinesis*. Taken from Barr et al. (2004).

At the beginning of mitosis Plk1 accumulates at the centrosomes, where it contributes to the formation of the mitotic spindle through phosphorylation of γ-tubulin (Casenghi et al., 2003, Casenghi et al., 2005); Plk1 also activates Cdk1 during this time and promotes its localization to centrosomes during prometaphase (Jackman et al., 2003). Moreover, Plk1 is also critical for the centrosomal localization of the APC/C during the initial stages of mitosis, and its activation, as it co-operates with Cdk1-Cyclin B1 to promote Cdc20 recruitment to the APC/C (Kraft et al., 2003, Golan et al., 2002). In this regard Plk1 also phosphorylates the APC/C inhibitor Emi1, allowing for its SCF-dependent poly-ubiquitylation and 26S proteasomal degradation, which is necessary for APC/C re-activation in G2 (Hansen et al., 2004, Moshe et al., 2004).

During early mitosis, Plk1 is found enriched at the kinetochores, where it is recruited through interaction of its PBD with multiple substrates primed by phosphorylation, such as Bub1 and the Chromosome Passenger Complex (CPC) component, Inner Centromeric Protein (INCENP) (Qi et al., 2006, Goto et al., 2006). Interestingly, Plk1 recruitment to kinetochores also relies upon its ability to create its own docking sites and self-regulate its recruitment; for instance, Plk1-dependent phosphorylation of the centromeric protein PBIP1 creates a docking site to facilitate its recruitment to kinetochores (Lee et al., 2008, Kang et al., 2006, Neef et al., 2003, Neef et al., 2007). Plk1 is enriched at unattached kinetochores and ensures the proper attachment of chromosomes to the mitotic spindle as Plk1 inhibition can impair this process (Lénárt et al., 2007). Plk1 also participates in the silencing of the SAC once chromosomes are properly attached to the mitotic spindle, and this involves Plk1-dependent phosphorylation of the protein, p31Comet, which is responsible for freeing Mad2 associated with the MCC complex, and for the disassembly of the MCC in a process that also requires the ATPase, TRIP13 (Kaisari et al., 2019).

Following metaphase-to-anaphase transition, Plk1 translocates to the midzone, where it plays an important role in the organization of the central spindle. Plk1 localization to the midzone is dependent upon its association with the Protein Regulator of Cytokinesis 1 (PRC1), which is inhibited prior to anaphase onset by Cdk1-Cyclin B1-dependent phosphorylation (Barr et al., 2004, Golsteyn et al., 1995). Whilst at the midzone, Plk1 phosphorylates the RhoGEF Ect2, which promotes Ect2 binding with centralspindlin and consequently triggers the activation of the RhoA GTPase responsible for the elongation of the central spindle, the formation of the midbody and cytokinesis (Petronczki et al., 2008, Petronczki et al., 2007, Yüce et al., 2005). Remarkably, this process is also controlled during early mitosis by Cdk1-dependent phosphorylation of Ect2, which prevents its premature phosphorylation by Plk1 (Yüce et al., 2005). During this time Plk1 also activates the protein phosphatase, Cdc14 which promotes the dephosphorylation of Cdh1, and its recruitment to the APC/C to allow the formation of active APC/C-Cdh1 complexes (van Leuken et al., 2009).

During telophase Plk1 translocates to the midbody where it regulates the early stages of cytokinesis. Through the phosphorylation of several substrates, including PRC1 and the Mitotic Kinesin-Like Protein 2 (MKLP2), Plk1 has a pivotal role in the regulation of the early stages of cytokinesis. Indeed, Plk1 inhibition at this stage promotes the disorganization of the central spindles, failure in cleavage furrow ingression, as well as the disruption of its own cellular distribution (Santamaria et al., 2007, Neef et al., 2003). Another partner of Plk1 during cytokinesis is the Golgi protein, Nir2, which is phosphorylated at the beginning of mitosis by Cdk1 to allow for Golgi disassembly. At the end of mitosis, Nir2 localizes at the midbody whereupon it is phosphorylated by Plk1, which is required for the completion of cytokinesis and for the re-assembly of the Golgi apparatus (Litvak et al., 2004).

At the end of mitosis Plk1 is degraded in an APC/C-Cdh1-dependent manner. Interestingly, Plk1 degradation occurs with slower kinetics compared to other late mitotic APC/C substrates such as Aurora A, where degradation starts immediately after anaphase onset. As such, it has been suggested that APC/C-Cdh1 activity might be coordinated by other mechanisms during late mitosis, aimed at controlling the timely degradation of substrates as cells prepare for cytokinesis and abscission. In this regard, a non-degradable Plk1 species contributes to a delay in cytokinesis, suggesting that Plk1 elimination at late times during cytokinesis is important for the completion of the final stage of mitosis (Lindon and Pines, 2004).

1.8.3 Aurora B

First discovered in yeast, Aurora B is a serine-threonine kinase responsible for the phosphorylation of substrates on the R/K-X-T/S-I/L/V consensus (Chan and Botstein, 1993, Cheeseman et al., 2002, Kimura et al., 1997). Together with INCENP, Survivin and Borealin, Aurora B is part of the CPC, and participates in ensuring correct chromosome attachment to the microtubules, sustaining the SAC, correcting chromosome bridges, and for the regulation of processes that control cytokinesis (Fig. 1. 10) (Taylor and Peters, 2008, Petronczki et al., 2007, Maiato et al., 2019, Hauf et al., 2003, D'Avino and Capalbo, 2016, Carmena et al., 2012).

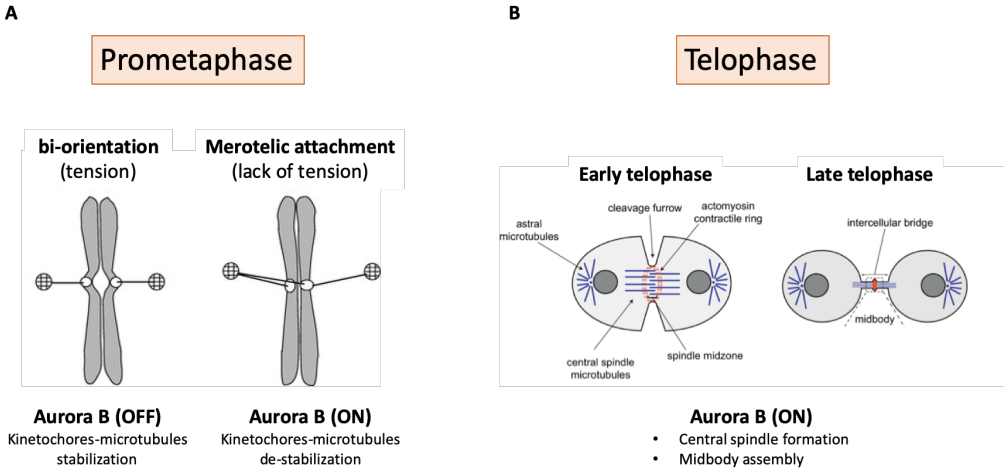

Figure 1. 10: **Aurora B role during mitosis.** (**A**) During *Prometaphase* Aurora B contributes to the destabilization of *Merotelic attachments.* Adapted from Tanaka (2005). (**B**) During *Telophase* Aurora B contributes to the *Central spindle formation* and to the the *Midbody assembly*. Adapted from D'Avino and Capalbo (2016).

Aurora B localizes at centromeres during prometaphase where it is activated through auto-phosphorylation of its T-loop, and trans-phosphorylation of its associated protein INCENP (Ma and Poon, 2011, Krenn and Musacchio, 2015). This process is facilitated by Plk1, which phosphorylates CPC component Survivin directly and primes Aurora B and its substrates for phosphorylation and activation (Rosasco-Nitcher et al., 2008). Aurora B localization at the centromeres also depends upon the kinase, Haspin, which is responsible for the phosphorylation of histone H3-T3 and the recruitment of the CPC through targeting Survivin (Wang et al., 2010, Hindriksen et al., 2017). At the centromeres, Aurora B plays a critical contribution in the maintenance of centromeric cohesion, a process mediated by the proteins Shugoshin (SGO1) and Haspin, which ensures sister chromatid cohesion until their segregation at the metaphase-to-anaphase transition (Ma and Poon, 2011, Dai et al., 2006).

The main role of Aurora B is to correct improper kinetochore-microtubule attachments and to sustain the SAC due through its localization to the inner kinetochores (Krenn and Musacchio, 2015). Proper attachment of chromosomes to the mitotic spindle is controlled

by two pathways: the SAC, which operates generally to promote cellular arrest in the presence of unattached kinetochores; and the Error Correction (EC) system, which operates locally to ensure the correct attachment of chromosomes to the mitotic spindle through the activity of Aurora B (Krenn and Musacchio, 2015, Biggins and Murray, 2001, Tanaka et al., 2002). Aurora B phosphorylates multiple substrates at the outer kinetochores and serves to destabilize merotelic kinetochore-microtubule attachments and stabilize bi-oriented kinetochore-microtubule attachments (Fig. 1.10 A). When chromosomes are bi-oriented, the mechanical tension created allows for a spatial separation between Aurora B and its substrates at the outer kinetochores, impeding Aurora B kinase activity and stabilizing correctly configured kinetochore-microtubule attachments. In contrast, in the absence of bi-orientation the lack of tension allows for Aurora B to phosphorylate its substrates at the outer kinetochore, which leads to the destabilization of the kinetochore-microtubule attachments and the sustainment of the SAC (Liu et al., 2009, Nezi and Musacchio, 2009, Hauf et al., 2003, Musacchio, 2011, Musacchio, 2015).

Following anaphase onset, Aurora B is no longer associated to the centromeres and it translocates to the midzone, where it contributes to the assembly and stabilization of the central spindle (Ma and Poon, 2011, Kelly and Funabiki, 2009, Carmena et al., 2012, Carmena et al., 2009, D'Avino and Capalbo, 2016). This is achieved primarily by Aurora B-directed phosphorylation of Centralspidlin, whose function is also controlled by Plk1. However, whilst Plk1s role is to favour the activation of the RhoA GTPase, Aurora B promotes the formation of the central spindle by inducing the formation of Centralspindlin clusters at the equatorial cortex, which are required for the stabilization of the central spindle (Fig. 1.10 B) (D'Avino and Capalbo, 2016, Minoshima et al., 2003, Ma and Poon, 2011, Petronczki et al., 2007). Aurora B also appears to participate in a novel checkpoint

mechanism occurring between anaphase and telophase, aimed at correcting the presence of chromosomes bridges, and, as such, delays furrow ingression in the presence of DNA within the central spindle. In this regard, the Aurora B-dependent phosphorylation of Cyclin B1 inhibits Cdk1 activity and thus facilitates the disassembly of chromosome bridges (D'Avino and Capalbo, 2016, Steigemann et al., 2009, Maiato et al., 2019). Akin to Plk1, Aurora B is targeted for degradation by the APC/C-Cdh1 during mitotic exit, which ensures the silencing of Aurora B signalling pathway and the progression of cells into G1 (Stewart and Fang, 2005).

1.9 Known functions of APC/C subunit APC5

Together with APC1, APC4 and APC15, APC5 is a component of the APC/C platform domain responsible for bridging the APC/C TPR domain and the catalytic core of the APC/C holoenzyme (Table 1.1) (Alfieri et al., 2017). APC5 is a 755 amino acid protein that, according to structural and bioinformatic analyses, is organized into three main alpha-helix domains: one encompassing residues 1-160, named $APC5^{N}$; the second, comprising residues 206-740, which is characterized by the presence of a conserved TPR motif and is therefore named $APC5^{TPR}$; and the third domain is the C-terminal region. An unstructured loop linker comprising residues 170-205 connects $APC5^{N}$ and $APC5^{TPR}$ and no interface interactions exist between these two APC5 domains, suggesting that the overall APC5 structure is stabilized by contacts with the APC4 subunit (Fig. 1.11 A). Within the APC/C holoenzyme, APC5 occupies a strategical position within the platform domain, which allows for multiple interactions with many other APC/C subunits, namely APC1, APC4, APC15 and APC8. Cryo-EM data suggests that APC15 seems to be essential for the stabilization of the $APC5^{N}$ domain, whereas APC8 functions as a bridge between $APC5^{N}$ and $APC5^{TPR}$, contributing to

the stabilization of the overall APC5 structure together with APC4 (Fig. 1.11 B) (Cronin et al., 2015).

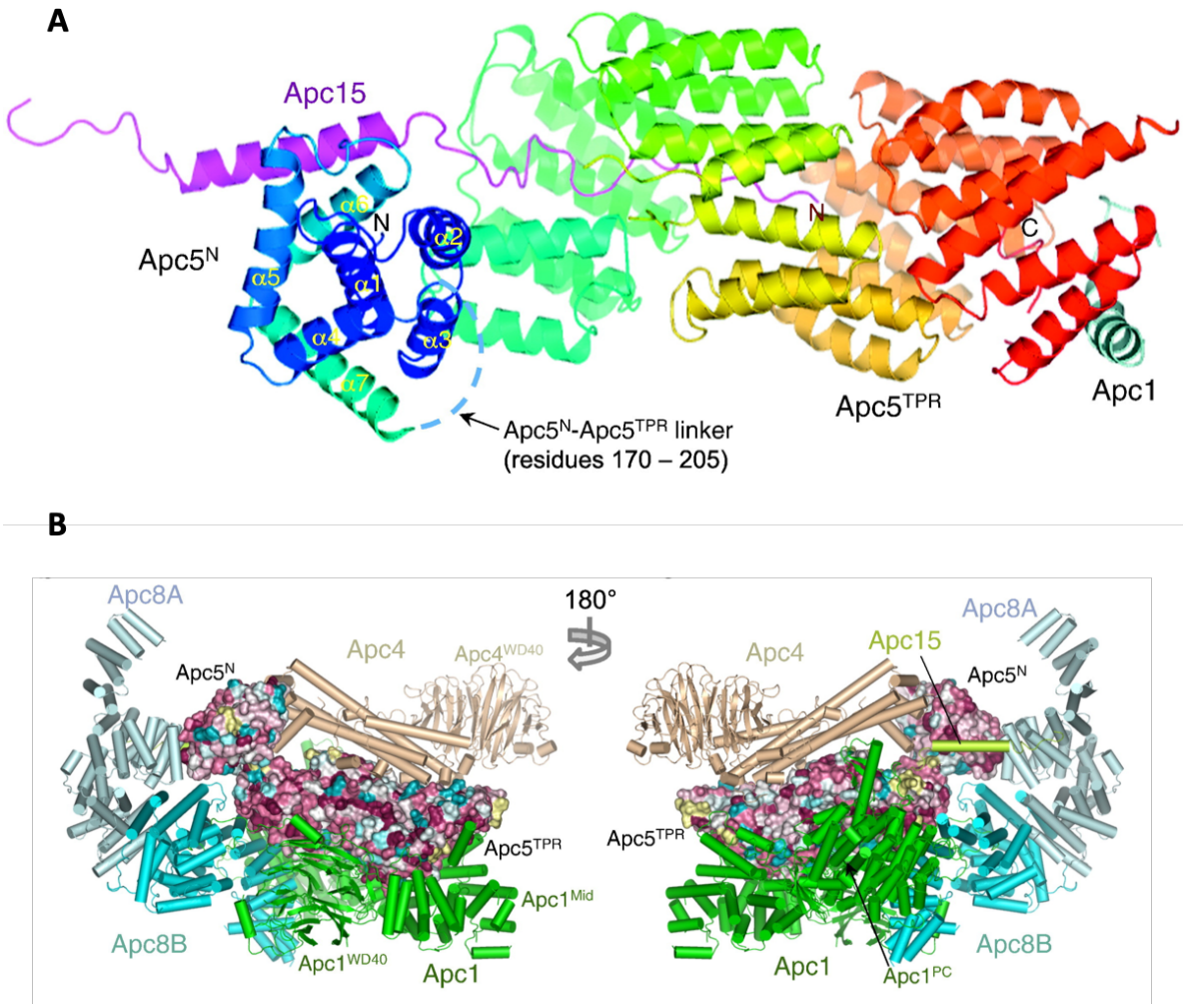

Figure 1. 11: **Structure of the APC/C subunit, APC5.** (**A**) Cartoon of EM structure of human APC5 colour-graded from blue to red from the N- to C-terminus. The small subunit APC15 that contacts APC5 is also shown (**B**) Surface of APC5 color-coded according to conservation (purple, conserved; cyan, unconserved). Contacting subunits APC1, APC4, APC8 and APC15 are also shown. Taken from Cronin et al. (2015).

As detailed earlier conformational changes within the APC/C are deemed critical in the regulation of APC/C E3 ubiquitin ligase activity. As APC5 has multiple intramolecular interactions with other APC/C subunits, conformational changes in APC5 structure are likely

to affect the overall structure of the APC/C that, potentially, could impact on APC/C activity. For instance, the alpha-helix C-terminal region of the APC5 has been predicted to fold back onto the $APC5^{TPR}$ domain, which together with the APC15 helix, creates a cavity within the C-terminus of $APC5^{TPR}$, which allows for the association of the APC/C activator, Cdh1. Given that APC4 is important in modulating the binding affinity of UbcH10 for the APC/C it is likely, given the high number of interactions between APC4 and APC5, that conformational changes occurring within APC5 might impact on UbcH10 interaction with the APC/C (Cronin et al., 2015).

It has been determined that APC5, as well as APC7, can associate with transcriptional co-activators CBP/p300, through protein-protein interaction domains conserved in adenovirus E1A (Turnell et al., 2005). CBP/p300 positively, promote progression through mitosis. As mentioned earlier, APC5 and APC7 are not substrates for CBP/p300-directed acetylation; APC3 is a target for CBP/p300-directed acetylation though how this affects APC/C function is not known. This study also determined that the APC5 and APC7 could stimulate CBP/p300-dependent transcription though the requirement for APC/C E3 ubiquitin ligase activity in this process is not known. It has been suggested that APC5 exists independently of the APC/C holoenzyme, and can participate in cellular processes independent of the APC/C (Turnell et al., 2005, Koloteva-Levine et al., 2004). Remarkably, a yeast three-hybrid screen using Internal Ribosome Entry Site (IRES)-containing mRNAs as bait, identified APC5 as a poly-A binding protein (PABP) protein which, when overexpressed, counteracted the ability of PABP to enhance translation. In this regard, fractionation studies suggested that APC3 did not co-fractionate with APC5-PABP complexes, suggesting a role independent of the APC/C holoenzyme (Koloteva-Levine et al., 2004).

1.10 Project aims

It is becoming increasingly clear that individual APC/C subunits, through protein-protein interactions and PTMs, play a critical role in the temporal regulation of the APC/C during the cell cycle (Zhang et al., 2016, Qiao et al., 2016, Fujimitsu et al., 2016). Despite these recent advances we still know very little about how individual APC/C subunits contribute to the overall function and regulation of the APC/C holoenzyme. With this in mind, the principal aim of the current project was to investigate the roles, and the regulation, of the APC/C platform subunit, APC5, in mitosis. APC5 was chosen for this study, not only because our laboratory has a long-standing interest in this protein, but because it has also clearly been shown to regulate mitosis, though how this is achieved at the molecular level is poorly understood (Alfieri et al., 2016, Neumann et al., 2006). As a starting-point for my studies, unpublished work in our laboratory suggested that APC5 protein levels might be reduced during mitosis.

My initial aims therefore were to investigate this phenomenon and more generally, to establish the precise role of APC5 in mitosis and determine how APC5 function is regulated. As such, the original objectives of the project were as follows:

- To confirm preliminary data that suggested APC5 was destabilized in mitosis.
- To establish the dynamics of APC5 destabilization during mitosis by employing stable FLAG-APC5 WT U2OS FRT clonal cell lines to investigate the stability and regulation of the FLAG-APC5 protein during mitosis and throughout the cell cycle.
- To understand the impact of APC5 mitotic destabilization on APC/C activity at a molecular level.

Intriguingly, by fulfilling our initial objectives, we discovered that the apparent mitotic destabilization of APC5 was not due to changes in the absolute levels of the protein. Instead, we determined that the 'reduction' in the APC5 levels during mitosis was due to an epitope-masking phenomenon, caused by the phosphorylation of APC5 during mitosis, which abrogated completely the binding avidity of a panel of monoclonal antibodies raised against APC5. In the light of this new evidence, and given the known, crucial role of phosphorylation in the regulation of APC/C activity, we decided to investigate this phosphorylation event further. We therefore changed our project aims, which focused on the investigation of APC5 phosphorylation in mitosis and on the role of APC5 phosphorylation in the regulation of APC/C activity. In order to fulfil these aims, we devised a number of new objectives, which were to:

- Identify the phosphorylation site on APC5 responsible for the epitope-masking phenomenon by exploiting the characteristic ability of our panel of monoclonal antibodies not to be able to bind the phosphorylated APC5 species.
- Identify the kinase(s) responsible for APC5 phosphorylation.
- Investigate the dynamics of APC5 phosphorylation in order to define when it occurs during the cell cycle.
- Establish the role of the SAC in the phosphorylation of APC5 during mitosis and moreover, the effect of genotoxic stress on APC5 phosphorylation.
- Determine the effect of APC5 mitotic phosphorylation on the regulation of APC/C activity.
- Investigate the localization of the phosphorylated APC5 species during mitosis.

In this regard, we anticipated that results of our studies into APC5 phosphorylation might provide new molecular insight into the complex mechanisms that regulate APC/C activity throughout the cell cycle, particularly during mitosis.

CHAPTER 2: MATERIALS AND METHODS

2.1 Tissue culture

2.1.1 Cell culture and maintenance

All cell lines employed in this project are listed in Table 2.1. RPE-1, U2OS and HeLa cell lines were maintained in HEPES-buffered Dulbecco's Modified Eagle Medium (DMEM; Sigma-Aldrich) supplemented with 8% v/v Foetal Calf Serum (FCS; Sigma-Aldrich) and 2mM L-glutamine (Sigma-Aldrich). U2OS FRT cell lines produced during the course of this study were maintained in DMEM-HEPES supplemented with 200µg/ml Hygromycin (Gibco). All cell lines used were cultured in a humidified incubator at 37°C, 5% v/v CO_2. For maintenance and propagation cells were washed once in Phosphate Buffer Saline (PBS; Oxoid) and trypsinised with TrypLE express (Life Technologies) at 37°C for 5 min, re-suspended in growth medium, centrifuged for 3 min at 300g at room temperature and seeded onto new dishes at the appropriate dilution. To ensure sterility all procedures were conducted under a Mars Safety Class hood 2 (Scanlaf).

Cell line	Description
RPE-1	human hTERT-immortalized Retinal Pigment Epithelial cells (ATCC number CRL-4000)
HeLa	human adenocarcinoma HPV-18 infected cervical epithelial cells (ATCC number CCL-2)
U2OS	human osteosarcoma (ATCC number HTB96)

U2OS FRT	U2OS cells carrying a FRT recombinant site (Dr. Garry Sedwick, University of Copenhagen)
FLAG-Cdc20 U2OS FRT	U2OS FRT cells expressing FLAG-Cdc20 under the control of a tetracycline-responsive promoter
FLAG-APC5 WT U2OS FRT	U2OS FRT cells expressing FLAG-APC5 WT under the control of a tetracycline-responsive promoter
FLAG-APC5 S195A U2OS FRT	U2OS FRT cells expressing FLAG-APC5 S195A under the control of a tetracycline-responsive promoter
FLAG-APC5 S195D U2OS FRT	U2OS FRT cells expressing FLAG-APC5 S195D under the control of a tetracycline-responsive promoter
FLAG-APC5 T232A U2OS FRT	U2OS FRT cells expressing FLAG-APC5 T232A under the control of a tetracycline-responsive promoter
FLAG-APC5 T232E U2OS FRT	U2OS FRT cells expressing FLAG-APC5 T232E under the control of a tetracycline-responsive promoter

Table 2. 1: **List of cell lines employed during this project**

2.1.2 Synchronization experiments and drug treatments

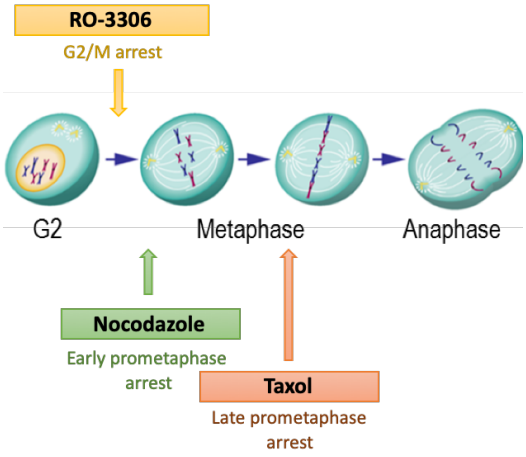

Figure 2. 1**: Synchronization experiments and drugs treatment.** Diagram showing the specific mitotic stage where cells arrest following the different synchronization treatments.

2.1.2.1 Synchronization of cells in mitosis

Synchronization in mitosis was achieved by incubating cells in DMEM-HEPES supplemented with 10µM nocodazole (Sigma-Aldrich) or 10µM taxol (Sigma-Aldrich). Typically, cells were grown on 25cm^2 (T25) or 75cm^2 (T75) sterile flasks; mitotic cells were isolated by mechanical shake-off and centrifugation for 3 min at 300g. Mitotic cells were then released back into the cell cycle after being washed twice with DMEM-HEPES at 37°C and subsequently incubated at 37°C in fresh DMEM-HEPES medium. Cells were then harvested at the appropriate time points post nocodazole/taxol withdrawal. Prior to synchronization U2OS FRT cell lines, carrying the gene of interest, were treated with 200µg/ml Doxycycline for 18h to induce expression of the recombinant gene. As and when needed, 10µM of the 26S proteasome inhibitor, MG132 was added to the cells 30 min following release from nocodazole or taxol treatment, in order to stabilize poly-ubiquitylated proteins as cells progressed through mitosis. All drugs were prepared in water.

2.1.2.2 Synchronization of cells at the G2/M border

Synchronization of cells at the G2/M border was achieved by incubating cells, grown on 6cm^2 or 10cm^2 sterile dishes, in DMEM-HEPES supplemented with 9µM RO-3306 (Sigma-Aldrich) for 18h and then harvested. Prior to synchronization U2OS FRT cell lines, carrying the gene of interest, were treated with 200µg/ml Doxycycline for 18h to induce expression of the recombinant gene. All drugs were prepared in water.

2.1.2.3 Treatment of cells with Reversine

Mitotically-arrested cells obtained by treatment with 10µM nocodazole or taxol were isolated by mechanical shake-off and transferred on to 10cm^2 sterile dishes in the continued presence of the synchronization agent. In order to overcome the SAC, 250nM Reversine (Tebu-bio) was added to the cells for the appropriate time prior to harvesting. As and when needed, 10µM of MG132 was added at the same time as Reversine to allow for the stabilization of poly-ubiquitylated proteins through inhibition of the 26S proteasome. Cells were harvested at the appropriate times post-treatment. All drugs were prepared in water.

2.1.2.4 Induction of cellular genotoxic stress

Genotoxic stress was induced by treatment of cells with 5-FluoroUracil (5-FU, 50µg/ml) or Carboplatin (Carbo-Pt; see legends for concentrations used) for 16h after which time they were harvested. Genotoxic stress was also induced, when appropriate, with UV irradiation at 25J/m^2. Cells were harvested at the appropriate times post-irradiation (see Figure legends for details). All drugs were prepared in water.

2.1.2.5 Inhibition of mitotic kinases

For the mitotic kinase inhibition experiments mitotically-arrested cells obtained by treatment with nocodazole were isolated by mechanical shake-off and transferred to fresh 10cm^2 dishes

in the continued presence of nocodazole. Cdk1 was inhibited by the addition of 9μM RO-3306 (Sigma-Aldrich); Plk1 was inhibited by the addition of 250nM BI-6727 (Cayman Chemical); Aurora B was inhibited by the addition of 10μM Hesperadin (Cayman Chemical). Inhibitors were added to cells alone, or in combination with 10μM 26S proteasome inhibitor, MG132 and harvested at the appropriate time points post-treatment. All drugs were prepared in water.

2.1.3 Generation of U2OS FRT cell lines

To generate clonal U2OS FRT cell lines, cells at 90% confluence on 10cm^2 sterile dishes were transfected with 1.5μg of the appropriate pcDNA5-FRT vector, 13.5μg of the pOG44 vector, that expresses the Flp recombinase necessary for the integration of the exogenous gene at the FRT recombinant site, and 15μl of the transfection reagent, Lipofectamine 2000 (Life Technologies) in the presence of reduced-serum medium, OptiMEM (Life Technologies). 24h post-treatment transfected cells were passaged on to four, fresh 10cm^2 dishes. After a further 48h cells were placed under selection by the addition of DMEM-HEPES supplemented with 200μg/ml Hygromycin B (Life Technologies). Discrete colonies were observed about 2 weeks post-transfection and individual colonies were isolated in sterile conditions using the Nikon eclipse TS100 microscope and seeded on to 24-well plates in the continued presence of DMEM-HEPES supplemented with 200μg/ml Hygromycin B. When cells reached confluency they were transferred onto one 10cm^2 dish that was kept as a stock and two 6cm^2 dishes to test the expression of the integrated gene. One of the two 6cm^2 dishes was subsequently treated with 200μg/ml of Doxycycline whilst the other was used as a non-induced control. 18h post-induction cells were harvested and cell lysates tested for expression of the exogenous gene product by Western blotting.

2.1.4 siRNA transfections

RNA interference was employed to silence the expression of the endogenous APC5 gene. Transfection was performed on cells at 30% confluence in OptiMEM with the transfection reagent, Lipofectamine RNAiMAX (Life Technologies) and 30nM silencing control siRNA (siCTRL) or 30nM siRNA directed towards APC5 (Table 2.2). The transfection mix was prepared by mixing the siRNA construct and the RNAiMAX separately in OptiMEM for 5 min at room temperature. The siRNA construct and Lipofectamine RNAiMAX solutions were then combined and incubated for an additional 30 min at room temperature. Cells were then washed twice with OptiMEM and maintained in OptiMEM. The transfection mix was then added drop-wise to cells which were then incubated for 6h at 37°C, 5% v/v CO_2. The transfection mix was then discarded and replaced with DMEM-HEPES medium.

For nocodazole-release experiments which utilized U2OS FRT cell lines expressing exogenous APC5 constructs, the siRNA transfection was performed 24h before the addition of the nocodazole, whilst Doxycycline induction of the exogenous gene was performed overnight on the same day of the transfection.

Gene	**siRNA construct sequence**
APC5	GCCAAGUGUUUAAACUGUAtt (Ambion)
siCTRL	CGUACGCGGAAUACUUCGAtt (Ambion)

Table 2.2: **siRNA constructs used during this project.** Underlined residues correspond to nucleotides mutated in the FLAG-APC5 species to incur siRNA resistance.

2.2 Protein biochemistry

2.2.1 Cell harvesting

2.2.1.1 Harvesting of whole cell lysates for Western blotting procedures

For preparation of cell lysates for Western blotting adherent cells were washed twice with cold PBS (4°C) and then incubated for 5 min with UTB lysis buffer (9M Urea, 50mM Tris-HCl pH 7.5, 0.15M β-mercaptoethanol) at room temperature. Cell lysates were then collected using a cell scraper and transferred to a clean, non-sterile eppendorf. To obtain lysates from mitotically-arrested cells, cells were isolated by mechanical shake-off and centrifugation at 300g for 3 min, washed twice with cold PBS (4°C) and resuspended in UTB lysis buffer. After harvesting, cells were sonicated using a Misonix Microson Ultrasonic Cell Disrupter on high power (setting 5) for 15 sec, centrifuged at 16200g at 4 °C for 30 min and stored at -80°C until required.

2.2.1.2 Cell harvesting for Immunoprecipitation

For Immunoprecipitation (IP) adherent cells were washed twice with cold PBS (4°C) and lysed in the most appropriate buffer for subsequent procedures (Table 2.3). Cells were typically incubated for 5 min at 4°C in lysis buffer, harvested with a cell scraper and then transferred to a clean, non-sterile eppendorf at 4°C. Mitotically-arrested cells were isolated by mechanical shake-off and centrifugation at 300g for 3 min, washed once with cold PBS (4°C) and resuspended in the most appropriate lysis buffer. All samples were mechanically homogenised using a dounce homogenizer with a tight pestle (Wheaton), centrifuged for 20 min at 16200g at 4°C to precipitate cellular debris, and the supernatant was collected with the use of a small gauge needle to avoid the collection of any lipid layer that accumulated on the surface of the supernatant.

Lysis buffer	Washing buffer
NETN 250mM NaCl 20 mM Tris (pH 7.5), 250 mM NaCl, 25 mM NaF, 25 mM β-glycerophosphate, 1 mM EDTA pH 8.0, 1% v/v Nonidet P-40	**NETN 250mM NaCl**
APC/C lysis buffer 20mM Tris pH 7.5, 100mM NaCl, 20mM β-glycerophosphate, 5mM $MgCl_2$, 0.2% v/v Nonidet P-40, 10% v/v glycerol, 1mM NaF, 0.5mM DTT	**APC/C washing buffer** 20mM Tris pH 7.5, 150mM NaCl, 0.02% v/v Tween 20
HiLo 50mM Tris pH 7.5, 0.825M NaCl, 1% v/v Nonidet-P40	**HiLo**

Table 2. 3: **Lysis buffers employed during this project for immunoprecipitation studies**

2.2.2 Bradford assay for determination of protein concentrations

The protein concentration of harvested cell lysates (as described in Sec. 2.2.1.1 and 2.2.1.2) was determined by comparing the absorbance at 595nm of 4µl of cell lysate with a standard curve generated by measuring the absorbance of 0µg, 5µg, 10µg, 20µg and 30µg of Bovine Serum Albumin (BSA; Sigma-Aldrich) diluted in 1ml of Bradford reagent (Bio-Rad). Absorbance of the samples was measured with a Cecil CE9200 spectrophotometer.

2.2.3 SDS-PAGE

50 µg of total protein was mixed with an equal volume of sample buffer (1 volume 10% v/v SDS: 2 volumes 9 M Urea, 50 mM Tris pH 7.4, 150 mM β -mercaptoethanol), boiled for 5

min at 95ºC and separated on a 10% w/v acrylamide gel (37.5/1 acrylamide/bisacrylamide, 0.1 M Tris-Bicine pH 8.0, 0.1 w/v SDS, 0.3% v/v TEMED [N, N, N', N;-tetramethylethylenediamine], 0.06% ammonium persulphate). The SDS-PAGE (Sodium Dodecyl Sulphate - Polyacrylamide Gel Electrophoresis) was performed overnight using a vertical gel electrophoresis system (Hoefer) in the presence of running buffer (0.1 M Tris, 0.1 M Bicine, 0.1% w/v SDS).

2.2.4 Western blotting procedure and Antibodies

SDS-PAGE gels were transferred to nitrocellulose membranes (PALL) at 280 mA for 6h in transfer buffer (25 M Tris, 192 mM glycine, 20% v/v methanol). The membranes were then blocked in blocking buffer, consisting of TBST (20 mM Tris-HCl pH 7.5, 150 mM NaCl, 0.1% v/v Tween 20) + 5% w/v Milk powder, for at least 45 min. The membranes were cut to the appropriate size and incubated overnight, on a rocker at 4ºC, with the appropriate primary antibody in blocking buffer (Table 2.4). Membranes were then washed with TBST for 30 min and incubated with the appropriate secondary antibody conjugated to Horseradish Peroxidase (HRP; Table 2.4) in blocking buffer for 3h at room temperature. The membranes were then washed 3 times for a total of 45 min and the antibody signal visualized with Immobilon Western Chemiluminescent reagent (Millipore) and X-ray film (Wolf Laboratories). Films were developed using an X-ograph developer.

Antiobody name	Cat.Num	Dilution	Species	Manufacturer
APC3	610455	1:2000	Mouse	BD Transduction Lab
APC4	sc-514895	1:1000	Mouse	Santa-Cruz Biotechnology
APC5 #229 polyclonal	A301-026A	1:500	Rabbit	Bethyl laboratories
APC5#10 monoclonal	-	1:10	Mouse	In house

APC5#22 monoclonal	-	1:10	Mouse	In house
APC5#23 monoclonal	-	1:10	Mouse	In house
APC5#24 monoclonal	-	1:10	Mouse	In house
APC5#33 monoclonal	-	1:2000	Mouse	In house
APC5#38 monoclonal	-	1:10	Rabbit	In house
APC5#4 monoclonal	-	1:2000	Mouse	In house
APC7	-	1:1000	Rabbit	In house
APC8	sc-524006	1:1000	Rabbit	Santa-Cruz Biotechnology
Aurora B	ab-2254	1:2000	Rabbit	Abcam
Bub1	ab-54893	1:1000	Mouse	Abcam
Cdc20	sc-245	1:2000	Mouse	Santa-Cruz Biotechnology
Cyclin A	sc-53227	1:500	Mouse	Santa-Cruz Biotechnology
Cyclin B1	sc-245	1:1000	Mouse	CRUK
FLAG	F3165	1:2000	Mouse	Sigma-Aldrich
Geminin	sc-13015	1:1000	Rabbit	Santa-Cruz Biotechnology
GST	Ab-1	1:500	Rabbit	Oncogene Science
Nek2A	610594	1:2000	Mouse	BD Transduction Lab
p53	DO-1	1:20	Mouse	David Lane
pAPC5 S195	740	1:1000	Rabbit	MRCPPU
pH3 Ser10	9701	1:3000	Rabbit	Cell Signalling
Plk1	sc-17783	1:2000	Mouse	Santa-Cruz Biotechnology
UbcH10	-	1:500	Rabbit	In house
α-Anti-mouse Ig HRP	P0447	1:2000	Goat	Dako

α-Anti-rabbit Ig HRP	P0399	1:3000	Swine	Dako
β-actin	A2228	1:40000	Mouse	Sigma-Aldrich

Table 2. 4: **Antibodies employed for Western blotting procedures during this project**

2.2.5 Immunoprecipitation

An appropriate amount of total protein (see Figure legends for individual experiments) isolated as described in section 2.2.1.2 was incubated, by rotation, overnight at 4°C in the presence of a specific antibody directed towards the protein of interest, or with the same amount of a control IgG derived from the same animal species. Immunocomplexes were then collected on protein G sepharose beads (KPL) by rotation for 3h at 4°C. Immunoprecipitates were then washed 5 times with the appropriate washing buffer (Table 2.3), with a centrifugation step at 16200g following each wash. Immunoprecipitates were then heated at 95ºC in sample buffer, separated by SDS-PAGE (see Sec. 2.2.3) together with 50µg of total protein from whole lysate used as a control, transferred to nitrocellulose and subjected to Western blotting (see Sec. 2.2.4)

2.2.6 λ-phosphatase treatment

λ-phosphatase treatment was performed using the Lambda Protein Phosphatase kit (New England BioLabs) on samples obtained by synchronization with nocodazole and taxol (Sec. 2.1.2.1) and isolated by IP (Sec. 2.2.5) in APC/C lysis buffer (Table 2.3). Following IP, beads were washed with 25mM Tris pH 7.4 before incubation for 1h at 30°C in 30µl of phosphatase buffer (3µl 10X NEBuffer for Protein Metallo Protease (PMP), 3µl of 10mM $MnCl_2$, 23µl nuclease free water) in the presence or absence of 1µl λ-phosphatase enzyme (that was replaced with nuclease free water for control samples). Following λ-phosphatase

treatment samples were separated by SDS-PAGE (see Sec. 2.2.3) and subjected to Western blotting analysis (see Sec. 2.2.4).

2.2.7 Expression and purification of recombinant GST proteins

The corresponding APC5 cDNA sequences to be expressed as a recombinant proteins were first cloned into the pGEX-4T1 vector (Sec. 2.3.1) and validated by Sanger sequencing. Validated clones were then used to transform *E.coli* RIPL codon-plus BL21 cells (Agilent Technologies) that were grown on Luria Broth (LB)-Agar supplemented with ampicillin (100µg/ml), as described in section 2.3.2. Single colonies of transformed bacteria were grown overnight in 25ml LB, supplemented with ampicillin (100µg/ml), by agitation at 220 rpm and 37°C. The following morning bacterial cultures were transferred into 500ml LB containing ampicillin (100µg/ml) and incubated by agitation at 37°C for approximately 3h to an O.D. of 0.6-0.7 at 600nm, after which time the temperature was reduced to 30°C and protein expression was induced 30 min later by the addition of 0.02% w/v isopropyl-β-D-1-thiogalactopyranoside (IPTG), followed by further incubation at 30°C at 220 rpm for 3h. To purify GST-tagged proteins bacteria were first pelleted by centrifugation for 5 min at 5000g at 4°C. BL21 cells were then incubated with GST lysis buffer (1mM EDTA pH 8.0 and 1% v/v Triton-X-100 in PBS), followed by four rounds of high powered sonication with the Misonix Microson Ultrasonic Cell Disrupter for 1 min on ice. The cell lysate was then centrifuged for 10 min at 20000g at 4°C, and the supernatant containing the GST protein of interest were transferred to a clean centrifuge tube. This step was repeated until the lysate became clear and the size of the pellet negligible (typically three centrifugation steps). The clarified lysate was then transferred in to a 50ml tube to which 1ml packed glutathione beads (Sigma-Aldrich) was added and the samples were incubated by rotation overnight at 4°C.

Samples were then centrifuged at 560g for 5 min and the glutathione beads washed three times in the GST lysis buffer, and twice with a wash solution of 1mM EDTA in PBS. The GST protein was eluted from the beads with 25mM glutathione in 50mM Tris pH 8.0 by rotation for 2h at 4°C. Eluted proteins were subject to three rounds of cellulose dialysis (molecular weight cut-off: 12000-14000 Da; Fisherbrand) in buffer containing 25mM Tris pH 8.0, 100mM NaCl, 1mM dithiothreitol and 10% v/v glycerol at 4°C. The concentration of the purified proteins was then calculated using the Bradford assay as described in section 2.2.2 and their purity was assessed by SDS-PAGE (Sec. 2.2.3).

2.3 Molecular biology

2.3.1 Cloning procedure

APC5 was amplified by PCR from a validated APC5 cDNA template (pcDNA5 FLAG-APC5 WT) using the appropriate PCR primers (Table 2.5) designed to incorporate specific restriction enzyme sites. PCR reactions were performed using HotStart Q5 Polymerase (New England BioLabs) in a total volume of 50µl containing: 10-50ng of template DNA, 500nM of the forward and reverse primers, 200µM dNTPs, 5µl 10X buffer and 1 Unit Q5 DNA polymerase (New England BioLabs). PCR reactions were carried out using a 2720 Thermal cycler PCR machine (Applied Biosystems) using the general protocol: 98°C for 30 sec, 25-35 cycles of 95°C for 10 sec, 50-72°C for 30 sec, 30 sec/kb at 72°C, 72°C for 2 min. PCR products were visualized following agarose-gel electrophoresis with SYBR Safe DNA stain. The DNA bands of interest were excised with a scalpel, and purified as described in section 2.3.7.

Next, the purified PCR products and the cloning vectors were subject to restriction enzyme digestion (New England BioLabs) for 3h at 37°C in water bath. Digestion reactions were

performed in a total volume of 50µl containing 500ng-2µg DNA, 5µl of 10X digestion buffer and 25 units of each restriction enzyme. The digested DNA was separated by agarose-gel electrophoresis, visualized with SYBR Safe DNA stain, and bands of interest purified as described in section 2.3.7.

Ligation of amplified DNA (insert) into the vector of choice was performed overnight at 16°C in a total volume of 30µl containing 3µl 10X T4 buffer, 1 unit of T4 DNA ligase, and insert:vector Molar ratios varying from 1:1 to 5:1; reactions were made up to 30µl with nuclease-free water (New England BioLabs). The ligation reaction mix was then incubated for 10 min at 65°C to inactivate the T4 DNA ligase. Library Efficiency DH5α (Invitrogen) competent cells were then added to these mixtures and bacteria transformation performed as described in section 2.3.2.

PCR Primers	**Sequence**
EcoRI APC5 1-400 For	AAGGAGAATTCATGGCCAGCGTCCACGAGAGCCTC
XhoI APC5 1-400 Rev	AAGGACTCGAGCCCAGCAAAAGCTCTCTTGTTGAAC

Table 2. 5: **Primers employed for the cloning of APC5.** Please note that the pcDNA5-FLAG-APC5 WT vector was used as a template to amplify APC5 1-400, and was already available in the laboratory when the project started.

2.3.2 Transformation of bacteria

Different strains of bacteria (Table 2.6) were used for DNA amplification (see Sec. 2.3.3 and 2.3.4). Typically, 100ng of purified plasmid DNA or 5µl of mini-prep plasmid DNA, was added to either 20µl Subcloning efficiency DH5α (Invitrogen), 20µl Library efficiency DH5α, or 20µl MAX efficiency Stbl2 competent (Invitrogen) cells. For QuickChange II site-directed mutagenesis 4µl of the reaction mix was added to 25µl of XL1-Blue supercompetent cells (Agilent Technologies). Plasmid DNA and bacteria were incubated on

ice for 30 min, followed by heat shock in a water bath at 42°C for 1 min, before being placed on ice for an additional 5 min. After this time, 400µl of LB medium (1% w/v NaCl, 1% w/v Tryptone (DIFCO), 0.5% w/v yeast extract (DIFCO)) was added to sub-cloning and library efficiency DH5α; 300µl of SOC medium (Invitrogen) was added to MAX Efficiency Stbl2 competent cells; 400µl of NZY medium (1% w/v NZ amine, 0.5% w/v yeast extract, 0.5% w/v NaCl, 12.3mM $MgSO_4$, 0.4% w/v glucose) was added to XL1-Blue supercompetent cells. Cells were then incubated for 1h in an orbital shaker at 37°C and plated onto LB-agar (1.5% w/v bacto-agar (DIFCO)) plates supplemented with ampicillin (100µg/ml; Sigma-Aldrich). The plates were left to dry at room temperature for 20 min and then transferred to an incubator overnight at 37°C to allow for bacterial growth.

Bacteria strain	**Manufacturer**
Subcloning efficiency DH5α	Invitrogen
Library efficiency DH5α	Invitrogen
MAX Efficiency Stbl2 competent	Invitrogen
XL1-Blue supercompetent	Agilent technologies
BL21-RIPL	Agilent technologies

Table 2. 6: **List of bacteria strains employed during this project**

2.3.3 Mini-prep of plasmid DNA

Following bacterial transformation, individual colonies were picked from LB-agar plates and grown overnight in 5ml LB supplemented with ampicillin (100µg/ml; Sigma-Aldrich), in an orbital shaker at 37°C. The following day bacteria were pelleted by centrifugation at 5000g for 5 min and the DNA purified using the GenElute plasmid mini-prep kit (Sigma-Aldrich). As such, bacteria were resuspended in 200µl of resuspension buffer supplemented

with RNase and lysed by inversion following the addition of 200µl of lysis buffer. After 5 min, 300µl of neutralization buffer was added to each sample which was again mixed by inversion. Lysates were then clarified by centrifugation and loaded onto DNA purification columns that had been washed previously with 500µl column preparation buffer. Columns were then centrifuged for 1 min at 16200g and the flow-through discarded. The columns were then washed successively, by the addition of 500µl of wash optional buffer and 750µl of washing solution containing 70% v/v ethanol and centrifugation at 16200g for 1 min. After the final wash the column was dried by centrifugation at 16200g for 1 min. After this step the column was placed in to a new collection tube and the plasmid DNA was eluted by the addition of 100µl of nuclease-free water and centrifugation at 16200g for 3 min. DNA concentration was quantified using a NanoDrop ND-1000 spectrophotometer (ThermoFisher Scientific) and the ND-1000 spectrophotometer v3.2 software (ThermoFisher Scientific). Samples were stored at -20°C until required.

2.3.4 Maxi-prep of plasmid DNA

For large-scale plasmid DNA preparations individual colonies were picked from LB-agar plates and incubated in 5ml LB supplemented with ampicillin (100µg/ml; Sigma-Aldrich) for 6h at 37°C in an orbital shaker. After this time the bacterial culture was transferred to 250ml LB supplemented with ampicillin (100µg/ml; Sigma-Aldrich) and left to grow overnight at 37°C in an orbital shaker. The following day bacteria were pelleted by centrifugation at 5000g for 10 min at 4°C and plasmid DNA was extracted with the NucleoBond Xtra Maxi kit (Macherey-Nagel). Bacteria were resuspended in 12ml of resuspension buffer supplemented with RNase. Bacteria were lysed by the addition of 12ml of lysis buffer, mixed by inversion, and incubated for 5 min at room temperature. Lysates

were then neutralized by the addition of 12ml of neutralization buffer; tubes were inverted until the cellular debris was precipitated. The samples were then transferred onto DNA purification columns that had been prepared previously by the addition of 25ml EQU solution. After DNA loading onto the columns, the columns were washed with 25ml washing buffer containing 70% v/v ethanol, after which the DNA was eluted upon the addition of 15ml elution buffer. 10.5 ml of isopropanol was then added to each sample to precipitate the plasmid DNA, which was pelleted by centrifugation at 27216g for 30 min and 4°C. Subsequent steps were performed in a sterile cabinet to preserve the sterility of the DNA. Precipitated DNA was washed twice with 1ml of 70% v/v ethanol. The DNA pellet was then left to air-dry for 15 min and an appropriate amount of nuclease-free water was then added to the samples. After hydration the DNA concentration was measured with a NanoDrop ND-1000 spectrophotometer (ThermoFisher Scientific) and the ND-1000 spectrophotometer v3.2 software (ThermoFisher Scientific).

2.3.5 Site-directed mutagenesis

Site-directed mutagenesis was performed on pcDNA5 FLAG-APC5 WT and pGEX-4T1 APC5 1-400 templates using the Quick-Change II Site-directed mutagenesis kit (Agilent Technologies) in a PCR reaction using the primers listed in Table 2.7. The PCR reaction was performed in a total volume of 50µl containing: 5µl of 10X reaction buffer, 10ng of DNA template, 500nM of forward and reverse primers, 200µM of dNTPs, 2.5 U/µl of Pfu Ultra DNA polymerase (Agilent Technologies) and nuclease-free water up to the required volume. PCR reactions were carried out using a 2720 Thermal cycler PCR machine (Applied Biosystems) using the following parameters: 95°C for 1 min, 18 cycles of 95°C for 50 sec, 60°C for 50 sec, 1min/kb at 68°C, 68°C for 9 min. Amplified DNA was then subjected to digestion with the restriction enzyme, Dpn1 (10U/µl) for 1h at 37°C in water bath. 4µl of

DNA was then added to 25µl of XL1-Blue supercompetent cells (Agilent Technologies) and the bacterial transformation was performed as described in section 2.3.2. Individual colonies were selected and mini-prep plasmid DNA purified as described in section 2.3.2. Sanger sequencing, as described in section 2.3.6 was used to validate the incorporation of the desired mutations.

Mutagenic primer	**Sequence**
APC5 S195A For	GAAGAACTTGATGTAGCTGTAAGAGAAGAGGAGG
APC5 S195 Rev	CCTCCTCTTCTCTTACAGCTACATCAAGTTCTTC
APC5 S195D For	GAAGAACTTGATGTAGATGTAAGAGAAGAGGAGG
APC5 S195D Rev	CCTCCTCTTCTCTTACATCTACATCAAGTTCTTC
APC5 S221D For	CTTTCTCAACAGGCTGATTTGCTAAAGAATGATG
APC5 S221D Rev	CATCATTCTTTAGCAAATCAGCCTGTTGAGAAAC
APC5 T232A For	GATGAGACTAAGGCCCTCGCTCCAGCTTCCTTGCAGAAG
APC5 T232A Rev	CTTCTGCAAGGAAGCTGGAGCGAGGGCCTTAGTCTCATC
APC5 T232E For	GATGAGACTAAGGCCCTCGAACCAGCTTCCTTGCAGAAG
APC5 T232E Rev	CTTCTGCAAGGAAGCTGGTTGAGGGCCTTAGTCTCATC

Table 2. 7: **List of primers for mutagenesis that were employed during this project.** All primers were produced by Sigma-Aldrich.

2.3.6 DNA sequencing

Sequencing reactions were performed by PCR in a volume of 20µl using the following method: 25 cycles of 96°C for 10s, 55°C for 5s, and 60°C for 4min. The sequencing reaction was: 10ng/µl sequencing primer (Table 2.8), 4µl 5x sequencing buffer, 1µl Big Dye Terminator (Applied Biosystems), 5µl of mini-prep DNA and nuclease-free water up to the required volume. After PCR, the DNA was precipitated, on ice for 30 min, by the addition

of 62.5µl absolute ethanol, 3µl 3 M Sodium Acetate, and 14.5µl nuclease-free water. Precipitated DNA was pelleted by centrifugation for 20 min at 16200g and washed twice with 100µl 70% v/v ethanol. After ethanol washes DNA was air-dried and re-suspended in 11µl HiDi and heated at 100°C for 5 min. DNA sequences were obtained using a 3500xl Genetic Analyser (Applied Biosystems) and analysed with BLAST (NCBI, NIH).

Sequencing Primers	Sequence
APC5 seq2 (1023) For	AGATACGCCGCTCTGAATCTTGCC
APC5 seq3 (1473) For	CTGGAGGCGGTGAATGCGGGCGTG
APC5 seq4 (1923) For	CTGCCCATGCTCCTGCAGGCTCTG
APC5 seq5 (677) For	AAAAATGGAAAAAGAAGAACTTGA
APC5 seq6 (671) For	TGAAAGAAAAATGGAAAAAGAAGA
APC5 seq7 (1707) For	ACGATTTCCGCCTAATAGTCAGCA
APC5 seq357 For	TACAAGTTAATTGAAGAGTCTTGT
pcDNA5 TO For	CGCAAATGGGCGGTAGGCGTG

Table 2. 8: **List of sequencing primers used during this project.** All primers were produced by Sigma-Aldrich.

2.3.7 Agarose-gel electrophoresis and DNA gel extraction

Agarose-gel electrophoresis was typically performed on a 0.8% w/v agarose (electrophoresis grade, Invitrogen) gel in 60ml of TBE (100mM Tris, 100mM boric acid, 2mM EDTA pH 8.3) in the presence of 1.5µl SYBR Safe (Life Technologies). Prior to loading, DNA was mixed with 6X gel-loading buffer (30% v/v glycerol, 0.25% w/v bromophenol blue and 0.25% w/v xylene cyanol FF). Gels were typically run at 60V for 45 min in 1X TBE. Gels were visualized with a Safe Imager (Invitrogen) and DNA gel extraction was performed with a QIAquick Gel extraction kit (Qiagen).

Individual bands of the correct size were excised from the agarose gel and then solubilised by the addition of 600µl of buffer QG at 55°C for 10 min. 200µl of isopropanol was then added to the solution, which was mixed by inversion, before being transferred to a QIAquick column and centrifuged for 1min at 16200g. The flow through was discarded and the column was washed with 500µl of QG buffer by centrifugation at 16200g for 1 min. The column was then washed with PE buffer by centrifugation at 16200g for 1 min. The column was then dried by centrifugation at 16200g for 1 min, and the DNA was eluted by centrifugation at 16200g for 2 min with 50µl of nuclease-free water.

2.4 Microscopy

2.4.1 Immunofluorescence

For immunofluorescence cells from a 10cm^2 dish were seeded onto multispot microscope glass slides (Hendley Ltd) at 20% density, as described in section 2.1.1. After 48h incubation the slides were washed with PBS before being fixed and permeabilised by incubation with methanol at -20°C for 15 min. Slides were then left to air-dry at room temperature and then blocked with heat inactivated normal goat serum (HINGS; 20% v/v HINGS, 0.2% w/v BSA in PBS) for 45 min at room temperature. Slides were washed in PBS and then incubated for 2h at room temperature with the appropriate primary antibodies diluted in blocking buffer (Table 2.9). Following the primary incubation, slides were washed twice with PBS for 15 min, and then incubated with the specific fluorophore-conjugated secondary antibodies (Table 2.9). Following incubation with the secondary antibodies, the slides were washed three times in PBS for 15 min and then air-dried. Slides were mounted in Vectashield (Vector Laboratories) containing DAPI (4',6-diamidino-2-phenylindole) and visualized either with

the Nikon Y-FL epi-fluorescence microscope or with the Zeiss LSM780 confocal microscope.

Antibody name	Cat.Num	Dilution	Species	Manufacturer
γ–tubulin	T6557	1:2000	Mouse	Sigma-Aldrich
pAPC5 S195	740	1:50	Rabbit	MRCPPU
Plk1	sc-17783	1:50	Mouse	Santa-Cruz
PRC1	sc-376983	1:50	Mouse	Santa-Cruz
α-mouse Alexa Fluor 594	A21203	1:100	Donkey	Life Technologies
α-rabbit Alexa Fluor 488	A21206	1:100	Donkey	Life Technologies
α-tubulin	T5168	1:2000	Mouse	Sigma-Aldrich

Table 2. 9: **List of antibodies used for immunofluorescence microscopy during this project**

2.4.2 Live cell imaging

For live cell imaging experiments one confluent 10cm^2 dish was plated onto 12-well plates at a density of 10% for siRNA transfection followed by DNA transfection experiments, and 20% solely for siRNA transfection experiments. The following day the siRNA transfection was performed as described in section 2.1.4 with a transfection mix containing 0.5µl RNAiMAX (Life Technologies), and 30nM of siCTRL or siAPC5 (Table 2.2) in a total volume of 100µl OptiMEM (Life Technologies). The day after siRNA transfection cells were incubated in the presence of 500mM SiR-DNA (Spirochrome) in DMEM-HEPES for at least 1h before starting the imaging data collection.

Images were captured using a Cell-IQ system (CM Technologies) equipped with phase and fluorescence modules using a 10X objective. Plates were housed within a chamber at a

controlled temperature of 37°C, 5% v/v CO_2. Images of the selected regions of interest on the plate were acquired every 3 min for at least 20h. Images were then processed to remove background fluorescence, using the appropriate software, before being exported as Windows media files (Cell-IQ Analyzer version 4.4.0). Cell counting was performed manually with the aid of the Cell Counter plugin in ImageJ Fiji (Schindelin et al., 2012) and statistical analyses was performed in R Studio using the Wilcoxon test function, which performs a non-parametric test for comparison of non-normally distributed samples based on their median values.

CHAPTER 3: IDENTIFICATION OF APC5 S195 AS A TARGET FOR PHOSPHORYLATION DURING MITOSIS

3.1 Introduction

APC5 is a 755 amino acid protein, which together with APC1, APC4 and APC15, constitutes the platform domain of the APC/C (Sivakumar and Gorbsky, 2015, Cronin et al., 2015, Alfieri et al., 2017, Watson et al., 2018). It is established that conformational changes that occur within the APC/C platform domain affect greatly the overall structure and function of the APC/C holoenzyme (Zhang et al., 2016, Fujimitsu et al., 2016). As such, phosphorylation of the APC3 and APC1 subunits by Cdk1-Cyclin B1 modifies APC/C structure, which is critical for the formation of an active APC/C-Cdc20 complex during mitosis (Zhang et al., 2016, Alfieri et al., 2016). Indeed, structural analyses conducted by the Barford laboratory have revealed the existence of an APC1 'inhibitory' helix that occupies the Cdc20-interacting site on the APC/C and inhibits APC/C activation until entry in to mitosis (Zhang et al., 2016). When Cdk1 becomes active through its association with Cyclin B1 at the beginning of mitosis, phosphorylation of APC3 and APC1 allows for the displacement of this APC1 'inhibitory' helix from the Cdc20-interaction site and allowing the formation of active APC/C-Cdc20 complexes responsible for the degradation of early APC/C mitotic substrates. Conformational changes within the APC/C platform domain have also been shown to occur following the association/dissociation of the MCC inhibitory complex with/from the APC/C, revealing the importance of the APC/C platform in the overall regulation of APC/C activity (Alfieri et al., 2016). APC15 helix dislocation has also been reported to be critical during metaphase for the dissociation of the MCC complex from the APC/C and for Cdc20 auto-ubiquitylation which is required to activate the APC/C after the

SAC has been satisfied (Lara-Gonzalez et al., 2012, Sivakumar and Gorbsky, 2015, Reddy et al., 2007, Kataria and Yamano, 2019, Mansfeld et al., 2011, Uzunova et al., 2012).

Interestingly, structural analysis of the APC/C in association with the SAC effector-MCC complex has revealed that APC5 conformational changes occur during mitosis concomitantly with the switching of the APC/C structure into its active form (Alfieri et al., 2016). As such, APC5 stability and PTM during mitosis could participate to the complex events aimed at regulating APC/C activity during mitosis. As such, the principal aim of this Chapter was to begin to investigate the function, and regulation, of APC5 in mitosis.

3.2 APC5 protein levels in mitosis

3.2.1 APC5 levels are reduced following nocodazole release in RPE-1 cells

Previous unpublished data from our laboratory suggested that APC5 protein levels are reduced during mitosis in HeLa cells. To validate these findings, we performed a nocodazole-release experiment using RPE-1 cells synchronized in mitosis through treatment with nocodazole, a spindle poison that, by impeding microtubule polymerization, activates a SAC-dependent cellular mitotic arrest and accumulation of APC/C substrates, such as Cyclin B1. Mitotically-arrested cells were collected by mechanical shake-off and released from mitotic-block through withdrawal of nocodazole and harvested at different time-points to track their progression and exit from mitosis. We then employed Western blotting analyses to assess the protein levels of various APC/C subunits and substrates in asynchronous cells and throughout mitosis (Fig. 3.1).

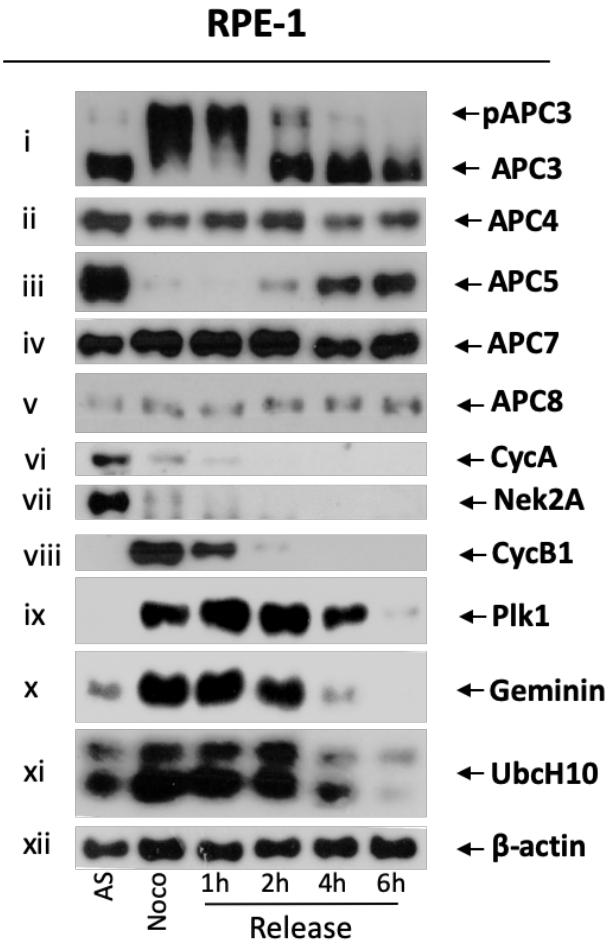

Figure 3. 1: **APC5 protein levels are reduced during mitosis.** Cell lysates from RPE-1 asynchronous cells (AS), nocodazole-arrested cells (Noco) and cells released from the mitotic arrest at different time-points (1h, 2h, 4h and 6h) were harvested in UTB lysis buffer. 50µg of total protein was separated by SDS-PAGE, transferred to a nitrocellulose membrane and the levels of various APC/C subunits, UbcH10 and APC/C mitotic substrates were determined by Western blotting. The levels of β-actin were used as a loading control. This data is representative of three individual experiments.

No significant alterations in the protein levels of the APC/C subunits APC4, APC7 and APC8 occurred during the time-course of the experiment (panel ii, iv and v, Fig. 3.1). A predominant, higher molecular weight band of APC3 was observed in mitotically-arrested cells compared to asynchronous cells, indicative of APC3 mitotic phosphorylation and well known hallmark for mitosis, which was reduced as cells exited mitosis and re-entered G1 (panel i, Fig. 3.1). Nocodazole treatment also promoted the accumulation of the APC/C

substrates, Cyclin B1, Plk1 and Geminin, relative to asynchronous cells, consistent with the SAC-dependent inhibition of the APC/C during prometaphase (panel viii, ix and x, Fig. 3.1). Upon SAC satisfaction following nocodazole withdrawal and activation of the APC/C-Cdc20 complex, Cyclin B1 levels were reduced dramatically and was completely degraded 2h following nocodazole release, indicative of mitotic exit. Protein levels of the APC/C-Cdh1 late mitotic substrates, Plk1 and Geminin, were also reduced following the release from the mitotic arrest and completely disappeared after 6h (panel ix and x, Fig. 3.1). In contrast, the protein levels of the SAC-insensitive APC/C substrates Nek2A and Cyclin A were already very low in nocodazole-treated cells, due to their ability to bind directly to the APC/C independently of the SAC activation status (panel vii and viii, Fig. 3.1). Interestingly, APC5 protein levels were also very low in mitotically-arrested cells compared to asynchronous cells and they were not restored until 4h following nocodazole-release (panel iii, Fig. 3.1). As such, APC5 protein levels appeared to mirror the pattern observed for the APC/C SAC-insensitive substrates Nek2A and Cyclin A, suggesting that APC5 might be degraded during the early stages of mitosis. Intriguingly, as APC5 protein levels started to reappear 4h post-release which is concomitant with the disappearance of an APC/C-Cdc20 active complex, the alterations in the levels of APC5 observed might suggest that APC5 is degraded during the early stage of mitosis in a SAC-independent APC/C-Cdc20-dependent fashion. Interestingly, after 4h release the levels of the APC/C E2 enzyme UbcH10 were also reduced compared to their levels in mitotically-arrested cells and the early stages of the nocodazole withdrawal (panel xi, Fig. 3.1). Taken together, the results of this experiment confirmed the previous findings from our laboratory suggesting that APC5 protein levels are reduced in mitosis.

3.2.2 APC5 levels are reduced independently of the SAC in mitosis

To investigate the timing of APC5 protein loss further, we decided to synchronize RPE1 and U2OS cells at various stages of mitosis using different drugs. Cells were thus arrested at the G2/M border by treatment with RO-3306, which by inhibiting Cdk1 activity mimics the G2/M checkpoint normally triggered in response to DNA damage (Vassilev, 2006, O'Connell et al., 2000). Cells were also arrested during the early stages of mitosis by treatment with nocodazole, which as previously indicated causes cells to arrest during prophase by impeding microtubule polymerization (Sec. 3.2.1). Mitotically-arrested cells were also obtained by treatment with taxol, which by impeding microtubule de-polymerization promotes cellular arrest throughout mitosis. Following these treatments, we harvested and quantified protein cell lysates and subjected them to Western blotting analyses to measure the levels APC5, as well as the levels of APC3 and known APC/C substrates Nek2A and Cyclin B1 (Fig. 3.2 A and B).

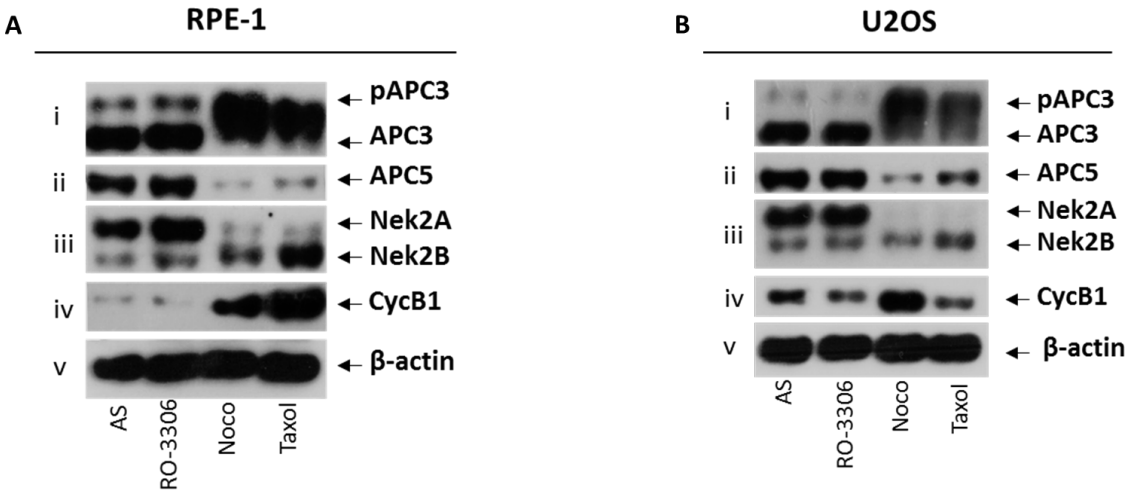

Figure 3. 2: **APC5 levels are reduced in mitosis in a SAC-independent manner.** Lysates from Asynchronous (AS), G2/M-arrested (RO-3306) and mitotically-arrested (Noco/Taxol) RPE-1 (**A**) and U2OS (**B**) cells were harvested in UTB Lysis Buffer. 50µg of total protein was separated by SDS-PAGE, transferred to a nitrocellulose membrane and the level of various APC/C subunits and substrates were detected by Western blotting. The levels of β-actin were used as a loading control. These data are representative of three individual experiments.

Consistent with our previous findings, a higher molecular weight band corresponding to phosphorylated APC3 appeared in mitotically-arrested cells, while in asynchronous and G2/M-arrested cells the major band was represented by the faster migrating, un-phosphorylated, form of APC3 (panel i, Fig. 3.2). For both cell lines the levels of Nek2A were reduced dramatically in mitotically-arrested cells compared to asynchronous and G2/M-arrested cells, consistent with its SAC-insensitive, APC/C-dependent, degradation (panel iii, Fig. 3.2). APC5 protein levels were also reduced considerably in mitotically-arrested cells compared to asynchronous cells, mimicking the destabilization pattern observed for the SAC-insensitive APC/C substrate Nek2A (panel ii, Fig. 3.2). Interestingly, no alterations in the levels of APC5 were observed in cells arrested at the G2/M border in comparison to asynchronous cells, indicating that the apparent destabilization of APC5 occurs specifically in mitosis (cf lane 1 and 2, panel ii, Fig. 3.2). Consistent with the SAC-dependent inhibition of the APC/C during prophase in the presence of a disrupted spindle, Cyclin B1 levels accumulated in mitotically-arrested cells compared to asynchronous and G2/M-arrested cells (panel iv, Fig. 3.2). However, the protein levels of Cyclin B1 were lower in taxol-treated U2OS cells than in RPE-1 cells, which interestingly mirrors the levels of APC5 in taxol-arrested U2OS cells, which could reflect the different sensitivities of these cell lines to taxol treatment (cf panel iv, Fig. 3.2 A and B). Overall, these data suggest that APC5 protein levels are reduced specifically in mitosis. As such, our findings suggest that APC5 might be degraded early in mitosis, independently of the SAC.

3.2.3 APC5 interaction with APC/C holoenzyme is ablated in mitosis

The data presented so far suggests that APC5 might be degraded during mitosis in a manner akin to the SAC-insensitive substrates, Nek2A and Cyclin A. However, as APC5 has been shown previously to play various roles independent of the APC/C holoenzyme, we

questioned whether the APC5 mitotic destabilization correlated positively the amount of APC5 present in the APC/C complex. To answer this question we conducted an APC3 co-IP assay using RPE-1 and U2OS cells synchronized with RO-3306, nocodazole or taxol (Fig. 3.3 A and B). Following cell cycle synchronization, cell lysates from RPE-1 and U2OS were incubated with an anti-APC3 specific antibody (α-APC3) or a control IgG (α-IgG) and following antibody collection upon Protein G Sepharose and separation by SDS-PAGE, Western blotting was employed to determine the levels of APC5 association with APC3, and hence the APC/C holoenzyme (panel iv, Fig. 3.3 A and B). For comparative purposes the ability of APC3 to associate with other APC/C subunits and Cdc20 was also determined (panel ii, iii and v, Fig. 3.3 A and B).

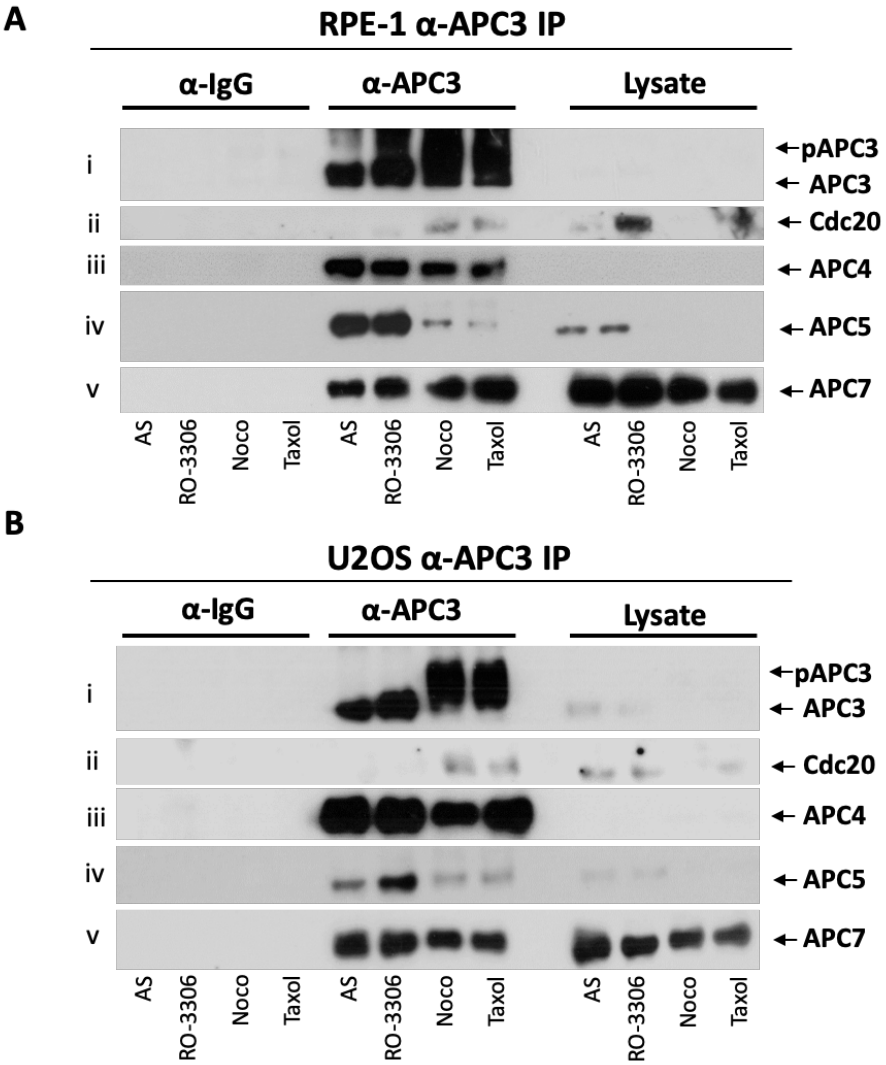

Figure 3. 3: **APC5 does not appear to be part of the APC/C holoenzyme during mitosis.** Lysates from Asynchronous (AS), G2/M-arrested (RO-3306) and mitotically-arrested (Noco/Taxol) RPE-1 (**A**) and U2OS (**B**) cells were obtained by incubation in NETN Lysis Buffer. 1.4 mg of total protein from RPE-1 cells (**A**) and 1.2mg of total protein from U2OS cells (**B**) were incubated overnight at 4°C with an APC3 specific antibody (α-APC3) or with normal mouse IgG (α-IgG) followed by 3h incubation at 4°C with Protein G Sepharose beads. Immunoprecipitated proteins and 50μg of total protein lysate were separated by SDS-PAGE, transferred to a nitrocellulose membrane and the levels of various APC/C subunits and Cdc20 were detected by Western blotting. These data are representative of three individual experiments.

As expected, the APC3-Cdc20 interaction occurred specifically in mitotically-arrested cells and was not detected in asynchronous, or in G2/M-arrested cells (panel ii, Fig 3.3 A and B). The ability of APC3 to interact with the APC/C subunits APC4 and APC7 was the same

under each condition tested (panel iii and v, Fig. 3.3 A and B). In contrast, in both RPE-1 and U2OS cell lines APC5 interaction with APC3 appeared to be reduced substantially in mitotically-arrested cells compared to asynchronous and G2/M-arrested cells (cf lane 5 and 6 with lane 7 and 8, panel iv, Fig. 3.3 A and B), suggesting that APC5 degradation is responsible for its dissociation from the APC/C holoenzyme during the early stages of mitosis. Overall, these results provide evidence that APC5 might be destabilized during mitosis and suggest, therefore, that APC5 might not be required for the APC/C-Cdc20 activity during the early stages of mitosis. As such, APC5 mitotic destabilization might represent a novel level of regulation of the APC/C holoenzyme occurring through direct ablation of one of its platform domain subunits.

3.3 APC5 as a potential APC/C substrate

Our data so far suggests that APC5 might be degraded early in mitosis in a similar manner to APC/C SAC-insensitive substrates. As the APC/C is the major regulator of protein stability during mitosis we reasoned that APC5 mitotic destabilization could be dependent upon APC/C mitotic activity.

3.3.1 APC5 protein sequence contains three conserved D-boxes

APC/C substrates are categorized by the presence of characteristic degron motifs within their primary sequence, such as D-boxes and KEN boxes, which are responsible for their APC/C-dependent degradation (Davey and Morgan, 2016). To consider the possibility that APC5 is an APC/C substrate, we performed an *in silico* analysis of the APC5 protein sequence with GPS-ARM 2.0, a software program that allows the detection of APC/C degrons (Liu et al., 2012). Those analyses led to the identification of three highly conserved potential minimal

D-boxes at positions: 54-57, 96-99 and 280-283 within APC5's primary sequence (Fig. 3.4 A and B).

A

Position	Peptide	Type
54-57	LME RRRL NQL	D-box
96-99	VQI RIKL MAE	D-box
280-283	YFD RLIL TGA	D-box

B

	D-box 54-57	D-box 96-99	D-box 280-283
APC5_HUMAN	LMERRRLNQLLLPLLQGP	SVQIRIKLMAEGELKDMEQ	SLLHYFDRLILTGAESKSNG
APC5_MOUSE	LVERRKLNQLLLPLLQGP	SVQIRIKLMAEGELKDMEQ	SLLHYFDRLILTGAEGKSNG
APC5_RAT	LVERRKLNQLLLPLLQGP	SVQIRIKLMAEGELKDLEQ	SLLHYFDRLILTGAEGKSNG
Q7ZVQ0_DANRE	LLDRRRLNKLILPLQQGP	AVKLRLFLMADGELQDMEH	SLLHYFDRLILSGAEGKSNG
Q0IH16_XENLA	LVEKRRLNKQILPLLQGP	SVHIRIKLMAEGELKDMEQ	SLLHYFDRLILTGAESKSNG
Q8TA45_DROME	TQRRRMFYMLVFKLIQEQ	AL------FDFSEIQNI--	ALHRALDRSPVRL----MS-
APC5_YEAST	TA---VFLRLISPTRPSL	ALTLMGYLEAINGLDSINR	SLHNYFDYKSTGN-------
APC5_SCHPO	-----PFLDLVLGYFNPN	LL--HERLWSLHSFEDIHE	NLCRYFDHIMHSD-------

Figure 3. 4: **APC5 primary sequence contains three D-boxes.** (**A**) Identification of APC5 D-boxes by GPS-Arm 2.0. (**B**) Clustal Omega multiple alignment of APC5 showing the conservation of the three D-boxes amongst different species.

3.3.2 APC5 protein levels are destabilized following Cdc20 overexpression

To ascertain a requirement for the APC/C in the potential mitotic destabilization of APC5, we decided to employ a U2OS FRT Doxycycline-inducible clonal cell line overexpressing FLAG-Cdc20 that was developed during the course of these studies (see Sec. 2.1.3, Chapter 2). Overexpression of the APC/C coactivator Cdc20 has been shown to be responsible for APC/C hyperactivation, premature degradation of APC/C substrates and uncontrolled progression through mitosis in many cancer types (Lehman et al., 2007, Wang et al., 2018, Wu et al., 2019). For our purposes we performed a nocodazole-release experiment (Fig. 3.5) either in presence (+ 200μg/ml Dox) or absence (-Dox) of overexpressed FLAG-Cdc20 and employed Western blotting to determine the levels of APC5, as well as other APC/C subunits and substrates (Fig. 3.5).

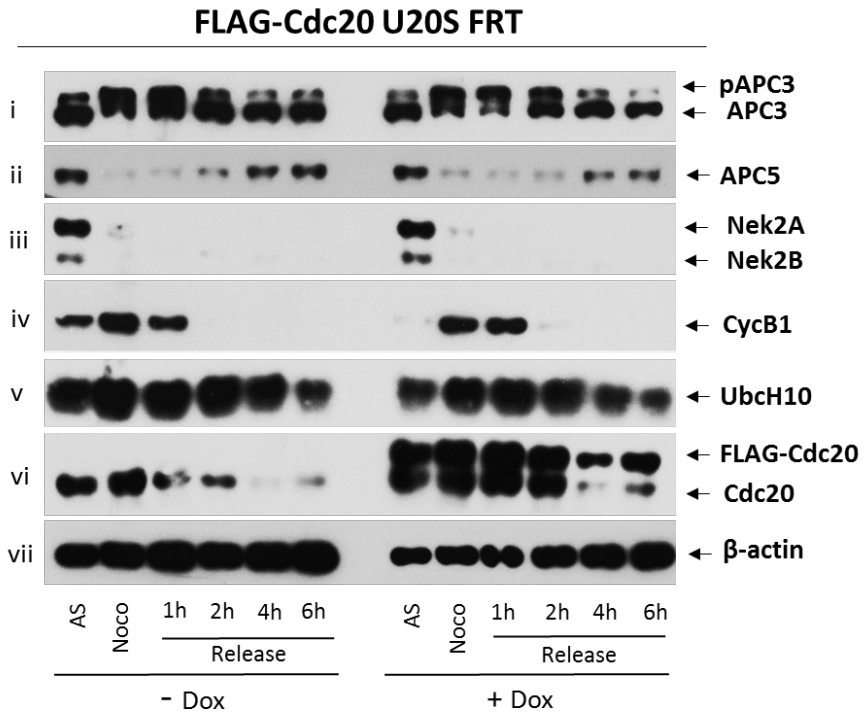

Figure 3. 5: **Effects of Cdc20 overexpression on APC5 protein levels.** Cell lysates from FLAG-Cdc20 U2OS FRT asynchronous cells (AS), nocodazole-arrested cells (Noco) and cells released from the mitotic arrest at different time points (1h, 2h, 4h and 6h) both in presence (+Dox) or absence (-Dox) of Doxycycline, and harvested in UTB Lysis Buffer. 50μg of total protein was separated by SDS-PAGE, transferred to a nitrocellulose membrane and the levels of various APC/C subunits, UbcH10, Cdc20 and APC/C mitotic substrates were determined by Western blotting. The levels of β-actin were used as a loading control. These data are representative of three individual experiments.

As expected, the results of this experiment showed that Cdc20 overexpression strongly affected APC/C activation causing premature degradation of Cyclin B1 and UbcH10 proteins in asynchronous cells, compared to control cells (panel iv and v, Fig. 3.5). However, no significant differences where observed in the levels of Nek2A under the same conditions, possibly because Nek2A might require appropriate PTM to be degraded (panel iii, Fig. 3.5). Interestingly, APC5 levels were reduced in the presence of overexpressed FLAG-Cdc20 in the nocodazole-release experiment, notably at late-times post-release, suggesting that APC5 could be an APC/C substrate at late times in mitosis, or in G1 (panel ii, Fig. 3.5).

To evaluate further the requirement for APC/C in the degradation of APC5, we performed Western blotting analyses to check the level of APC5 and other APC/C substrates using the FLAG-Cdc20 U2OS FRT Doxycycline-inducible cell line synchronized with RO-3306, nocodazole or taxol, either in the presence, or absence of Dox (Fig. 3.6). Cdc20 overexpression was shown to promote the degradation of well-known APC/C substrates such as Cyclin B1 and Cyclin A in asynchronous and G2/M-arrested cells compared to control cells, without altering the levels of Nek2A (panel iii, iv and v, Fig. 3.6). Likewise, APC5 levels were reduced following Cdc20 overexpression in all synchronization conditions tested, suggesting a role for the APC/C-Cdc20 complex in its degradation (panel ii, Fig. 3.6).

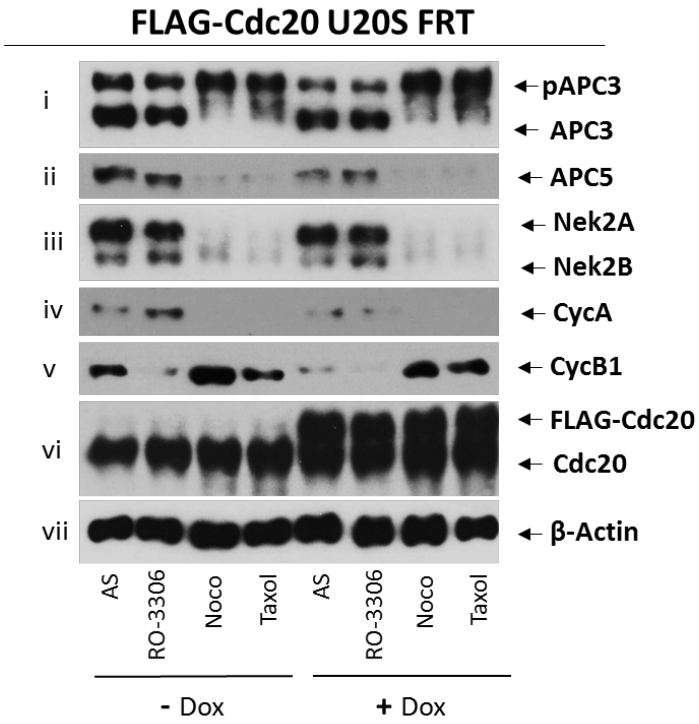

Figure 3. 6: **Effects of Cdc20 overexpression on APC5 protein levels.** Lysates from asynchronous (AS), G2/M-arrested (RO-3306) and mitotic-arrested (Noco/Taxol) FLAG-Cdc20 U2OS FRT cells either in presence (+Dox) or absence (-Dox) of Doxycycline were harvested in UTB Lysis Buffer. 50µg of total protein was separated by SDS-PAGE, transferred to a nitrocellulose membrane and the level of various APC/C subunits, Cdc20 and substrates were determined by Western blotting. The levels of β-actin were used as a loading control. These data are representative of three individual experiments.

The results obtained thus far suggest that APC/C-Cdc20 might have a role in the degradation of APC5. If so, APC5 degradation in mitosis would represent an auto-regulatory mechanism through which APC/C E3 ligase activity could be fine-tuned during mitosis and G1.

3.4 Generation of Doxycycline inducible FLAG-APC5 WT U2OS FRT cell lines

To investigate further the levels of the APC5 protein in mitosis and validate our previous findings, we generated a number of clonal, Doxycycline-inducible, FLAG- APC5 WT U2OS FRT cell lines (Fig. 3.7). First, we co-transfected U2OS FRT cells with a pcDNA5 FRT-FLAG-APC5 WT together with the pOG44 vector, which express for the Flp recombinase. This allowed for the stable integration of the recombinant gene in the U2OS FRT cells genome within a FLP Recombination Target (FRT) under the control of a hybrid, human cytomegalovirus (CMV)/$TetO_2$ promoter responsive to Doxycycline (Dox). Efficient integration of the recombinant gene also allowed for constitutive expression of a Hygromycin-resistance gene, which we used to select clones which had integrated FLAG-APC5 into the recombination site. FLAG-APC5 WT efficiently transfected cells that produced individual colonies in the presence of Hygromycin (200µg/ml) were isolated to generate clonal cell lines (see Sec. 2.1.3, Chapter 2).

3.4.1 FLAG-APC5 U2OS FRT cell lines efficiently express FLAG-APC5 protein following Doxycycline induction

We tested the ability of the clonal cell lines to express FLAG-APC5 WT in the presence of Doxycycline (Dox; 200 µg/ml) by Western blotting using a specific antibody directed toward the FLAG-Tag of the recombinant protein (Fig. 3.7).

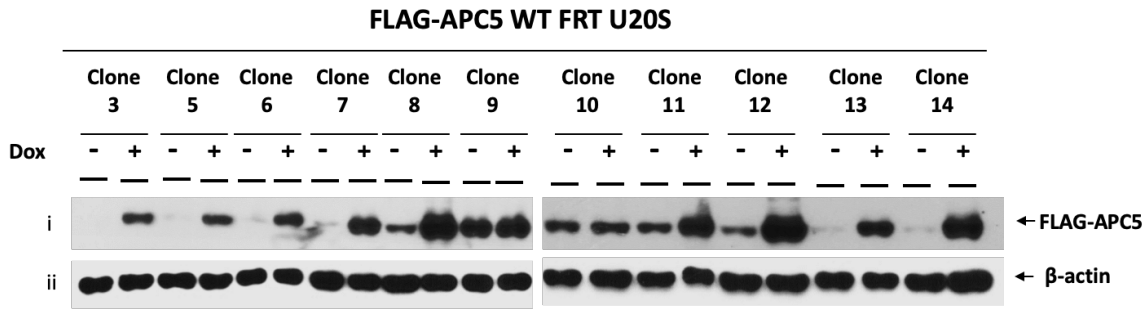

Figure 3. 7: **Expression of wild-type (WT) FLAG-Apc5 in U2OS cells treated with doxycycline.** Lysates from non-induced (Dox-) and doxycycline-induced (Dox+) FLAG-APC5 WT U2OS FRT clones were harvested in UTB lysis buffer. 50µg of total protein was separated by SDS-PAGE, transferred to a nitrocellulose membrane and the level of FLAG-APC5 was detected using an α-FLAG specific antibody by Western blotting. The levels of β-actin were used as a loading control.

The results obtained indicated that most of the U2OS FRT cell lines generated expressed FLAG-APC5 WT following Dox treatment, although some of the cell lines showed low level leakage of FLAG-APC5 WT expression in the absence of Dox. We subsequently selected clone 13 (FLAG-APC5 WT U2OS FRT #13) for experiments going forward, as FLAG-APC5 WT protein levels were good following Dox induction, with minimal FLAG-APC5 WT expression in the absence of Dox (lane 19 and 20, panel i, Fig. 3.7).

3.4.2 FLAG-APC5 WT protein levels are not destabilized during mitosis

To investigate whether the FLAG-APC5 WT recombinant gene product behaved as endogenous APC5, we decided to look at the level of the FLAG-APC5 protein under different synchronization conditions. We therefore compared FLAG-APC5 protein levels in asynchronous, G2/M and mitotically-arrested cells (Fig. 3.8 A).

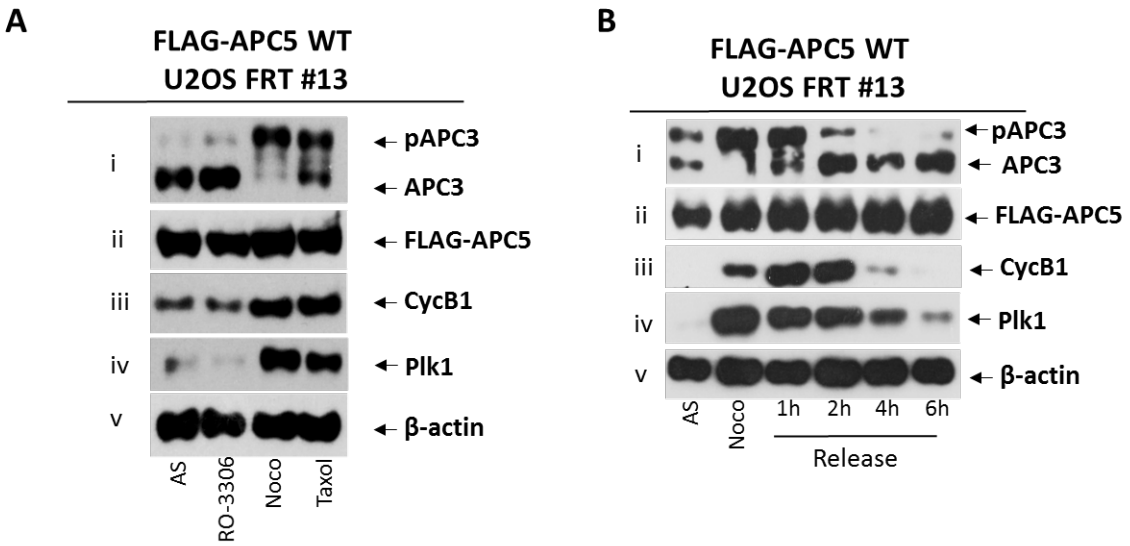

Figure 3. 8: **FLAG-APC5 WT levels do not change during mitosis. (A)** Lysates from asynchronous (AS), G2/M-arrested (RO-3306) and mitotically-arrested (Noco/Taxol) FLAG-APC5 WT U2OS FRT Clone 13 (#13) doxycycline-induced cells were harvested in UTB lysis buffer. **(B)** Cell lysates from FLAG-APC5 WT Flp-in U2OS Clone 13 (#13) doxycycline-induced asynchronous cells (AS), nocodazole-arrested cells (Noco) and cells released from the mitotic arrest at different time points (1h, 2h, 4h and 6h) were harvested by treatment with UTB lysis buffer. In both experiments 50µg of total protein was separated by SDS-PAGE, transferred to a nitrocellulose membrane and the level of FLAG-APC5 was detected with an α-FLAG specific antibody by Western blotting together with APC3 and some APC/C well-known mitotic substrates. The levels of β-actin were used as a loading control. These data presented is representative of three individual experiments.

In contrast to the findings with the APC5 monoclonal antibody (mAb), Western blot analysis suggested that FLAG-APC5 WT protein levels were not altered during mitosis relative to interphase cells and G2/M-arrested cells (panel ii, Fig. 3.8 A). Likewise, when we performed a nocodazole-release experiment using the FLAG-APC5 WT U2OS FRT cells, Western blot analyses revealed that FLAG-APC5 protein levels were not altered in mitosis or following nocodazole withdrawal (panel ii, Fig. 3.8 B). As the results obtained from our FLAG-APC5 WT U2OS FRT cells failed to recapitulate the destabilization of endogenous APC5 in mitosis observed in RPE-1 cells, we started to reason whether the alterations in the levels of APC5 were to be attributable to other factors. Interestingly, one obvious crucial difference in the experiments performed with endogenous APC5 and those performed with FLAG-

APC5 was the use of different antibodies to detect APC5 levels by Western blot. In fact, in all experiments conducted using RPE-1 and U2OS cells endogenous APC5 levels in mitosis were detected using an α-APC5 mAb developed in-house, which showed destabilization of the protein. On the other hand, FLAG-APC5 WT protein levels were detected in Western blotting using an antibody directed toward the FLAG-Tag of APC5, which revealed no alterations in the level of the recombinant FLAG-APC5 species in mitosis. As the two antibodies bind to different epitopes they show completely different results for APC5 levels during mitosis, we speculated that the APC5 mAb's binding affinity for its epitope might be different in mitosis and interphase.

3.5 PTM masks the APC5 epitope in mitosis

PTMs occurring on proteins can alter their function, localization and stability, as well as affect their interaction with other proteins (Pickart and Eddins, 2004). Interestingly PTMs, such as phosphorylation, acetylation and ubiquitylation, are crucial in the fine-tuning of cell division and in the regulation of APC/C activity (Kraft et al., 2003, Kataria and Yamano, 2019, Alfieri et al., 2017). Given their strong impact in such processes, we questioned whether the differences observed in the α-APC5 mAb binding affinity was due to PTMs occurring in the APC5 epitope during mitosis.

3.5.1 α-APC5 antibody screening

Although our initial results suggested that endogenous APC5 was degraded early in mitosis, potentially in an APC/C-dependent manner, the evidence obtained with the FLAG-APC5 WT U2OS FRT cell lines indicated that the level of the FLAG-APC5 species in mitosis remained unaltered relative to asynchronous cells, which were predominantly in interphase (Fig. 3.8). These results led to the hypothesis that the APC5 epitope recognized by our APC5

mAb might be masked in mitosis. For this reason, we conducted antibody screening to test the ability of various α-APC5 mAbs produced in our laboratory to recognize APC5 in asynchronous and mitotically-arrested RPE-1 and HeLa cells (Fig. 3.9).

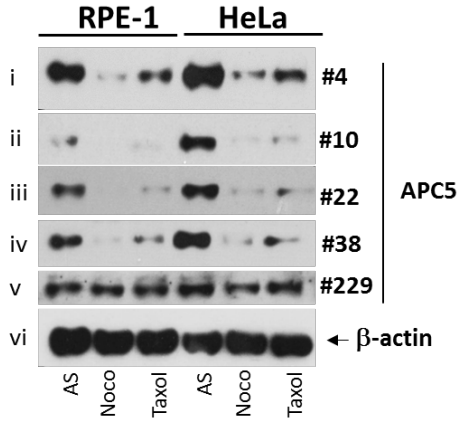

Figure 3. 9: **α-APC5 mAbs do not recognize APC5 in mitosis.** Lysates from asynchronous (AS) and mitotically-arrested (Noco/Taxol) RPE-1 and HeLa cells were harvested in UTB lysis buffer. 50µg of total protein was separated by SDS-PAGE, transferred to a nitrocellulose membrane and the levels of APC5 were detected with various α-APC5 mAbs (#4, #10, #22, #38) and with a polyclonal α-APC5 antibody (#229, Bethyl) by Western blotting. The levels of β-actin were used as a loading control. These data are representative of three individual experiments.

Interestingly, for both cell lines the results of this experiment revealed that all of the α-APC5 mAbs tested, and routinely used in the laboratory, APC5 protein levels were apparently reduced in mitosis compared to asynchronous conditions (panel i, ii, iii and iv, Fig. 3.9). To measure APC5 levels in mitosis further we purchased an α-APC5 polyclonal antibody from Bethyl Labs. The polyclonal α-APC5 antibody, akin to the α-FLAG specific antibody, determined that APC5 protein levels were not reduced in mitosis (panel v, Fig. 3.9). Remarkably, even though the mAbs used to detect APC5 were produced through immunization of the animal against the full-length APC5 protein, the antibody screening results suggest that all the α-APC5 mAbs bind to the same epitope, which might be masked during mitosis.

3.5.2 APC5 is phosphorylated in mitosis

As phosphorylation of multiple APC/C subunits, including APC1 and APC3, has been shown to be indispensable for the activation of the APC/C-Cdc20 complex (Qiao et al., 2016, Zhang et al., 2016, Golan et al., 2002), we reasoned that APC5 might similarly be phosphorylated in mitosis. Therefore, to address the hypothesis that PTM masks the APC5 epitope in mitosis, we decided to perform a λ-Phosphatase (λPPase) assay. To do this, we co-immunoprecipitated APC5 with an α-APC7 specific antibody from asynchronous and mitotically-arrested RPE-1 cells under non-denaturing conditions and we analysed its protein levels by Western blotting using the α-APC5 mAb, #4 prior to, and after, λPPase treatment (Fig. 3.10).

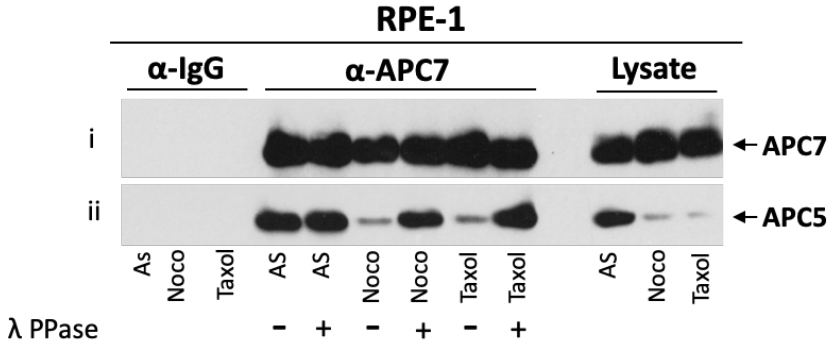

Figure 3. 10: **APC5 is phosphorylated in mitosis.** Lysates from asynchronous (AS) and mitotically-arrested (Noco/Taxol) RPE-1 cells were harvested in APC/C lysis buffer. 0.6 mg of total protein was incubated overnight at 4°C with an APC7 (α-APC7) polyclonal antibody or with normal rabbit IgG (α-IgG), followed by 3h incubation at 4°C with Protein G Sepharose beads (20µl packed). Following IP, beads were incubated for 1h at 30°C in the presence or absence of λ-Phosphatase. IPs, together with 50µg of total protein lysate was separated by SDS-PAGE, transferred to a nitrocellulose membrane and the levels of APC5 and APC7 were detected by Western Blotting. This data is representative of three individual experiments.

The results of this experiment revealed that there were no differences in APC5 protein levels in asynchronous cells treated with λPPase (cf lane 4 and 5, panel ii, Fig. 3.10). On the

contrary, λPPase treatment completely restored APC5 level in mitosis compared to non-treated samples protein (cf lane 6+7 and 8+9, panel ii, Fig. 3.10). Together, these data confirmed our hypothesis that PTM in mitosis masks the α-APC5 mAb epitope, and suggests, moreover, that APC5 is phosphorylated in mitosis and that the α-APC5 mAbs do not bind to this post-translationally modified form of APC5.

3.6 Investigating the dynamics of APC5 phosphorylation

Results presented so far have determined that APC5 is phosphorylated early in mitosis and this PTM is lost as cells exit mitosis and proceed into G1. As such, we found that α-APC5 mAbs are unable to bind their epitope on APC5 when it is phosphorylated in mitosis. We therefore decided to exploit the change in the binding affinity of the APC5 mAbs to study the dynamics of APC5 phosphorylation/dephosphorylation in mitosis and understand its physiological effects on the APC/C holoenzyme.

3.6.1 Weakening the SAC promotes APC5 de-phosphorylation

APC/C mitotic activity is tightly regulated. The premature activation of the APC/C in prometaphase is inhibited by the SAC that targets and inhibits the co-activator Cdc20 and blocks the formation of an active APC/C-Cdc20 complex until all chromosomes are attached to the spindle in a bi-oriented manner and ready to undergo segregation in anaphase (Lara-Gonzalez et al., 2012, Musacchio, 2015, Musacchio and Salmon, 2007).

As the timing of APC5 phosphorylation overlaps with the SAC-dependent inhibition of the APC/C, we questioned whether this phosphorylation event was directly due to SAC activation. To study this possibility, we treated mitotically-arrested RPE-1 cells, obtained by treatment with nocodazole, with the SAC inhibitor Reversine, a drug commonly used to weaken the SAC by inhibiting the SAC-signalling protein Mps1 (Santaguida et al., 2010,

Lara-Gonzalez et al., 2012). Cells were therefore harvested at different time points post-Reversine treatment (30', 1h, 2h, 3h, 4h, 5h and 6h) and Western blotting analysis was employed to compare the levels of various APC/C substrates and the phosphorylation status of APC3 and APC5 in asynchronous, mitotically-arrested cells and during the Reversine-dependent inhibition of the SAC (Fig. 3.11).

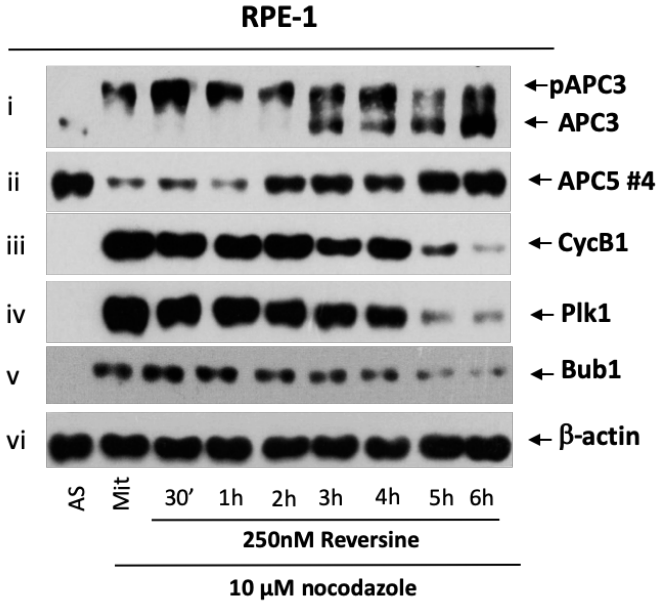

Figure 3. 11: **Disruption of the SAC in the presence of nocodazole promotes APC5 de-phosphorylation.** Lysates from asynchronous (AS), mitotically-arrested cells (Mit) and cells treated with 250nM of Reversine in the presence of 10µM nocodazole harvested at different time (30', 1h, 2h, 3h, 4h, 5h and 6h) were harvested in UTB lysis buffer. 50µg of total protein was separated by SDS-PAGE, transferred to a nitrocellulose membrane and the levels of APC5 were detected with an α-APC5 mAb (#4). The levels of APC3, CycB1 and Plk1 were used as a control for APC/C activity, whereas the levels of Bub1 were used as a control for the SAC activation status. The levels of β-actin were used as a loading control. This data is representative of three individual experiments.

As expected, nocodazole treatment of RPE-1 cells caused the accumulation of APC/C substrates Cyclin B1 and Plk1 compared to asynchronous cells, as a consequence of the disruption of the mitotic spindle which triggers mitotic arrest (cf lane 1+2, panel iii and iv, Fig. 3.11). Under the same conditions, the protein levels of Bub1, a well-established

component of the SAC signalling pathway, as well as an APC/C substrate, appeared to be reduced in mitotically-arrested cells compared to asynchronous conditions, as a consequence of the mitotic arrest imposed by the treatment with nocodazole (cf lane 1+2, panel v, Fig. 3.11). As expected, concomitant treatment with Reversine caused SAC satisfaction regardless of the disruption of the spindle. As such, SAC-dependent inhibition was overridden causing premature degradation of the APC/C substrates Cyclin B1, Plk1 and Bub1, especially at late times post-treatment compared to mitotically-arrested cells not treated with Reversine (cf lane 3, 4, 5, 6, 7, 8, 9 with lane 2, panel iii, iv and v, Fig. 3.11). Likewise, the high molecular weight APC3 band, corresponding to the mitotic phosphorylated form was markedly increased in mitotically-arrested cells treated with nocodazole alone compared to asynchronous cells (cf lane 1 and 2, panel i, Fig. 3.11). As a consequence of Reversine treatment, APC3 phosphorylation was reduced significantly 3h post-treatment compared to cells only treated with nocodazole, confirming that Reversine stimulated mitotic progression (panel i, Fig. 3.11). Interestingly, while the APC5 band disappeared in mitotically-arrested cells compared to interphase cells, as a consequence of its phosphorylation, treatment with Reversine caused a reduction in APC5 phosphorylation at the early stages of the time course followed by a complete loss of phosphorylation as cells progressed through mitosis (panel ii, Fig. 3.11).

To expand upon these observations, we repeated the experiment, but, this time induced mitotic arrest with taxol. As such, mitotically-arrested RPE-1 cells obtained by treatment with taxol were isolated by mechanical shake-off, treated with Reversine and harvested at different time points (30', 1h, 2h, 3h, 4h, 5h and 6h). As before, Western blot analysis was performed to look at the levels of various APC/C substrates and at the phosphorylation status of APC3 and APC5 (Fig. 3.12).

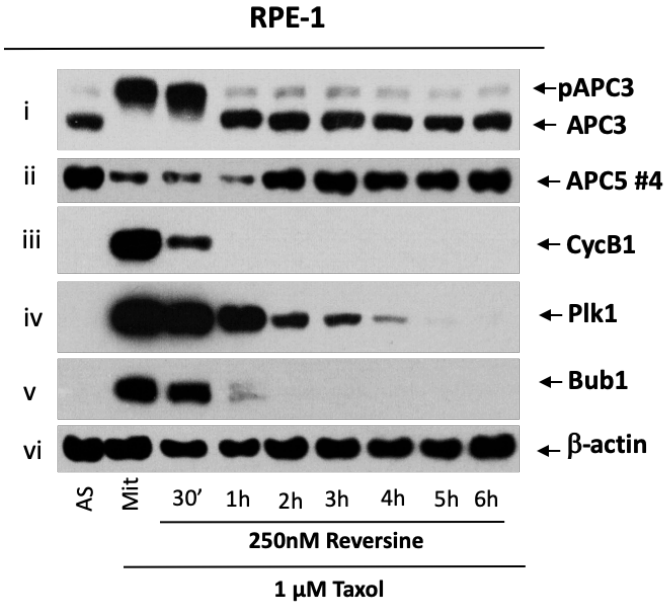

Figure 3. 12: **Disruption of the SAC in the presence of taxol reduces APC5 phosphorylation.** Lysates from asynchronous (AS), mitotically-arrested cells (Mit) and cells treated with 250nM of Reversine in the presence of 10μM Taxol harvested at different time (30', 1h, 2h, 3h, 4h, 5h and 6h) were harvested in UTB lysis buffer. 50μg of total protein was separated by SDS-PAGE, transferred to a nitrocellulose membrane and the levels of APC5 were detected with an α-APC5 mAb (#4). The level of APC3, CycB1 and Plk1 were used as a control for APC/C activity, whereas the levels of Bub1 were used as a control for the SAC activation status. The levels of β-actin were used as a loading control. This data is representative of three individual experiments.

Western blot analyses revealed that activation of the SAC in response to taxol treatment caused the accumulation of the APC/C substrates Cyclin B1, Plk1 and Bub1, as well as the appearance of the high molecular weight APC3 species, relative to asynchronous cells (panel i, iii, iv and v, Fig. 3.12). As seen previously, Reversine treatment of mitotically-arrested cells triggered the activation of the APC/C-Cdc20 complex and the consequent degradation of the APC/C substrates Cyclin B1, Plk1 and Bub1 (panel iii, iv and v Fig. 3.12). Interestingly, as taxol treatment arrests cells throughout mitosis compared to nocodazole, which arrests cells is prophase, the degradation of APC/C substrates was faster, with complete loss of Bub1 and Cyclin B1 after 1h post-Reversine treatment (panel iii and v, Fig. 3.12). Plk1 levels were also reduced at a faster rate in Reversine-treated taxol cells, compared

to Reversine-treated nocodazole cells (cf panel iv Fig. 3.11 and Fig. 3.12). Reversine treatment also promoted APC5 de-phosphorylation, as confirmed by the increase of APC5 levels 2h post-Reversine treatment (panel ii, Fig. 3.12). Interestingly, whilst Reversine promoted the dephosphorylation of APC5 more gradually in cells treated with nocodazole, Reversine caused a more drastic loss of APC5 phosphorylation in taxol-treated cells, with complete recovery of the interphase levels of APC5 2h following Reversine addition (cf panel ii, Fig. 3.11 and 3.12).

Taken together, the results of these experiments revealed that weakening the SAC correlates positively with the loss of APC5 mitotic phosphorylation, suggesting a potential direct involvement of the SAC in the phosphorylation of APC5 during mitosis. However, as Reversine treatment of mitotically-arrested cells obtained with either nocodazole or taxol caused cells to escape mitosis regardless the disruption of the mitotic spindle, it is not possible to establish whether the loss of APC5 phosphorylation is a direct consequence of weakening the SAC, or is instead due to cells progressing from mitosis to G1. Moreover, as APC5 de-phosphorylation occurs more quickly when cells were arrested with taxol compared to nocodazole, these data suggest that APC5 de-phosphorylation might be due to mitotic exit rather than to a direct effect of the SAC (cf panel ii, Fig. 3.11 and 3.12).

3.6.2 26S proteasome inhibition sustains APC5 mitotic phosphorylation

Our data so far indicates that APC5 de-phosphorylation occurs as cells exit mitosis and progress towards G1, suggesting that APC5 phosphorylation occurs specifically during mitosis (Fig. 3.1). We also found that inhibiting the SAC with Reversine promotes APC5 de-phosphorylation indicating a potential role for the SAC in phosphorylating APC5 during mitosis (panel ii, Fig. 3.11 and 3.12). However, Reversine treatment also causes cells to

escape mitosis and enter G1, leaving the possibility that the loss of APC5 mitotic phosphorylation following Reversine-treatment might be due to normal mitotic progression and exit rather than to the SAC inhibition. As mitotic exit is normally driven by the 26S proteasome-mediated degradation of ubiquitylated substrates, mainly produced though the E3-ubiquitin activity of the APC/C (Peters, 2006, Sivakumar and Gorbsky, 2015, Pray et al., 2002, Mocciaro and Rape, 2012), we reasoned that we could establish the role for the SAC on APC5 phosphorylation by impeding mitotic cell exit using the 26S proteasome inhibitor, MG132 (Potapova et al., 2006).

Therefore, we repeated the Reversine treatment of nocodazole-arrested cells in the presence of MG132, which blocks mitotic progression even when the SAC is overridden by Reversine. For this experiment, we isolated mitotically-arrested RPE-1 cells obtained by treatment with nocodazole and treated them either with Reversine only, or with Reversine and MG132, for 2h and 4h. Following these treatments the levels of various APC/C mitotic substrates and the phosphorylation status of APC3 and APC5 were analysed by Western blotting, and compared to their levels in asynchronous conditions or in cells treated with nocodazole alone (Fig. 3.13).

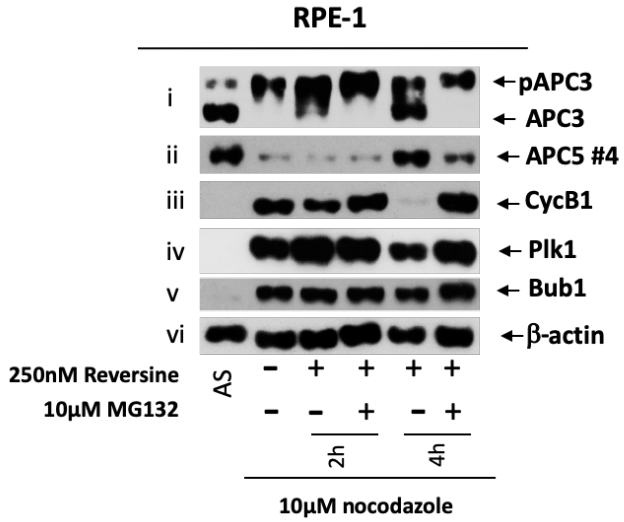

Figure 3. 13: **APC5 phosphorylation is maintained when the 26S proteasome is inhibited following SAC satisfaction by Reversine.** Lysates from asynchronous (AS), mitotically-arrested cells (lane 2), mitotically-arrested cells treated with 250nM Reversine for 2h and 4h (lane 3 and 5) and mitotically-arrested cells treated with 10 μM MG132 and 250nM Reversine for 2h and 4h (lane 4 and 6) were harvested in UTB lysis buffer. 50μg of total protein was separated by SDS-PAGE, transferred to a nitrocellulose membrane. The phosphorylation status of APC5 was detected by the inability of the α-APC5 mAb #4 to bind its epitope when phosphorylated. The level of APC3, CycB1 and Plk1 were used as a controls for APC/C activity, whereas the levels of Bub1 were used as a control for the SAC activation status. The levels of β-actin were used as a loading control. This data is representative of three individual experiments.

Consistent with our previous findings, treatment of nocodazole-arrested cells with Reversine caused cells to escape mitosis with an appropriate reduction in the levels of Cyclin B1, Plk1 and Bub1 compared to cells treated with nocodazole alone (panel iii, iv and v, Fig. 3.13). Accordingly, phosphorylation of APC3 was reduced markedly following Reversine treatment (panel i, Fig. 3.13). However, concomitant treatment of nocodazole-arrested cells with Reversine and MG132 for 2 and 4 hours caused cells to stall in mitosis, as demonstrated by the restoration in the levels of Cyclin B1, Plk1 and Bub1 which were comparable to those observed in mitotically-arrested cells (panel iii, iv and v, Fig. 3.13). Similarly, the mitotic APC3 phosphorylation status was restored when Reversine-treated cells were incubated with MG132, confirming that in the presence of MG132 Reversine could not promote mitotic exit

(panel i, Fig. 3.13). No differences were observed in APC5 phosphorylation status following 2h Reversine treatment either in the presence or absence of MG132 (panel ii, Fig. 3.13). Interestingly however, whilst 4h treatment with Reversine alone caused the complete loss of APC5 phosphorylation, APC5 phosphorylation was maintained to some extent when Reversine-treated cells were also treated with MG132 (panel ii, Fig. 3.13), suggesting that APC5 phosphorylation is not dependent on an active SAC.

To confirm these data, we decided to look at the phosphorylation status of APC5 in RPE-1 cells released from mitotic arrest in the presence of MG132, to see whether 26S proteasome inhibition could alone, maintain APC5 phosphorylation status. To do this, we synchronized cells in mitosis by treatment with nocodazole and released them from mitotic arrest either in the presence or absence of MG132 (Fig. 3.14). Cells were harvested at different time points and Western blotting analyses were performed to evaluate the phosphorylation status of APC5 and the levels of various substrates known to be targeted for degradation in mitosis by the APC/C (Fig. 3.14).

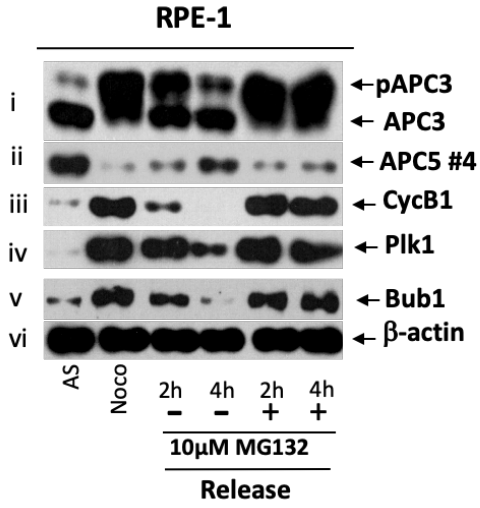

Figure 3. 14: **Blocking mitotic progression through 26S proteasome inhibition maintains APC5 phosphorylation status.** Cell lysates from asynchronous RPE-1 cells (AS), nocodazole-arrested cells (Noco) and cells released from the mitotic arrest at different time-points (1h, 2h, 4h and 6h) were harvested in UTB lysis buffer. 50μg of total protein was separated by SDS-PAGE, transferred to a nitrocellulose membrane and the levels of various APC/C subunits, UbcH10 and APC/C mitotic substrates were determined by Western blotting. The levels of β-actin were used as a loading control. This data is representative of three individual experiments.

As expected, releasing mitotically-arrested cells in the presence of MG132 prevented them from exiting mitosis, as indicated by the accumulation of the known APC/C substrates Cyclin B1, Plk1 and Bub1 relative to cells released in the absence of MG132 (panel iii, iv and v, Fig. 3.14). Accordingly, APC3 remained phosphorylated in cells released from the mitotic block in the presence of MG132, whilst APC3 from cells released in the absence of MG132 was not phosphorylated (panel i, Fig. 3.14). Interestingly, APC5 was de-phosphorylated following nocodazole withdrawal in the absence of MG132 compared to mitotically-arrested cells, whilst APC5 phosphorylation was maintained when cells were released in to medium containing MG132 (cf lane 3+4 and 5+6, panel ii, Fig. 3.14).

Overall, the results of our experiments indicate that APC5 is phosphorylated by a mitotic kinase by a mechanism that is largely independent of SAC activity. Indeed, APC5 is de-

phosphorylated as cells progress through mitosis in the presence of a weakened SAC (Fig. 3.11 and 3.12), whilst APC5 phosphorylation is maintained when cells are stalled in mitosis through inhibition of the 26S proteasome (Fig. 3.14). Taken together, these results suggest that APC5 phosphorylation is temporally coordinated in mitosis. As such, we hypothesize that the phosphorylation of APC5 in mitosis might regulate APC/C activity.

3.6.3 APC5 phosphorylation status is not affected by genotoxic stress

Apart from its role in the control of mitotic progression, the APC/C has been found to play a central role in cellular checkpoint activation in response to DNA damage. In fact, genotoxic stress caused by either chemical or physical agents, can trigger APC/C-Cdh1 activation in G2 phase to promote Plk1 degradation, the stabilization of Claspin and the Claspin-mediated activation of Chk1 (Stracker et al., 2009). As our data suggested that APC5 is phosphorylated in mitosis when the APC/C is active, we questioned whether APC5 could be phosphorylated when the APC/C is re-activated during G2 phase in response to DNA damage.

To evaluate this possibility we subjected RPE-1 cells to DNA damage through a series of DNA damage-inducing treatments and investigated the phosphorylation status of APC5. Specifically, we treated cells with UV ionization, 5-Fluor-Uracil (5-FU), or Carbo-Pt and employed Western blot analysis to determine whether genotoxic stress affected APC5 phosphorylation status (Fig. 3.15 A, B and C).

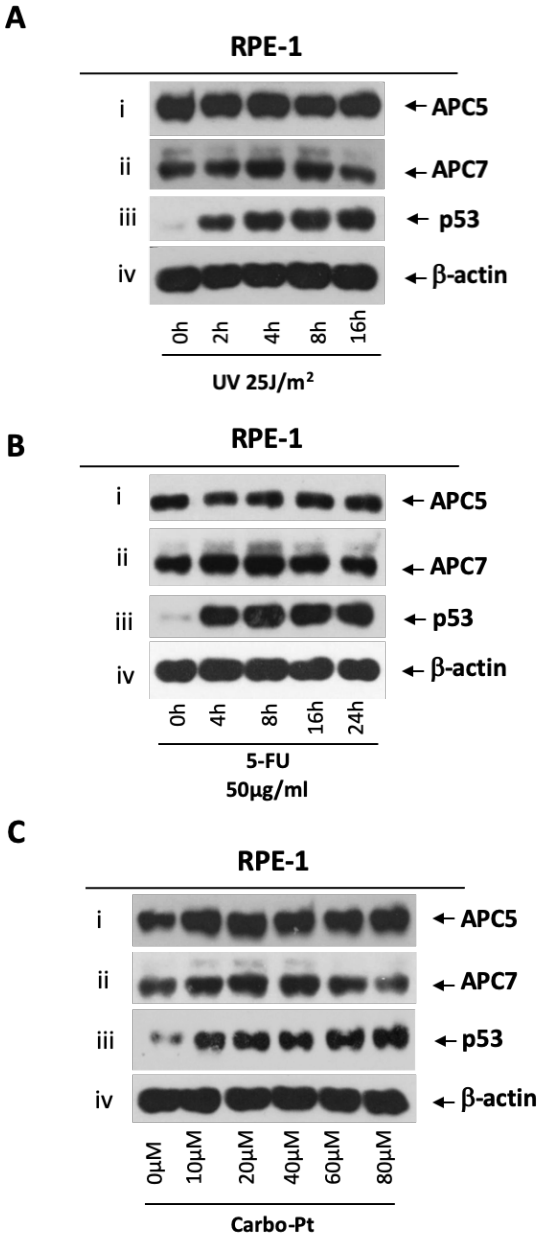

Figure 3. 15: **APC5 phosphorylation is not induced by DNA damage.** (**A**) Cell lysates from UV-treated (25J/m^2), (**B**) 5-FU-treared (50µg/ml) and (**C**) Carbo-Pt-treated (16h post-treatment) RPE-1 cells were harvested in UTB lysis buffer. 50µg of total protein was separated by SDS-PAGE, transferred to a nitrocellulose membrane and the levels of APC5, APC7 and p53 were determined by Western blotting. The levels of β-actin were used as a loading control. This data is representative of three individual experiments.

Consistent with DNA damage all the treatments performed were able to cause increases in the protein levels of p53 compared to untreated cells (panel iii, Fig. 3.15 A, B and C). Despite

this, DNA damage did not affect the phosphorylation status of APC5 (panel i, Fig. 3.15 A, B and C). These data suggest that APC5 phosphorylation upon the residue recognized by our α-APC5 mAbs are restricted to mitosis and it is not affected by DNA damage. Interestingly however, a higher molecular weight band, which might correspond to a phosphorylated APC7 species, was observed in these experiments and it seemed particularly high following 5-FU treatment, suggesting that the cellular response induced by this genotoxic agent might have a potential role on the regulation of APC7 (panel ii, Fig. 3.15 A, B and C).

3.7 Identification of the mitotic kinase responsible for APC5 phosphorylation

Mitotic kinases such as Cdk1, Plk1 and Aurora A and B are key in the regulation of many events during mitosis, including the regulation of the SAC and the activity of the APC/C (Carmena et al., 2009, Nigg, 2001, Cuijpers and Vertegaal, 2018, Golan et al., 2002). As cells progress through mitosis towards G1 the activity of these mitotic kinases is no longer required and cells inactivate these pathways in order to complete mitosis. In this context, APC/C E3 ligase activity is critical in many ways. For instance, once all chromosomes are aligned to the mitotic spindle in metaphase and the SAC is satisfied, the APC/C inactivates Cdk1 by orchestrating the proteasomal degradation of Cyclin B1, allowing for mitotic exit(Sivakumar and Gorbsky, 2015). Similarly, Plk1 and Aurora A are degraded by the APC/C-Cdh1 active complex following anaphase onset and during the later stages of mitosis, and this has been reported to be critical for mitotic exit and for cytokinesis (Lindon and Pines, 2004, Ma and Poon, 2011). On the other hand, Aurora B kinase remains active until cytokinesis, as its activity seems to be required for a proper separation of cells after mitosis through its phosphorylation of the Nuclear distribution protein c (NudC) (Weiderhold et al., 2016).

The data presented thus far suggests that APC5 phosphorylation occurs specifically during mitosis and that it is reduced as cells progress through, and exit mitosis (Fig. 3.1, 3.2 and 3.10). We have also determined that APC5 phosphorylation is linked directly to the 26S proteasome-mediated degradation of mitotic substrates and, therefore, to the activation status of the APC/C (Fig. 3.14). Given these findings, we reasoned that APC5 phosphorylation might be regulated by mitotic kinases, such as Cyclin B1-Cdk1 and Plk1 that are also degraded in an APC/C-dependent manner (Clute and Pines, 1999, Lindon and Pines, 2004). To identify the mitotic kinase/s responsible for APC5 mitotic phosphorylation, we investigated the effect of mitotic kinases inhibition upon the phosphorylation status of APC5 in mitosis.

3.7.1 Cdk1 inhibition in mitosis prevents APC5 phosphorylation

To investigate the involvement of Cyclin B1-Cdk1 in the phosphorylation of APC5 in mitosis, we employed the well-known specific Cdk1 inhibitor, RO-3306. However, as treatment of mitotically-arrested cells with RO-3306 has been shown previously to cause mitotic slippage (Chan et al., 2008), we also treated cells with the 26S proteasome inhibitor, MG132, to arrest cells in mitosis so that we could look at the direct effect of Cdk1 inhibition on the phosphorylation status of APC5 in mitosis. As such, RPE-1 cells were synchronized in mitosis by treatment with nocodazole. Mitotically-arrested cells were then isolated by mechanical shake-off and treated either with the Cdk1 inhibitor RO-3306 alone or in the presence of both the 26S proteasome inhibitor, MG132 and nocodazole, and harvested after 2h and 4h post-RO-3306 treatment. We then carried out Western blot analysis to look at the effect of Cdk1 inhibition on the levels of various APC/C substrates, such as Cyclin B1, Plk1 and Bub1 and the phosphorylation status of APC3 and APC5 (Fig. 3.16).

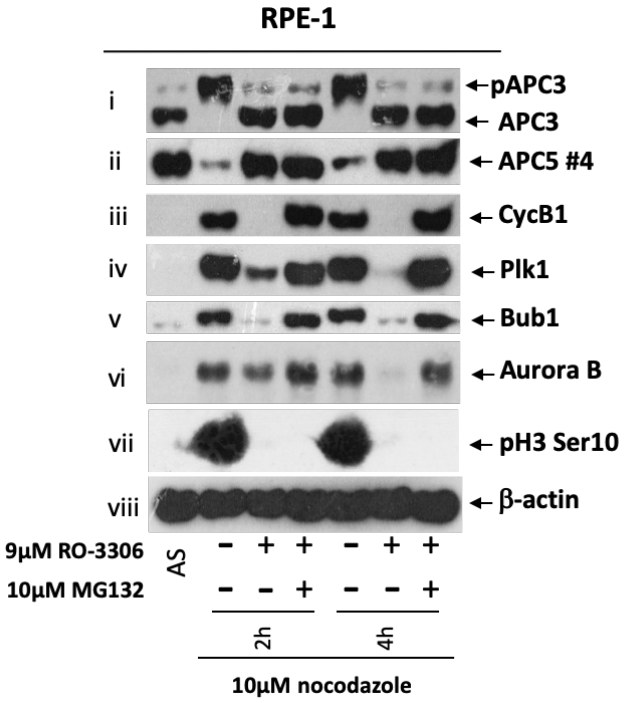

Figure 3. 16: **Cdk1 inhibition attenuates APC5 phosphorylation in nocodazole-arrested cells.** Lysates from asynchronous (AS), mitotically-arrested cells (lane 2 and 5), mitotically-arrested cells treated with 9μM RO-3306 for 2h and 4h (lane 3 and 6) and mitotically-arrested cells treated with 9μM RO-3306 and 10μM MG132 for 2h and 4h (lane 4 and 7) were harvested in UTB lysis buffer. 50μg of total protein was separated by SDS-PAGE, transferred to a nitrocellulose membrane (PALL). The phosphorylation status of APC5 was detected by the inability of the α-APC5 mAb #4 to bind its epitope when phosphorylated. The phosphorylation status of APC3 was used either as a control for the mitotic arrest and as a control for Cdk1 inhibition. pH3 Ser10 was used as a marker for mitosis. The levels of CycB1 and Plk1 were used as a control for APC/C activity, whereas the levels of Bub1 were used as a control for the SAC activation status. The levels of β-actin were used as a loading control. This data is representative of three individual experiments.

As expected, inhibition of Cyclin B1-Cdk1 activity in the presence of nocodazole promoted progression through mitosis, as indicated by the loss of phosphorylated pH3 Ser10 (panel vii, Fig. 3.16), with complete loss of Cyclin B1, Plk1 and Bub1 following RO-3306 treatment, relative to cells mitotically-arrested with nocodazole alone (panel iii, iv, v, Fig. 3.16). Despite the recovery of a strong signal for APC5 in cells treated with the Cdk1 inhibitor in the presence of nocodazole (cf lane 3+4 and 5+6, panel ii, Fig. 3.16), indicating the loss of its mitotic phosphorylation, it was impossible to discern whether this effect was

due to Cdk1 inhibition rather than to mitotic slippage. However, simultaneous treatment of cells with RO-3306 and MG132, in the presence of nocodazole, efficiently blocked cells in mitosis, as demonstrated by the similar levels of Cyclin B1, Plk1 and Bub1 in cells only treated with nocodazole, and cells treated with RO-3306 and MG132 in the presence of nocodazole (cf lane 2+4 and 5+7, panel iii, iv and v Fig. 3.16). This experimental approach allowed for the evaluation of the direct effect of Cdk1 inhibition on APC/C phosphorylation in mitosis. Indeed, a consequence of Cdk1 inhibition in mitosis was that the APC3 higher molecular weight band, corresponding to its mitotic phosphorylated form, was completely lost in cells treated simultaneously with RO-3306 and MG132 (cf lane 2+4 and 5+7, panel i, Fig. 3.16). Interestingly, inhibition of Cdk1 in mitotically-arrested cells also led to the complete restoration of the APC5 band compared to asynchronous cells, indicating that APC5 does not undergo phosphorylation when Cdk1 is inhibited (panel ii, Fig. 3.16). Overall, the results of this experiment revealed that Cdk1 might be responsible for APC5 mitotic phosphorylation.

3.7.2 Plk1 inhibition in mitosis reduces APC5 phosphorylation

So far, our data suggests that Cyclin B1-Cdk1 might be responsible for APC5 phosphorylation in mitosis. However, as many proteins serve as substrates for multiple kinases, especially during mitosis when the phosphorylation pathways are intrinsically linked to one another creating complex regulatory networks (Cuijpers and Vertegaal, 2018), we wanted to investigate the requirement for others mitotic kinases in the phosphorylation of APC5. It is acknowledged that Cdk1 and Plk1 share various substrates, especially during mitosis (Cuijpers and Vertegaal, 2018, Elia et al., 2003a, Elia et al., 2003b, Neef et al., 2003, Neef et al., 2007). In particular, it has been reported that Cdk1 phosphorylation is required to prime Plk1 substrates by generating docking sites recognized specifically by Plk1 through

its PDB-binding domain, which is ultimately responsible for Plk1-dependent phosphorylation of its substrates (Jang et al., 2002, Elia et al., 2003a, Elia et al., 2003b, Neef et al., 2007, Neef et al., 2003).

To evaluate the role played by Plk1 in the phosphorylation of APC5, we inhibited Plk1activity in mitosis employing the Plk1 inhibitor, BI-6727 (Rudolph et al., 2009). RPE-1 cells arrested in mitosis by treatment with nocodazole were initially isolated by mechanical shake-off and subjected to treatment with BI-6727 alone or in the presence of MG132, which was used as previously to prevent cells escaping mitosis. Following these treatments cells were harvested after 2h and 4h and the cells lysates were analysed by SDS-PAGE coupled to Western blotting to determine the levels of various APC/C substrates and the phosphorylation status of APC5 (Fig. 3.17).

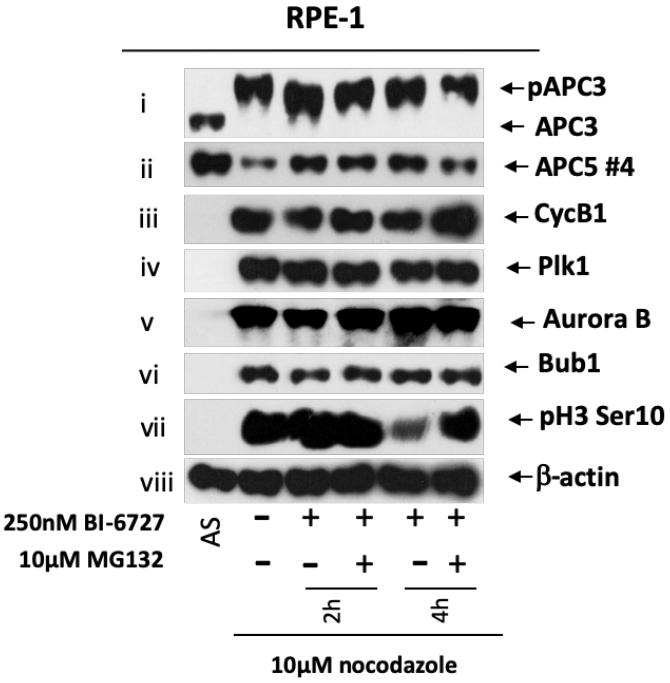

Figure 3. 17: **Plk1 inhibition attenuates APC5 phosphorylation in nocodazole-arrested cells.** Lysates from asynchronous (AS), mitotically-arrested cells (lane 2), mitotically-arrested cells treated with 250nM BI-6727 for 2h and 4h (lane 3 and 5) and mitotically-arrested cells treated with 250nM BI-6727 and 10μM MG132 for 2h and 4h (lane 4 and 6) were harvested in UTB lysis buffer. 50μg of total protein was separated by SDS-PAGE, transferred to a nitrocellulose membrane. The phosphorylation status of APC5 was detected by the inability of the α-APC5 mAb #4 to bind its epitope when phosphorylated. The levels of APC3, CycB1 and Plk1 were used as a control for APC/C activity, whereas the levels of Bub1 were used as a control for the SAC activation status. The levels of pH3 Ser10 were used as a marker for mitosis. The levels of β-actin were used as a loading control. This data is representative of three individual experiments.

The results of this experiment revealed that inhibition of Plk1 during mitosis was not sufficient to allow cells to escape mitosis, as showed by the comparable levels of the APC/C substrates Cyclin B1, Plk1 and Bub1 in mitotically-arrested cells treated with nocodazole alone and cells treated with Plk1 inhibitor in the presence or absence of MG132 (cf lane 2+3 and 4 and 2+5 and 6, panel iii, iv and v, Fig. 3.17). Cell cycle status was also confirmed by the phosphorylation status of the histone H3-Ser10 residue which appeared unaltered in almost all conditions tested compared to cells only treated with nocodazole (cf lane 2+3 and 4 and 2+5 and 6, panel vii, Fig. 3.17). A reduction in the phosphorylation of histone H3-

Ser10 was observed only after 4h in mitotic cells treated with the Plk1 inhibitor (panel vii, Fig. 3.17), which might be due to a potential reduction of Aurora B activity during the late mitotic stage, as a consequence of Plk1 inhibition (Rosasco-Nitcher et al., 2008, Cuijpers and Vertegaal, 2018). However, these results indicated that cells were arrested in mitosis and that the SAC kept the APC/C inactive during the entire time course of the experiment. Indeed, the phosphorylation status of APC3 was not altered following treatment with BI-6727 alone or in the presence of MG132 (cf lane 3+5 and 4+6, panel i, Fig. 3.17). This suggests that although Plk1 contributes towards APC3 phosphorylation during mitosis, its inhibition does not affect the slower migrating rate of APC3 on SDS-PAGE imposed by CyclinB1-Cdk1-dependent phosphorylation. Interestingly, inhibition of Plk1 caused the, almost complete, recovery of the APC5 band in all conditions tested (cf lane 2+3, 4, 5 and 6, panel ii, Fig. 3.17). However, the intensity of the APC5 band appeared lower in comparison to asynchronous cells, indicating that APC5 phosphorylation might not be lost completely when Plk1 is inhibited. Overall, the results of these experiments suggest that Plk1, as well as Cdk1, is responsible for APC5 phosphorylation during mitosis. Intriguingly, as both Cdk1 and Plk1 activity is abrogated as cells exit mitosis, concomitant with the loss of APC5 phosphorylation, it cannot be excluded that both kinases are implicated in a regulatory pathway operating on the APC/C through the phosphorylation of APC5. However, from the data so far obtained is not possible to discern the contribution of these mitotic kinases in the phosphorylation of APC5 during the early stage of mitosis.

3.7.3 Aurora B inhibition in mitosis attenuates APC5 phosphorylation

To investigate the role of Aurora B kinase upon APC5 phosphorylation in mitosis we used the well-known Aurora B inhibitor Hesperadin (Hauf et al., 2003). As previously described for other inhibitor studies, we isolated mitotically-arrested RPE-1 cells obtained by treatment

with nocodazole and then treated them with Hesperadin alone, or with Hesperadin plus MG132, in the presence of nocodazole. Cells were harvested after 2 and 4 hours following drug treatment and the cell lysates were analysed by Western Blot to evaluate the levels of various APC/C substrates and the phosphorylation status of APC5 (Fig. 3.18).

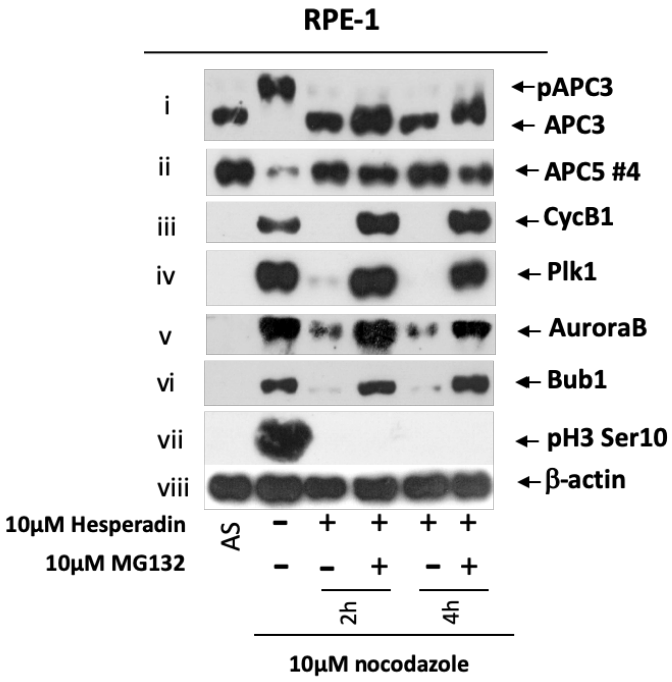

Figure 3. 18: **Aurora B inhibition attenuates APC5 phosphorylation in nocodazole-arrested cells.** Lysates from asynchronous (AS), mitotically-arrested cells (lane 2), mitotically-arrested cells treated with 10μM Hesperadin for 2h and 4h (lane 3 and 5) and mitotically arrested cells treated with 10μM Hesperadin and 10μM MG132 for 2h and 4h (lane 4 and 6) were harvested in UTB lysis buffer. 50μg of total protein was separated by SDS-PAGE, transferred to a nitrocellulose membrane. The phosphorylation status of APC5 was detected by the inability of the α-APC5 mAb #4 to bind its epitope when phosphorylated. The level of APC3, CycB1 and Plk1 were used as a control for APC/C activity, whereas the levels of Bub1 were used as a control for the SAC activation status. The level of pH3 Ser10 was used as a control for Aurora B inhibition. The levels of β-actin were used as a loading control. This data is representative of three individual experiments.

As for Cdk1 inhibition (Fig. 3.16), inhibition of Aurora B kinase in mitotically-arrested cells enabled cells to escape mitosis, as indicated by the reduction in the levels of the APC/C substrates Cyclin B1, Plk1 and Bub1 after 2h and 4h treatment with Hesperadin when

compared to mitotically-arrested cells only treated with nocodazole (cf lane 2+3 and 5, panel iii, iv and v, Fig. 3.18). In agreement with this observation the higher molecular weight APC3 band corresponding to its mitotically phosphorylated form was lost in cells treated with Hesperadin compared to mitotically-arrested cells (cf lane 2+3 and 5, panel i, Fig. 3.18). Furthermore, the levels of Aurora B were also reduced following the mitotic slippage imposed by Hesperadin, reflecting also the loss of histone H3-Ser10 phosphorylation, a widely recognized Aurora B substrate, compared to mitotically-arrested cells only treated with nocodazole (cf lane 2+3 and 5, panel vii, Fig. 3.18). As a consequence of mitotic slippage, APC5 phosphorylation status was abrogated under these conditions (cf lane 2+3 and 5, panel ii, Fig. 3.18). However, akin to the Cdk1 inhibition experiment, co-treatment with the 26S proteasome inhibitor, MG132, and Hesperadin was sufficient to prevent mitotic slippage, as evidenced by the similar levels of the APC/C substrates Cyclin B1, Plk1 and Bub1 in cells only treated with nocodazole and cells treated with the Aurora B inhibitor plus MG132 (cf lane 2+4 and 6, panel iii, iv and v, Fig. 3.18). Similarly, APC3 phosphorylation was preserved in cells co-treated with Hesperadin and MG132 compared to mitotically-arrested cells (cf lane 2+4 and 6, panel i, Fig. 3.18). As expected, inhibition of Aurora B caused the complete loss of the histone H3-Ser10 phosphorylation, as Aurora B is responsible for histone H3-Ser10 phosphorylation in mitosis. Interestingly, under the same conditions phosphorylation of APC5 was completely lost and its levels appeared similar to those observed in asynchronous cells, indicating that Aurora B might also play a role in the phosphorylation of APC5 (cf lane 1+4 and 6, panel ii, Fig. 3.18).

Overall, our data has revealed that APC5 is phosphorylated during mitosis and that multiple kinases might be responsible for this event. In fact, inhibition of Cdk1, Plk1 and Aurora B could all restore the binding capacity of our α-APC5 mAb for APC5, indicating that all these

inhibitory treatments could abrogate APC5 mitotic phosphorylation. It is not yet clear however whether all these kinases participate directly towards the phosphorylation of APC5. In fact, the three kinase inhibitors all recovered the APC5 un-phosphorylated band when cells were arrested in mitosis (Fig. 3.16, Fig. 3.17 and Fig. 3.18). It cannot be excluded however that only one of these kinases is directly responsible for the mitotic phosphorylation of APC5 and that the other kinases might only affect this event indirectly. Therefore, unequivocal identification of the APC5 residue phosphorylated in mitosis is critical to understanding the pathway responsible for APC5 mitotic phosphorylation as well as the kinases responsible for this phosphorylation event.

3.8 APC5 phospho-site fine-mapping

Results obtained so far have helped establish that APC5 is likely to be almost entirely phosphorylated at one particular residue during mitosis. We found that our in-house mAbs directed towards APC5 all bind to the same epitope and fail to recognize APC5 when APC5 is phosphorylated in mitosis (Fig. 3.9). Moreover, we found that inhibition of any of the mitotic kinases: Cdk1, Plk1 and Aurora B was able to restore the binding capacity for these mAb's for APC5 in mitosis, indicating that all of these kinases could play a role in the phosphorylation of a specific APC5 residue during mitosis (Fig. 3.16, Fig. 3.17 and Fig. 3.18). However, we cannot as yet unequivocally state which of these kinases is directly responsible for APC5 phosphorylation. As mitotic kinases target distinct sites within consensus sequences, we deemed it important to establish which APC5 residue is phosphorylated during mitosis, as this would help identify the kinase responsible.

3.8.1 α-APC5 mAbs recognize the same epitope in APC5

To establish which APC5 residue is phosphorylated in mitosis we decided to take advantage

of the fact that all our mAbs against APC5 bind to the same epitope. We therefore decided to perform a fine mapping exercise to identify the α-APC5 epitope in APC5. To do this we generated four GST-APC5 Fragments that cover the entire open reading frame of the APC5 protein (Fr1, Fr2, Fr3 and Fr4, Fig. 3.19). Importantly, the GST-APC5 fragments were expressed in bacteria, and as such they were not phosphorylated. Following purification on GST-agarose we performed Western blotting to test the ability of various α-APC5 mAbs (#4, #22, #23, #24, #33 and #38) to bind to the GST-APC5 fragments. We also used an α-GST specific antibody to validate protein loading (Fig. 3.19).

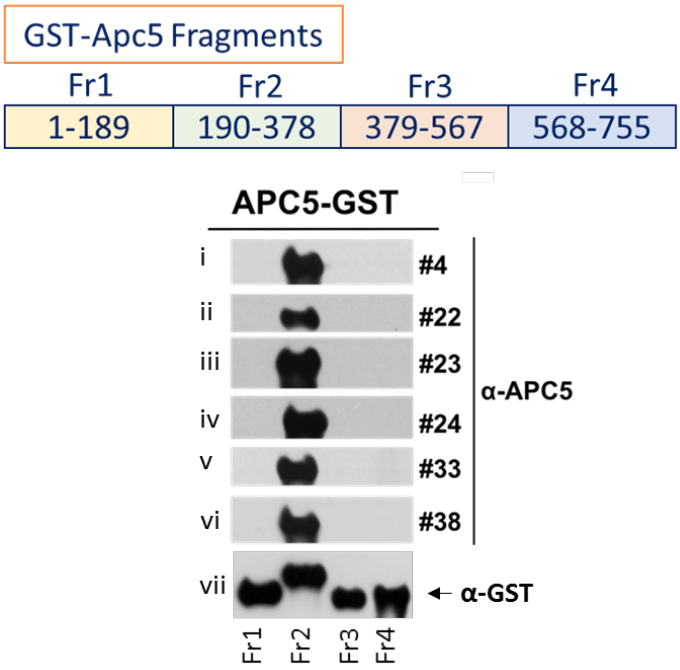

Figure 3. 19: **α-APC5 mAbs all bind to a region of APC5 encompassing residues 190-378.** 100 ng of GST-Apc5 purified fragments (Fr1, Fr2, Fr3 and Fr4) were separated by SDS-PAGE, transferred to a nitrocellulose membrane and subject to Western blotting with α-APC5 mAbs (#4, #22, #23, #24, #33, #38). The GST specific antibody (α-GST) was used as loading control. This data is representative of three individual experiments.

Western blot analyses confirmed that all the α-APC5 mAbs tested bound to the same GST-APC5 Fragment, Fragment 2 (Fr2), which corresponds to the region 190-378 of the APC5 amino acid sequence. The α-GST antibody was able to bind all the fragments through their

GST-Tag, verifying equal protein loading.

3.8.2 α-APC5 mAbs all bind to an epitope located between residues 190-237 within GST-APC5 Fragment 2

To fine-map the APC5 site of phosphorylation further, we generated GST-APC5 fragments of Fragment 2. Following their purification they were used to determine the binding avidity of the α-APC5 mAbs (#4, #22, #23, #24, #33 and #38) by Western blotting (Fig. 3.20).

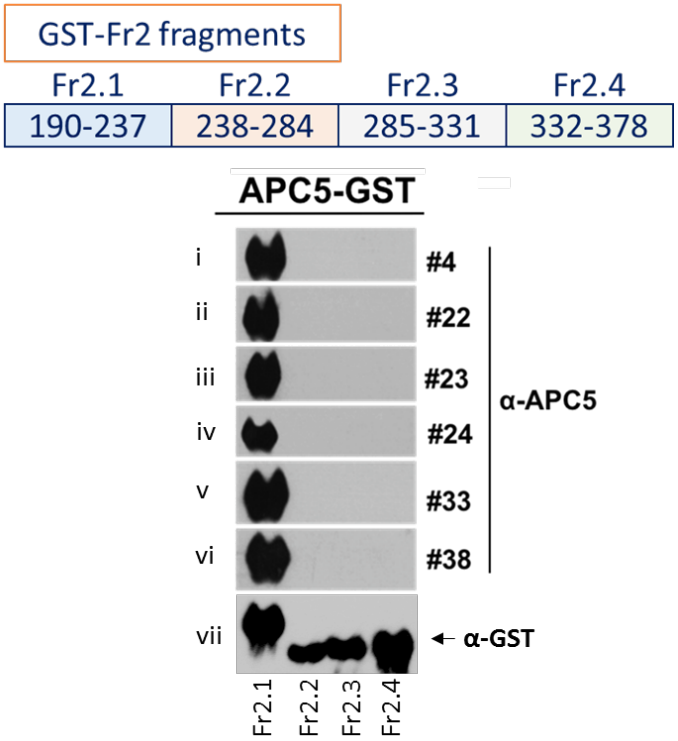

Figure 3. 20: **α-APC5 mAbs all bind to a region of APC5 encompassing residues 190-237.** 100 ng of purified GST-APC5 Fragment2 fragments (Fr2.1, Fr2.2. Fr2.3 and Fr2.4) were separated by SDS-PAGE, transferred to a nitrocellulose membrane and the α-APC5 mAbs (#4, #22, #23, #24, #33, #38) binding site was detected via Western Blotting. The GST specific antibody (α-GST) was used as loading control. This data is representative of three individual experiments.

Western blot analyses revealed that the α-GST antibody bound to all the GST-APC5 fragments, whilst the α-APC5 mAbs tested only bound to one region of Fragment 2, corresponding to amino acids 190-237.

3.8.3 APC5 region encompassing residues 190-237 contains consensus sites for mitotic kinases

The data obtained so far suggests that the APC5 mitotic phosphorylation site exists between amino acids 190-237. We therefore performed a multiple alignment over this region to identify potential consensus kinase motifs and evaluate their conservation among different species (Fig. 3.21).

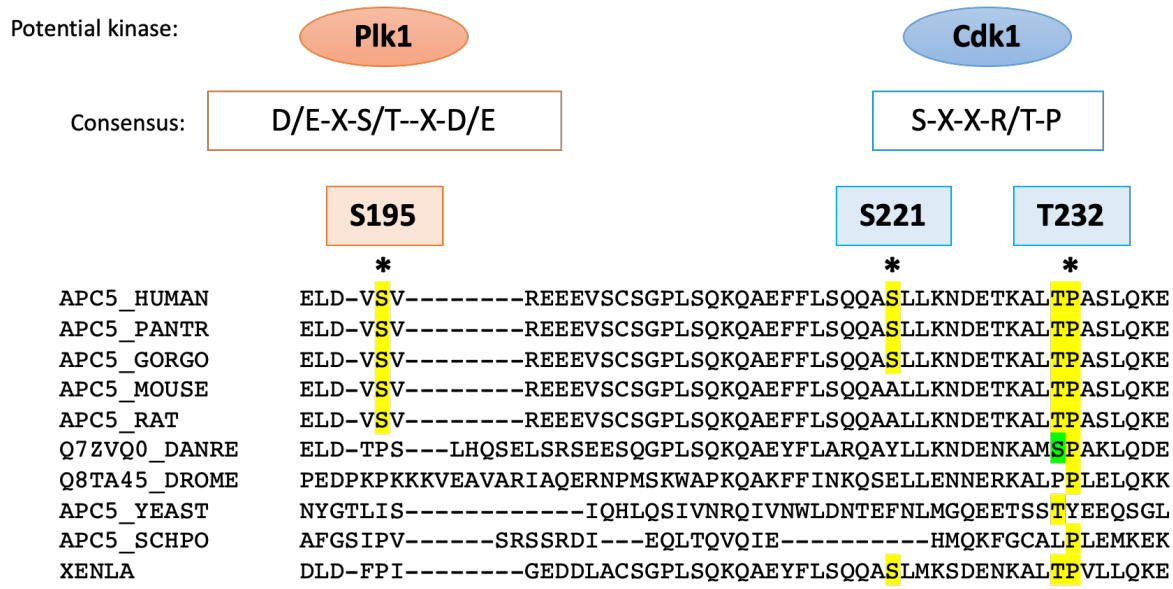

Figure 3. 21: **APC5 190-237 contains one potential phosphorylation site for Plk1 and two potential phosphorylation sites for Cdk1.** Clustal Omega multiple alignment of the APC5 region encompassing residues 190-237 from different species showing putative phosphorylation sites, kinase consensuses and their conservation (Clustal Omega, 2019).

The results of our *in silico* analysis identified three putative phosphorylation sites within the region 190-237: S195, which corresponds to a potential Plk1 site (D/E-X-S/T-X-X-D/E); and S221 and T232, which correspond to potential Cdk1 site (S-X-X-R/T-P) (Nakajima et al., 2003, Holt et al., 2009).

3.8.4 APC5 is phosphorylated in mitosis on S195

Consistent with our previous findings related to the involvement of Cdk1 and Plk1 in the mitotic phosphorylation of APC5, the use of bacterially purified GST-fragments of APC5 led to the identification of three potential phosphorylation sites within the 190-237 region of APC5 that could serve as potential substrate for Plk1 (S195) or Cdk1 (S221 and T232).

To identify unequivocally the APC5 residue that is phosphorylated in mitosis and is responsible for the mitotic epitope-masking phenomenon, we decided to undertake a site-directed mutagenesis approach (see Sec. 2.3.5, Chapter 2). To do this, we generated a GST-APC5 fragment comprising amino acids 1-400 (GST-APC5 1-400), which was used as a template to generate phospho-serine (S) and phospho-threonine (T) mimics by substitution of the S195 and S221 with aspartic acid (D) and substitution of the T232 residue with a glutamic acid (E) (Fig. 3.22 A). This site-directed mutagenesis approach allowed us to successfully generate GST-APC5 1-400: S195D, S221D, and T232E single mutants (Fig. 3.22 B) that were then used for Western blot analysis to test the ability of two α-APC5 mAbs (#4 and #24) to recognize to these GST-APC5 mutants (Fig. 3.22).

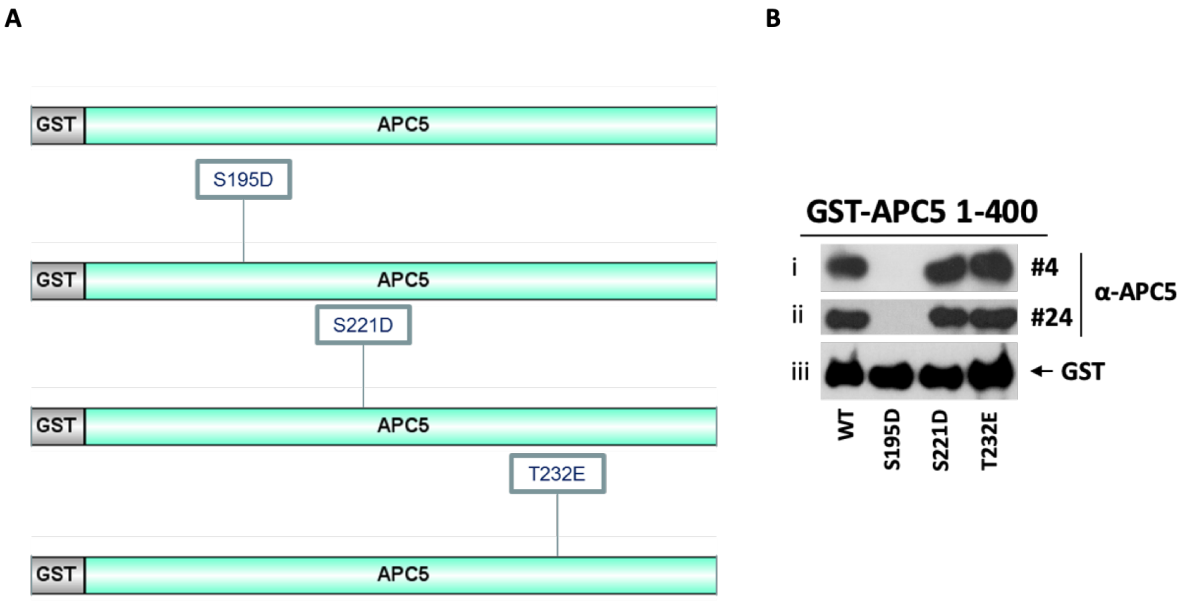

Figure 3. 22: **APC5 mitotic phosphorylation occurs on the Plk1 consensus site S195.** (**A**) Schematic representation of GST-APC5 1-400 WT, S195D, S221D and T232E. (**B**) 100 ng of purified GST-APC5 1:400 purified proteins corresponding to the WT and to the APC5 phospho-mimicking mutants S195D, S221D and T232E were separated by SDS-PAGE, transferred to a nitrocellulose membrane and the ability of the α-APC5 mAbs #4 and #24 to recognize their epitope was detected via Western Blotting. The GST specific antibody (α-GST) was used as loading control. This data is representative of three individual experiments.

The Western blot results revealed that the S195D phospho-mimic prevented the α-APC5 mAbs from recognizing the APC5 epitope, whilst phospho-mimics S221D and T232E did not mask the APC5 epitope. Taken together, these results suggest that phosphorylation of APC5 S195 in mitosis is responsible for the epitope-masking phenomenon, and that the cellular pool of APC5 is almost entirely phosphorylated on this residue during mitosis. The kinase responsible for APC5 S195 phosphorylation during mitosis is likely to be Plk1.

3.9 Discussion

Although initial observations suggested that APC5 might be degraded early in mitosis in a SAC-insensitive manner (Fig. 3.1 and 3.2), studies with our FLAG-APC5 U2OS FRT cell

lines revealed that FLAG-APC5 protein levels were not altered in mitosis relative to asynchronous cells (Fig. 3.8 A and B). In the light of these results we fine-mapped the epitope for our collection of α-APC5 mAbs, which demonstrated that all of the mAbs raised against APC5 bound to the same epitope, which was recognized in asynchronous cells, but not mitotic cells (Fig. 3.9). As the APC/C is subject to extensive phosphorylation in mitosis (Qiao et al., 2016, Zhang et al., 2016, Golan et al., 2002, Kraft et al., 2003, Fujimitsu et al., 2016, Herzog et al., 2005, Hegemann et al., 2011) we postulated that phosphorylation of APC5 during mitosis might mask the epitope for our α-APC5 mAbs such that it appears that APC5 protein levels are reduced in mitosis, when in fact APC5 phosphorylation masks antibody recognition. Consistent with this hypothesis λ-phosphatase treatment of α-APC7 IPs restored the ability of our α-APC5 mAbs to recognize APC5 in mitosis (Fig. 3.10).

Looking at the dynamics of APC5 phosphorylation during mitosis we determined that APC5 phosphorylation was strictly dependent upon cell cycle status and was not affected by genotoxic stress (Fig. 3.14 and 3.15). Moreover, the use of Reversine to overcome the SAC indicated that APC5 is de-phosphorylated as cells progress though mitosis (Fig. 3.11 and 3.12). Overall, these data allowed us to define the timing of APC5 phosphorylation, which occurs following mitotic entry and is sustained throughout the APC/C-mediated degradation of Cyclin B1 and Bub1, and the commencement of Plk1 degradation (e.g. Fig 3.1). As the APC/C activation status changes during this time, passing from SAC-dependent inhibition to Cdc20-mediated activation, it is possible that APC5 phosphorylation in mitosis could contribute to the fine-tuning of APC/C mitotic activity. In support of this idea, cryo-EM studies indicate that APC5 conformation is altered dramatically (shifts downwards), relative to the whole APC/C holoenzyme when the SAC is satisfied, and occurs concomitantly with the dislocation of the APC15 helix (Fig. 1.6) (Alfieri et al., 2016). As PTMs can strongly

affect protein conformation by changing the charge-status of the residues they modify, PTMs are often used by cells as a rapid mechanism to regulate enzyme activity through the modulation of intra- and inter- molecular interactions (Paleologou et al., 2008, Hunter, 2012). As such, APC5 phosphorylation, which, according to our data, occurs upon almost the entire cellular pool of APC5 during mitosis (Fig. 3.10), could contribute towards the regulation of APC/C activity during the different stages of mitosis.

To shed light on the effect of APC5 phosphorylation in the regulation of the APC/C holoenzyme activity, it was critical to identify unequivocally the specific APC5 phosphorylation site and the mitotic kinase responsible for this phosphorylation event. To do this we adopted a fine-mapping approach using GST-APC5 fragments corresponding to the entire open-reading frame of the APC5 protein. To do this we employed a panel of α-APC5 mAbs produced in our laboratory to identify the APC5 residue that is subject to phosphorylation during mitosis. This approach allowed us to map the antibody epitope on APC5 to the amino acid sequence corresponding to residues 190-237 of the APC5 protein (Fig. 3.19 and 3.20). As our mAbs all recognised the same epitope on APC5 this approach worked extremely well. Whilst designing these experiments we also considered using phage display to generate a random peptide library that could be expressed on the phage surface to identify the α-APC5 mAb epitope (Fack et al., 1997), but fortunately, this approach was not needed.

Multiple alignment of the APC5 sequence corresponding to the region encompassing residues 190-237 revealed the presence of three, potentially conserved, phosphorylation sites that could, theoretically, be targeted by Plk1 (S195) or Cdk1 (S221, T232) according to kinase consensus motifs (Fig. 3.21) (Nakajima et al., 2003, Holt et al., 2009). Interestingly,

a PhosphoSite Plus search of APC5 revealed that all three sites had been identified previously as being phosphorylated during mitosis in various mass spectrometric screens (Herzog et al., 2005, Steen et al., 2008, Hegemann et al., 2011). However, no information about the extent of protein phosphorylation, nor the physiological effect of these phosphorylation events upon APC/C activity have been reported to date. As Cdk1 and Plk1 play crucial roles in the regulation of mitotic progression, including the Cdk1-dependent regulation of APC/C activity (Fujimitsu et al., 2016), it was essential to define unequivocally the APC5 phosphorylation site recognised by our α-APC5 mAbs. To do this we undertook a site-directed mutagenesis approach aimed at mimicking phosphorylation of these three potential sites. We therefore generated a GST-APC5 1-400 fragment and used it as a template to produce the S195D, S221D and T232E phospho-mimic mutants (Fig. 3.22 A and B). Using these mutants we determined that the APC5 mitotic phosphorylation site recognized by our α-APC5 mAb corresponded to the putative Plk1-targeted residue, S195 (Fig. 3.22 C).

A requirement for Plk1 in the mitotic phosphorylation of APC5 was consistent with the results we obtained when we inhibited Plk1 activity during mitosis (Fig. 3.17). However, a role for Cyclin B1-Cdk1 in APC5 mitotic phosphorylation cannot be excluded. As APC5 T232 is a potential Cdk1 phosphorylation site, which has been reported to be phosphorylated during mitosis (Steen et al., 2008), it is possible that prior Cdk1-dependent phosphorylation on this site is required for Plk1 to phosphorylate APC5 at S195. Consistent with this hypothesis, inhibition of Cdk1 kinase activity in mitotically-arrested cells also resulted in the attenuation of APC5 phosphorylation during mitosis (Fig. 3.16). Interestingly, it appeared that Aurora B kinase activity also contributed towards APC5 mitotic phosphorylation at S195 (Fig. 3.18). Given the extensive crosstalk between the various

mitotic kinases it is possible that Aurora B regulation of Cdk1, or Plk1 activities, also modulates S195 phosphorylation (Cuijpers and Vertegaal, 2018). Moreover, in addition to the Plk1-Cdk1 axis already discussed, some reports suggest that Aurora B kinase is activated by substrates previously phosphorylated by both Plk1 and Cdk1 mitotic kinases (Cuijpers and Vertegaal, 2018, Petronczki et al., 2008). Indeed, Aurora B-dependent phosphorylation of the MCAK (Mitotic Centromere-Activated Kinesin) protein is influenced by Cdk- and Plk1-mediated phosphorylation of the same protein (Ritter et al., 2015). Therefore, it is possible that the Cdk1 and Plk1-dependent activation of Aurora B could facilitate APC5 S195 phosphorylation by one of these three kinases, which is most likely to be Plk1 based on the known specificities of these kinases. This, however, awaits clarification.

Overall, we found that APC5 is phosphorylated at S195 at the beginning of mitosis and remains phosphorylated at least until the commencement of APC/C-mediated degradation of SAC-sensitive substrates (Fig. 3.11-3.14). As this phosphorylation event occurs concomitantly with various regulatory processes affecting APC/C activity, including SAC inhibition of the APC/C, the switching of the APC/C into the active conformation and the interaction of the APC/C with its co-activators, it will be interesting in the future to determine the impact of APC5 S195 phosphorylation on the function of the APC/C holoenzyme (Kraft et al., 2003, Golan et al., 2002, Fujimitsu et al., 2016, Lara-Gonzalez et al., 2012). Indeed, as APC5 is part of the APC/C platform domain that is responsible for connecting the catalytic core to the TPR domain of the holoenzyme (Chang et al., 2015), this phosphorylation event could potentially, cause extensive conformational changes that might alter APC/C function during mitosis, akin to the regulation of APC/C activity by the Cdk1-dependent phosphorylation of APC1 and APC3 (Zhang et al., 2016).

CHAPTER 4: INVESTIGATING THE ROLE OF APC5 AND APC5 S195 PHOSPHORYLATION IN MITOSIS

4.1 Introduction

Our investigations so far have established that Plk1 phosphorylates the APC/C platform subunit APC5 at S195 during mitosis and that Cdk1 might play a role in the regulation of this phosphorylation event. Indeed, inhibition of both Plk1 and Cdk1 kinases during mitosis attenuated APC5 phosphorylation (Fig. 3.16 and 3.17). It was clear from our data that almost the entire cellular pool of APC5 is phosphorylated upon S195 during mitosis (Fig. 3.10). Akin to APC1 and APC3 phosphorylation that allows the APC/C holoenzyme to acquire its active conformation during mitosis (Zhang et al., 2016), we anticipate that APC5 mitotic phosphorylation could similarly represent an important level of regulation for the APC/C's mitotic activity. With this in mind, we therefore decided to investigate APC5 phosphorylation in more detail, to understand its biological role and its impact on APC/C function in mitosis. To fulfil these aims, as it will be discussed in more detail during this chapter, we decided to generate a series of stable, Doxycycline-inducible U2OS FRT monoclonal cell lines that either mimic (FLAG-APC5 S195D) or ablate (FLAG-APC5 S195A) S195 phosphorylation, to be used as a tool to investigate the role of S195 phosphorylation (pS195) on APC/C activity and regulation. Additionally, to clarify the role played by the Cdk1 mitotic kinase in the regulation of the, purported, Plk1-dependent phosphorylation of APC5, we also generated U2OS FRT monoclonal cell lines that either mimic or inhibit phosphorylation of the APC5 residue, T232 (FLAG-APC5 T232E and FLAG-APC5 T232A, respectively). This decision was based on data published by Kirschner's group, who determined that APC5 was phosphorylated at T232 during mitosis

(Steen et al., 2008). As T232 and S195 lie close to each other within APC5's primary sequence, and T232 is part of a typical Cdk1 consensus, we considered it appropriate to investigate the relationship between these two phosphorylation sites, and clarify the role played by Plk1 and Cdk1 in the phosphorylation of S195. Moreover, to understand in more detail the role of APC5 in mitosis we investigated the molecular and biological consequences of APC5 knockdown. The results from these investigations are presented in this chapter.

4.2 FLAG-APC5 phospho-mutant U2OS FRT cell lines

4.2.1 Generation of FLAG-APC5 S195A and S195D U2OS FRT stable cell lines

To start our investigation into the physiological role of APC5 phosphorylation at S195 during mitosis, we employed site-directed mutagenesis, described previously (Sec. 3.8.4, Chapter 3), to generate the phospho-mimicking FLAG-APC5 S195D mutant using our pcDNA5 FRT FLAG-APC5 WT as a template. We similarly generated the FLAG-APC5 phosphorylation-defective mutant, FLAG-APC5 S195A by substituting the serine residue with an alanine, to create a form of the APC5 that could no longer be phosphorylated at this residue. Once these pcDNA5 FLAG-APC5 mutants were validated by Sanger sequencing, they were used to generate U2OS FRT monoclonal cell lines, that in response to Dox expressed the FLAG-tagged mutant forms of the APC5 protein, i.e. FLAG-APC5 S195A and FLAG-APC5 S195D. These cell lines were generated in an identical manner to that described previously for FLAG-APC5 WT U2OS FRT cell lines (Sec. 3.4.1, Chapter 3). The ability of these cell lines to express mutant APC5 species, in response to Dox, was validated by Western blotting (Fig. 4.1 A and B).

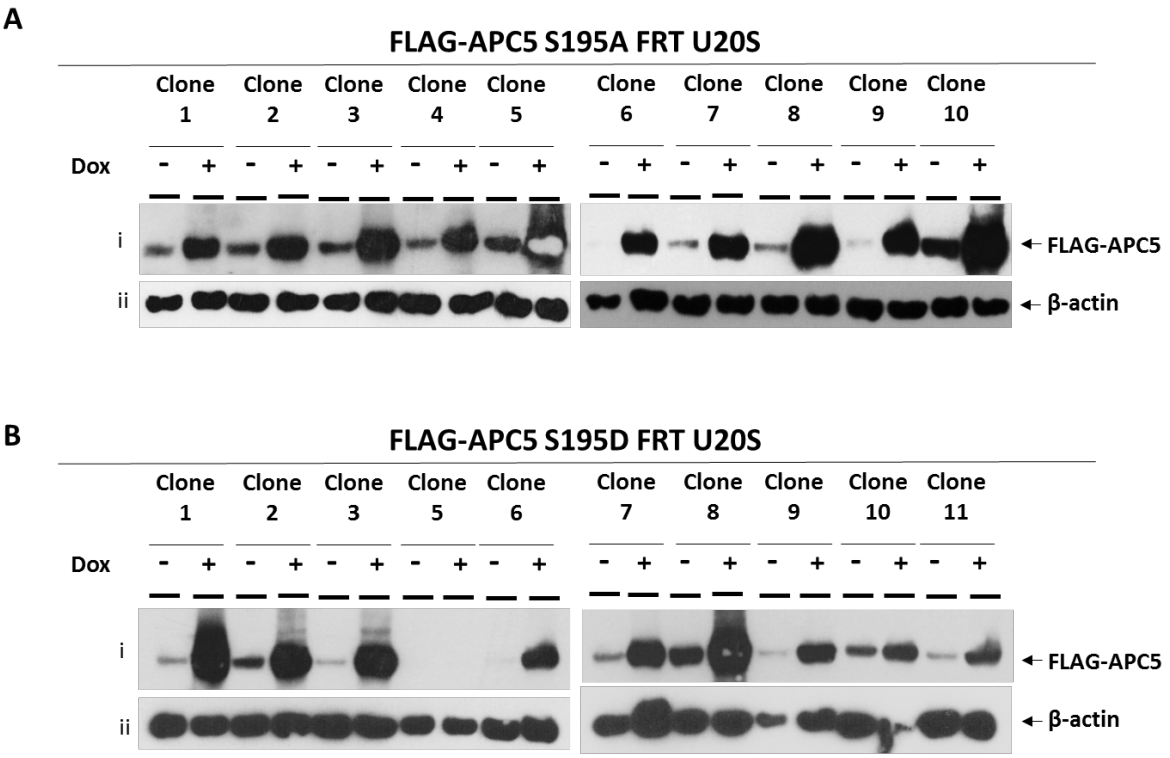

Figure 4. 1: **Expression of FLAG-APC5 S195A and S195D phospho-mutants in U2OS cells treated with doxycycline.** Lysates from doxycycline-induced (Dox+) and non-induced (Dox-) FLAG-APC5 S195A (**A**) and S195D (**B**) U2OS FRT clones were harvested in UTB lysis buffer. 50µg of total protein was separated by SDS-PAGE, transferred to a nitrocellulose membrane and the level of FLAG-APC5 was detected using an α-FLAG specific antibody by Western blotting. The levels of β-actin were used as a loading control.

The Western blotting results revealed that both FLAG-APC5 S195A and FLAG-APC5 S195D U2OS FRT monoclonal cell lines were generated successfully, and most of the clones expressed FLAG-APC5 protein following Dox induction with relatively low levels of exogenously-expressed proteins in the absence of Dox (panel i, Fig. 4.1 A and B). Based on these results, we selected FLAG-APC5 S195A Clone 8 (#8, Fig. 4.1 A) and FLAG-APC5 S195D Clone 3 (#3, Fig. 4.1 B) for further experiments.

4.2.2 Generation of FLAG APC5 T232A and T232E U2OS FRT stable cell lines

Given the potential role of Cdk1 in regulating APC5 phosphorylation at S195 by Plk1 during mitosis (Sec. 3.7.1, Chapter 3), site-directed mutagenesis was also employed to generate the

phospho-mimicking and phospho-inhibitory forms of APC5 T232, i.e T232A and T232E, respectively. Once again, these mutants were created using the pcDNA5 FLAG-APC5 WT construct as a template, and the resulting sequence-validated constructs were then employed to generate U2OS FRT monoclonal stable cell lines that could express the mutant forms FLAG-APC5 T232A and FLAG-APC5 T232E in response to Dox treatment. The efficiency of this procedure was again assessed by Western blot (Fig. 4.2, A and B).

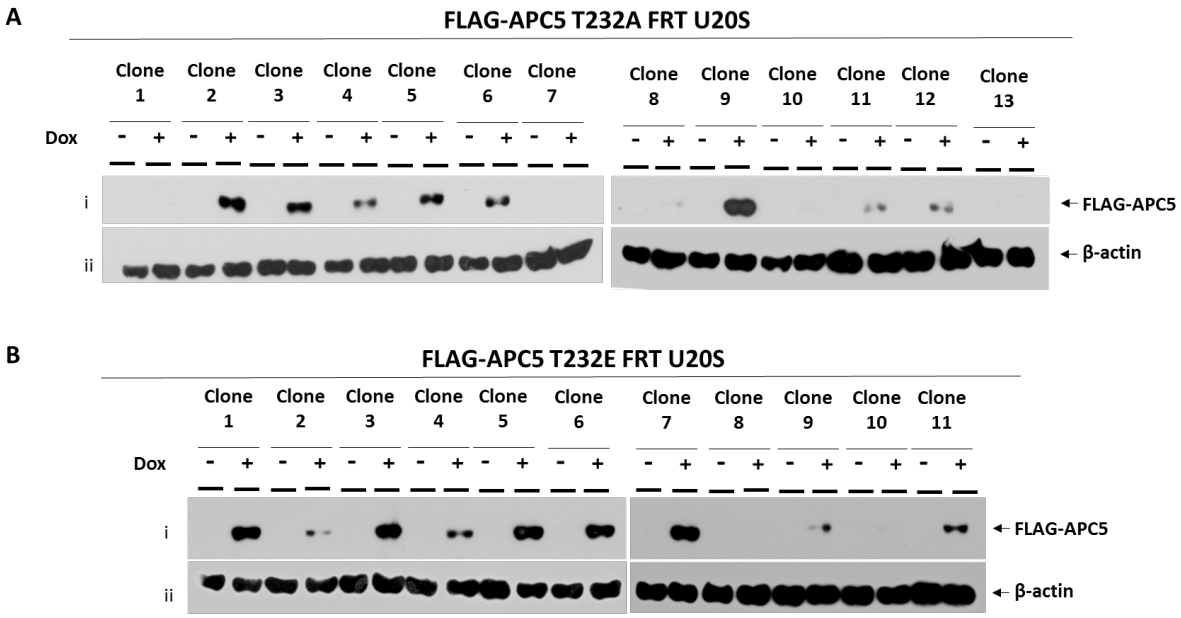

Figure 4. 2: **Expression of FLAG-APC5 T232 phospho-mutants in U2OS cells treated with doxycycline.** Lysates from doxycycline-induced (Dox+) and non-induced (Dox-) FLAG-APC5 T232A (**A**) and T232E (**B**) U2OS FRT clones were harvested in UTB lysis buffer. 50µg of total protein was separated by SDS-PAGE, transferred to a nitrocellulose membrane and the level of FLAG-APC5 was detected using an α-FLAG specific antibody by Western blotting. The levels of β-actin were used as a loading control.

Western blotting results confirmed the efficient generation of stable U2OS FRT monoclonal cell lines expressing good levels of FLAG-APC5 T232A and FLAG-APC5 T232E recombinant proteins following Dox induction (panel i, Fig. 4.2 A and B). Among the various clones generated, FLAG-APC5 T232A Clone 9 (#9, Fig. 4.2 A) and FLAG-APC5 T232E Clone 1 (#1, Fig. 4.2 B) were selected for future experiments.

4.2.3 FLAG-APC5 mutant proteins are incorporated into the APC/C holoenzyme

The successful generation of the U2OS FRT monoclonal cell lines expressing the S195 and T232 phospho-mimicking and inhibitory species of APC5, provided us with a potential tool to study the role of APC5 mitotic phosphorylation on the APC/C holoenzyme activity and its regulation during mitosis. However, as the APC/C is a multi-subunit protein complex, it was paramount to establish, in the first instance, whether these exogenous APC5 species were incorporated successfully into the active APC/C complex. To address this, we tested the ability of all exogenous FLAG-APC5 species to interact with the APC/C subunit, APC7, following Dox-induction of both asynchronous and mitotically-arrested U2OS FRT monoclonal cell lines, obtained by treatment with nocodazole. As such, we performed a series of IP assays from each of the selected U2OS FRT cell lines using an α-APC7 Ab, and then performed Western blotting analyses to validate the ability of FLAG-APC5 species to interact with APC7, and hence the APC/C holoenzyme (Fig. 4.3 A, B, C, D, E).

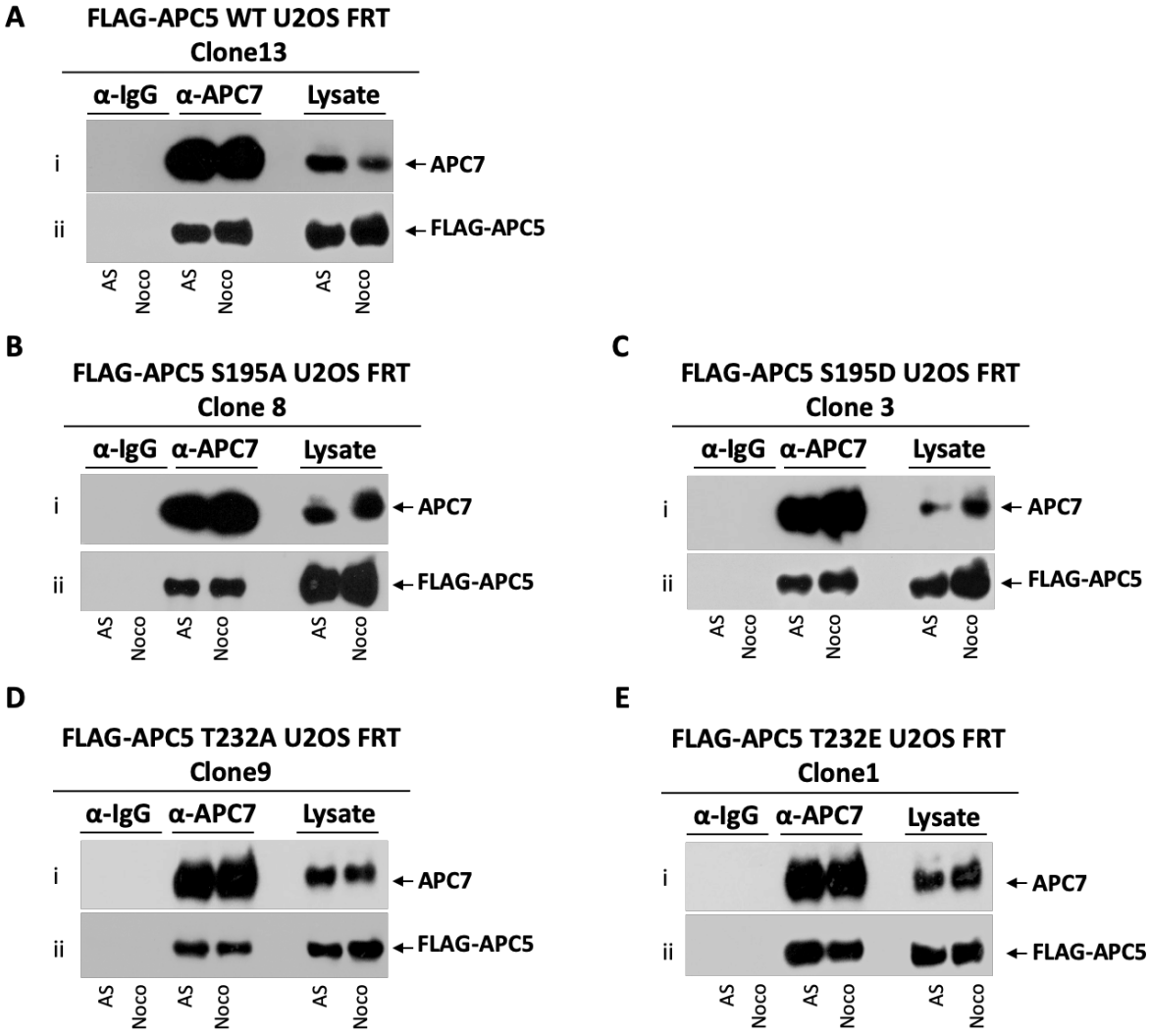

Figure 4. 3: **FLAG-APC5 species are incorporated into the APC/C holoenzyme.** Lysates from asynchronous (AS) and mitotically-arrested (Noco) FLAG-APC5 WT (**A**), FLAG-APC5 S195A (**B**), FLAG-APC5 S195D (**C**), FLAG-APC5 T232A (**D**) and FLAG-APC5 T232E (**E**) U2OS FRT cells were obtained by incubation in APC/C Lysis Buffer. An equal amount of total protein from AS and Noco cells was incubated overnight at 4°C with an APC7 specific antibody (α-APC7) or with normal rabbit IgG (α-IgG) followed by collection of immunoprecipitates upon Protein G Sepharose beads. Immunoprecipitated proteins and 50μg of total protein lysate were separated by SDS-PAGE, transferred to a nitrocellulose membrane and the levels of APC7 and FLAG-APC5 were detected by Western blotting. These data are representative of three individual experiments.

The results of these IPs revealed that all exogenously-expressed FLAG-APC5 species from our stable U2OS FRT cell lines were incorporated efficiently into the APC/C holoenzyme in both asynchronous and mitotic cells (panel ii, Fig. 4.3 A, B, C, D and E). Indeed, IP with

an α-APC7 Ab, co-precipitated the FLAG-APC5 species in all instances (panel ii, Fig. 4.3 A, B, C, D and E). Fortunately, control IPs with a rabbit IgG antibody in both asynchronous and in mitotically-arrested cells did not co-precipitate FLAG-APC5 (cf lane 1+3 and 2+4, Fig. 4.3 A, B, C, D and E). Overall, these data indicate that the FLAG-APC5 species are incorporated effectively into the APC/C complex, in both asynchronous and mitotic cells. As such our FLAG-APC5 U2OS FRT cell lines are a, potential, valuable tool to investigate the effect of the APC5 phosphorylation at S195 and T232 on the APC/C activity.

4.3 FLAG-APC5 U2OS FRT stable cell lines as a tool to investigate the physiological effects of APC5 phosphorylation during mitosis

Once we established that the FLAG-APC5 proteins were appropriately incorporated within the APC/C complex (Fig. 4.3), we decided to use the newly generated FLAG-APC5 U2OS FRT cell lines to investigate the physiological role of APC5 phosphorylation at S195 in the regulation of APC/C activity in mitosis.

4.3.1 Expression of FLAG-APC5 proteins in the presence of endogenous APC5 delays mitotic progression

In the first instance, we utilised our U2OS FRT monoclonal cell lines expressing the FLAG-APC5 S195 mutants to investigate the effect of altering APC5 phosphorylation status on the APC/C activity by looking at the ability of cells to progress through mitosis. For this purpose, we performed a series of nocodazole-release experiments using the FLAG-APC5 WT #13, FLAG-APC5 S195A #8 and FLAG-APC5 S195D #3 U2OS FRT cell lines, in the presence or absence, of exogenously-expressed proteins (Fig. 4.4, 4.5 and 4.6). These experiments were performed as described previously for the FLAG-Cdc20 U2OS FRT cell line, where cells were arrested in mitosis by treatment with nocodazole, either with, or

without, prior induction with Dox, and then released into the cell cycle by nocodazole withdrawal (Sec. 3.3.2, Chapter 3). Western blotting analyses were then employed to evaluate the effect of the FLAG-APC5 expression on mitotic progression, by looking at the degradation pattern of some APC/C substrates and at the phosphorylation status of the APC/C subunits APC3 and APC5 (Fig. 4.4, 4.5 and 4.6).

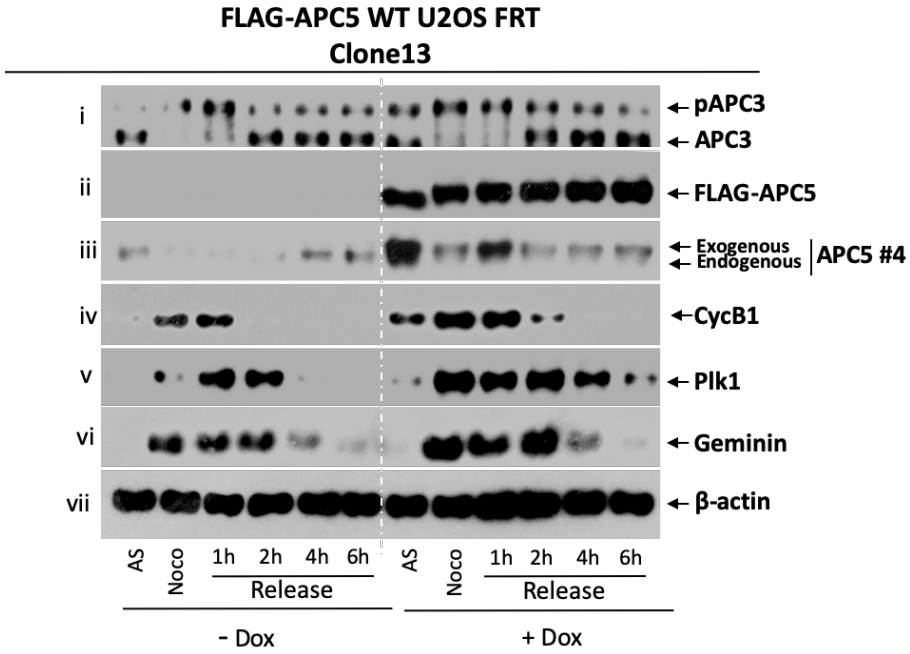

Figure 4. 4: **Effects of FLAG-APC5 WT expression on mitotic progression.** Cell lysates from U2OS FRT FLAG-APC5 WT #13 asynchronous cells (AS), nocodazole-arrested cells (Noco) and cells released from the mitotic arrest at different time points (1h, 2h, 4h and 6h), both in presence or absence of Dox (-/+ Dox), were harvested in UTB lysis buffer. 50µg of total protein was separated by SDS-PAGE, transferred to a nitrocellulose membrane and the levels of APC3, APC5, and FLAG-APC5, together with the levels of the APC/C mitotic substrates Cyclin B1, Plk1 and Geminin were determined by Western blotting. The levels of β-actin were used as a loading control. These data are representative of three individual experiments.

Consistent with our previous data, FLAG-APC5 WT levels were constant in asynchronous and mitotically-arrested cells, and following nocodazole withdrawal; as anticipated no FLAG-APC5 WT was detected in the absence of Dox (panel ii, Fig. 4.4). Consistent with

APC5 mitotic species not being recognized by the α-APC5 mAb #4, both endogenous APC5 and FLAG-APC5, represented by the slightly shifted higher molecular weight band, were low in nocodazole-arrested cells and during the initial stages of the mitotic release either in the presence or absence of Dox (panel iii, Fig. 4.4). Although it appeared that FLAG-APC5 was de-phosphorylated 1h after nocodazole withdrawal, as detected by the α-APC5 mAb #4 in the Dox-treated samples, the overall phosphorylation status of APC5 did not appear compromised during mitosis following Dox induction, suggesting that the FLAG-APC5 WT species is subjected to the same level of phosphorylation as endogenous APC5 during mitosis (panel iii, Fig. 4.4). Western blot detection of APC/C substrates and APC3 phosphorylation status, revealed that expression of FLAG APC5 WT caused a delay in mitotic expression (Fig. 4.4). Indeed, although cells were synchronized successfully in mitosis both in the presence or absence of Dox treatment, as indicated by the appearance of the hyper-phosphorylated APC3 form, and by the accumulation of the APC/C substrates Cyclin B1, Plk1 and Geminin in nocodazole-treated cells, these proteins persisted for longer following nocodazole withdrawal for those cells treated with Dox, relative to untreated samples (panel i, iv, v and vi, Fig. 4.4). Interestingly, Dox-treated cells also seemed to accumulate higher amounts of the APC/C substrates Cyclin B1, Plk1 and Geminin during the mitotic arrest compared to the corresponding Dox-untreated cells (cf lane 2 and 8, panel iv, v and vi, Fig. 4.4). Moreover, Dox-treated cells took longer to induce the degradation of these proteins following nocodazole-release compared to cells not treated with Dox, suggesting that the APC/C was working less efficiently when FLAG-APC5 WT was expressed (panel iv, v and vi, Fig. 4.4). Also, the APC3 phosphorylated form seemed to persist longer following nocodazole withdrawal when cells were treated with Dox compared to Dox untreated cells, possibly because of the persistence of Cyclin B1 which is responsible

for this phosphorylation event (panel i, Fig. 4.4). Taken together, these data indicate that FLAG-APC5 WT expression in the presence of endogenous APC5 might interfere with the normal mitotic progression of U2OS FRT cells by altering the APC/C holoenzyme mitotic activity.

Although the data obtained with the cell cycle studies with the FLAG-APC5 WT species were not promising, we decided to repeat the experiment using the FLAG-APC5 S195A and S195D U2OS FRT cell lines to get, at least, an indication of whether cell lines expressing mutant FLAG APC5 species differed in their ability to progress throughout mitosis, relative to the WT FLAG APC5 species. To investigate this possibility FLAG-APC5 S195A #8 and FLAG-APC5 S195D #3 U2OS FRT cells, either treated or untreated with Dox, were synchronized in mitosis by treatment with nocodazole and then released from the mitotic arrest by nocodazole withdrawal. Cells were then harvested at different time points and Western blot analyses were employed to determine the levels of the APC/C subunits APC3, APC5 and FLAG-APC5, as well as APC/C substrates Cyclin B1, Plk1 and Geminin to investigate the dynamic rate of mitotic progression (Figs. 4.5 and 4.6).

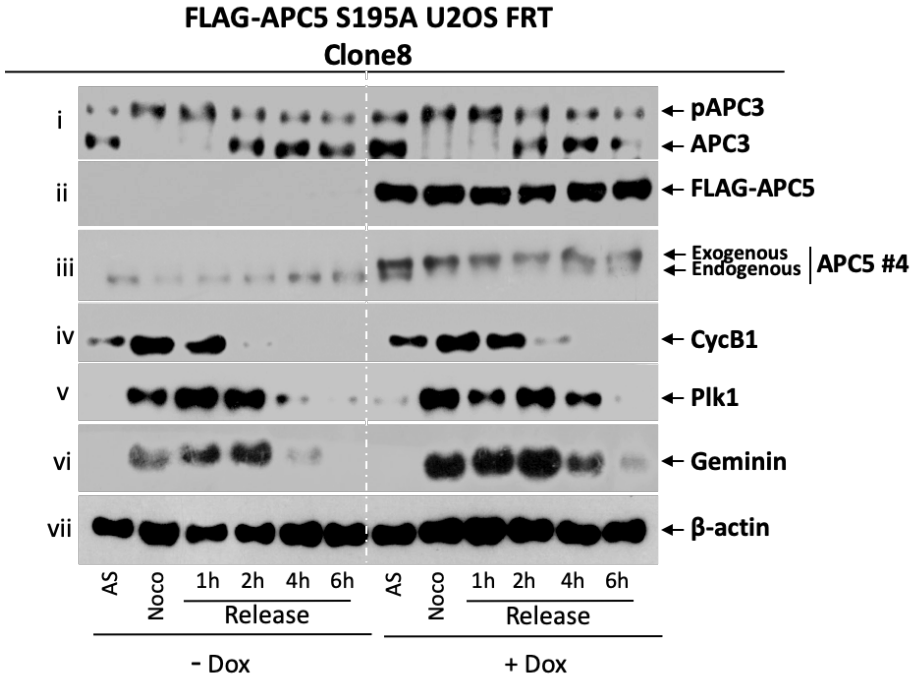

Figure 4. 5: **Effects of FLAG-APC5 S195A expression on mitotic progression.** Cell lysates from U2OS FRT FLAG-APC5 S195A #8 asynchronous cells (AS), nocodazole-arrested cells (Noco) and cells released from the mitotic arrest at different time points (1h, 2h, 4h and 6h) both in presence or absence of Dox (-/+ Dox), were harvested in UTB lysis buffer. 50μg of total protein was separated by SDS-PAGE, transferred to a nitrocellulose membrane and the levels of APC3, APC5, and FLAG-APC5 and mitotic substrates Cyclin B1, Plk1 and Geminin were determined by Western blotting. The levels of β-actin were used as a loading control. These data are representative of three individual experiments.

Consistent with our studies with FLAG-APC5 WT, FLAG-APC5 S195A was not detected in the absence of Dox treatment, but was expressed to high levels in the presence of Dox and remained stable following nocodazole treatment, and withdrawal (panel ii, Fig. 4.5). As expected, the results obtained for endogenous APC5 with the α-APC5 mAb #4, in the absence of Dox induction, were in perfect agreement with our previous nocodazole-release results (Fig. 3.1); the phosphorylation status of endogenous APC5 during mitosis was not compromised in the FLAG-APC5 S195A U2OS FRT cells in the absence of exogenously expressed FLAG-APC5 S195A (panel iii, Fig. 4.5). On the contrary, a higher molecular weight band, corresponding to the non-phosphorylatable form of APC5 S195A, was detected

at all time by the α-APC5 mAb #4 following Dox treatment, as it is not affected by the epitope-masking phenomenon (panel iii, Fig. 4.5). Looking at the dynamics of mitotic progression, the results for FLAG-APC5 S195A were similar to those obtained for FLAG-APC5 WT #13 U2OS FRT cells (Fig. 4.4). Indeed, the levels of the APC/C substrates Cyclin B1, Plk1 and Geminin again appeared to be higher in mitotically-arrested cells treated with Dox, relative to the Dox-untreated cells (cf lane 2 and 7, panel iv, v and vi Fig. 4.5). Likewise, the rate of their degradation following nocodazole withdrawal was slower in Dox-treated samples compared to Dox-untreated cells, suggesting that the expression of the FLAG-APC5 S195A recombinant protein caused a delay in the progression of cells through mitosis, in a similar manner to the one elicited by FLAG-APC5 WT (cf panel iv, v and vi, Fig. 4.4 and 4.5). Consistent with prolonged Cyclin B1 expression in Dox-treated cells the phosphorylation status of APC3 was higher following nocodazole-release of the FLAG-APC5 S195A expressing cells compared to cells only expressing endogenous APC5 (panel i, Fig. 4.5). Although the delay observed during mitosis by this mutant form of APC5 might reflect an alteration in APC/C activity, the results obtained did not differ significantly from FLAG-APC5 WT cells, such that we cannot determine whether inhibition of APC5 phosphorylation at S195 affects APC/C holoenzyme activity or mitotic progression (Fig. 4,4 and 4.5).

We next performed the same experiment with the FLAG-APC5 S195D U2OS FRT stable cell line #3, which expresses a phospho-mimicking APC5 mutant corresponding to a constitutively phosphorylated form of APC5. Western blot analyses were again employed to evaluate the effect of the expression of the recombinant protein on the dynamics of mitotic progression (Fig. 4.6).

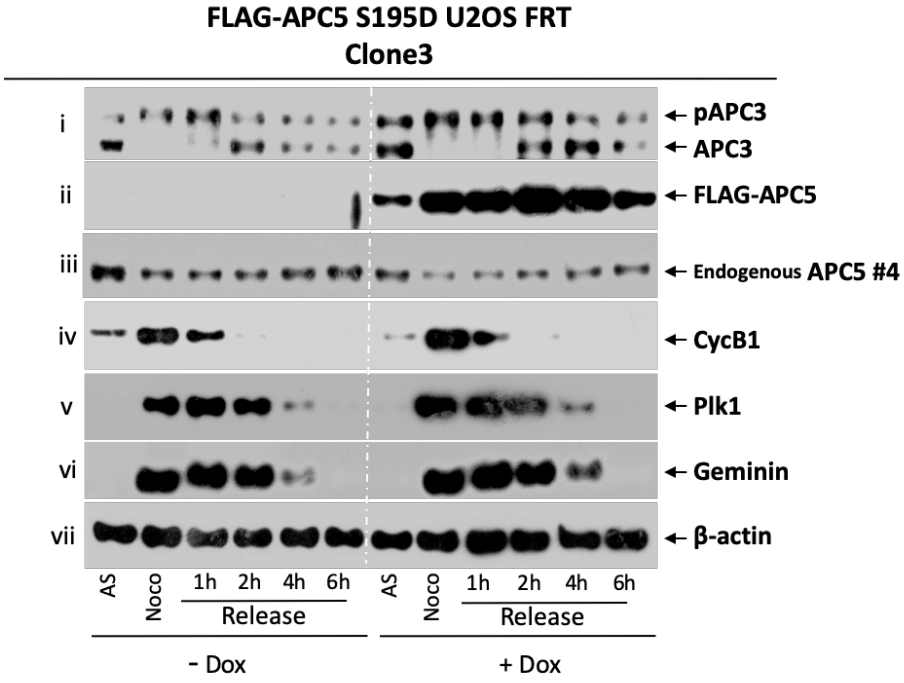

Figure 4. 6: **Effects of FLAG-APC5 S195D expression on mitotic progression.** Cell lysates from U2OS FRT FLAG-APC5 S195D #3 asynchronous cells (AS), nocodazole-arrested cells (Noco) and cells released from the mitotic arrest at different time points (1h, 2h, 4h and 6h) both in presence or absence of Dox (-/+ Dox), were harvested in UTB lysis buffer. 50µg of total protein was separated by SDS-PAGE, transferred to a nitrocellulose membrane and the levels of APC3, APC5, and FLAG-APC5, as well as the levels of the APC/C mitotic substrates Cyclin B1, Plk1 and Geminin were determined by Western blotting. The levels of β-actin were used as a loading control. These data are representative of three individual experiments.

As expected Western blotting revealed that the FLAG-APC5 S195D protein was not detected in the absence of Dox treatment, but was detected following Dox induction (panel ii, Fig. 4.6). Interestingly, in the presence of Dox there was a noticeable increase in the levels of the FLAG-APC5 S195D protein in mitotically-arrested cells and during the early stages of the mitotic release compared to interphase, potentially suggesting that APC5 protein stability increases during mitosis when it is phosphorylated (panel ii, Fig. 4.6). As established previously the phosphorylation status of endogenous APC5 was unaltered in the monoclonal FLAG-APC5 S195D U2OS FRT cells both in the presence or absence of Dox

(panel iii, Fig. 4.6). Interestingly however, different from what observed with the FLAG-APC5 WT or S195A cell lines, no higher molecular weight band corresponding to the recombinant FLAG-APC5 S195D protein species was detected at any time by the α-APC5 mAb #4 (cf panel iii, Fig. 4.4, 4.5 and 4.6). These results are considered to be a consequence of the FLAG-APC5 S195D form completely masking the APC5 mAb #4 epitope at all time points (cf panel iii, Fig. 4.4, 4.5 and 4.6). Moreover, and in contrast with what observed with the FLAG-APC5 WT and S195A cell lines, Western blotting with FLAG-APC5 S195D cells revealed no major differences in the levels of the APC/C substrates Cyclin B1, Plk1 and Geminin in nocodazole-arrested cells either treated or untreated with Dox, or in their degradation pattern following nocodazole withdrawal (cf lane 1+6 and 7+12, panel iv, v and vi, Fig. 4.6). APC3 phosphorylation also appeared slightly increased in mitotically-arrested cells expressing FLAG-APC5 S195D compared to cells only expressing endogenous APC5, which might suggest an effect of APC5 S195 constitutive phosphorylation on the phosphorylation status of APC3 during mitosis (cf lane 2+3 and 8+9, panel i, Fig. 4.6).

As FLAG-APC5 WT and S195A expression caused a mitotic delay, S195D expression did not. Taken together these data suggest that the FLAG-APC5 S195D species, which mimics a S195 phosphorylated form of APC5, potentially accelerates mitotic progression by increasing the APC/C mitotic activity against its substrates, as well as APC3 phosphorylation during mitosis (cf Fig. 4.4, 4.5 and 4.6). However, as expression of FLAG-APC5 WT delayed mitotic progression relative to cells expressing endogenous APC5 alone (Fig. 4.4), this dataset did not allow firm conclusions regarding the effect of APC5 phospho-mutants on mitotic progression dynamics to be drawn. We therefore needed to consider experimental alternatives to determine the 'real' effect of APC5 mitotic phosphorylation at position S195 on the overall activity of the APC/C in mitosis.

4.3.2 Doxycycline-inducible expression of FLAG-APC5 wild-type or mutant protein from U2OS FRT cells does not compensate for the knock-down of endogenous APC5

Given that exogenous expression of WT and S195A FLAG-APC5 species delayed mitotic progression in the presence of endogenous APC5, we reasoned that the expression of endogenous APC5 might have created an experimental artefact that accounted for the delayed normal mitotic progression of these cells. Therefore, we next decided to look at the effect of our exogenously-expressed FLAG-APC5 proteins on mitotic progression in the absence of the endogenous APC5 protein. To do this we took advantage of the fact that our original pcDNA5 APC5 WT FRT construct, had previously be rendered siRNA-resistant through mutation of 5 nucleotides that lie within the siAPC5 sequence (whilst retaining WT APC5 protein sequence). To validate these siRNA-resistant cells we transfected both Dox-treated and untreated FLAG-APC5 WT #13 U2OS FRT cells with a siRNA Luciferase control (siCTRL) or a siRNA targeted against the endogenous APC5 (siAPC5) gene (Fig. 4.7).

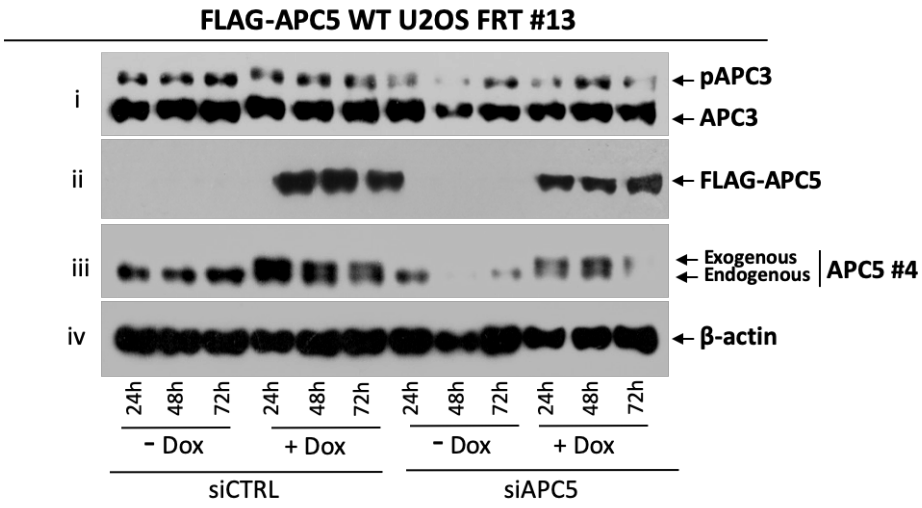

Figure 4. 7: **Exogenous FLAG-APC5 proteins are siRNA-resistant.** Lysates from FLAG-APC5 WT #13 U2OS FRT cells -/+Dox treated with either a silencing control siRNA (siCTRL) or with a siRNA towards APC5 (siAPC5) were collected in UTB lysis buffer at different time points (24h, 48h and 72h). 50µg of total protein from each sample was separated by SDS-PAGE, transferred to a nitrocellulose membrane and the levels of FLAG-APC5, endogenous APC5 and APC3 were determined by Western blotting. The levels of β-actin were used as a loading control. This data is representative of three individual experiments.

The Western blot results showed that in the absence of Dox treatment, the levels of endogenous APC5 detected with the α-APC5 mAb #4 were greatly reduced following the siAPC5 treatment compared to the siCTRL samples (panel iii, Fig. 4.7). Conversely, the signal detected by the α-FLAG specific Ab indicated that the levels of FLAG-APC5 WT were not reduced greatly following siRNA treatment against APC5, confirming that the FLAG-APC5 recombinant species was resistant to siAPC5 treatment (panel ii, Fig. 4.7).

Having established that our FLAG-APC5 recombinant proteins are resistant to siAPC5 treatment, we then decided to repeat the nocodazole-release experiments with our U2OS FRT monoclonal cell lines expressing FLAG-APC5 WT, FLAG-APC5 S195A and FLAG-APC5 S195D, in the absence of endogenous APC5. In this series of experiments, following initial treatment of cell lines with the siCTRL or the siAPC5 siRNA oligonucleotides, all

samples were treated with Dox to induce the expression of the recombinant FLAG-APC5 recombinant species. Cells were then synchronized in mitosis by treatment with nocodazole and finally released back into the cell cycle following nocodazole withdrawal. Western blotting analysis was then employed to follow mitotic progression by looking at the levels of various APC/C substrates and APC3 phosphorylation status (Fig. 4.8, 4.9 and 4.10).

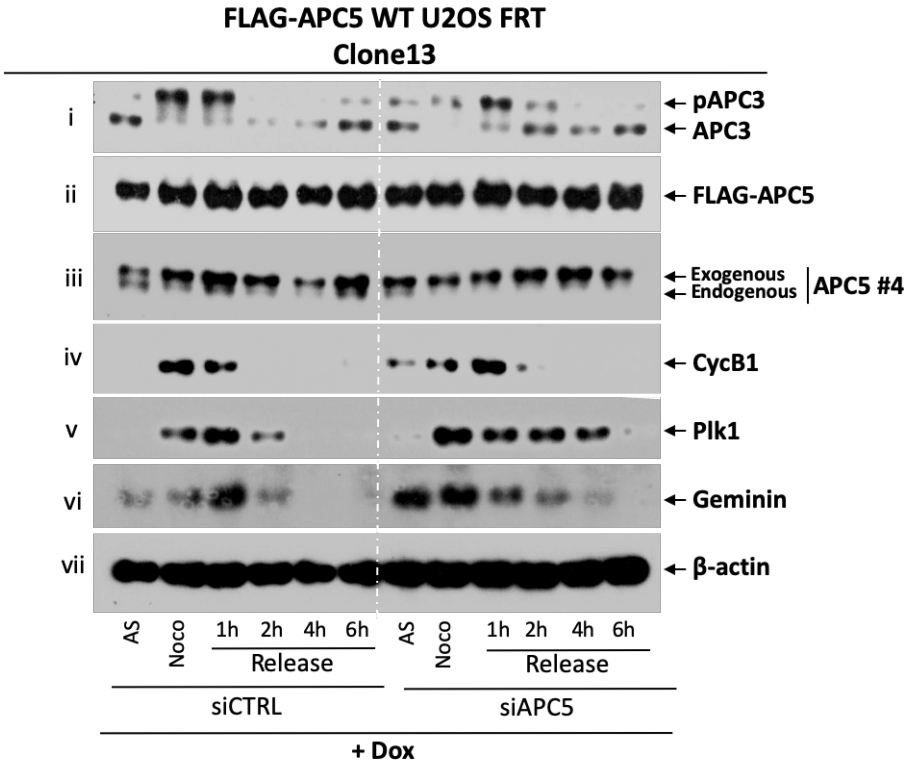

Figure 4. 8: **FLAG-APC5 WT expression does not compensate for the loss of endogenous APC5**. Following treatment of U2OS FRT cells with Dox and then siRNA, a nocodazole-release experiment was performed and lysates collected in UTB lysis buffer. 50µg of total protein, from asynchronous (AS), nocodazole-arrested cells (Noco) and cells harvested at different time-points post-release (1h, 2h, 4h and 6h), was separated by SDS-PAGE, transferred to a nitrocellulose membrane and the levels of FLAG-APC5, endogenous APC5, APC3 and some APC/C mitotic substrates were determined by Western blotting. The levels of β-actin were used as a loading control. This data is representative of three individual experiments.

Consistent with previous results, Western blotting indicated that FLAG-APC5 WT protein levels were stable at all times during the experiment regardless of whether they had been

treated with siCTRL or the siAPC5 oligonucleotides (panel ii, Fig. 4.8). On the contrary, endogenous APC5 levels were reduced greatly in samples treated with siAPC5 in comparison to the siCTRL-treated samples whilst the exogenous APC5 form recognised by the APC5 mAb #4 was not (panel iii, Fig. 4.8). Western blot analyses of APC/C substrates Cyclin B1, Plk1 and Geminin indicated that the siAPC5-dependent depletion of endogenous APC5 was responsible for a slight increase in their overall levels, both in asynchronous and in mitotically-arrested cells compared to siCTRL-treated samples (panel iv, v and vi, Fig. 4.8). Moreover, siAPC5 treatment of FLAG-APC5 WT #13 U2OS FRT cells caused a deceleration in the degradation pattern of these APC/C substrates, particularly Plk1, compared to siCTRL-treated cells, suggesting that APC/C activity was reduced in these cells (panel iv, v and vi, Fig. 4.8); no significant changes were observed in the phosphorylation status of APC3 however (panel i, Fig.4.8). Overall, the results of this experiment showed that FLAG-APC5 WT expression, in the absence of endogenous APC5, causes a delay in the progression of these cells through mitosis, suggesting that FLAG-APC5 WT might not be able to compensate for the loss of endogenous APC5 in this regard (Fig. 4.8).

To establish whether APC5 S195 phosphorylation affected mitotic progression the same experimental procedure was performed using U2OS FRT monoclonal cell lines expressing either the FLAG-APC5 phosphorylation-defective, S195A or the phospho-mimic, S195D proteins (Fig. 4.9 and 4.10).

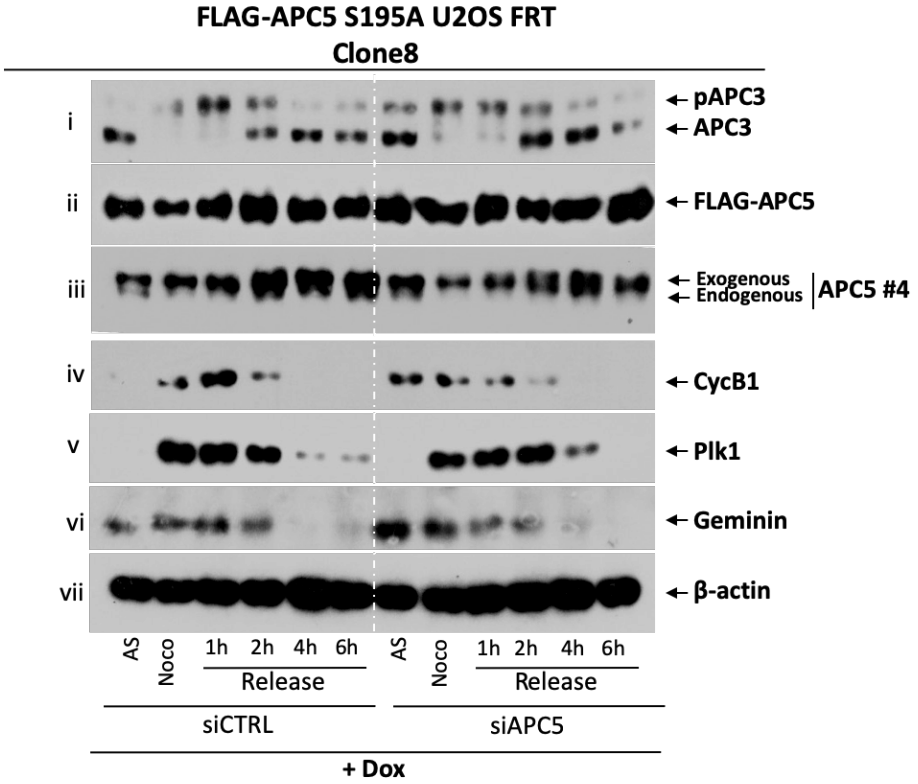

Figure 4. 9: **Exogenously-expressed FLAG-APC5 S195A delays mitotic progression in the absence of endogenous APC5.** Following treatment of U2OS FRT cells with Dox and then siRNA, a nocodazole-release experiment was performed and lysates collected in UTB lysis buffer. 50µg of total protein from asynchronous (AS), nocodazole-arrested cells (Noco) and cells harvested at different time-points post-release (1h, 2h, 4h and 6h) was separated by SDS-PAGE, transferred to a nitrocellulose membrane and the levels of FLAG-APC5, endogenous APC5, APC3 and some APC/C mitotic substrates were determined by Western blotting. The levels of β-actin were used as a loading control. This data is representative of three individual experiments.

Western blot with α-FLAG and α-APC5 mAbs revealed that like FLAG-APC5 WT, the exogenously-expressed FLAG-APC5 S195A gene was resistant to the siAPC5 treatment (panel ii and iii, Fig. 4.9). Again, whilst no alteration in the overall levels, or phosphorylation status, of APC3 were detected following the siRNA treatment (panel i, Fig. 4.9), FLAG-APC5 S195A expression, in the absence of endogenous APC5 protein, delayed the degradation of all the APC/C substrates Cyclin B1, Plk1 and Geminin compared to siCTRL (panel iv, v and vi, Fig. 4.9). These data are similar to those observed for the FLAG-APC5 WT species (cf Fig 4.8 and Fig. 4.9).

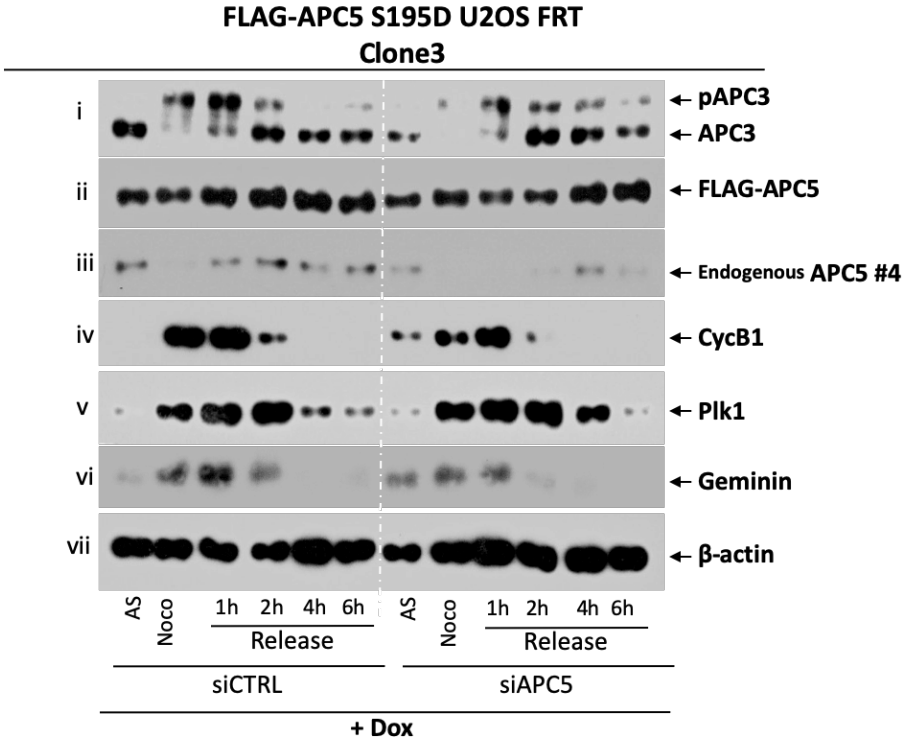

Figure 4. 10: **Exogenously-expressed FLAG-APC5 S195D does not affect normal mitotic progression.** Following treatment of U2OS FRT cells with Dox and then siRNA, a nocodazole-release experiment was performed and lysates collected in UTB lysis buffer. 50μg of total protein from asynchronous (AS), nocodazole-arrested cells (Noco) and cells harvested at different time-points post-release (1h, 2h, 4h and 6h) was separated by SDS-PAGE, transferred to a nitrocellulose membrane and the levels of FLAG-APC5, endogenous APC5, APC3 and some APC/C mitotic substrates were determined by Western blotting. The levels of β-actin were used as a loading control. This data is representative of three individual experiments.

Western blot with α-FLAG and α-APC5 mAbs revealed that like WT and S195A APC5 species the FLAG-APC5 S195D species was resistant to the siAPC5 treatment (panel ii and iii, Fig. 4.10). No additional bands, corresponding to the slower migrating FLAG-APC5 recombinant protein, was detected in these cells with the α-APC5 mAb #4 due to the constitutively phosphorylated status of the S195D mutant that masks the Ab epitope (panel iii, Fig. 4.10). Western blot analyses did not reveal any major differences in the levels, or degradation pattern of APC/C substrates Cyclin B1, Plk1 and Geminin in siAPC5-treated cells compared to siCTRL-treated cells (panel iv, v and vi, Fig. 4.10); no alteration in the

overall levels, or phosphorylation status, of APC3 were detected following the siRNA treatment (panel i, Fig. 4.10) Taken together these data suggest that, expression of S195D accelerates mitotic progression, relative to WT, or S195A APC5 species, indicating potentially that APC5 S195 phosphorylation does modulate the timing of mitotic progression (cf Fig. 4.8 and Fig. 4.10). However, as FLAG-APC5 WT was not able to compensate for the loss of endogenous APC5 and allow for a timely progression through mitosis, and that FLAG-APC5 S19SA was no different from FLAG-APC5 WT, we came to the conclusion that despite the vast effort in generating these reagents, that they were ultimately, not suitable for establishing the role of APC5 S195 phosphorylation in mitotic progression.

4.4 APC5 depletion delays mitotic progression

Although our studies with the FLAG-APC5 U2OS FRT cells did not help to establish a clear relationship between APC5 mitotic phosphorylation and the regulation of the APC/C during mitosis, the results obtained provided some insight into the potential role played by APC5 during mitosis. Indeed, our data suggested that modulating APC5 protein levels in the cell might interfere with the normal progression of cells through mitosis. Given these findings we decided to use different cell models to address in more detail whether modulation of APC5 protein levels affects mitotic progression. To this end we decided to use RPE-1 and HeLa cells both of which have proved, consistently, to be faithful models for studying mitosis (Floyd et al., 2008, Neumann et al., 2010).

4.4.1 APC5 knockdown delays mitotic progression both in RPE-1 and HeLa cells

To elucidate the role played by APC5 in the normal mitotic progression, we initiated a new series of experiments to look at the effect of APC5 knockdown on the ability of RPE-1 cells to progress through mitosis. Initially therefore, we conducted a pilot experiment to evaluate

RPE-1 sensitivity to different amounts of siAPC5 oligonucleotides. As such, asynchronous RPE-1 cells subjected to treatment with a siCTRL or with different amount of a siAPC5 siRNA oligonucleotides were harvested 48h post-transfection; Western blotting analysis revealed that APC5 protein levels were knocked down by the siAPC5 oligonucleotides to similar levels at all concentrations used (cf lane 2, 3 and 4 with lane 1; Fig. 4.11). Western blotting also revealed that there were no alterations in the protein levels of APC3 between the siCTRL and the siAPC5-treated samples, suggesting that knocking down APC5 in asynchronous cells does not affect APC3 stability (panel i, Fig. 4.11).

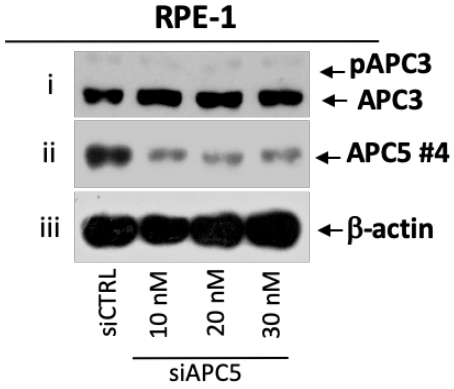

Figure 4. 11**: RPE-1 cells are sensitive to APC5 knockdown.** RPE-1 cells were treated with a silencing control siRNA (siCTRL) or different amounts of a siRNA targeted towards APC5 (10nM, 20nM and 30nM siAPC5). Lysates were harvested after 48h in UTB lysis buffer. 50µg of total protein from each sample was separated by SDS-PAGE, transferred to a nitrocellulose membrane and the levels of APC5 and APC3 were determined by Western blotting. The levels of β-actin were used as a loading control. This data is representative of three individual experiments.

Once the efficiency of the APC5 knockdown was confirmed, our next step was to investigate the effect of APC5 knockdown during the normal mitotic progression of RPE-1 cells. To do this RPE-1 cells were initially treated with a siCTRL or with siAPC5 siRNA oligonucleotides and then subjected to a nocodazole-release experiment where cells were initially synchronized in mitosis by treatment with nocodazole and, following nocodazole

withdrawal, their ability to progress throughout mitosis was determined by Western blotting for well-known APC/C substrates cyclin B1, Plk1, Geminin and Bub1, as well as at the levels of APC5 and the phosphorylation status of APC3 (Fig. 4.12).

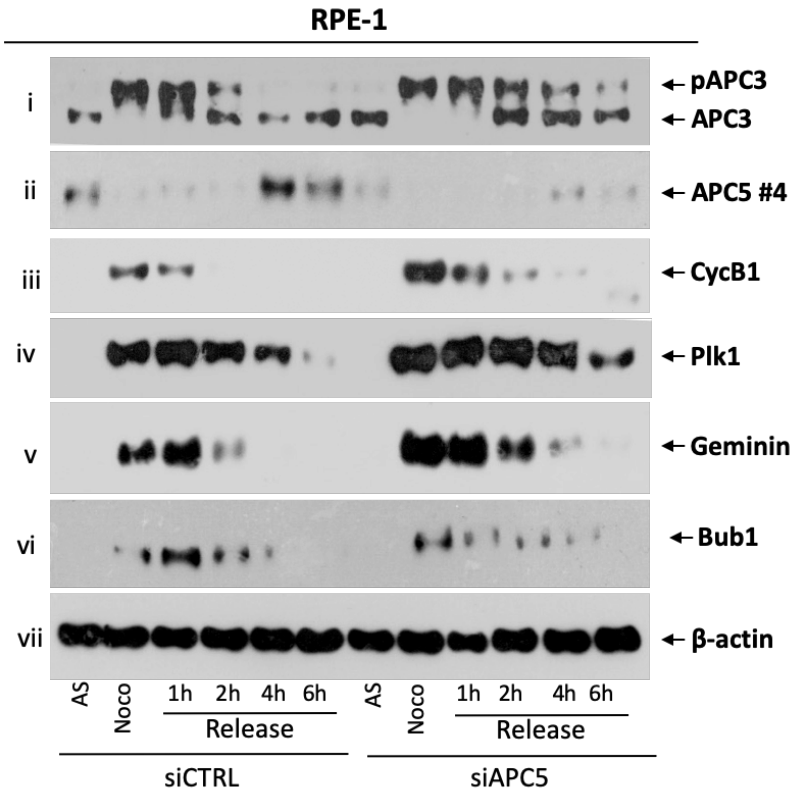

Figure 4.12: **APC5 silencing affects mitotic progression in RPE-1 cells.** RPE-1 cells were treated with a siRNA targeted against APC5 or a control siRNA and subjected to a nocodazole release experiment. Lysates were collected in UTB lysis buffer at the appropriate times. 50µg of total protein from asynchronous (AS), nocodazole-arrested cells (Noco) and cells harvested from the mitotic release at different time-points (1h, 2h, 4h and 6h) was separated by SDS-PAGE, transferred to a nitrocellulose membrane and the levels of APC5, APC3 and some APC/C mitotic substrates were determined by Western blotting. The levels of β-actin were used as a loading control. This data is representative of three individual experiments.

Consistent with earlier results (Fig 4.11) Western blotting revealed that APC5 was successfully knocked-down in asynchronous cells following siAPC5 treatment (panel ii, Fig. 4.12). Although the epitope-masking phenomenon associated with APC5 mitotic phosphorylation (Chapter 3), greatly reduced detectable levels of APC5 in all samples treated, treatment with siAPC5 oligonucleotides reduced these levels further compared to

the siCTRL samples (panel ii, Fig. 4.12). Interestingly, the protein levels of all the APC/C substrates tested, Cyclin B1, Plk1, Geminin were increased at all time-points following nocodazole-release of siAPC5-treated cells, relative to siCTRL samples (panel iii, iv, v and vi, Fig. 4.12). As such, APC5 knockdown appeared to slow down the degradation of these APC/C substrates, suggesting that APC5 depletion reduces the E3 ubiquitin ligase activity of the APC/C holoenzyme. Consistent with this view APC3 phosphorylation was prolonged in siAPC5-treated cells released from the mitotic arrest compared to the same samples treated with the siCTRL, suggesting that the time taken for siAPC5-treated cells to progress through mitosis was extended (panel i, Fig. 4.12). Indeed, 2h and 4h post nocodazole withdrawal, APC3 phosphorylation was still very high in siAPC5-treated samples relative to siCTRL cells (cf lane 10 and 11 with lane 4 and 5, panel i, Fig. 4.12). Together, these data suggest that APC5 knockdown affects the normal ability of cells to progress throughout mitosis reflected by an extension in the time taken for cells to progress through mitosis, which might be due to a reduction in APC/C E3 ubiquitin ligase activity.

Given the effect of knocking down APC5 on mitotic progression in RPE-1 cells, we wished to corroborate these findings in HeLa cells. Initially therefore, we conducted a pilot experiment to determine the efficiency of APC5 knockdown in HeLa cells. Asynchronous HeLa cells were thus treated with 30nM siCTRL or 30nM siAPC5 siRNA oligonucleotides and harvested after 24h, 48h and 72h post-transfection. Western blot analyses revealed that APC5 was efficiently knocked down at all timepoints investigated (panel ii, Fig. 4.13), and that APC3 levels, and phosphorylation status, was not altered, appreciably (panel i, Fig. 4.13).

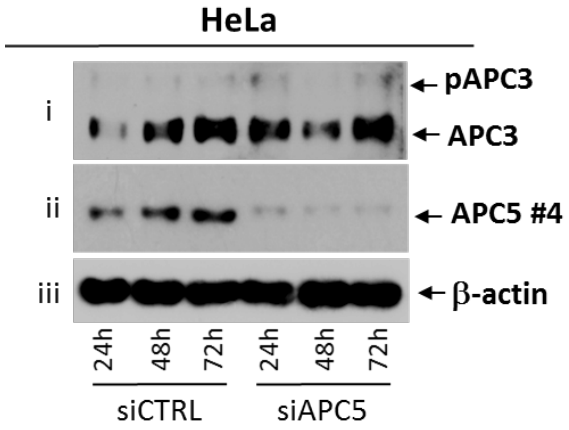

Figure 4. 13: **HeLa cells are sensitive to siAPC5 knockdown.** HeLa cells were treated with a silencing control siRNA (siCTRL) or with a siRNA targeted against APC5 (siAPC5). Lysates were harvested in UTB lysis buffer at different time points post-transfection (24h, 48h and 72h). 50µg of total protein from each sample was separated by SDS-PAGE, transferred to a nitrocellulose membrane and the levels of APC5 and APC3 were determined by Western blotting. The levels of β-actin were used as a loading control. This data is representative of three individual experiments.

We next investigated the effects of APC5 knockdown on HeLa cell progression through mitosis. We therefore treated HeLa cells with siCTRL and siAPC5 oligonucleotides and subjected these cells to a nocodazole-release experiment (Fig 4.14).

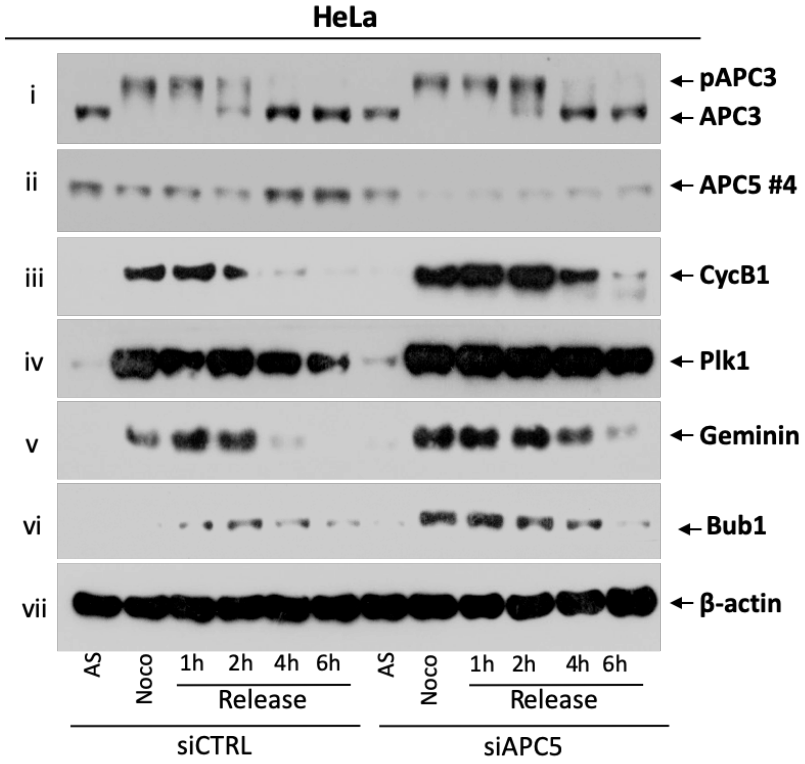

Figure 4.14 **APC5 silencing affects mitotic progression in HeLa cells.** HeLa cells were treated with an siRNA targeted against APC5 or a control siRNA and subjected to a nocodazole release experiment. Lysates were collected in UTB lysis buffer at the appropriate times. 50µg of total protein from asynchronous (AS), nocodazole-arrested cells (Noco) and cells harvested from the mitotic release at different time-points (1h, 2h, 4h and 6h) was separated by SDS-PAGE, transferred to a nitrocellulose membrane and the levels of APC5, APC3 and some APC/C mitotic substrates were determined by Western blotting. The levels of β-actin were used as a loading control. This data is representative of three individual experiments.

As expected, APC5 protein levels were reduced greatly in samples treated with siAPC5 oligonucleotides compared to siCTRL-treated samples, confirming the successful depletion of the APC5 protein (panel ii, Fig. 4.14). Consistent with the notion that APC5 depletion reduces APC/C activity and slows progression of cells through mitosis, the levels of the APC/C substrates Cyclin B1, Plk1, Geminin and Bub1 were increased significantly, at all timepoints investigated, in HeLa cells depleted of APC5 compared to siCTRL cells (panel iii, iv, v and vi, Fig. 4.14). Moreover, APC3 phosphorylation was prolonged in siAPC5-treated cells relative to siCTRL cells also suggestive of these cells taking longer to progress

through mitosis (panel i, Fig 4.14). Taken together APC5 knockdown experiments suggest that reduction of APC5 levels reduces APC/C E3 ligase activity and prolongs the time taken for cells to progress through mitosis.

4.4.2 Time-lapse microscopic imaging indicates that APC5 knockdown affects progression through mitosis

As the data obtained from RPE-1 and HeLa cells revealed that APC5 knockdown causes a delay in progression through mitosis (Fig. 4.12 and 4.14) we decided to investigate this phenotype further. We therefore decided to conduct a time-lapse microscopic imaging experiment in RPE-1 cells to measure the time taken by siCTRL-treated cells and siAPC5-treated cells to complete mitosis following NEBD (see Sec.2.4.2, Chapter 2). Twenty-four hours post-knockdown RPE-1 DNA was labelled with the cell-permeable, fluorescent DNA stain, SiR-DNA and 2h later cells were imaged every 3 min for approximately 24h by the CellQ live cell imager. The data set obtained was then analysed manually with the aid of the Cell Counter plugin using the ImageJ Fiji software package (Schindelin et al., 2012), to measure the time taken by individual cells to progress from NEBD to metaphase-to-anaphase transition and from anaphase to the completion of cytokinesis. The use of the fluorescent DNA stain allowed for a clear visualization of chromosome condensation, making it easier to follow and time accurately the mitotic progression of individual cells.

The live-cell imaging experiments revealed that RPE-1 cells treated with siAPC5 oligonucleotides displayed mitotic-arrest, mitotic-delay and cytokinesis-defect phenotypes, when compared to siCTRL-treated RPE-1 cells (Fig. 4.15). These experiments revealed that following APC5 knockdown on average 53% of these cells were unable to undergo metaphase-to-anaphase transition and existed in either a prophase or metaphase-arrest -like

state after NEBD (Fig. 4.15). Although 46% of APC5 knockdown cells, were on average able to complete mitosis, their transition was delayed significantly, whilst 1% of cells, on average, failed to complete cytokinesis after chromosome segregation (Fig. 4.15).

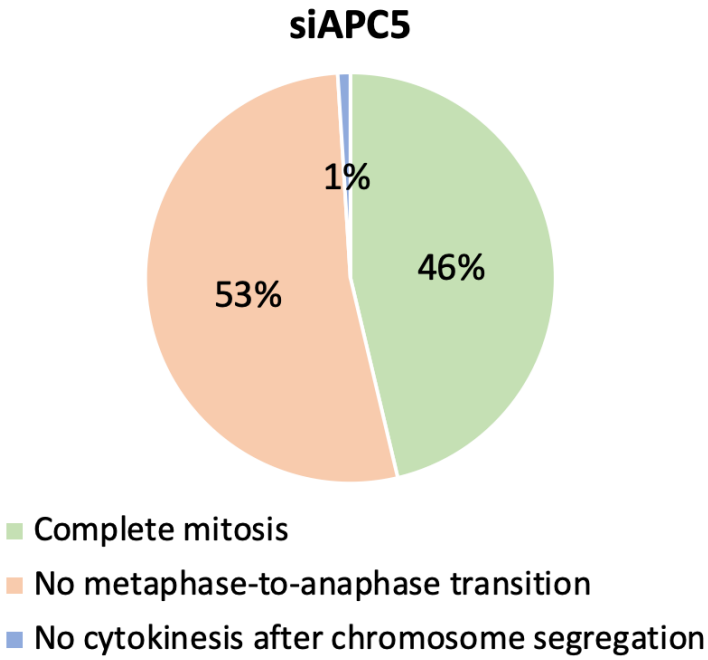

Figure 4.15: **APC5 knockdown affects the ability of RPE-1 to progress through mitosis.** Pie chart representing the average percentage of mitotic events following siAPC5 treatment of RPE-1 cells. This data represents the average of three independent experiments. A total of 70-80 cells were counted per sample for each independent experiment.

More detailed analyses allowed us to measure the difference in the time taken by APC5 knockdown cells, relative to siCTRL-treated cells, to progress from NEBD to anaphase and from anaphase to cytokinesis. These analyses revealed that for those APC5-knockdown cells that did progress through mitosis both passage from NEBD to anaphase and from anaphase to cytokinesis were delayed significantly as a consequence of APC5 knockdown (Fig. 4.16, 4.17 and 4.18). Representative images below illustrate that siCTRL chromosomes were perfectly aligned to the metaphase plate after about 15-18 min following NEBD, and underwent metaphase-to-anaphase transition after about 21 min post-NEBD (Fig. 4.16, A). RPE-1 cells treated with the siAPC5 oligonucleotides, however, suffered a marked delay in

their chromosome segregation pattern following NEBD, such that metaphase-to-anaphase transition was initiated 72 mins post NEBD (Fig. 4.16, B). Moreover, 53% of siAPC5-treated RPE-1 cells failed in undergo metaphase-to-anaphase transition after NEBD and chromosome condensation and went back to an interphase-like status after 120 min (Fig. 4.16, C). These data suggest that APC5 depletion has a significant impact on APC/C mitotic activity (Fig. 4.16).

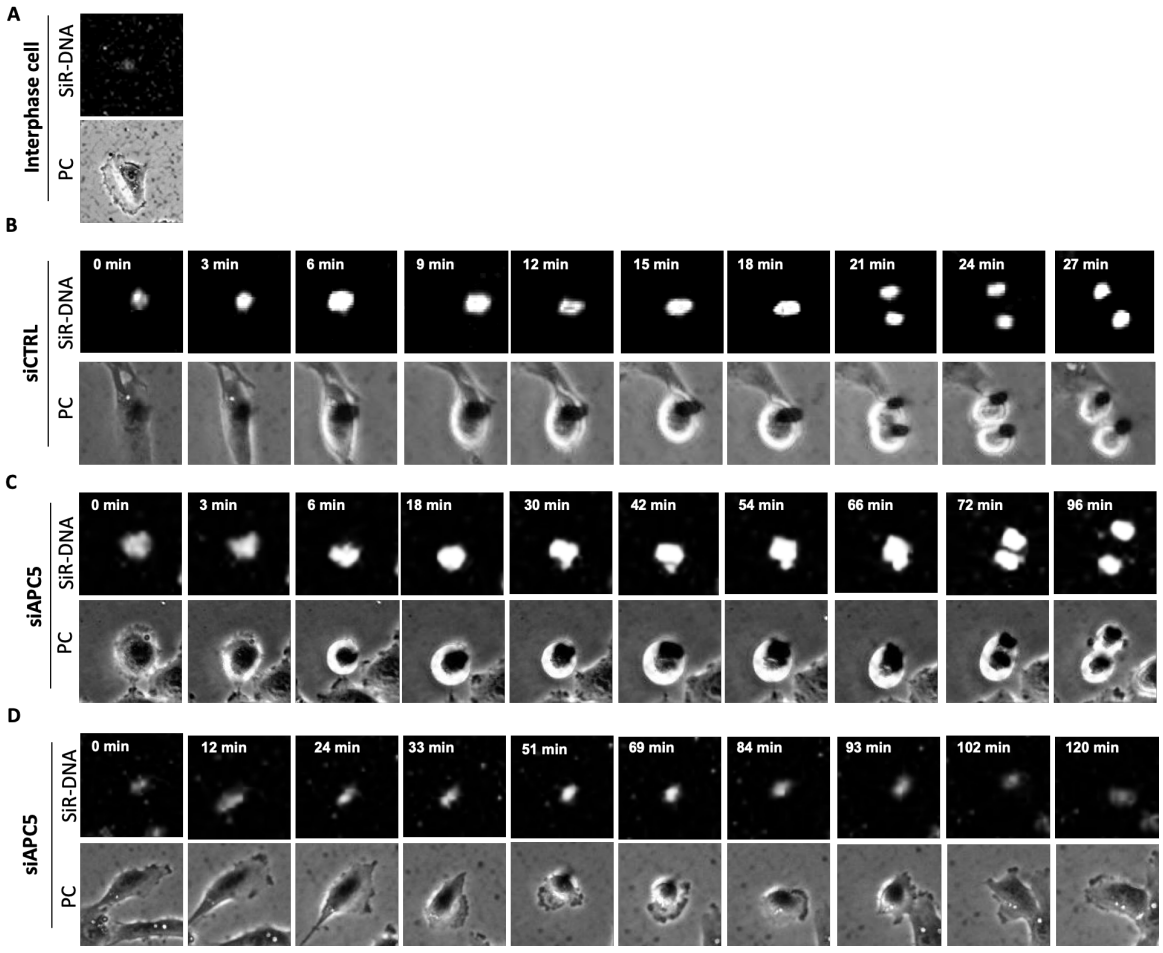

Figure 4. 16: **APC5 depletion delays normal mitotic progression.** Phase-contrast (PC) and fluorescent (SiR-DNA) live cell images of interphase (**A**) and RPE-1 cells progressing through mitosis after siCTRL (**B**) or siAPC5 (**C** and **D**) treatments. Representative image from three independent live cell imaging experiments.

Further inspection of the data revealed that the mitotic progression of siCTRL-treated cells was uniformly distributed, showing an average time to progress from NEBD to anaphase of about 22 min (mean and median), whilst data obtained for siAPC5-treated cells was more scattered, with about 50% of cells taking an average of approximately 61 min (median) to complete the same metaphase-to-anaphase transition following NEBD. These data suggest that APC5 depletion might either impact chromosome attachment to the mitotic spindle and/or APC/C activation once the SAC has been satisfied (Fig. 4.17). Further analyses revealed that the time required for cytokinesis completion following metaphase-to-anaphase transition for siCTRL cells was about 93 min (mean and median), whilst the siAPC5-treated cells which did complete mitosis took an average of 153 min (median, Fig. 4.18).

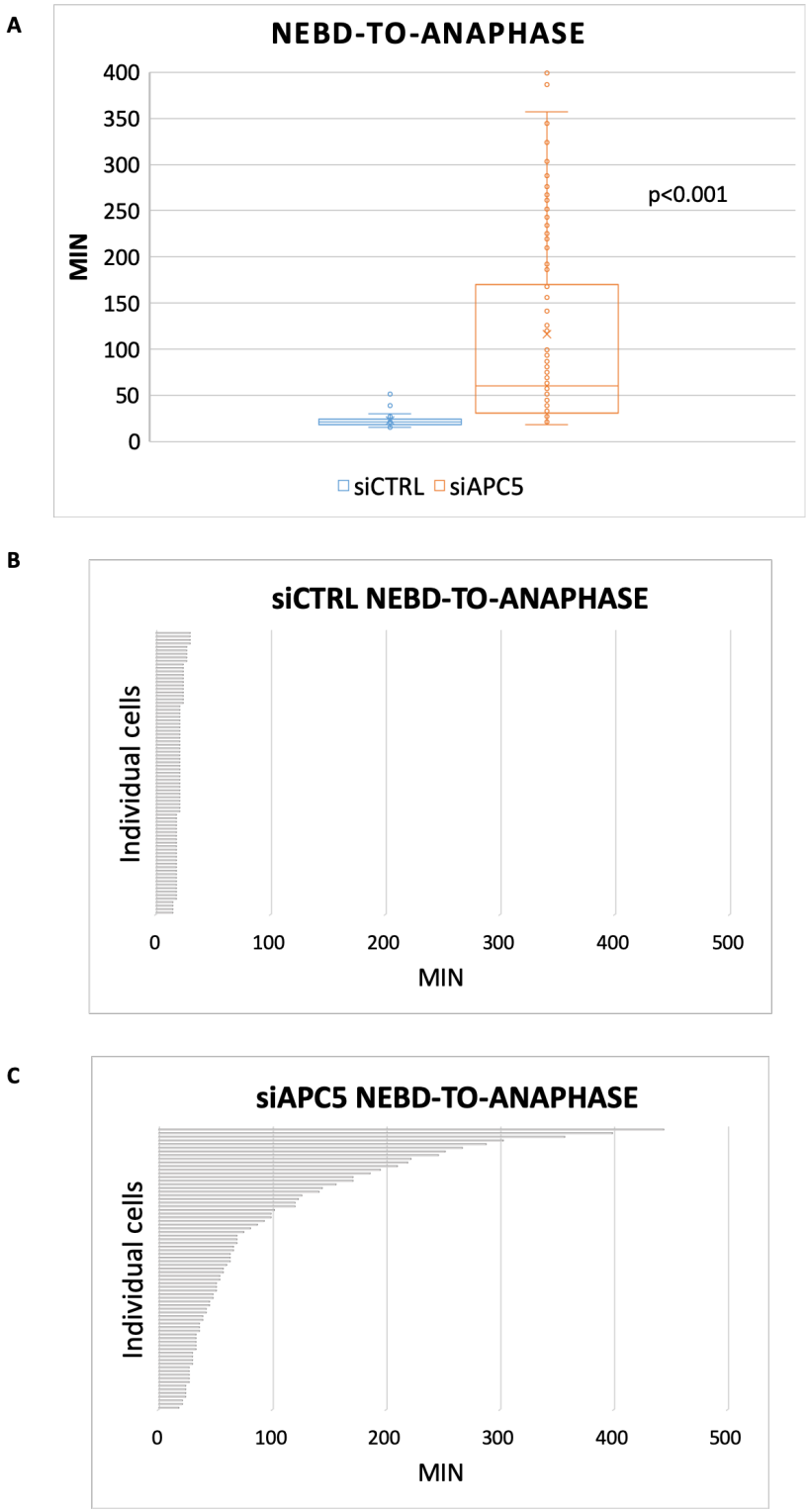

Figure 4. 17: **APC5 knockdown delays mitotic progression from NEBD-to-anaphase.** (**A**) Box plot illustrating RPE-1 cells progression from NEBD to anaphase. (**B** and **C**) Bar charts showing time taken by individual RPE-1 cells to progress from NEBD to anaphase following siCTRL (**B**) or siAPC5 (**C**) oligonucleotide treatment. Data obtained from three independent live cell imaging experiments. A total of 70-80 cells were counted per sample in each independent experiment.

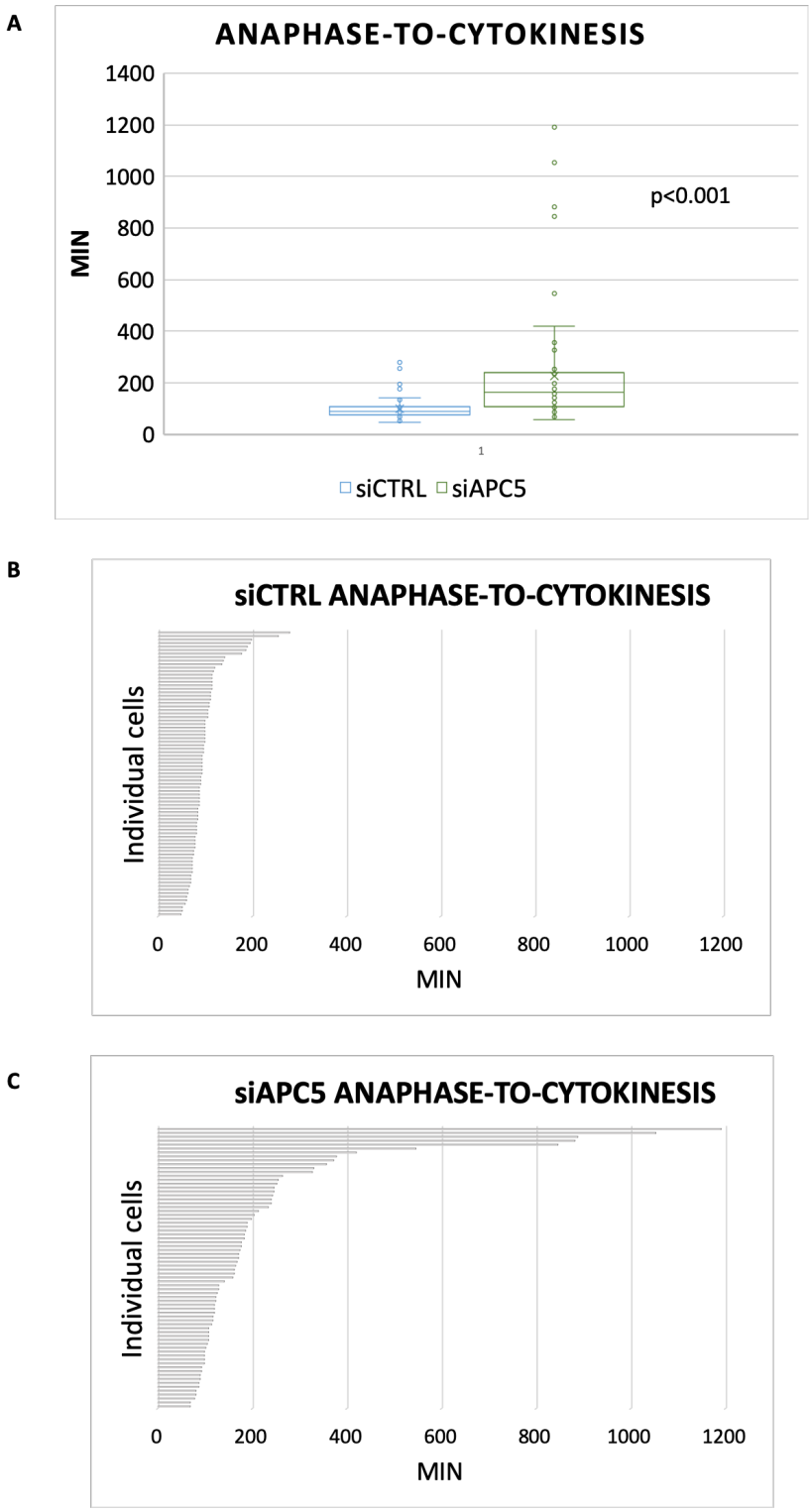

Figure 4. 18: **APC5 knockdown delays progression from anaphase-to-cytokinesis.** (**A**) Box plots illustrating time taken by RPE-1 cells to progress from anaphase to cytokinesis. (**B** and **C**) Bar charts showing time taken by individual RPE-1 cells to progress from anaphase to cytokinesis following siCTRL (**B**) or siAPC5 (**C**) oligonucleotide treatment. Data obtained from three independent live cell imaging experiments. A total of 70-80 cells were counted per sample in each independent experiment.

Taken together, these data indicate that APC5 depletion affects significantly mitotic progression of RPE-1 cells by, presumably, interfering with the molecular processes that regulate metaphase-to-anaphase transition and cytokinesis. As such these data suggest a critical role for APC5 in modulating the activity of the APC/C complex throughout mitosis.

4.5 Discussion

Although previously published mass spectrometry screens had revealed that APC5 residues, S195 and T232 were phosphorylated during mitosis (Herzog et al., 2005, Steen et al., 2008, Hegemann et al., 2011), no experimental detail, about the extent of APC5 phosphorylation or the possible physiological role played by these PTMs in the regulation of APC/C mitotic activity exists. In contrast, data obtained in our previous chapter revealed that almost the entire pool of APC5 is phosphorylated during mitosis at the Plk1 consensus site, S195 (Fig. 3.21) (Nakajima et al., 2003), and that this phosphorylation event might be dependent upon the activity of Plk1, Cdk1 and Aurora B mitotic kinases (Fig. 3.1, 3.16, 3.17 and 3.22). Based on this evidence, and the fact that APC/C activity is modulated by phosphorylation during mitosis (Zhang et al., 2016, Fujimitsu et al., 2016, Golan et al., 2002, Qiao et al., 2016), the aim of the studies presented in this chapter was to investigate the role of APC5 mitotic phosphorylation at S195 in the regulation of the APC/C. Moreover, as the APC5 residue T232 is likely phosphorylated by Cdk1 (Holt et al., 2009), and Cdk1 often primes substrates for Plk1-dependent phosphorylation (Fig. 3.22) (Elia et al., 2003a, Elia et al., 2003b, Neef et al., 2007), we also aimed to establish whether T232 phosphorylation was an essential prerequisite for S195 phosphorylation.

Unfortunately, however, our experimental approach failed to answer these important questions. In this regard, we were able to generate stable monoclonal U2OS FRT cell lines

that expressed FLAG-tagged APC5 recombinant proteins corresponding to the WT species and S195 and T232 phospho-mutants that incorporated successfully into the APC/C holoenzyme (Fig. 3.7, 4.2 and 4.3). However, when we looked at the mitotic behaviour of these U2OS FRT cell lines following Dox induction, we found that the FLAG-APC5 WT was not able to recapitulate the normal mitotic progression expected of these cells (Fig. 4.4 and 4.8). Moreover, expression of exogenous FLAG-APC5 S195A and S195D species, did not have a dramatic effect on the ability of cells to progress through mitosis, either in the presence or absence of endogenous APC5 (Fig. 4.5, 4.6, 4.9 and 4.10). Nevertheless, cells expressing FLAG-APC5 WT and FLAG-APC5 S195A were delayed in mitosis compared to FLAG-APC5 S195D U2OS FRT cells in all conditions tested (Fig. 4.4-4.6 and 4.8- 4.10). As such, our data might suggest that the constitutive phosphorylation of APC5 at S195 augments mitotic APC/C activity. If so, it is interesting to speculate that APC5 phosphorylation at S195 might participate in the activation of the APC/C in mitosis by promoting conformational changes in the APC/C that facilitates Cdc20 association with the holoenzyme (Zhang et al., 2016). Akin to the inter-subunit regulation between APC3 and APC1 during mitosis, where the Cdk-1 dependent phosphorylation of APC3 promotes the phosphorylation of APC1, it is possible that APC5 phosphorylation at S195 could, similarly promote APC3 and APC1 phosphorylation, as an upstream regulator of these APC/C subunits (Fujimitsu et al., 2016). However, as FLAG-APC5 WT U2OS FRT cells were delayed in their progression through mitosis (Fig. 4.4 and 4.8), these hypotheses could not be confirmed, and definitive conclusions could not be drawn.

It is possible that the levels of the recombinant FLAG-APC5 species expressed in our U2OS FRT cell lines were not adequate to compensate for the loss of endogenous APC5 following the siAPC5 treatment (Fig. 4.8-4.10). Moreover, notwithstanding the fact we selected U2OS

FRT clones which appeared to express FLAG-APC5 species to similar levels following Dox induction (Fig. 3.7, 4.1 and 4.2), it cannot be excluded that subtle differences in the expression of the different FLAG-APC5 species also impacted on the rate of cellular progression through mitosis. As such, it might be that the FLAG-APC5 S195D species was expressed to higher levels than the FLAG-APC5 WT and FLAG-APC5 S195A species and that might explain the faster progression of those cells through mitosis (Fig. 4.8- 4.10). Also, it cannot be excluded that despite their incorporation into the APC/C holoenzyme (Fig. 4.3), the FLAG-APC5 species might alter the overall structure of the APC/C, causing a reduction in its overall enzymatic activity and hence the slower rate of mitotic progression observed for FLAG-APC5 WT U2OS FRT cells (Fig. 4.4 and 4.8). Another potential concern is the utility of U2OS cell lines to study mitosis, as they are not used routinely for such studies, despite there being no indications in the literature that they are not a good model system to study mitosis. In fact, whilst TERT-immortalized RPE-1 cells have no genetic alterations, and are considered a good model to study mitosis (Floyd et al., 2008, American Type Culture Collection (ATCC), 2019), U2OS cells might have accumulated genetic mutations or genomic aberrations that dysregulate progression through mitosis. However, whilst HeLa cells, like U2OS cells, are tumour-derived, their progression through mitosis does not differ significantly from RPE-1 cells, which makes HeLa cells a good model for the study of mitosis (Neumann et al., 2010). However, one caveat worth noting is that although HeLa cells are used extensively to study mitosis, they are cancer-derived cells, and as such, they might be subjected to alterations in checkpoint control systems operating during the cell cycle. Moreover, HeLa cells possess an integrated human papilloma virus (HPV) genome within their genome. As such, HeLa cells express the viral oncoprotein E7, which has been implicated in the regulation of APC/C activity during mitosis (Yu and Munger, 2013).

Therefore, results obtained using HeLa cells in our study need to be evaluated carefully. Given also that U2OS cells are cancer-derived cells, obtained by osteosarcoma, we were unsure whether the FLAG-APC5 U2OS FRT clonal cell lines were an appropriate model to study the effects of APC5 phosphorylation under physiological conditions and acknowledge the need for a different approach to understand the role of APC5 phosphorylation at S195 and to ascertain its effect on APC/C activity.

Given the considerations outlined above it would be worthwhile to generate clonal RPE-FRT or HeLa-FRT cell lines that express the different FLAG-APC5 species to re-evaluate the effects of S195 phosphorylation on the process of mitosis. Alternatively, we could express the FLAG-APC5 species transiently in these cells to study their effects. In either of these scenarios, we would also assess the affinity of the FLAG-APC5 WT, S195A and S195D species for Cdc20 binding and validate the hypothesis that APC5 phosphorylation promotes APC/C mitotic activation in a manner akin to the phosphorylation of APC3 and APC1 (Fujimitsu et al., 2016, Zhang et al., 2016). We could similarly test whether APC5 mitotic phosphorylation has any effect on Cdh1 and/or UbcH10 binding to the APC/C, as structural analyses have suggested that APC5 conformational changes are also required for the association of these proteins with the APC/C (Cronin et al., 2015).

We could also use these approaches to evaluate whether APC5 S195 phosphorylation affects the ability of the APC/C to interact with protein substrates, such that APC5 S195 phosphorylation could generate a substrate-binding module, which might help establish the APC/C hierarchy for its targets (Davey and Morgan, 2016). Indeed, SUMOylated APC4 functions as a molecular adaptor and helps recruit the APC/C substrate, KIF18B to the APC/C (Eifler et al., 2018). In support of this idea homozygous mutants of the *Drosophila*

APC5 orthologue, ida, limit the APC/C-dependent degradation of Cyclin B1 without affecting the degradation of Securin (Bentley et al., 2002), suggesting that APC5 is important in the modulating the ability of the APC/C to target substrates during mitosis.

Although we have not been able, thus far, to evaluate the physiological role of APC5 mitotic phosphorylation at S195, studies presented within this chapter have provided important information about the role of APC5 in mitosis. Indeed, our experiments revealed that APC5 depletion by RNAi not only caused a delay in the mitotic progression of both RPE-1 and HeLa cells (Fig. 4.12 and 4.14), but also limited, substantially RPE-1 cells' ability to progress through mitosis (Fig. 4.15- 4.18). As such, our findings are consistent with those reported by Neumann and colleagues in their MitoCheck project, where a systematic approach was adopted to identify those human proteins that regulate mitosis and mitotic progression (Neumann et al., 2010). Using a siRNA library directed towards a total of 22,000 genes in HeLa cells, this study identified more than a thousand genes, that when knocked-down, gave a mitotic phenotype. As expected, knock-down of many of the APC/C subunits impaired cellular progression through mitosis, with more dramatic effects associated to the ablation of the APC/C catalytic subunits APC2, APC11 and APC10, as well as APC3. According to their report knockdown of these specific APC/C subunits led to segregation problems, lagging chromosomes and chromosomes bridges, nuclei morphological alterations, cellular arrest in metaphase and mitotic delays/arrest (Neumann et al., 2010). By contrast, knock-down of other APC/C subunits, i.e. APC4, APC6, and APC13 were instead more generally classified as causing metaphase delays/arrest or mitotic delays/arrest; whilst APC1 and APC7 knock-down was associated with an increase in cell proliferation (Neumann et al., 2010). Reasonably, due to the huge amount of information obtained through this high-throughput approach, following their initial screening and validation

Neumann and colleagues only focused on the phenotypic characterization of a small subset of candidates, and no extra information were provided relative to most of the genes identified (Neumann et al., 2010).

Similar to what was reported for APC4, APC6 and APC13, the MitoCheck project revealed that APC5 knock-down caused mitotic delay/arrest and metaphase alignment problems (Neumann et al., 2010). Our time-lapse microscopic analyses confirmed these observations, as well as providing a more detailed characterization of the APC5 knock-down phenotype. Indeed, through our live cell imaging experiments we determined that 53% of RPE-1 cells arrested in mitosis following siAPC5 treatment, whilst 46% completed mitosis, albeit with a marked delay in the time taken to exit mitosis (Fig. 4.15). Specifically, whilst control cells took on average of 22 min to progress from NEBD-to-anaphase and 90 min to complete cytokinesis thereafter, siAPC5-treated cells were delayed significantly ($p<0.001$) in their progression through mitosis, and took on average 60 min to progress from NEBD-to-anaphase and 153 min to complete cytokinesis following anaphase onset (medians, Fig. 4.17 and 4.18).

Interestingly, similar mitotic defects were also reported for the knockdown of the *Drosophila* APC5 homologous ida (Bentley et al., 2002), that shares 65% of similarity with the human APC5 (Yu et al., 1998). According to this study, homozygous deficient of ida were subjected to severe development problems related to cell proliferation and cell cycle control, such that ida mutants arrested in a prometaphase-like state with condensed chromosomes, suggesting a critical role for APC5 in mitosis that is conserved from metazoan to humans (Bentley et al., 2002). Akin to our study presented here, the *Drosophila* study also established that some

ida mutant cells were able to undergo metaphase-to-anaphase transition, but that they became aneuploid with aberrant, hyper-condensed chromosomes (Bentley et al., 2002).

Given that we observe obvious mitotic defects when we knock-down APC5 in RPE-1 cells (Fig. 4.15- 4.18) it would be extremely interesting to see if we could transiently express our siRNA-resistant FLAG-tagged APC5 species to determine whether APC5 WT, or the S195 or T232 phospho-mutant species were able to reverse the effects of APC5 knockdown on mitotic progression. Indeed, it has been shown previously that phospho-mimicking mutations or phospho-inhibitory mutations can alter the activation status of an enzyme to affect biological processes (e.g. Otto et al. (2017), Paleologou et al. (2008)). For instance, the modification of all S and T residues to E in the enzyme guanylyl-cyclase (GC)-A, which is responsible for hormone-dependent changes in blood pressure, recapitulates the phosphorylation-dependent activation of guanylyl cyclase activity (Otto et al., 2017). However, not all phospho-mimics recapitulate the biological effect of phosphorylation. For instance, phosphorylation at S129 in α-Synuclein inhibits fibrillation of α-Synuclein, whilst the phospho-mimetic SD and SE mutants are unable to recapitulate this effect (Paleologou et al., 2008). In light of theses studies it will be interesting to see whether APC5 phospho-mimicking species behaves akin to natively phosphorylated APC5 S195 species in the regulation of APC/C activity.

Interestingly, structural analysis of the APC/C, in complex with the MCC, have suggested that the dissociation of MCC from the APC/C upon SAC satisfaction necessitates conformational changes in the APC15 platform subunit. These conformational changes promote the autoubiquitylation of Cdc20 associated with the MCC and consequent release of the MCC from the APC/C (Alfieri et al., 2016, Reddy et al., 2007, Mansfeld et al., 2011,

Uzunova et al., 2012). Interestingly, these structural analyses also revealed that concomitant with changes in APC15 conformation, APC5 shifts upwards and facilitates the association of UbcH10 with the holoenzyme (Fig. 1.6) (Alfieri et al., 2016). Given that knockdown of APC5 causes a mitotic arrest phenotype, it will be interesting to see if the APC5 S195 or T232 phospho-mutant species regulate MCC complex dissociation and/or UbcH10 binding.

Overall, data presented in this chapter has revealed a critical role for the APC/C subunit, APC5 in the regulation of APC/C activity during mitosis, suggesting a potential role for APC5 S195 phosphorylation in the mitotic functions of the APC/C. The precise role of APC5 S195 phosphorylation in the regulation of the APC/C in the context of mitosis, however, awaits further characterization.

CHAPTER 5: CHARACTERIZATION OF ENDOGENOUSLY PHOSPHORYLATED APC5 S195 SPECIES IN MITOSIS

5.1 Introduction

In an attempt to investigate the role of the APC5 S195 phosphorylation on APC/C activity during mitosis, we previously utilized cell lines that were engineered to express FLAG-APC5 phospho-mutants in a TET-inducible manner (Chapter 4). Although the results obtained did not allow us to establish the role of APC5 S195 phosphorylation with certainty, overall, the data generated suggested that APC5 S195 phosphorylation might be important for APC/C function during mitotic progression (Fig 4.10). Moreover, as depletion of APC5 protein levels by RNAi had a very strong impact on the ability of both RPE-1 and HeLa cells to progress through mitosis (Fig. 4.13 and 4.14) it is likely that APC5 PTMs are key to APC5 function in this regard. To investigate the role of endogenous APC5 S195 phosphorylation under normal physiological conditions we decided to generate an anti-APC5 S195 phospho-specific Ab, which fortunately, proved successful. Details of the Ab generation and characterisation as well as an investigation into endogenous APC5 S195 phosphorylation under physiological conditions are described in this chapter.

5.2 Following APC5 phosphorylation under physiological conditions

5.2.1 Generation of an α-pAPC5 S195-specific antibody

Having determined that APC5 is phosphorylated at S195 during mitosis we wished to monitor endogenous APC5 S195 phosphorylation directly under various physiological conditions. For this reason, we employed the MRC Protein Phosphorylation Unit in Dundee to generate a phospho-specific Ab against the phosphorylated S195 APC5 protein species (α-pAPC5 S195). To do this they made a peptide equivalent to the APC5 region under

investigation and incorporated a phosphorylated serine residue corresponding to the S195 residue that is phosphorylated in the native protein (Peptide 1: ANAPC5 - C-KEELDVS*VREEEV – where S* is pS195). This peptide was then coupled to carrier proteins BSA (Bovine Serum Albumin), or KLH (Keyhole Limpet Hemocyanin) through an N-terminal cysteine residue, not found in the native protein, before being injected into rabbits for immunization. At 6, 10 and 14 weeks post-injection serum was isolated and the α-phospho-APC5 (pAPC5) S195 Ab affinity purified using the phospho-peptide (Peptide 1) coupled to Sepharose. To purify further the phospho-Ab and eliminate the presence of any Ab's that could still react with the un-phosphorylated form of APC5, the α-phospho-APC5 Ab was incubated with an un-phosphorylated peptide (Peptide 2 ANAPC5 - C-KEELDVSVREEEV) coupled to Sepharose prior to use. Overall, this process allowed for the isolation of a rabbit α-pAPC5 S195-specific Ab, which ideally, would only have affinity for the mitotically, phosphorylated APC5 S195 species of APC5.

5.2.2 α-pAPC5 S195 Ab binds to phosphorylated APC5 during mitosis in numerous cell types

Once the purified α-pAPC5 S195 Ab was isolated we wanted initially to establish its ability to recognize specifically, the phosphorylated S195 APC5 species during mitosis from different cell lines. With this purpose in mind, we harvested whole cell lysates either obtained from asynchronous, or mitotically-arrested RPE-1, U2OS FRT, HeLa, A549 and H1299 cells treated with nocodazole. We then performed SDS-PAGE and Western blot analyses to validate the binding avidity of the α-pAPC5 S195 Ab for the mitotic, phosphorylated form of APC5. For comparison we compared the reactivity of the phospho-Ab with our α-APC5 mAb #4, which does not bind to APC5 during mitosis, and with a

commercial polyclonal α-APC5 Ab, capable of detecting the APC5 protein at all stages of the cell cycle (Fig. 5.1). We also determined the levels of the APC/C substrates, Cyclin B1 and Plk1 and the phosphorylation status of APC3 as indicators of cell cycle status (Fig. 5.1).

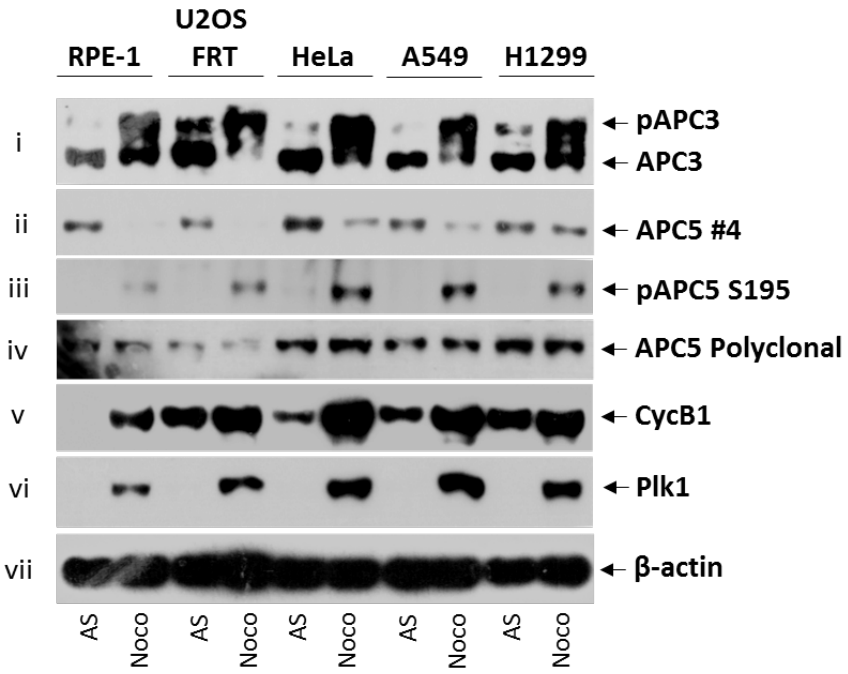

Figure 5.1: **α-pAPC5 S195 Ab recognizes phosphorylated APC5 preferentially during mitosis in multiple cell lines.** Cell lysates from RPE-1, U2OS FRT, HeLa, A549 and H1299 asynchronous (AS) and nocodazole-arrested cells (Noco) were harvested in UTB lysis buffer. 50μg of total protein was separated by SDS-PAGE, transferred to a nitrocellulose membrane and the levels of APC5 were determined by Western blotting with three different antibodies (APC5 #4, pAPC5 S195 and APC5 polyclonal Ab), as well as the levels of APC3, Cyclin B1 and Plk1. The levels of β-actin were used as a loading control. This data is representative of three individual experiments.

As expected, a higher molecular weight band was observed for APC3 in nocodazole-treated samples compared to asynchronous conditions in all cell types, indicating APC3 mitotic phosphorylation and confirming the effectiveness of the synchronization procedure (panel i, Fig. 5.1). Although some differences under asynchronous conditions were observed for Cyclin B1 from different cell types, its levels, as well as those for Plk1, were overall higher in mitotically-arrested cells relative to asynchronous cells for all cell types used, confirming

the typical accumulation of APC/C mitotic substrates in nocodazole-treated cells (panel v and vi, Fig. 5.1). The absolute levels of APC5 also differed between cell lines with higher levels observed in HeLa, A549 and H1299 cells compared to RPE-1 and U2OS FRT cell lines (panel ii, iii and iv, Fig. 5.1). Nevertheless, consistent with our previous findings, no significant differences were observed when comparing APC5 protein levels in asynchronous and mitotically arrested-cells of the same cell type when using the α-APC5 polyclonal Ab, confirming the ability of this Ab to recognize the APC5 species independently of S195 phosphorylation status (panel iv, Fig. 5.1). In contrast, the APC5 signal was almost completely lost in all mitotically-arrested cells when detected with the α-APC5 mAb #4, consistent with previous observations that this Ab possesses low binding affinity for its epitope when APC5 is phosphorylated in mitosis (panel ii, Fig. 5.1). In agreement with our hypothesis that APC5 is phosphorylated at S195 specifically during mitosis the α-pAPC5 S195 Ab only detected APC5 in mitotically-arrested cells in all cell lines used (panel iii, Figure 5.1). Signal intensity differences between cell lines were observed that might reflect the differences in the overall levels of APC5 in these different cell lines; importantly, the α-pAPC5 S195 Ab did not show any binding affinity for APC5 in asynchronous conditions (panel iii, Fig. 5.1). Overall, these results establish that the α-pAPC5 S195 Ab binds with high avidity to the phosphorylated APC5 S195 epitope during mitosis. These data also suggest that the phosphorylation of APC5 S195 in mitosis is conserved between different cell lines.

5.2.3 α-pAPC5 S195 binds specifically to APC5

The strong and specific immunoreactivity of the α-pAPC5 S195 Ab for APC5 from different mitotically-arrested cell types (Fig. 5.1), suggests selectivity, and specificity of this Ab for the mitotic APC5 phosphorylated species. Given these results we next wanted to ascertain

whether the Western blot signal detected corresponded genuinely to APC5, or if it was a non-specific protein, not related to APC5, that is recognized by the α-pAPC5 S195 Ab during mitosis. For this reason, we decided to test the ability of the α-pAPC5 S195 Ab to recognise this immunoreactive species following APC5 knock-down by RNAi. To do this, asynchronous and mitotically-arrested RPE-1 and HeLa cells were treated for 24 hours with a siRNA targeted against APC5, or alternatively, treated with a control, non-silencing siRNA for the same length of time. The levels of APC5, as well as the levels of APC3 and Cyclin B1, were then tested by Western blotting (Fig. 5.2 A and B).

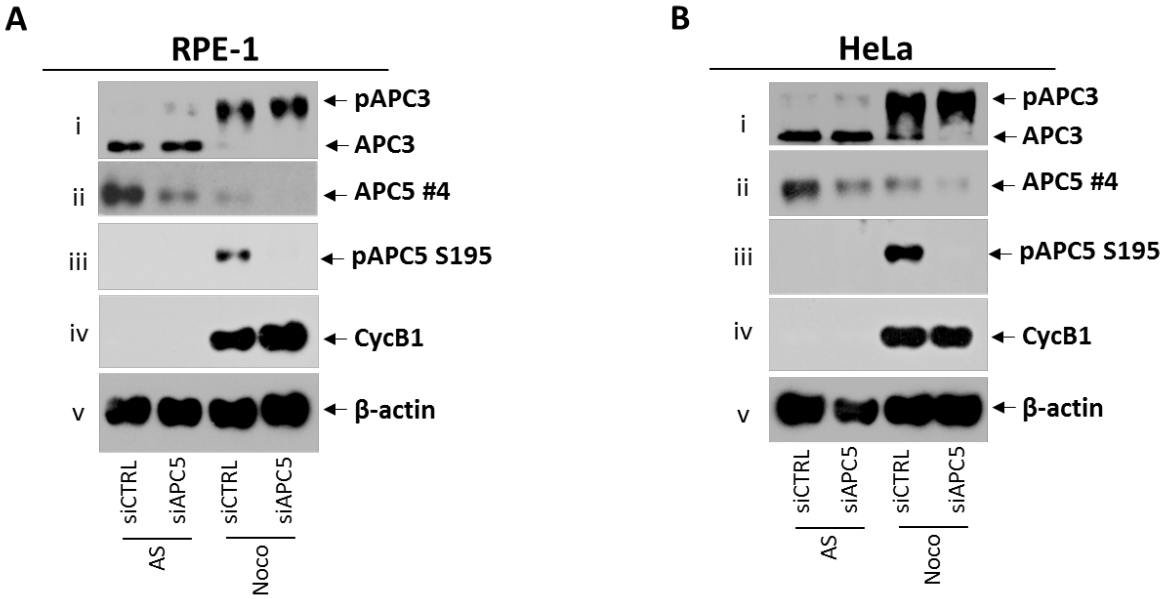

Figure 5.2: **The α-pAPC5 S195 Ab recognizes APC5 specifically.** Asynchronous (AS) and mitotically-arrested (Noco) RPE-1 (**A**) and HeLa (**B**) cells were treated with an siRNA against APC5 (siAPC5) or with a control siRNA (siCTRL) for 24 hours and then harvested in UTB lysis buffer. 50μg of total protein was separated by SDS-PAGE, transferred to a nitrocellulose membrane and the levels of APC5 were determined by Western blotting with two different antibodies (APC5 #4 and pAPC5 S195); the levels of APC3 and Cyclin B1 were also determined. The levels of β-actin were used as a loading control. This data is representative of three individual experiments.

Western blotting results established that the typical slower migrating mitotic form of APC3 and its hypophosphorylated derivative present in asynchronous cells, were not affected by

APC5 knockdown, relative to siCTRL samples (panel i, Fig. 5.2 A and B). Similarly, Cyclin B1 levels accumulated in mitotically-arrested cells and were not compromised following siAPC5 treatment, relative to siCTRL samples (panel iv, Fig. 5.2 A and B), indicating that APC5 knockdown does not have an effect on the overall levels of this protein. In contrast, APC5 protein levels were completely abrogated, both in asynchronous and in mitotically-arrested cells, following the siRNA treatment directed against APC5 (panel ii and iii, Fig. 5.2 A and B). Crucially, in this regard, the ability of the α-APC5 #4 mAb to detect non-phosphorylated APC5 in asynchronous cells, and the ability of α-pAPC5 S195 Ab to recognise the mitotic form of APC5, was lost as a consequence of APC5 knock-down, relative to siCTRL samples (cf lane 1+2 and 3+4, panel ii and iii, Fig. 5.2 A and B). These data demonstrate therefore, the specificity of the α-pAPC5 S195 Ab for APC5 during mitosis, thus ruling out the possibility that it cross-reacts non-specifically with other proteins of a similar molecular weight during mitosis.

5.2.4 The α-pAPC5 S195 Ab binds specifically to phosphorylated APC5

To establish further the specificity of our custom-made α-pAPC5 S195 Ab for the mitotically phosphorylated form of APC5, we also performed a protein phosphatase assay, similar to the one described in chapter 3 (Fig. 3.10), to evaluate whether the α-pAPC5 S195 Ab recognizes phosphorylated APC5 specifically, and does not recognize the unphosphorylated APC5 derivative. For this purpose, we co-IP'd APC5 using an α-APC7 Ab both from asynchronous and mitotically-arrested RPE-1 and HeLa cells, and incubated IPs with, or without, λ-phosphatase (see Sec. 2.2.6, Chapter 2). We then performed a Western blot to examine the effects of λ-phosphatase treatment on the levels of pAPC5 S195, as well as the levels and changes in the phosphorylation status of APC7 (Fig. 5.3).

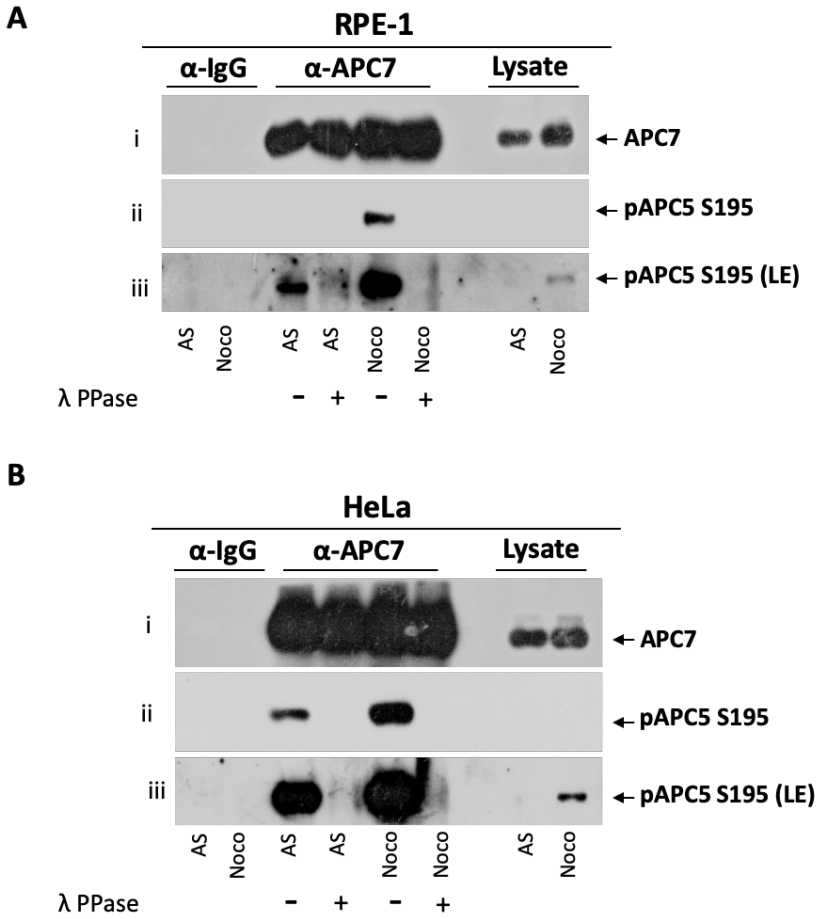

Figure 5.3: **The α-pAPC5 S195 Ab recognizes specifically phosphorylated APC5.** Lysates from asynchronous (AS) and mitotically-arrested (Noco) RPE-1 (**A**) and HeLa (**B**) cells were harvested in APC/C lysis buffer. An equal amount of total protein was incubated overnight at 4°C with an APC7 (α-APC7) Ab or with a normal rabbit IgG (α-IgG), followed by 3h incubation at 4°C with Protein G Sepharose beads. Following IP, Protein G beads were incubated for 1h at 30°C in the presence or absence of λ-phosphatase. IPs, together with 50μg of total protein lysate were separated by SDS-PAGE, transferred to a nitrocellulose membrane and the levels of pAPC5 and APC7 were detected by Western blotting. Longer exposure (LE) is shown to visualize lysate. This data is representative of three individual experiments.

Western blot analyses revealed that APC7 was immunoprecipitated efficiently from both cell lines from asynchronous and mitotically-arrested cells, validating our experimental protocol (panel i, Fig. 5.3 A and B). No differences were observed in the overall levels, or migration pattern, of APC7 following λ-phosphatase treatment (cf lane 3+4 and 5+6 panel i, Fig. 5.3 A and B). These data suggest that dephosphorylation of APC7 has no effect on the

binding affinity of the α-APC7 Ab for its antigen. In contrast, however, λ-phosphatase treatment abolished completely the binding avidity of the α-pAPC5 S195 Ab for its antigen in mitotically-arrested RPE-1 and HeLa cells (panel ii, Fig. 5.3 A and B). This APC5 species was also detected at low levels in asynchronous RPE-1 and HeLa cells, presumably reflecting the higher mitotic index of these cells; long exposures are presented to see APC5 immunoreactivity in cell lysates (cf panel ii and iii, Fig. 5.3 B). Overall, these data establish that the α-pAPC5 S195 Ab recognizes specifically the mitotically-phosphorylated form of APC5, making it a suitable tool to interrogate the phosphorylation status of endogenous APC5 during mitosis.

5.3 Detection of APC5 S195 phosphorylation under physiological conditions

5.3.1 Detection of phosphorylated APC5 S195 species during mitosis

Having confirmed formerly that the α-pAPC5 S195 Ab recognizes specifically the phosphorylated form of APC5 and does not recognize other proteins of the same molecular weight in mitosis (Fig. 5.1 and 5.2), we wanted to continue our investigation looking at APC5 S195 phosphorylation during mitotic progression. For this reason, we repeated the nocodazole release experiments described previously (Sec. 3.2, Chapter 3). Thus, following nocodazole-release and serum re-addition we harvested our cells at different time points to follow APC5 phosphorylation during mitotic progression by Western blotting using our specific α-pAPC5 S195 Ab (Fig. 5.4 A and B). Akin to the other nocodazole-release experiments conducted so far, we also looked at the levels of the APC/C substrates Cyclin B1 and Plk1, as well as at the levels and at the phosphorylation status of APC3 to follow cells as they exited mitosis (Fig. 5.4 A and B).

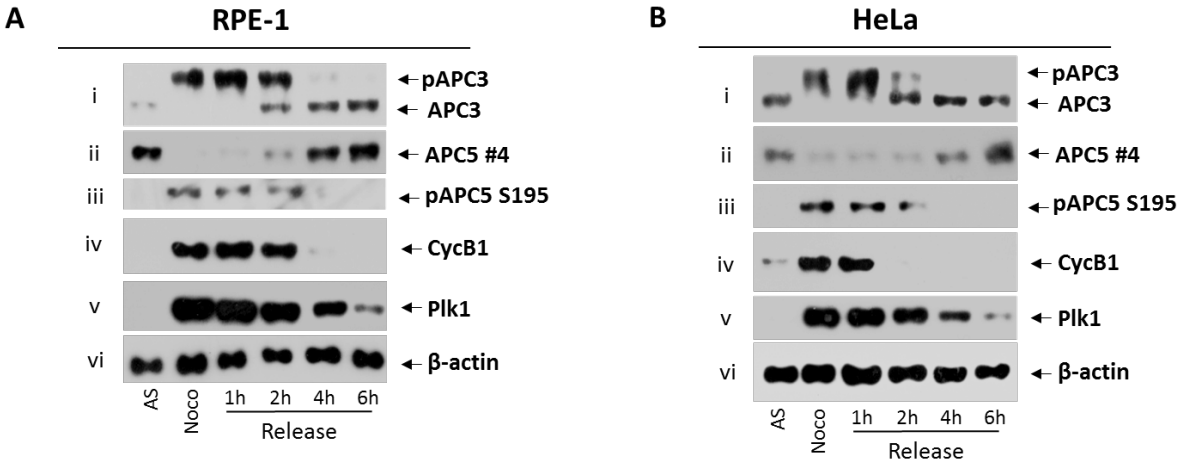

Figure 5.4: **APC5 S195 is phosphorylated specifically during mitosis.** RPE-1 (**A**) and HeLa (**B**) cell lysates from asynchronous (AS), nocodazole-arrested cells (Noco) and cells released from the mitotic arrest at different time-points were harvested in UTB lysis buffer. 50μg of total protein was separated by SDS-PAGE, transferred to a nitrocellulose membrane and the binding avidity of APC5 #4 mAb and α-pAPC5 S195 Ab for their antigens, as well as the levels of APC3, Cyclin B1 and Plk1 were determined by Western blotting. The levels of β-actin were used as a loading control. This data is representative of three individual experiments.

As anticipated a higher molecular weight band for APC3 was detected in mitotically-arrested cells compared to asynchronous cells, which was gradually reduced as cells progressed through mitosis (panel i, Fig. 5.4 A and B). Consistent with this, Cyclin B1 and Plk1 levels were elevated in mitotically-arrested cells compared to asynchronous cells, and they were progressively lost after the release from nocodazole, in both RPE-1 and HeLa cells (panel iv and v, Fig. 5.4 A and B). Consistent with earlier observations APC5 was phosphorylated in mitosis, as noted by the increase in the detection of the phosphorylated APC5 species with the α-pAPC5 S195 Ab, and the loss of the APC5 #4 mAb avidity for APC5 in both RPE-1 and HeLa cells (panel ii and iii, Fig. 5.4 A and B). Taken together these results indicate that the entire APC5 cellular pool is phosphorylated at S195 during mitosis, and increased our confidence that we could track endogenous APC5 protein phosphorylation during mitosis.

To confirm that APC5 phosphorylation is restricted to mitosis we also repeated our cell cycle synchronization experiments with different cell cycle drugs (Sec. 3.2.2, Chapter 3). For this purpose, RPE-1 and HeLa cell lysates were harvested following the synchronization of cells at the G2/M border with the Cdk1 inhibitor, RO-3306, or following a mitotic arrest with either nocodazole or taxol; asynchronous cell lysates were also harvested. The phosphorylation status of APC5 was then detected by Western blotting (Fig. 5.5 A and B). Cyclin B1, Plk1 and APC3 levels were also determined to establish the effectiveness of the respective synchronization treatments (Fig. 5.5 A and B).

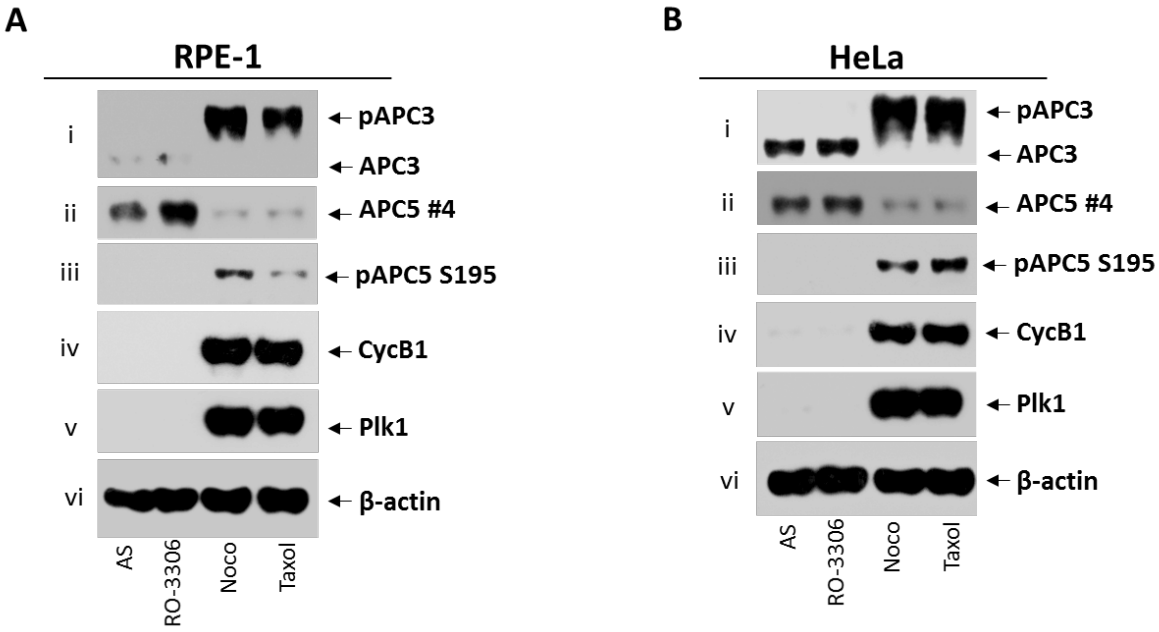

Figure 5.5: **APC5 phosphorylation at S195 is restricted to mitosis.** Lysates from Asynchronous (AS), G2/M-arrested (RO-3306) and mitotic-arrested (Noco/Taxol) RPE-1 (**A**) and HeLa (**B**) cells were harvested in UTB Lysis Buffer. 50µg of total protein was separated by SDS-PAGE, transferred to a nitrocellulose membrane and the phosphorylation status of APC5, as well as the levels of APC3, Cyclin B1 and Plk1 were all detected by Western blotting. The levels of β-actin were used as a loading control. These data are representative of three individual experiments.

As expected, the slower migrating, phosphorylated, form of APC3 was only detected in mitosis and it was not present in asynchronous cells, or in cells arrested at the G2/M border

(cf lane 1 and 2 with 3 and 4, panel i, Fig. 5.5 A and B). Likewise, Cyclin B1 and Plk1 could only be detected in mitotically-arrested samples (cf lane 1 and 2 with 3 and 4, panel iv and v, Fig. 5.5 A and B). Interestingly, the α-pAPC5 S195 Ab only detected APC5 phosphorylated at S195 in mitotic cells and did not detect any phosphorylated APC5 in cells arrested at the G2/M border; Western blot analyses with the α-APC5 #4 mAb confirmed these observations (panel ii and iii, Fig. 5.5 A and B). The reason for the apparent loss in phosphorylated APC5 S195 signal in taxol-arrested RPE-1 cells compared to nocodazole-treated cells is not clear as phosphorylated APC5 S195 levels are comparable in nocodazole and taxol-treated HeLa cells (cf lane 3 and 4, panel iii, Fig. 5.5 A and B). Together, these data establish with certainty that APC5 S195 is phosphorylated as cells enter and progress through mitosis, and is not phosphorylated in G2 cells (panel iii, Fig. 5.4 and 5.5 A and B).

5.3.2 Reciprocal co-immunoprecipitation reveals that the α-pAPC5 S195 Ab can be used for immunoprecipitation

As we have established that the α-pAPC5 S195 Ab reacts specifically with the phosphorylated APC5 S195 species during mitosis, we next wanted to determine whether this Ab could also be used for IP so that we could, ultimately, relate S195 phosphorylation status to the dynamic APC/C interactome or APC/C PTM's in mitosis, although we recognized that IP with the phospho-specific Ab would preclude the identification of proteins(s) that interact specifically with this phospho-APC5 S195 residue itself. To evaluate the ability of the α-pAPC5 S195 Ab for IP, we conducted a series of reciprocal co-IPs experiments, both in RPE-1 and HeLa cells, in which we tested the ability of the α-pAPC5 S195 Ab to co-IP the APC/C subunit, APC7 from asynchronous and mitotically-arrested cells. In this regard we performed reciprocal IP's with the α-APC7 Ab to establish the

efficiency of the α-pAPC5 S195 Ab to IP the APC/C holoenzyme in both cell lines (Fig. 5.6 and 5.7 A and B).

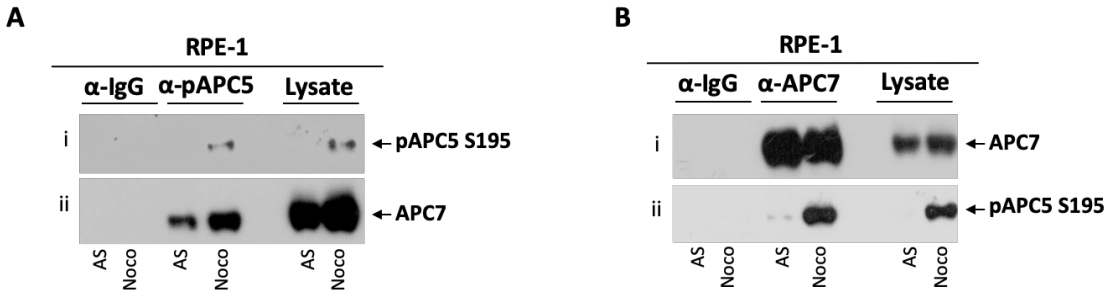

Figure 5.6: **The α-pAPC5 S195 Ab is suitable for IP in RPE-1 cells.** Lysates from Asynchronous (AS) and mitotically-arrested (Noco) RPE-1 cells were harvested in APC/C lysis buffer. An equal amount of total protein from AS and Noco cells was incubated overnight at 4°C either with the pAPC5 S195 specific Ab (α-pAPC5, **A**), with an APC7 specific Ab (α-APC7, **B**) or with normal rabbit IgG (α-IgG, **A** and **B**) followed by 3h incubation at 4°C with Protein G Sepharose beads. Immunoprecipitated proteins and 50μg of total protein (Lysate) was separated by SDS-PAGE, transferred to a nitrocellulose membrane and the levels of pAPC5 S195 and APC7 were detected by Western blotting. These data are representative of three individual experiments.

Western blotting results revealed the presence of a band corresponding to the pAPC5 S195 species present mostly in mitotically-arrested cells with little, or no signal for phosphorylated APC5 in asynchronous cell lysates (panel i, Fig. 5.6 A). Interestingly, the α-pAPC5 S195 Ab also co-IP'd APC7 suggesting that this phosphorylated APC5 species is a component of the APC/C (panel ii, Fig. 5.6 A). In support of this notion, the α-APC7 Ab co-immunoprecipitated the pAPC5 S195 species specifically from mitotic cells (panel ii, Fig. 5.6 B). Although the efficiency of the α-pAPC5 S195 to IP APC7, was reduced relative to the α-APC7 Ab it did co-IP a proportion of the APC/C complex. Taken together, these data suggest that the α-pAPC5 S195 Ab is suitable for conducting IP experiments (Fig. 5.6 A and B).

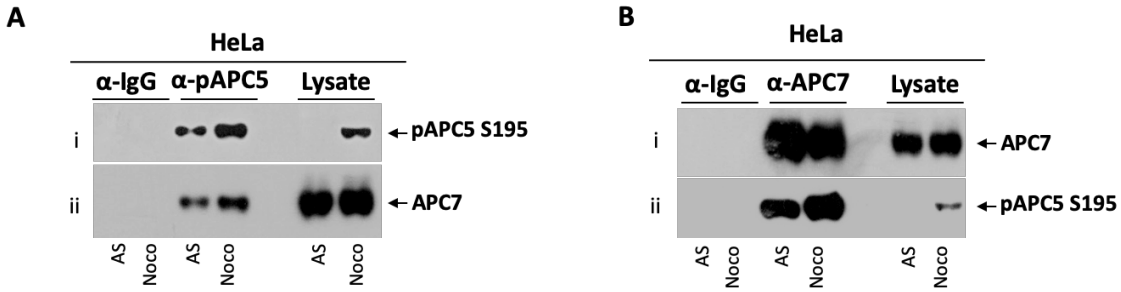

Figure 5.7: **The α-pAPC5 S195 Ab is suitable for IP in HeLa cells.** Lysates from Asynchronous (AS) and mitotically-arrested (Noco) HeLa cells were obtained by incubation in APC/C lysis buffer. An equal amount of total protein from AS and Noco cells was incubated overnight at 4°C either with the pAPC5 S195 specific Ab (α-pAPC5, **A**), with an APC7 pAb (α-APC7, **B**) or with normal rabbit IgG (α-IgG, **A** and **B**) followed by 3h incubation at 4°C with Protein G Sepharose beads. Immunoprecipitated proteins and 50μg of total protein (Lysates) was separated by SDS-PAGE, transferred to a nitrocellulose membrane and the levels of pAPC5 S195 and APC7 were detected by Western blotting. These data are representative of three individual experiments.

Similar results were also observed following reciprocal co-IP experiments conducted in HeLa cells (Fig. 5.7 A and B). Indeed, IP's with the α-pAPC5 S195 Ab clearly indicated its ability to pulldown APC7 from both asynchronous and nocodazole-arrested cells (panel ii, Fig. 5.7 A). As before, a low amount of phosphorylated APC5 S195 was also immunoprecipitated from asynchronous cells, consistent with the presence of mitotic cells in asynchronous HeLa cultures (panel i, Fig. 5.7 A). As for RPE-1 cells, the ability of the α-pAPC5 S195 Ab to IP the APC/C was reduced relative to the ability of the α-APC7 Ab but demonstrated clearly its ability to co-IP APC7 (panel ii, Fig. 5.7 B).

Overall, the results of these experiments confirmed the suitability of the α-APC5 S195 phospho-Ab for IP, even though its efficiency was lower than the α-APC7 Ab (Fig. 5.6 and 5.7, A and B).

5.4 α-pAPC5 S195 Ab as a tool to investigate the kinase responsible for APC5 phosphorylation at S195

Given that we can track APC5 S195 phosphorylation directly with the α-pAPC5 S195 Ab we also decided to repeat the series of experiments presented in Chapter 3 that attempted to identify the mitotic kinase(s) that targeted S195 for phosphorylation during mitosis (Fig. 3.16-3.18).

5.4.1 Cdk1 inhibition reduces the levels of the pAPC5 S195 species in mitosis

To re-assess the requirement for Cdk1 in APC5 S195 phosphorylation during mitosis, lysates previously obtained from RPE-1 cells synchronized in mitosis by treatment with nocodazole and treated with the Cdk1 kinase inhibitor RO-3306, either in the presence, or absence, of the 26S proteasome inhibitor MG132 for 2h and 4h, were used for Western blotting and the evaluation of APC5 phosphorylation status using the α-pAPC5 S195 Ab. Please note that this figure was generated by combining the pAPC5 blot with blots presented in Chapter 3 (Fig. 3.16 and 5.8).

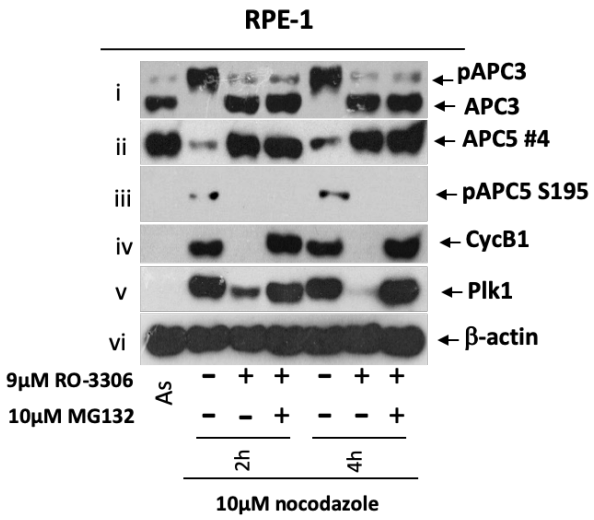

Figure 5.8: **Cdk1 inhibition attenuates APC5 phosphorylation in nocodazole-arrested cells.** Lysates from asynchronous (AS), mitotically-arrested cells (lane 2 and 5), mitotically-arrested cells treated with 9μM RO-3306 for 2h and 4h (lane 3 and 6) and mitotically-arrested cells treated with 9μM RO-3306 and 10μM MG132 for 2h and 4h (lane 4 and 7) were harvested in UTB lysis buffer. 50μg of total protein was separated by SDS-PAGE, transferred to a nitrocellulose membrane. The phosphorylation status of APC5 was detected by the inability of the α-APC5 mAb #4 to bind its epitope when phosphorylated, and the ability of the α-pAPC5 S195 Ab to recognize pAPC5. The phosphorylation status of APC3 was used both as a control for the mitotic arrest and as a control for Cdk1 inhibition. The levels of CycB1 and Plk1 were used as controls for APC/C activity and the levels of β-actin were used as a loading control. The blots corresponding to APC3, APC5 #4, CycB1, Plk1 and β-actin are taken by Fig. 3.16, whereas pAPC5 S195 is specific to this figure. This data is representative of three individual experiments.

As discussed extensively in Chapter 3 (Sec. 3.7.1, Chapter 3), Cdk1 inhibition of mitotically-arrested cells causes the phenomenon of mitotic escape even in the presence of nocodazole, which can be overcome by the concomitant addition of MG132. Consistent with these properties, in the absence of the 26S proteasome inhibitor the levels of Cyclin B1 and Plk1, as well as the APC3 hyperphosphorylated form, were very low when Cdk1 activity was inhibited. However, the levels of the APC/C substrates remained high when MG132 was also added, indicating a cellular mitotic arrest under conditions where Cdk1 was inhibited (panel i, iv and v, Fig. 5.8). The efficiency of the Cdk1 inhibition treatment under these circumstances was also confirmed by the loss of APC3 phosphorylation after 2h and 4h

when MG132 was also present, as hyperphosphorylation of APC3 is due to Cdk1 mitotic activity (panel i, Fig. 5.8) (Fujimitsu et al., 2016, Golan et al., 2002). In these conditions, we could observe the recovery of the APC5 signal detected by the α-APC5 mAb #4, which we related to the loss of APC5 mitotic phosphorylation when Cdk1 kinase is inhibited (panel ii, Fig. 5.8 and Sec. 3.7.1, Chapter 3). Consistent with these observations the α-pAPC5 S195 Ab did not detect pAPC5 when Cdk1 was inhibited confirming our hypothesis that Cdk1 participates in the phosphorylation of APC5 S195 during mitosis (cf lane 2+4 and 5+7, panel iii, Fig. 5.8) though whether this is direct, or indirect remains to be established.

5.4.2 Plk1 inhibition reduces the levels of the pAPC5 S195 species in mitosis

To confirm our data on the potential role played by the mitotic kinase Plk1 in the phosphorylation of APC5 during mitosis, we re-ran samples from the experiment presented in Chapter 3, where Plk1 was inhibited during mitosis either in the presence, or absence, of the 26S proteasome inhibitor, MG132 (Sec. 3.7.2, Chapter 3). Thus, lysates obtained by treatment of RPE-1 cells with nocodazole and with the Plk1 inhibitor BI-6727, in presence, or absence, of MG132 for 2h and 4h, were separated by SDS-PAGE and subjected to Western blotting to determine the levels of the pAPC5 S195 species. The results of these analyses are presented alongside previous Western blots for APC3, Cyclin B1, Plk1 and β-actin (Fig. 3.17 and Fig. 5.9).

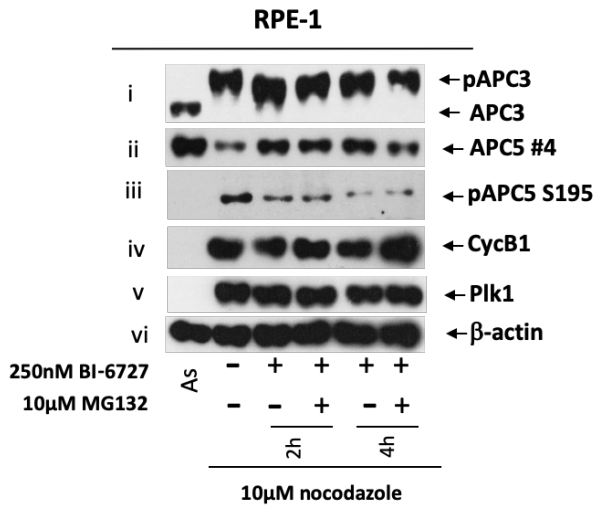

Figure 5. 9: **Plk1 inhibition attenuates APC5 phosphorylation in nocodazole-arrested cells.** Lysates from asynchronous (AS), mitotically-arrested cells (lane 2), mitotically-arrested cells treated with 250nM BI-6727 for 2h and 4h (lane 3 and 5) and mitotically-arrested cells treated with 250nM BI-6727 and 10μM MG132 for 2h and 4h (lane 4 and 6) were harvested in UTB lysis buffer. 50μg of total protein was separated by SDS-PAGE and then transferred to a nitrocellulose membrane. The phosphorylation status of APC5 was detected by the inability of the α-APC5 mAb #4 to bind its epitope when phosphorylated, and the ability of the α-pAPC5 S195 Ab to recognize pAPC5. The levels of APC3, CycB1 and Plk1 were used as controls for APC/C activity, whereas the levels of β-actin were used as a loading control. The blots corresponding to APC3, APC5 #4, CycB1, Plk1 and β-actin are taken by Fig. 3.17, whereas pAPC5 S195 is specific for this figure. This data is representative of three individual experiments.

As discussed previously in Chapter 3, Western blotting results revealed that cells arrested in mitosis with nocodazole remained in mitosis when Plk1 was inhibited with BI-6727, and did not exit mitosis. Indeed, APC/C substrates Cyclin B1 and Plk1 remained elevated in the presence of BI-6727, and APC3 remained hyperphosphorylated (panel i, iv and v, Fig. 5.9 and Sec. 3.7.2, Chapter 3). Consistent with a role for Plk1 in the phosphorylation of APC5 S195, Plk1 inhibition restored the ability of α-APC5 mAb #4 to recognise the unphosphorylated form of APC5, whilst Western blotting with the α-pAPC5 S195 Ab determined that the levels of pAPC5 S195 were reduced dramatically when Plk1 was

inhibited (panel ii and iii, Fig. 5.9; panel ii Fig. 3.17). These data indicate that Plk1 has a role in the phosphorylation of S195 during mitosis.

5.4.3 Aurora B inhibition greatly reduces pAPC5 S195 protein levels in mitosis

Akin to the Cdk1 and Plk1 inhibitor studies we also re-assessed the role of Aurora B kinase in the mitotic phosphorylation of APC5 (Sec. 3.7.3, Chapter 3). As such, RPE-1 cells lysates obtained by treatment with nocodazole followed by the addition of the Aurora B kinase inhibitor Hesperadin, either in presence or absence of MG132, collected 2h and 4h post-treatment, were used to determine the levels of the pAPC5 S195 protein species using the α-pAPC5 S195 Ab. The results of these analyses are presented alongside previous Western blots for APC3, Cyclin B1, Plk1 and β-actin (Fig. 3.18 and Fig. 5.10).

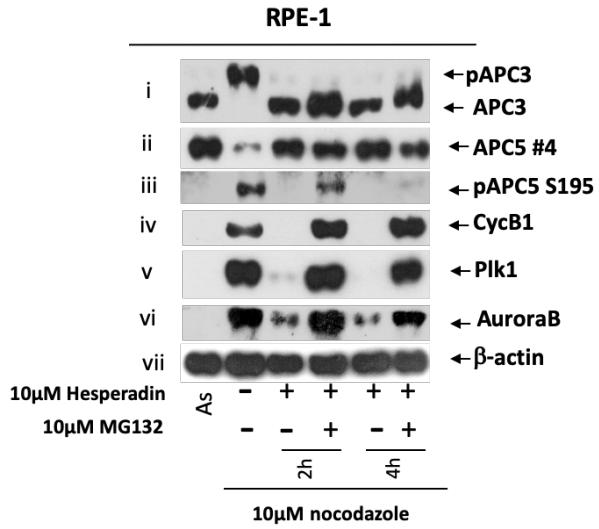

Figure 5. 10: **Aurora B attenuates APC5 phosphorylation in nocodazole-arrested cells.** Lysates from asynchronous (AS), mitotically-arrested cells (lane 2), mitotically-arrested cells treated with 10μM Hesperadin for 2h and 4h (lane 3 and 5) and mitotically-arrested cells treated with 10μM Hesperadin and 10μM MG132 for 2h and 4h (lane 4 and 6) were harvested in UTB lysis buffer. 50μg of total protein was separated by SDS-PAGE and transferred to nitrocellulose. The phosphorylation status of APC5 was detected by the inability of the α-APC5 mAb #4 to bind its epitope when phosphorylated, as well as using the α-pAPC5 S195 Ab. The levels of APC3, CycB1 and Plk1 were used as controls for APC/C activity, whereas the levels of β-actin were used as a loading control. The blots corresponding to APC3, APC5 #4, CycB1, Plk1 and β-actin are taken from Fig. 3.18, whereas pAPC5 S195 is specific for this figure. This data is representative of three individual experiments.

As discussed in Chapter 3, the experimental procedure adopted allowed for the successful inhibition of the Aurora B kinase in mitotically-arrested cells in the presence of the 26S proteasome inhibitor, MG132. Indeed, in the presence of Hesperadin and nocodazole alone, cells escaped mitosis as evidenced by the low levels of Cyclin B1, Plk1 and Aurora B after 2h and 4h compared to cells only treated with nocodazole (panel iv, v and vi, Fig. 5.10). However, upon addition of MG132 these APC/C substrates were elevated, suggesting the successful arrest of cells in mitosis when Aurora B was inhibited (panel iv, v and vi, Fig. 5.10). Under these circumstances, APC3 was hypophosphorylated in all samples regardless by the presence of MG132, or not (panel i, Fig. 5.10). These data suggest that like Cdk1

(Golan et al., 2002, Fujimitsu et al., 2016) Aurora B kinase contributes towards APC3 phosphorylation in mitosis (panel i, Fig. 5.10). Pertinent to our investigation, APC5 phosphorylation was also lost in mitotically-arrested cells when Aurora B was inhibited, as indicated by the recovery of the signal for the α-APC5 mAb #4 and the loss of pAPC5 S195 using the phospho-specific Ab, particularly 4h post-treatment (panel ii and iii, Fig. 5.10). These data suggest that Aurora B also plays a role in APC5 S195 phosphorylation during mitosis.

5.5 α-pAPC5 S195 Ab binding avidity for the FLAG-APC5 S195A, S195D, T232A and T232E phospho-mutants in mitosis

As the α-pAPC5 S195 Ab can detect the pAPC5 S195 species under physiological conditions by Western blotting, we decided to exploit this feature to investigate its binding avidity for the FLAG-APC5 phospho-mutants generated previously (Sec. 4.2.1, Chapter 4). In this regard we aimed to evaluate whether FLAG-APC5 S195A and FLAG-APC5 S195D that represent the constitutively unphosphorylated and phosphorylated derivatives of S195, respectively, are recognized by the phospho-specific Ab. In a similar scenario we also decided to test whether the α-pAPC5 S195 Ab would recognize the FLAG-APC5 T232A and T232E phospho-mutants in mitosis (Sec. 4.2.2, Chapter 4), which would assess directly the requirement for T232 phosphorylation in the regulation of S195 phosphorylation. Indeed, Plk1 phosphorylation of its substrates is often dependent upon the substrates prior phosphorylation by Cdk1 at a site proximal to the residues phosphorylated directly by Plk1 (Elia et al., 2003a, Jang et al., 2002). As APC5 T232 is a potential Cdk1 site that was found to be phosphorylated during mitosis in a previous mass spectrometric screen (Steen et al.,

2008), this question seemed highly pertinent to understanding the regulation of S195 phosphorylation.

5.5.1 The α-pAPC5 S195 Ab does not recognize the S195A and S195D mutants

To investigate whether S195A and S195D are recognized by the α-pAPC5 S195 Ab we performed an IP assay using our FLAG-APC5 WT, S195A and S195D U2OS FRT cell lines, that had been arrested in mitosis by nocodazole. Lysates obtained from mitotically-arrested cells were incubated with a mouse α-FLAG specific Ab directed towards the FLAG-APC5 species or with a mouse α-IgG control Ab. We then precipitated the immunocomplexes on Protein G Sepharose beads and performed Western blotting to determine the binding avidity of the α-pAPC5 S195 Ab for the FLAG-APC5 WT, FLAG-APC5 S195A and FLAG-APC5 S195D species (Fig. 5.11).

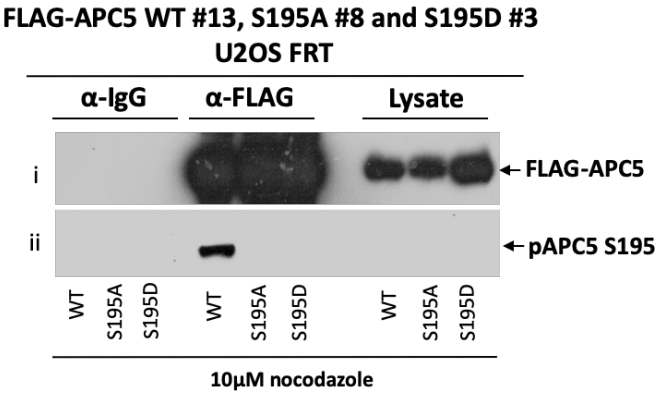

Figure 5. 11: The **pAPC5 S195 Ab does not recognize the APC5 S195A and S195D phospho-mutants.** Lysates from mitotically-arrested FLAG-APC5 WT (WT), FLAG-APC5 S195A (S195A) and FLAG-APC5 S195D (S195D) U2OS FRT cells were subject to immunoprecipitation with a FLAG specific Ab (α-FLAG) or with normal mouse IgG (α-IgG) followed by isolation of the immunocomplexes with Protein G Sepharose beads. Immunoprecipitated proteins and 50μg of total protein (Lysate) were separated by SDS-PAGE, transferred to a nitrocellulose membrane and the levels of FLAG-APC5 and pAPC5 S195 were detected by Western blotting. These data are representative of three individual experiments.

Western blot analysis revealed that the FLAG-APC5 species were successfully immunoprecipitated in all the cell lines employed, as indicated by the strong immunoreactivity of the α-FLAG Ab in our Western blot (panel i, Fig. 5.11). However, further analyses revealed that the α-pAPC5 S195 Ab was only able to react with the FLAG-APC5 WT species and did not recognize S195A or S195D (panel ii, Fig. 5.11). The loss of binding for the FLAG-APC5 S195A species was not surprising as the substitution of the S residue with an A prevents phosphorylation at this site (panel ii, Fig. 5.11). The loss of FLAG-APC5 S195D reactivity was similarly not unexpected, as previous studies have indicated whilst S to D changes can sometimes mimic biological activities of phosphorylated S residues, D is not similar enough, structurally, to pS to be recognized by phospho-specific antibodies (panel ii, Fig. 5.1) (Pearlman et al., 2011); The lack of detection of pAPC5 S195 in the WT lysate presumably reflects the fact that we used 2 mg of lysate for immunoprecipitation and only 50 μg for the lysate input (cf lane 4 and 7, Fig. 5.11).

5.5.2 APC5 mitotic phosphorylation at S195 does not seem to be dependent upon Cdk1 phosphorylation of T232

To evaluate the requirement for T232 phosphorylation by Cdk1, as a pre-requisite for S195 phosphorylation, we isolated FLAG-APC5 WT, T232A and T232E species (described in Sec. 4.2.2, Chapter 4) from mitotically-arrested U2OS FRT cells by immunoprecipitation and analysed APC5 S195 phosphorylation directly by Western blot (Fig. 5.12).

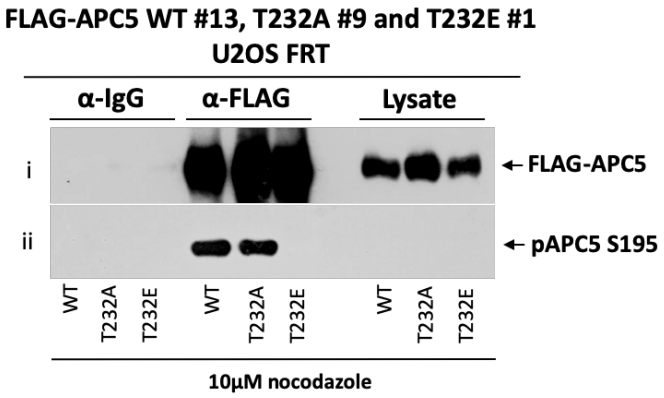

Figure 5. 12: **Investigating the requirement for APC5 T232 phosphorylation in the regulation of S195 phosphorylation.** Lysates from mitotically-arrested FLAG-APC5 WT (WT), FLAG-APC5 T232A (T232A) and FLAG-APC5 T232E (T232E) U2OS FRT cells were subject to immunoprecipitation with a FLAG specific Ab (α-FLAG) or with normal mouse IgG (α-IgG) followed by isolation of the immunocomplexes with Protein G Sepharose beads. Immunoprecipitated proteins and 50μg of total protein (Lysate) were separated by SDS-PAGE, transferred to a nitrocellulose membrane and the levels of FLAG-APC5 and pAPC5 S195 were detected by Western blotting. These data are representative of three individual experiments.

Western blot analyses revealed that the α-FLAG Ab immunoprecipitated FLAG-APC5 species efficiently from all cell lines employed (panel i, Fig. 5.12). Analyses revealed that the WT APC5 species was phosphorylated on S195, whilst mutation of T to A at residue 232 did not affect the ability of this species to be phosphorylated at S195 during mitosis (panel ii, Fig. 5.12). In contrast the putative, phospho-mimicking FLAG-APC5 T232E species, inhibited S195 phosphorylation during mitosis (panel ii, Fig. 5.12). These data, potentially, suggest that Cdk1 phosphorylation of T232 inhibits APC5 S195 phosphorylation, which is in contrast to the published role of Cdk1-directed phosphorylation as a requirement for Plk1-targeted phosphorylation (Elia et al., 2003a, Elia et al., 2003b, Jang et al., 2002). As both S195 and T232 are known to be phosphorylated in mitosis (Herzog et al., 2005, Steen et al., 2008, Hegemann et al., 2011) this experiment suggests that the mitotic phosphorylation of S195 and T232 in APC5 are coordinated temporally.

5.6 Investigating the cellular localization of pAPC5 S195 by immunofluorescence

As the α-pAPC5 S195 Ab worked well for Western blotting and immunoprecipitation we next investigated whether this reagent could be used in immunofluorescence to determine the cellular localization of pAPC5 S195 during mitosis as this might give valuable new insight into APC/C function during mitosis.

5.6.1 pAPC5 S195 localizes at centrosomes during prophase and metaphase and migrates to midbodies following anaphase in RPE-1 and HeLa cells

To determine the specific cellular location of the pAPC5 S195 species during mitosis we grew RPE-1 and HeLa cells on 12-well slides, and then fixed and permeabilized them in methanol at -20°C for 15 min prior to their primary incubation with the specific α-pAPC5 S195 Ab and subsequent incubation with an α-rabbit Alexa Fluor-488 secondary Ab (see Sec.2.4.1, Chapter 2). Slides were then mounted on to a coverslip with the DAPI-containing Vectashield and visualized with a Nikon Y-FL epi-fluorescent microscope to ascertain the specific localization of the pAPC5 S195 species during the different mitotic stages (Fig. 5.13 A and B).

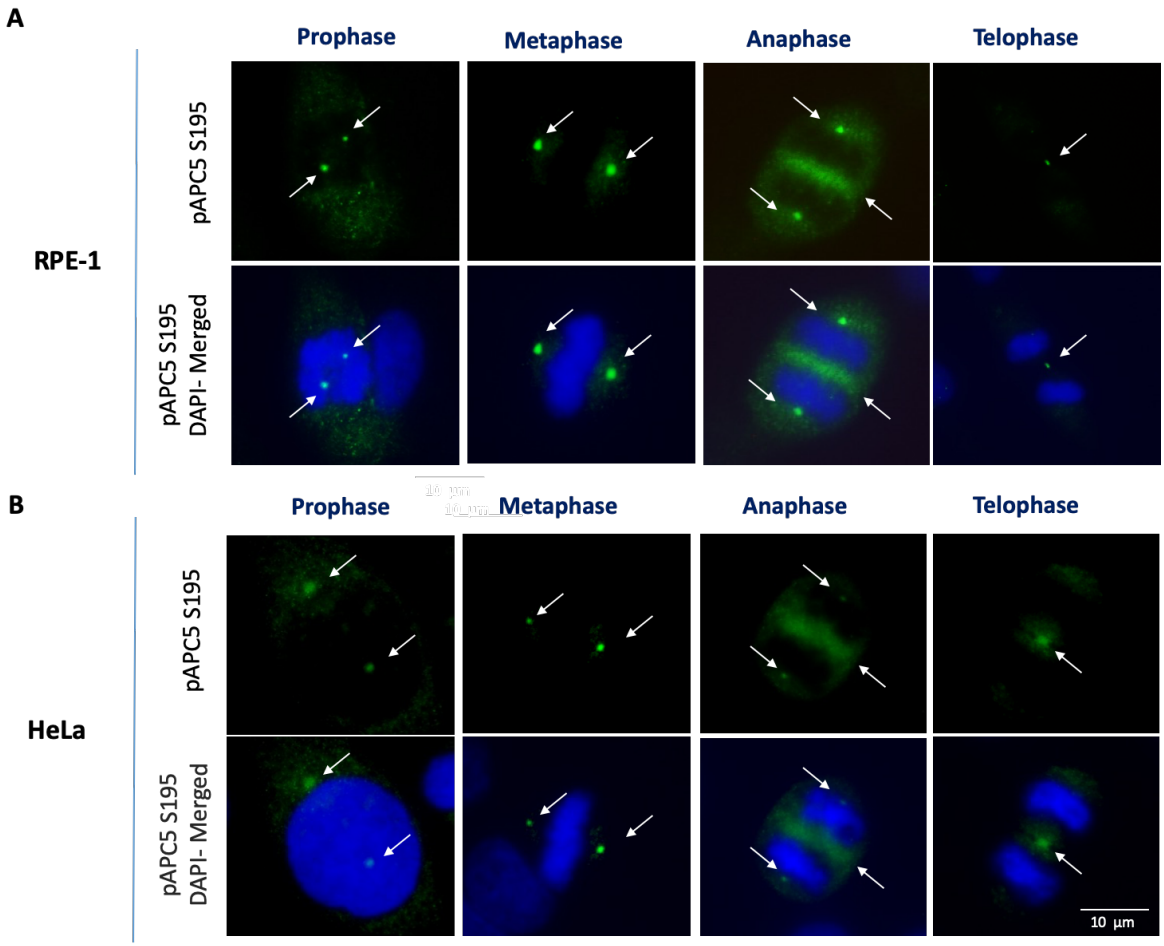

Figure 5.13: **Phospho-APC5 S195 localizes at centrosomes and the midbody during mitosis in both RPE-1 and HeLa cells.** RPE-1 (**A**) and HeLa (**B**) cells grown on 12-well slides were fixed and permeabilized in methanol. pAPC5 localization was detected by IF using the rabbit α-pAPC5 S195 primary Ab and an Alexa Fluor-488 secondary Ab. Slides were mounted in DAPI-containing Vectashield and then visualized with the Nikon Y-FL epi-fluorescent microscope. These data are representative of three individual experiments.

The results of these experiments were striking. Indeed, not only we were able to successfully visualize a clean green signal corresponding to the pAPC5 S195 species, we could clearly establish the localization pattern for the pAPC5 S195 species during the different mitotic phases both in RPE-1 and HeLa cells (Fig. 5.13 A and B). It was apparent that the phospho-APC5 species was detectable during prophase and metaphase where it appeared to localize with centrosomes and where it stayed until anaphase onset (panel Prophase, Metaphase and Anaphase, Fig. 3.13 A and B). Interestingly, these studies also revealed that following

metaphase-to-anaphase transition, pAPC5 S195 migrates towards the area between the segregating chromosomes, to eventually occupy the transient structures, in the midzone between dividing cells, known as midbodies (panel Telophase, Fig. 5.13 A and B). This localization pattern was aided by the visualization of DNA by the nuclear stain, DAPI (panel Prophase, Metaphase, Anaphase, Telophase, pAPC5 S195 and DAPI-Merged, Fig. 5.13 A and B). Overall, these data revealed that pAPC5 S195 has a distinctive and specific localization pattern during mitosis.

5.6.2 pAPC5 S195 co-localizes with APC/C substrates Plk1 and PRC1 during mitosis

Given the results obtained using the whole-field epi-fluorescent microscope, which disclosed precious information about the specific localization of the pAPC5 S195 species during mitosis, we initiated a new series of studies to evaluate whether pAPC5 S195 species co-localized with known centrosomal markers and APC/C substrates. In this regard, it is interesting to note that centrosomes represent the main region where Cyclin B1 degradation occurs once the SAC is satisfied at metaphase (Jackman et al., 2003). The localization of pAPC5 S195 species to the midbody is also interesting, in so far as there are no reports to date suggesting that the APC/C is recruited to these sites, but it is known that a number of APC/C substrates are recruited to midbodies during telophase, including the mitotic kinase Plk1, PRC1 and Anillin (Zhao and Fang, 2005, Mollinari et al., 2002, Adriaans et al., 2019, Lindon and Pines, 2004). As such, the presence of the pAPC5 S195 protein species at these sites might relate to the role of the APC/C in targeting these proteins for degradation at the end of mitosis. To investigate the colocalization of pAPC5 S195 with centrosomes and APC/C substrates, RPE-1 cells were grown on 12-well slides, fixed and permeabilized in methanol, and co-stained with the α-pAPC5 S195 rabbit Ab and mouse Abs directed towards α-tubulin, γ-tubulin, Plk1 and PRC1. Slides were then incubated with appropriate Alexa-

Fluor 488 and 594 secondary Abs. Images were collected using the Zeiss LSM780 confocal microscope in order to evaluate co-localization of the pAPC5 S195 protein with centrosomal markers and APC/C substrates (Figs. 5.14-5.17).

Confocal microscopy confirmed the distribution pattern of the pAPC5 S195 established previously (Fig. 5.13). pAPC5 S195 co-localized with both α and γ-tubulin, and particularly γ-tubulin at centrosomes during prophase and metaphase until anaphase onset, though a small proportion of pAPC5 S195 was also detectable, in some instances, at centrosomes during anaphase (Fig. 5.14 and 5.15,). Upon anaphase onset the phosphorylated APC5 S195 species relocalized to the midzone between segregating chromosomes, and during telophase, the entire cellular pool of pAPC5 S195 appeared to be localized to midbodies (panel, Fig. 5.14 and 5.15).

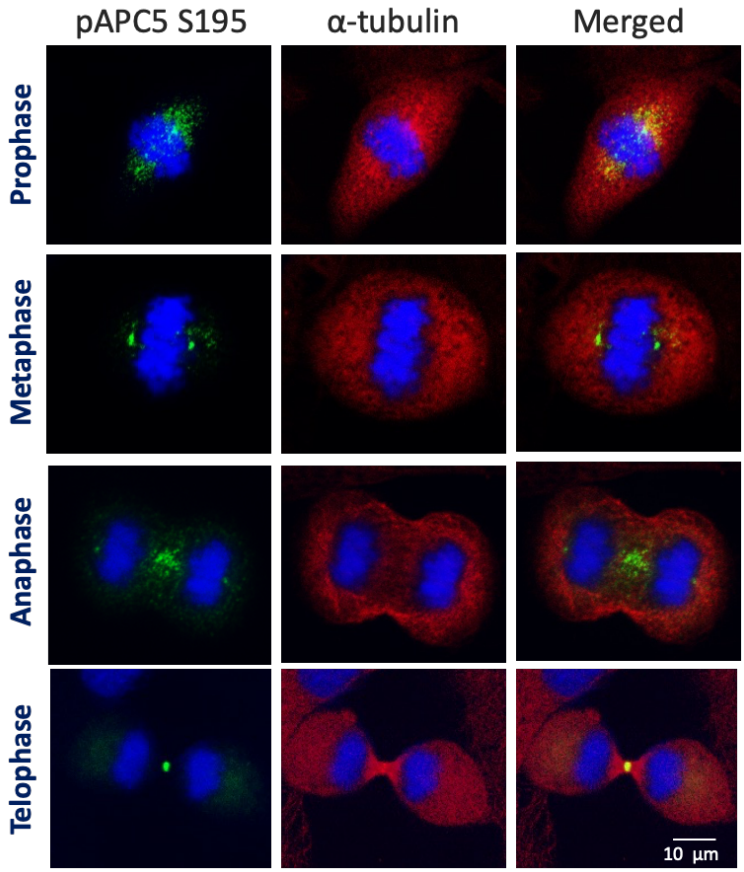

Figure 5.14: **pAPC5 localizes at centrosomes until metaphase-to-anaphase transition and then translocates to the midzone at anaphase and midbody during telophase.** RPE-1 cells grown on 12-well slides were fixed and permeabilized in methanol. pAPC5 localization was detected using the rabbit α-pAPC5 S195 primary Ab and a rabbit Alexa Fluor-488 secondary Ab, whilst an α-tubulin mAb raised in mice and a mouse Alexa Fluor-594 secondary Ab were used to detect α-tubulin. DNA staining was observed with DAPI; stained cells were visualized with the Zeiss LSM780 confocal microscope. These data are representative of three individual experiments.

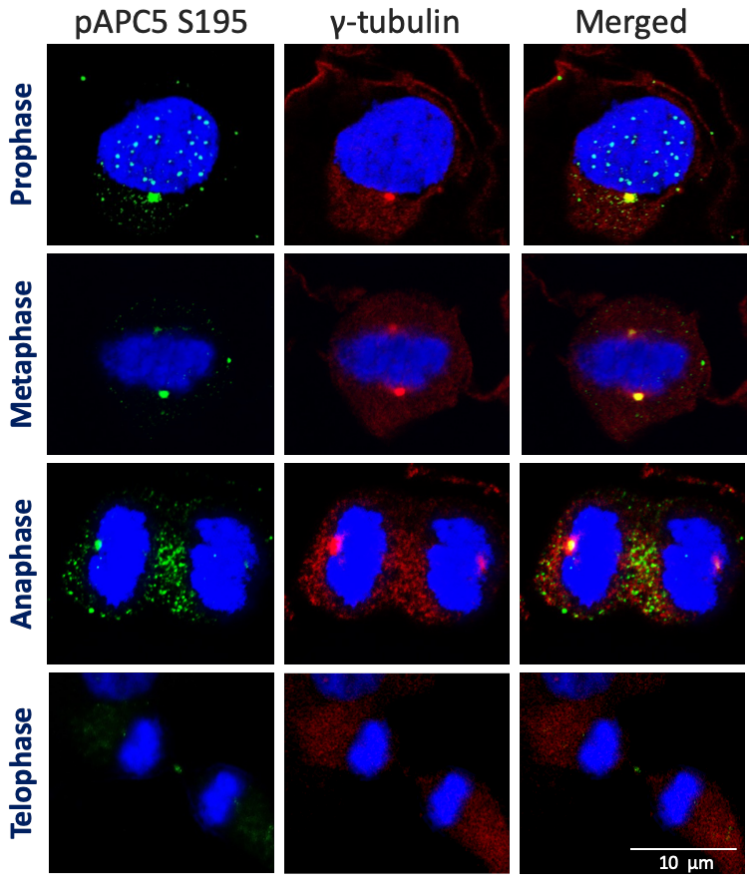

Figure 5.15: **pAPC5 localizes at the centrosomes until metaphase-to-anaphase transition and translocates to the midbody during telophase.** RPE-1 cells grown on 12-well slides were fixed and permeabilized in methanol. pAPC5 localization was detected using the rabbit α-pAPC5 S195 primary Ab and a rabbit Alexa Fluor-488 secondary Ab, whilst a γ-tubulin mAb raised in mice and a mouse Alexa Fluor-594 secondary Ab were used to detect γ-tubulin. DNA staining was observed with DAPI; stained cells were visualized with the Zeiss LSM780 confocal microscope. These data are representative of three individual experiments.

Further co-localization studies revealed that pAPC5 S195 co-localized with the mitotic kinase, Plk1 during metaphase, anaphase and telophase (Fig 5.16). Closer inspection of Plk1 and pAPC5 S195 co-localization during telophase suggested that these proteins did not exactly co-localize but were found juxtaposed in the area of the midbody, with Plk1 concentrated in the central region of the midbody and the pAPC5 S195 species occupying the flanking regions (Fig 5.16). Taken together, these data suggest a close, functional

relationship between pAPC5 S195 and Plk1 during mitosis that warrants further investigation.

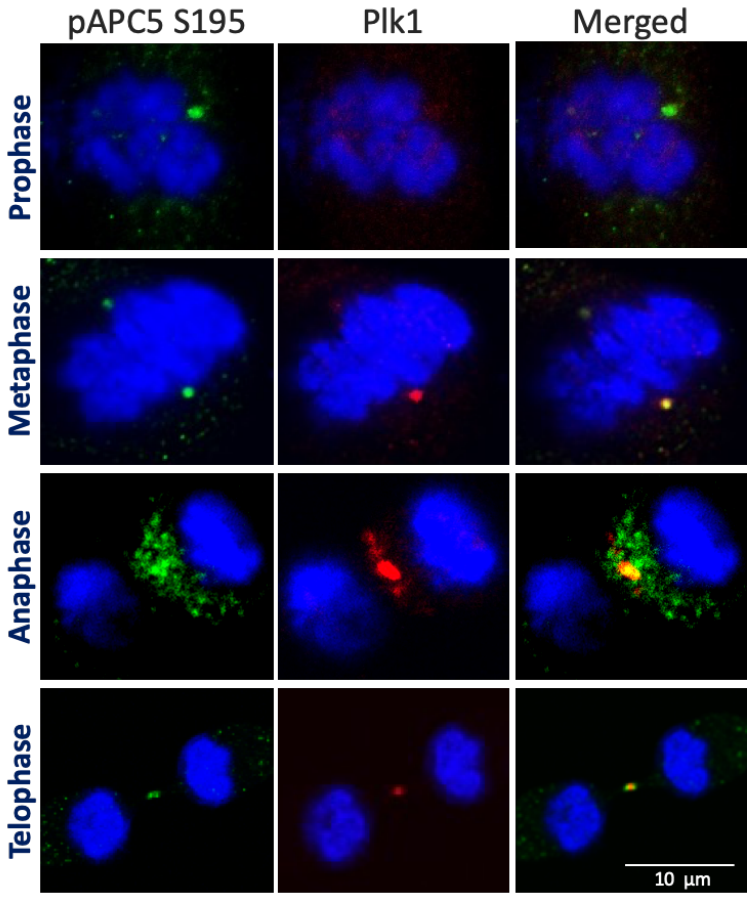

Figure 5.16: **pAPC5 S195 colocalizes with Plk1 during mitosis.** RPE-1 cells grown on 12-well slides were fixed and permeabilized in methanol. pAPC5 localization was detected using the rabbit α-pAPC5 S195 primary Ab and a rabbit Alexa Fluor-488 secondary Ab, whilst a Plk1 mAb raised in mice and a mouse Alexa Fluor-594 secondary Ab were used to detect Plk1. DNA staining was observed with DAPI; stained cells were visualized with the Zeiss LSM780 confocal microscope. These data are representative of three individual experiments.

As the APC/C substrate PRC1 is a known regulator of cytokinesis and aids the translocation of Plk1 to the midbodies after anaphase onset, through its ability to move along the microtubules (Neef et al., 2007, Petronczki et al., 2008), we also investigated whether pAPC5 S195 co-localizes with PRC1 during mitosis. Confocal microscopy revealed that

PRC1 does not localize at the centrosomes during prophase and metaphase, but it is instead associated with microtubules (Fig. 5.17). However, from anaphase onset PRC1 concentrated in the midzone where it co-localized to some extent with the pAPC5 S195 species (Fig. 5.17). During telophase PRC1 and pAPC5 S195 co-localized absolutely in the midbodies, suggesting that pAPC5 S195 and PRC1 are functionally related (Fig. 5.17). Taken together these co-localization studies have offered new insights into pAPC5 S195 localization, and putative functions, in mitosis.

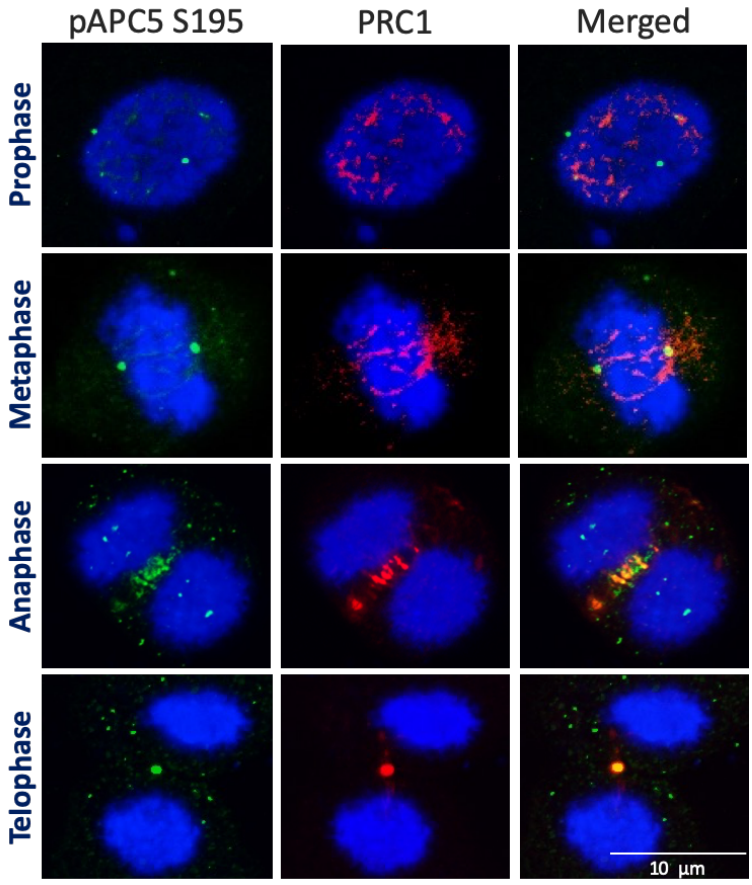

Figure 5.17: **pAPC5 mirrors the APC/C substrate PRC1 distribution in mitosis.** RPE-1 cells grown on 12-well slides were fixed and permeabilized in methanol. pAPC5 S195 localization was detected using the rabbit α-pAPC5 S195 primary Ab and a rabbit Alexa Fluor-488 secondary Ab, whilst a PRC1 mAb raised in mice and a mouse Alexa Fluor-594 secondary Ab were used to detect PRC1. DNA staining was observed with DAPI; stained cells were visualized with the Zeiss LSM780 confocal microscope. These data are representative of three individual experiments.

5.7 Discussion

To fulfil our aim of characterizing APC5 phosphorylation at S195 during mitosis and shed light on its effect on APC/C activity, we needed to develop reagents that could monitor APC5 phosphorylation directly under physiological conditions. For this reason, we raised an Ab against an APC5 peptide encompassing the phosphorylated S195 residue that recognized APC5 pS195 specifically (Sec. 5.2.1). The newly generated Ab was validated successfully, revealing that it recognised the pAPC5 S195 species specifically in mitosis in multiple cell lines (Fig. 5.1); specificity was validated further in RPE-1 and HeLa cell lines (Figs. 5.2 and 5.3). Analyses revealed that APC5 S195 was phosphorylated specifically occur during mitosis, appearing during prophase and disappearing as cells exited from mitosis, strengthening our hypothesis that phosphorylation of APC5 S195 was important in regulating APC/C activity in mitosis (Figs 5.4 and 5.5) (Zhang et al., 2016, Golan et al., 2002, Kraft et al., 2003). Indeed, we have already discussed the potential role for APC5 mitotic phosphorylation at S195 in the regulation of APC3 and APC1 phosphorylation, which is necessary for the association of Cdc20 with the APC/C (Sec. 4.5, Chapter 4) (Zhang et al., 2016, Chang et al., 2014, Fujimitsu et al., 2016).

Given the strategic position of the APC5 subunit within the APC/C structure, where it is in contact with multiple subunits, including APC8 and APC1 (Chang et al., 2014, Cronin et al., 2015), it is possible that the mitotic phosphorylation of APC5 S195 contributes to APC/C activation through alternative mechanisms. In particular, the APC8 subunit of the APC/C has been identified as being important in coordinating the recruitment of Cdc20 and Cdh1 to the APC/C, through its C-box domain, which provides an interaction site for these APC/C activators (Zhang et al., 2016, Alfieri et al., 2016, Matyskiela and Morgan, 2009). Interestingly, the APC1 inhibitory loop masks this C-box domain on APC8 when the APC/C

is inactivated, but upon mitotic phosphorylation of APC1, the Cdc20/Cdh1 binding site on APC8 becomes accessible (Zhang et al., 2016, Fujimitsu et al., 2016, Qiao et al., 2016, Matyskiela and Morgan, 2009). Moreover, association of Cdh1 to the APC/C, which does not require APC1 phosphorylation, has been shown to occur through a direct interaction between APC1 and Cdh1, which causes the rotation of APC8 within the APC/C that is critical for the association of the co-activator with the holoenzyme (Fig. 5.18) (Chang et al., 2014).

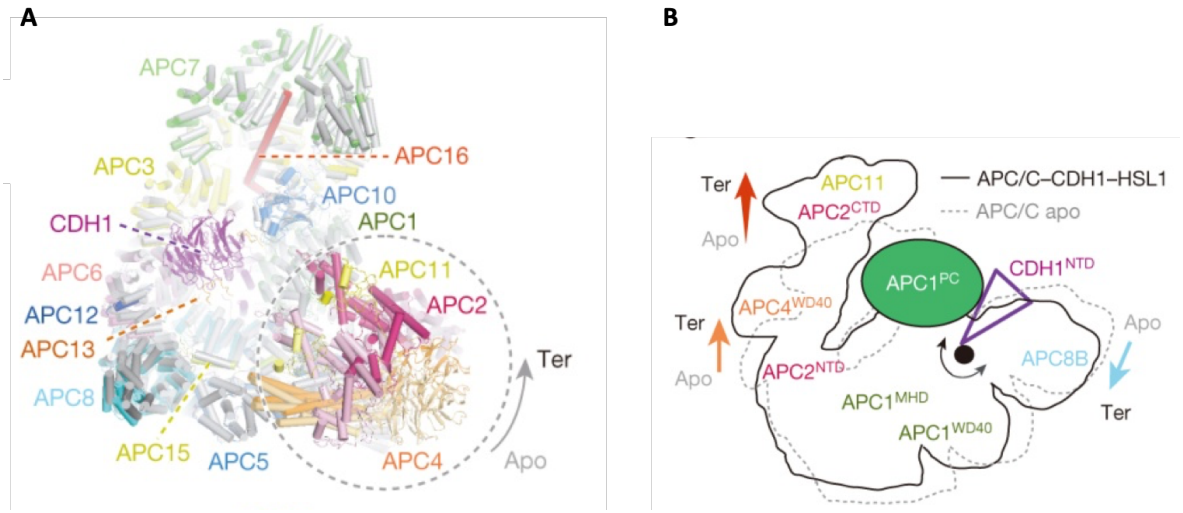

Figure 5. 18: **Cdh1 association with the APC/C requires conformational changes involving APC8.** (**A**) Superimposition of the Apo (grey) and ternary complex APC/C-Cdh1-HSL1 (colour referring to individual subunits) from reconstructed human APC/C at 7.4 Å. Taken from Chang et al. (2014). (**B**) Schematic representation of the superimposition of Apo (grey dots) and APC/C-Cdh1-HSL1 ternary complex (black line) showing platform displacement due to the association with Cdh1. Taken from Chang et al. (2014).

Interestingly, the APC5 S195 residue is positioned within an unstructured loop region, at the interface between APC8 and APC5 (Fig. 5.19 A) (Cronin et al., 2015). As such, APC5 phosphorylation at S195 during mitosis might contribute to the conformational changes observed in APC8 necessary for the association of Cdc20 and Cdh1 co-activators (Chang et al., 2014). Unfortunately however, as this region of APC5 is unstructured we cannot make

firm predictions about the role of APC5 pS195 in the association of Cdc20 with APC8 Fig. 5.19 B).

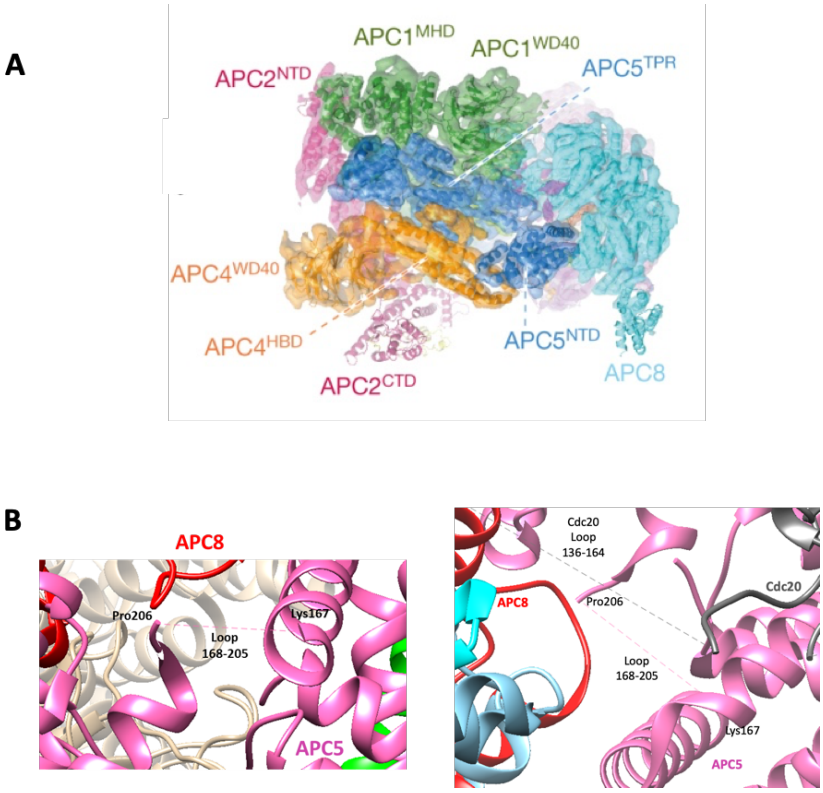

Figure 5. 19: **APC5 loop region encompassing S195 lies within close proximity to APC8.** (**A**) Electron microscopy image of human APC/C at 7.4 Å resolution showing APC1, APC2, APC4 and APC8 subunits. Taken from Chang et al. (2014). (**B**) Cartoon representation of the interface region between APC8 and Cdc20 (right) with the APC5 loop region encompassing 168-205 amino acids (PBD 5G05 corresponding to human APC/C EM structure at 3.4 Å, released by Zhang et al. (2016), analysed with Chimera software by the author.

Intriguingly, a study in fission yeast revealed that the Plk1 orthologue, Plo1 interacts with the APC8 yeast orthologue, Cut23, and this seems to be critical for APC/C mitotic activity (May et al., 2002). Indeed, Cut23 mutants impaired in their ability to associate with Plo1, arrested in metaphase, and only by overexpression of Plo1 could the mitotic arrest be overridden. As no Plk1 phosphorylation sites were identified in Cut23 the authors hypothesiszed that Cut23 acted as a docking molecule for Plk1 which could then

phosphorylate other APC/C subunits (May et al., 2002). Given the relative positions of APC5 and APC8 in the APC/C (Cronin et al., 2015, Chang et al., 2014), and that APC5 S195 conforms to a Plk1 consensus site (Nakajima et al., 2003), it is reasonable to suggest that APC5 S195 is phosphorylated by Plk1 during mitosis, through Plk1 interaction with APC8. However, multiple alignments presented in Chapter 3, suggested that the APC5 S195 residue was not conserved in *Schizosaccharomyces pombe* (Fig. 3.21). However, as Clustal Omega uses algorithms to optimise alignments between all sequences considered, we questioned whether reducing the number of species in the multiple alignment analysis would give a better indication as to whether the S195 residue was conserved between human and budding yeast. We therefore repeated the multiple alignment including only sequences from human, mouse, *Drosophila* and *Schizosaccharomyces pombe* (Fig. 5.20) (Clustal Omega, 2019).

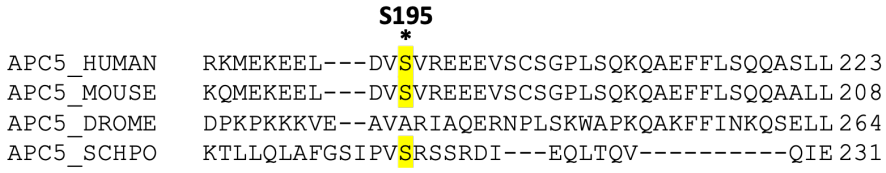

Figure 5. 20: **APC5 S195 might be conserved in S.pombe in a multiple alignment containing fewer species.** Clustal Omega multiple alignment of the APC5 sequence showing that the S195 residue in potentially conserved in *Schizosaccharomyces pombe* (Clustal Omega, 2019).

Interestingly, the new alignment revealed that S195 might be conserved between the human and the budding yeast APC5 protein sequences, suggesting that this residue in *Schizosaccharomyces pombe* could theoretically be targeted in mitosis by Plo1 in association with Cut23 (May et al., 2002). In this regard it would be extremely interesting to establish whether human APC5 S195 phosphorylation was dependent upon Plk1 association with APC8.

Within this chapter we also reported that the pAPC5 S195 Ab was suitable for conducting IP experiments (Fig. 5.6 and 5.7). Although we cannot use this Ab directly to assess whether APC5 pS195 serves as a binding module for an unknown interactor, we anticipate that our Ab could be used to analyse the PTM status (including phosphorylation) of the APC/C when S195 is phosphorylated. Protein phosphorylation is often used as a regulatory switch and can either effect enzymic activity directly or serve to recruit new binding partners by operating as protein-protein interaction modules (Hunter, 2012, Pearlman et al., 2011). Interestingly, the fission yeast Cut23 mutants impaired in their association with Plo1, showed a dramatic reduction in APC/C catalytic activity, as noted by the accumulation in the APC/C substrates Cyclin B1 and Securin (May et al., 2002). As such, it could be argued that Plk1 phosphorylation of the APC5 S195 site, might serve to create a docking site that recruits substrates to the APC/C for degradation.

Using the α-pAPC5 S195 Ab we also re-affirmed the proposition that Cdk1, Plk1 and Aurora B mitotic kinases all contribute to the regulation of APC5 phosphorylation at S195 (Fig. 5.8, 5.9 and 5.10). Indeed, protein phosphorylation during mitosis involves intense crosstalk between different mitotic kinases (Cuijpers and Vertegaal, 2018). Given our results with the kinase inhibitors it is possible that Cdk1 and Aurora B kinases phosphorylate APC5 S195 independent of Plk1. However, given that S195 conforms to a known Plk1 consensus motif and Plk1 is known to be recruited to substrates via the ability of its Polo-box to bind substrates already phosphorylated at other residues (e.g. PRC1 during anaphase) (Neef et al., 2007), it is perhaps more likely that Cdk1 and Aurora B kinases phosphorylate APC5 upon other residues, or other APC/C subunits, to facilitate the Plk1-directed phosphorylation of APC5 S195. Indeed, Marc Kirschner's group identified the APC5 residue, T232, that lies within a Cdk1 consensus motif as being phosphorylated in mitotically-arrested cells (Steen

et al., 2008) that could potentially recruit Plk1. However, data presented in this chapter suggests that T232 phosphorylation is not a pre-requisite for S195 phosphorylation. In this regard, whilst our α-pAPC5 S195 Ab recognized S195 phosphorylation on FLAG-APC5 WT species in mitosis, S195 was not phosphorylated on the T232 phospho-mimetic, FLAG-APC5 T232E species, but was phosphorylated on the phospho-inhibitory FLAG-APC5 T232A species, in mitosis (Fig. 5.12). As such, and in contrast to what is known about Cdk1 priming of its substrates (Elia et al., 2003a, Elia et al., 2003b, Neef et al., 2007, Neef et al., 2003), these data suggest Cdk1-dependent phosphorylation of T232 does not create a Plk1 docking site allowing for the Plk1-dependent phosphorylation of APC5 S195 but might in fact inhibit S195 phosphorylation (Fig. 5.12).

It is possible therefore that these two APC5 phosphorylation events are mutually exclusive and occur at different times during mitosis to regulate the APC/C in a temporally-coordinated manner. For instance, differential phosphorylation of T232 and S195 residues during mitosis, might differentially affect Cdc20 and Cdh1 association, which are already known to be cell-cycle dependent (Sivakumar and Gorbsky, 2015). In this regard, Cdh1 association to the APC/C has been shown to be independent upon the phosphorylation status of APC1 and APC3 (Kataria and Yamano, 2019, Sivakumar and Gorbsky, 2015, Alfieri et al., 2017), yet Cdh1 interacts at the same site on the APC/C as Cdc20 such that other phosphorylation events on the APC/C might facilitate Cdh1 association with the APC/C. As APC5 phosphorylation at S195 persists until the later stages of mitosis, it is interesting to speculate that S195 and T232 phosphorylation regulates Cdc20 and/or Cdh1 association and dissociation with the APC/C.

Although our α-pAPC5 S195 Ab recognised the phosphorylated APC5 S195 species during mitosis, our data revealed that in addition to not recognising the phospho-inhibited mutant FLAG-APC5 S195A species, it similarly, did not recognise the FLAG-APC5 S195D phospho-mimetic species (Fig. 5.11). These results were not surprising, as it has been reported previously that phospho-specific Ab's fail to recognise phosphomimetic amino acids, D and E, due to differences in their structures relative to phosphorylated S and T residues (Pearlman et al., 2011). However, the lack of binding affinity of our pAPC5 S195 Ab for the FLAG-APC5 S195D species, does not exclude the possibility that the FLAG-APC5 S195D species retains biological activity and will overcome cellular phenotypes caused by the depletion of endogenous APC5.

Our IF studies allowed us to characterize the cellular localization of the pAPC5 S195 species during mitosis (Figs. 5.13-5.17). In this regard, we found that the pAPC5 S195 species localized to centrosomes during prophase through to metaphase whereupon it migrated to the central furrow after metaphase-to-anaphase transition, and eventually resided at midbodies during telophase (Figs. 5.13-5.17). As such, pAPC5 S195 species localization is coincident with the centrosomal localization of Cyclin B1 during the early stages of mitosis where Cyclin B1 degradation has also been proposed to occur (Jackman et al., 2003). Interestingly, the distribution pattern of the pAPC5 S195 species following metaphase-to-anaphase transition appears to mirror the localization of the mitotic kinase Plk1 and its docking partner, PRC1, both of which, as well as being APC/C substrates, are required for cytokinesis (Fig. 5.16 and 5.17) (Mollinari et al., 2002, Lindon and Pines, 2004, Petronczki et al., 2008, Golsteyn et al., 1995). Although our data indicated that pAPC5 S195 species accumulated at midbodies at the end of mitosis (Figs. 5.13-5.17) the APC/C has not been previously shown to localize at midbodies, despite the fact that known APC/C substrates,

PRC1 and Plk1, accumulate at these sites during telophase and cytokinesis. As such, it is our intention to isolate midbodies and establish whether the APC/C is, in fact, recruited to these sites to promote substrate degradation. This hypothesis is very appealing, especially considering that in addition Plk1 and PRC1, other APC/C-Cdh1 substrates, such as Anillin, KiF4 and Aurora B, all accumulate at midbodies during telophase to coordinate cytokinesis (Zhu and Jiang, 2005, Lindon, 2008, Stewart and Fang, 2005, Minoshima et al., 2003, Zhao and Fang, 2005).

Given that APC/C-Cdh1 association occurs at anaphase onset (Kataria and Yamano, 2019, Sivakumar and Gorbsky, 2015), it is intriguing that late APC/C-Cdh1 substrates such as Plk1 and PRC1 are still present during telophase. Although there has been some speculation about the potential role for the APC/C in the regulation of cytokinesis, mainly based on the differential ordering of late APC/C substrate degradation (Lindon and Pines, 2004), exact mechanism underlying this process is not known. In this regard, and based on the evidence that the pAPC5 S195 species mirrors Plk1 distribution during mitosis (Fig. 5.16), it is possible that the Plk1-dependent phosphorylation of APC5 at S195 will promote APC/C localization at the midbodies, where it is needed for the degradation of its substrates and for completion of cytokinesis (Lindon, 2008). Indeed, our co-localization studies with Plk1, suggest that the pAPC5 S195 species is found juxtaposed to Plk1 at the midbodies, suggesting that the pAPC5 species is excluded from the centre of the midbody (Fig. 5.16), which might prevent the premature degradation of the APC/C substrates that localize in this zone. Unfortunately, the fine details of pAPC5 S195 localization in the co-localization experiments were lost, possibly due to a high colour saturation that reduced the resolution of the telophase images (Fig. 5.14, 5.15, 5.17). As such, we need to refine these analyses to

determine the precise localization of the pAPC5 S195 species within the midbodies at the very late stages of mitosis.

Overall, the data presented in this chapter suggests that pAPC5 S195 might play a critical role throughout mitosis in the regulation of the APC/C. Its localization at centrosomes prior to metphase-to-anaphase transition suggests that pAPC5 S195 participates in the degradation of APC/C-Cdc20 substrates. Moreover, pAPC5 S195 localization to midbodies suggests that the APC/C plays a direct role in cytokinesis and implies that a novel regulatory system exists to control APC/C activity during telophase to prevent the premature degradation of late APC/C substrates.

CHAPTER 6: FINAL DISCUSSION

6.1 The APC/C: a fascinating world to discover

The APC/C is a master regulator of cell life and ultimately, cell fate. It plays a central role in the regulation of cell division, where it orchestrates the ordered degradation of maybe, 100+ substrates to ensure the unidirectional progression of cells through the cell cycle (Sivakumar and Gorbsky, 2015, Peters, 2006, Zhou et al., 2016). Recent studies have suggested that APC/C activity is regulated by PTMs, such as phosphorylation. It has been shown that phosphorylation of APC/C subunits promotes APC/C conformational changes that regulate the overall activity of the holoenzyme (Qiao et al., 2016, Zhang et al., 2016, Chang and Barford, 2014, Chang et al., 2014). Mass spectrometry has contributed massively to defining APC/C subunit, and residue-specific, PTMs, revealing the existence of more than one hundred APC/C phosphorylation sites, many of which are mitotic-specific (Qiao et al., 2016, Herzog et al., 2005, Steen et al., 2008, Hegemann et al., 2011). Although the functionality of some of these phosphorylation sites are well-characterized, revealing for instance the paramount importance of APC3 and APC1 phosphorylation in the mitotic activation of the APC/C holoenzyme during the early stage of mitosis (Zhang et al., 2016, Fujimitsu et al., 2016), the role of most of these phosphorylation events, as well as the role played by many of the APC/C individual subunits, remain unclear (Qiao et al., 2016).

In this regard, the main focus of the present study was to characterize the function of the APC/C platform subunit, APC5, during mitosis. Our data determined that APC5 function was absolutely required for mitosis in diploid, TERT-immortalized RPE-1 cells, such that the RNAi-mediated depletion of APC5 was typified by mitotic arrest or significant delays in mitotic progression (Figs 4.15-4.18). These results are consistent with those reported by

the MitoCheck project who observed mitotic defects following APC5 knockdown in the HeLa cervical cancer-derived cell line, as well as with data obtained with the APC5 *Drosophila* homologous, ida, where homozygous ida mutants had mitotic defects and some APC/C substrates were elevated (Neumann et al., 2010, Bentley et al., 2002). Our investigation was also crucial in establishing that almost the entire cellular pool of APC5 is phosphorylated during mitosis at S195 (Fig. 3.10 and 3.22), suggesting that this PTM event is crucial in the regulation of APC/C activity during mitosis. Despite studies from the Peters and Kirschner groups that have suggested that APC5 is phosphorylated on only two or three residues during mitosis (Hegemann et al., 2011, Steen et al., 2008), an annotation of multiple mass spectrometric screens suggest that APC5 is subject to extensive residue-specific phosphorylation and ubiquitylation (Fig 6.1) (PhosphoSitePlus, 2019). The role of these PTMs remains unknown. As such, it would be valuable to establish, by additional mass spectrometric studies, whether these phosphorylation events are genuine, and if so, characterize their effects on APC5 function, in the context of the entire APC/C (Fig. 6.1) (PhosphoSitePlus, 2019).

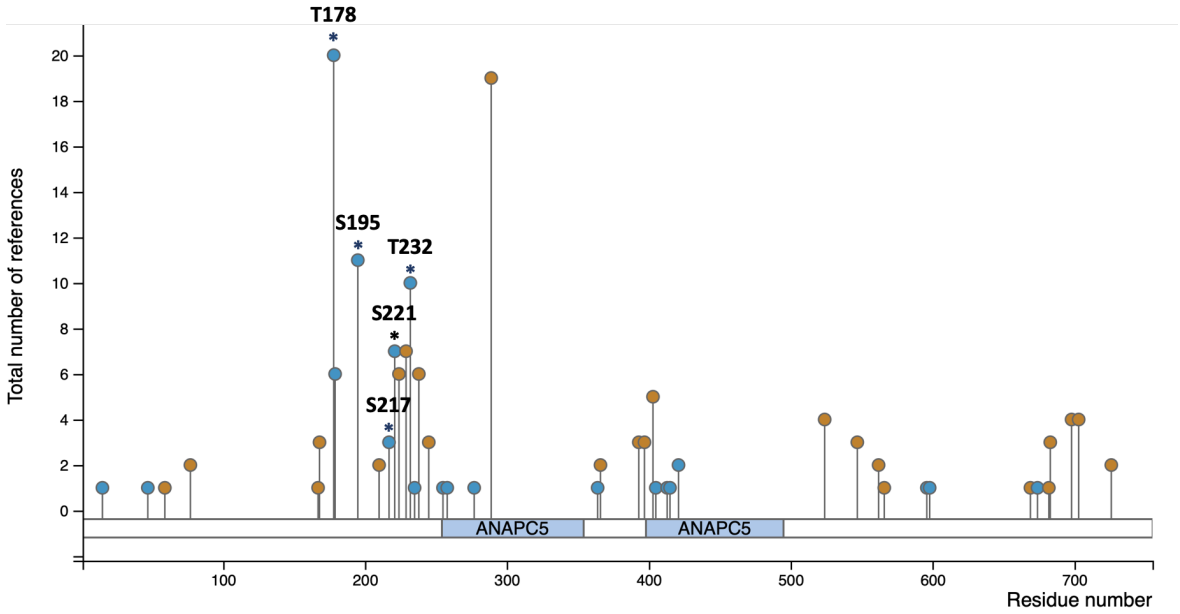

Figure 6. 1: **APC5 residues modified by PTM**. Annotation of multiple mass spectrometric screens has suggested that APC5 is subject to PTM on numerous residues (blue dots corresponding to phosphorylation; yellow/brown corresponding to ubiquitylation). Taken from PhosphoSitePlus (2019).

Given that our studies identified S195 as a major target for phosphorylation during mitosis future investigations should be focused on the functional characterization of this phosphorylation event in order to clarify its role in the regulation of the APC/C. In this regard, it will be interesting to establish whether expression of FLAG-APC5 S195A or FLAG-APC5 S195D mutants can rescue the mitotic phenotype observed following APC5 knockdown in RPE-1 cells. Additionally, it would be extremely interesting to make a human or Xenopus recombinant APC/C complex that incorporates the FLAG-APC5 S195A and FLAG-APC5 S195D mutants such that we could assess their structure and gauge their ability, *in vitro,* to target APC/C substrates for degradation (Fujimitsu et al., 2016, Qiao et al., 2016, Zhang et al., 2016, Alfieri et al., 2016). Indeed, comparison of the cryo-EM structures of these two recombinant APC/C complexes might be critical in determining the effects of APC5 S195 phosphorylation on APC/C conformation. In this regard, although the

S195 APC5 residue itself will not be observed, as it exists within a loop region that is not visible in cryo-EM structures, the effect of APC5 S195 phosphorylation will be imprinted on the overall structure of the APC/C complex.

Such an approach would also potentially, help characterize the role of APC5 S195 phosphorylation in the temporal activation of the APC/C through APC3 and APC1 phosphorylation (Fujimitsu et al., 2016, Qiao et al., 2016, Zhang et al., 2016), where we might be able to assess whether APC5 S195 phosphorylation lies upstream, or downstream of APC3 and APC1 phosphorylation. Given the intimate association between APC5 and APC4, which is considered important in the positioning of the APC2 catalytic subunit and the association of UbcH10 with the APC/C (Cronin et al., 2015), conformational changes associated with APC5 S195 phosphorylation might also provide interesting insights as to whether APC5 S195 phosphorylation modulates these effects. Moreover, such structural analyses would also reveal the effect of APC5 S195 phosphorylation on APC8 conformational changes which might impact on the ability of Cdc20 and Cdh1 to associate with the APC/C (Chang et al., 2014). APC/C degradation assays with known APC/C substrates using reconstructed APC/C-APC5 S195A and APC/C-S195D complexes, might also be useful in establishing the functional relevance of this phosphorylation event, particularly in relation to the phosphorylation status of APC3 and APC1 (Fujimitsu et al., 2016), and its ability to modulate APC/C association with Cdc20, Cdh1 or UbcH10 (Kramer et al., 2000, Pray et al., 2002). These studies are obviously dependent on the ability of the D residue to faithfully re-capitulate the effects phosphorylated S residues, which we know, from other studies is not necessarily a given (Paleologou et al., 2008, Pearlman et al., 2011), particularly as phospho-specific antibodies do not recognise S residues that have been changed to D.

It is well known that protein phosphorylation often creates novel protein-protein interaction modules that affect protein function (Hunter, 2012, Pearlman et al., 2011). Indeed, APC4 SUMOylation allows for APC/C substrate, KIF18B, to be recruited to the APC/C for degradation (Eifler et al., 2018). As such, APC5 phosphorylation at S195 during mitosis might, through interaction with specific substrates, facilitate selectively the degradation of APC/C substrates and contribute to the hierarchical degradation of APC/C substrates during mitosis (Davey and Morgan, 2016). Moreover, given that our data suggests that there is an intimate relationship between APC5 S195 and T232 phosphorylation, which might be indicative of fine-tuning of APC/C activity (Fig. 5.12), it might be that T232 phosphorylation modulates the function of APC5 species that are phosphorylated on S195. Whilst we might be able to use recombinant APC/C complexes to determine the ability of S195 and T232, as outlined above, to associate with activators, regulators or substrates these studies are open to interpretation given the structural differences between pS and D and pT and E. Potentially, a better way to determine if pS195 serves to create a specific binding motif for activators, regulators or substrates is to perform phospho-peptide pull down assays using an APC5 loop region peptide that is phosphorylated at the S residue, corresponding to S195; an unphosphorylated APC5 loop region peptide would serve to discriminate phopsho-specific binding avidities. This approach has been used successfully, previously (Schulze and Mann, 2004, Tinti et al., 2013). In this regard we would use peptides as bait and cellular extracts from different mitotic stages as a source of potential interacting proteins. We would then perform pulldowns coupled to either mass spectrometry for an unbiased approach, or Western blot analysis with APC/C substrates, activators, or regulators in a more targeted-approach. These studies would help establish whether APC5 S195 phosphorylation is important in recruiting cellular proteins to the APC/C.

The studies detailed in this thesis have been important in establishing that pAPC5 S195 species are localized at centrosomes from prophase until anaphase, and at midbodies at the late stages of mitosis (Fig. 5.13-5.17). Although, the role of APC/C complexes containing pAPC5 S195 species at these locations is unknown it has been established previously that Cyclin B1 is degraded at centrosomes (Clute and Pines, 1999). As APC/C substrates such as Plk1 and PRC1, amongst others, accumulate at midbodies and regulate the process of cytokinesis it might be that APC/C complexes possessing pAPC5 S195 species might regulate the degradation of these substrates. Despite this, the APC/C has never been shown to localize to midbodies. As such our work in this area is novel and might give rise to a new area of research focused on the investigation of APC/C function at midbodies during cytokinesis. In this regard, we need to establish, through the isolation of purified midbodies, the presence of the APC/C holoenzyme at these structures, and more accurately determine, by confocal microscopy, the relationship between pAPC5 S195 and APC/C substrates. It is interesting to note, in this regard, that a small but significant proportion of APC5 knockdown cells failed to undergo cytokinesis following chromosome segregation (Fig. 4. 15). As such, it would be important to establish whether S195A or S195D APC5 species could rescue the ability of APC5 knockdown cells to undergo cytokinesis.

As discussed in the introduction (Sec. 1.7, Chapter 1), multiple APC/C subunit mutations are found in numerous cancer types, were they have been postulated to contribute to the hyperproliferative behaviour of cancer cells, as well as to metastasis and invasion, genome instability and aneuploidy (Xin et al., 2018, Qiu et al., 2017, Qiu et al., 2016, Kang et al., 2009). Indeed, predictive phenotype analyses of the many missense mutations identified within various APC/C subunits in different cancer types, have highlighted their potential to dysregulate APC/C activity, confirming the role played by the APC/C in the maintenance of

genome stability (Sansregret et al., 2017). As we have shown that APC5 knockdown typically results in mitotic arrest or a delay in the ability of cells to progress through mitosis (Fig. 4.15-4.18), our data might explain why APC5 missense mutations are not commonly associated with cancer phenotypes (Fig 6.2)(cBioPortal, 2019), as alteration in APC5 functions might represent a disadvantage for cellular proliferation. As can be seen from the data presented in Fig 6.2, mutations in APC5 occur at low frequency in a limited number of cancers, and do not compare to the frequency of mutations in known tumour suppressors, such as p53 (typically greater than 50% for most human cancers), or oncogenes, such as Ras (approximately 30% for colorectal cancer). Given, also that mutations are distributed through APC5 and do not occur at hot-spots, it is unlikely that APC5 mutations are cancer-causing and more likely that they are passenger mutations that contribute to the cancer phenotype rather than being a causative agent, or being required for maintenance of the cancer phenotype; interestingly S195 has not been shown to be mutated in human cancer suggesting that its inactivation would be detrimental to APC/C activity. There are perhaps, one or two cancer types however, where the relationship between APC5 and cancer should be explored in more detail. In particular APC5 is mutated in almost 6% of uterine cancers (Figure 6.2). It would be interesting from a structure-function perspective to determine how individual mutations observed in uterine cancers affect APC/C structure and consequently, APC/C activity, as it is known that both Cdc20 and UbcH10 overexpression induces cancers through the hyperactivation of the APC/C (Pallante et al., 2005, Van Ree et al., 2010, Wang et al., 2018, Wu et al., 2013).

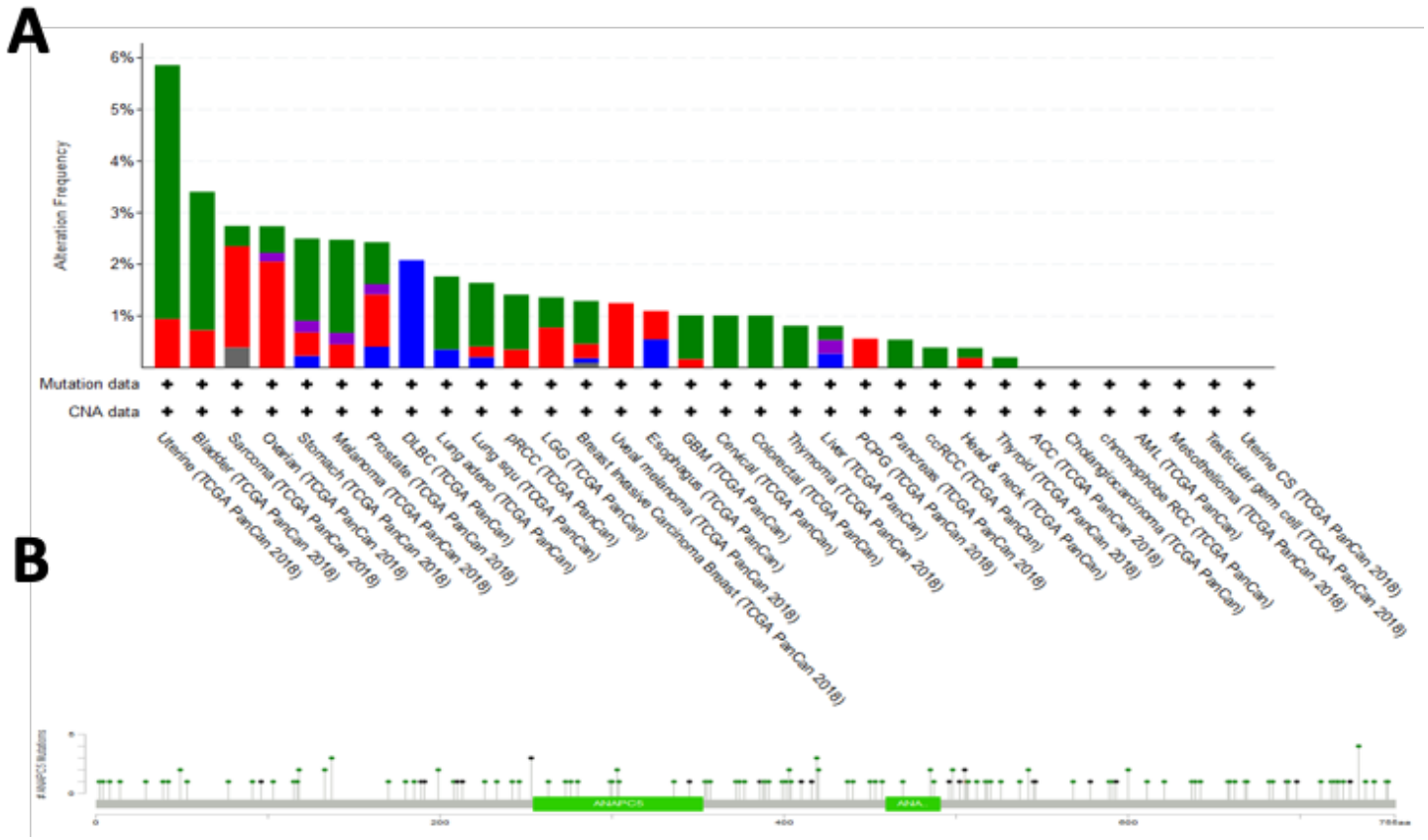

Figure 6.2: **APC5 mutation in human cancer**. (**A**) cBioPortal data taken from TCGA PanCancer Atlas Studies Combined study (10967 total samples, 32 studies) displaying APC5 mutations in different human cancers. Colour legend as follows: amplification (red), mutation (green), deletion (blue), multiple alterations (grey) and fusion (purple). (**B**) Residues subjected to mutation including 109 missense (green dots), 26 truncating (black dots) and 1 in-frame mutation. Taken from cBioPortal (2019).

Overall, the studies detailed here have helped characterize further the mitotic functions of the APC/C at a molecular level, implicating pAPC5 S195 in regulating APC/C function throughout mitosis from prophase to cytokinesis and identifying potential new roles for the APC/C in the regulation of mitosis. In consideration of what has been discussed here, future studies in APC5 will help define APC5 function during each phase of mitosis.

LIST OF REFERENCES

ABE, S., NAGASAKA, K., HIRAYAMA, Y., KOZUKA-HATA, H., OYAMA, M., AOYAGI, Y., OBUSE, C. & HIROTA, T. 2011. The initial phase of chromosome condensation requires Cdk1-mediated phosphorylation of the CAP-D3 subunit of condensin II. *Genes & development,* 25**,** 863-874.

ADRIAANS, I. E., BASANT, A., PONSIOEN, B., GLOTZER, M. & LENS, S. M. 2019. PLK1 plays dual roles in centralspindlin regulation during cytokinesis. *J Cell Biol,* 218**,** 1250-1264.

AJEAWUNG, N. F., NGUYEN, T. T. M., LU, L., KUCHARSKI, T. J., ROUSSEAU, J., MOLIDPEREE, S., ATIENZA, J., GAMACHE, I., JIN, W. & PLON, S. E. 2019. Mutations in ANAPC1, Encoding a Scaffold Subunit of the Anaphase-Promoting Complex, Cause Rothmund-Thomson Syndrome Type 1. *The American Journal of Human Genetics,* 105**,** 625-630.

ALFIERI, C., CHANG, L., ZHANG, Z., YANG, J., MASLEN, S., SKEHEL, M. & BARFORD, D. 2016. Molecular basis of APC/C regulation by the spindle assembly checkpoint. *Nature,* 536**,** 431.

ALFIERI, C., ZHANG, S. & BARFORD, D. 2017. Visualizing the complex functions and mechanisms of the anaphase promoting complex/cyclosome (APC/C). *Open Biol,* 7.

AMERICAN TYPE CULTURE COLLECTION (ATCC). 2019. *The Global Bioresource Center* [Online]. Available: https://www.lgcstandards-atcc.org/?geo_country=gb [Accessed].

ARCHAMBAULT, V., LEPINE, G. & KACHANER, D. 2015. Understanding the polo kinase machine. *Oncogene,* 34**,** 4799.

BARR, F. A., SILLJÉ, H. H. & NIGG, E. A. 2004. Polo-like kinases and the orchestration of cell division. *Nature reviews Molecular cell biology,* 5**,** 429.

BASHIR, T., DORRELLO, N. V., AMADOR, V., GUARDAVACCARO, D. & PAGANO, M. 2004. Control of the SCF Skp2–Cks1 ubiquitin ligase by the APC/C Cdh1 ubiquitin ligase. *Nature,* 428**,** 190.

BASSERMANN, F., FRESCAS, D., GUARDAVACCARO, D., BUSINO, L., PESCHIAROLI, A. & PAGANO, M. 2008. The Cdc14B-Cdh1-Plk1 axis controls the G2 DNA-damage-response checkpoint. *Cell,* 134**,** 256-267.

BENTLEY, A., WILLIAMS, B. C., GOLDBERG, M. L. & ANDRES, A. J. 2002. Phenotypic characterization of Drosophila ida mutants: defining the role of APC5 in cell cycle progression. *Journal of Cell Science,* 115**,** 949-961.

BIGGINS, S. & MURRAY, A. W. 2001. The budding yeast protein kinase Ipl1/Aurora allows the absence of tension to activate the spindle checkpoint. *Genes & development,* 15**,** 3118-3129.

BOUTROS, R., DOZIER, C. & DUCOMMUN, B. 2006. The when and wheres of CDC25 phosphatases. *Current opinion in cell biology,* 18**,** 185-191.

BRITO, D. A. & RIEDER, C. L. 2006. Mitotic checkpoint slippage in humans occurs via cyclin B destruction in the presence of an active checkpoint. *Current Biology,* 16**,** 1194-1200.

BROWN, N. G., VANDERLINDEN, R., WATSON, E. R., WEISSMANN, F., ORDUREAU, A., WU, K. P., ZHANG, W., YU, S., MERCREDI, P. Y., HARRISON, J. S., DAVIDSON, I. F., QIAO,

R., LU, Y., DUBE, P., BRUNNER, M. R., GRACE, C. R. R., MILLER, D. J., HASELBACH, D., JARVIS, M. A., YAMAGUCHI, M., YANISHEVSKI, D., PETZOLD, G., SIDHU, S. S., KUHLMAN, B., KIRSCHNER, M. W., HARPER, J. W., PETERS, J. M., STARK, H. & SCHULMAN, B. A. 2016. Dual RING E3 Architectures Regulate Multiubiquitination and Ubiquitin Chain Elongation by APC/C. *Cell,* 165**,** 1440-1453.

BUSCHHORN, B. A., PETZOLD, G., GALOVA, M., DUBE, P., KRAFT, C., HERZOG, F., STARK, H. & PETERS, J.-M. 2011. Substrate binding on the APC/C occurs between the coactivator Cdh1 and the processivity factor Doc1. *Nature structural & molecular biology,* 18**,** 6.

CAHILL, D. P., LENGAUER, C., YU, J., RIGGINS, G. J., WILLSON, J. K., MARKOWITZ, S. D., KINZLER, K. W. & VOGELSTEIN, B. 1998. Mutations of mitotic checkpoint genes in human cancers. *Nature,* 392**,** 300.

CAPPELL, S. D., CHUNG, M., JAIMOVICH, A., SPENCER, S. L. & MEYER, T. 2016. Irreversible APCCdh1 inactivation underlies the point of no return for cell-cycle entry. *Cell,* 166**,** 167-180.

CAPPELL, S. D., MARK, K. G., GARBETT, D., PACK, L. R., RAPE, M. & MEYER, T. 2018. EMI1 switches from being a substrate to an inhibitor of APC/C CDH1 to start the cell cycle. *Nature,* 558**,** 313.

CARMENA, M., RUCHAUD, S. & EARNSHAW, W. C. 2009. Making the Auroras glow: regulation of Aurora A and B kinase function by interacting proteins. *Current opinion in cell biology,* 21**,** 796-805.

CARMENA, M., WHEELOCK, M., FUNABIKI, H. & EARNSHAW, W. C. 2012. The chromosomal passenger complex (CPC): from easy rider to the godfather of mitosis. *Nature reviews Molecular cell biology,* 13**,** 789.

CASENGHI, M., BARR, F. A. & NIGG, E. A. 2005. Phosphorylation of Nlp by Plk1 negatively regulates its dynein-dynactin-dependent targeting to the centrosome. *Journal of cell science,* 118**,** 5101-5108.

CASENGHI, M., MERALDI, P., WEINHART, U., DUNCAN, P. I., KÖRNER, R. & NIGG, E. A. 2003. Polo-like kinase 1 regulates Nlp, a centrosome protein involved in microtubule nucleation. *Developmental cell,* 5**,** 113-125.

CBIOPORTAL. 2019. Available: http://www.cbioportal.org [Accessed].

CHAN, C. S. & BOTSTEIN, D. 1993. Isolation and characterization of chromosome-gain and increase-in-ploidy mutants in yeast. *Genetics,* 135**,** 677-691.

CHAN, Y. W., MA, H. T., WONG, W., HO, C. C., ON, K. F. & POON, R. Y. 2008. CDK1 inhibitors antagonize the immediate apoptosis triggered by spindle disruption but promote apoptosis following the subsequent rereplication and abnormal mitosis. *Cell Cycle,* 7**,** 1449-1461.

CHANG, L. & BARFORD, D. 2014. Insights into the anaphase-promoting complex: a molecular machine that regulates mitosis. *Current opinion in structural biology,* 29**,** 1-9.

CHANG, L., ZHANG, Z., YANG, J., MCLAUGHLIN, S. H. & BARFORD, D. 2014. Molecular architecture and mechanism of the anaphase-promoting complex. *Nature,* 513**,** 388.

CHANG, L., ZHANG, Z., YANG, J., MCLAUGHLIN, S. H. & BARFORD, D. 2015. Atomic structure of the APC/C and its mechanism of protein ubiquitination. *Nature,* 522**,** 450.

CHEESEMAN, I. M., ANDERSON, S., JWA, M., GREEN, E. M., KANG, J.-S., YATES III, J. R., CHAN, C. S., DRUBIN, D. G. & BARNES, G. 2002. Phospho-regulation of kinetochore-microtubule attachments by the Aurora kinase Ipl1p. *Cell,* 111**,** 163-172.

CHEN, Q., ZHANG, X., JIANG, Q., CLARKE, P. R. & ZHANG, C. 2008. Cyclin B1 is localized to unattached kinetochores and contributes to efficient microtubule attachment and proper chromosome alignment during mitosis. *Cell research,* 18**,** 268.

CHOI, E., CHOE, H., MIN, J., CHOI, J. Y., KIM, J. & LEE, H. 2009. BubR1 acetylation at prometaphase is required for modulating APC/C activity and timing of mitosis. *The EMBO journal,* 28**,** 2077-2089.

CLUSTAL OMEGA. 2019. *Multiple Sequence Alignment* [Online]. Available: https://www.ebi.ac.uk/Tools/msa/clustalo/ [Accessed].

CLUTE, P. & PINES, J. 1999. Temporal and spatial control of cyclin B1 destruction in metaphase. *Nature cell biology,* 1**,** 82.

CRONIN, N. B., YANG, J., ZHANG, Z., KULKARNI, K., CHANG, L., YAMANO, H. & BARFORD, D. 2015. Atomic-resolution structures of the APC/C subunits Apc4 and the Apc5 N-terminal domain. *Journal of molecular biology,* 427**,** 3300-3315.

CUIJPERS, S. A. & VERTEGAAL, A. C. 2018. Guiding mitotic progression by crosstalk between post-translational modifications. *Trends in biochemical sciences,* 43**,** 251-268.

D'AVINO, P. P. & CAPALBO, L. Regulation of midbody formation and function by mitotic kinases. Seminars in cell & developmental biology, 2016. Elsevier, 57-63.

DA FONSECA, P. C., KONG, E. H., ZHANG, Z., SCHREIBER, A., WILLIAMS, M. A., MORRIS, E. P. & BARFORD, D. 2011. Structures of APC/C Cdh1 with substrates identify Cdh1 and Apc10 as the D-box co-receptor. *Nature,* 470**,** 274.

DAI, J., SULLIVAN, B. A. & HIGGINS, J. M. 2006. Regulation of mitotic chromosome cohesion by Haspin and Aurora B. *Developmental cell,* 11**,** 741-750.

DAVEY, N. E. & MORGAN, D. O. 2016. Building a Regulatory Network with Short Linear Sequence Motifs: Lessons from the Degrons of the Anaphase-Promoting Complex. *Mol Cell,* 64**,** 12-23.

DE ANTONI, A., PEARSON, C. G., CIMINI, D., CANMAN, J. C., SALA, V., NEZI, L., MAPELLI, M., SIRONI, L., FARETTA, M. & SALMON, E. D. 2005. The Mad1/Mad2 complex as a template for Mad2 activation in the spindle assembly checkpoint. *Current Biology,* 15**,** 214-225.

DI FIORE, B., DAVEY, N. E., HAGTING, A., IZAWA, D., MANSFELD, J., GIBSON, T. J. & PINES, J. 2015. The ABBA motif binds APC/C activators and is shared by APC/C substrates and regulators. *Developmental cell,* 32**,** 358-372.

DI FIORE, B. & PINES, J. 2010. How cyclin A destruction escapes the spindle assembly checkpoint. *The Journal of cell biology,* 190**,** 501-509.

DIAZ-MARTINEZ, L. A., TIAN, W., LI, B., WARRINGTON, R., JIA, L., BRAUTIGAM, C. A., LUO, X. & YU, H. 2015. The Cdc20-binding Phe box of the spindle checkpoint protein BubR1 maintains the mitotic checkpoint complex during mitosis. *Journal of Biological Chemistry,* 290**,** 2431-2443.

DIFFLEY, J. F. 2004. Regulation of early events in chromosome replication. *Current Biology,* 14**,** R778-R786.

DONG, S., HUANG, F., ZHANG, H. & CHEN, Q. 2019. Overexpression of BUB1B, CCNA2, CDC20, and CDK1 in tumor tissues predicts poor survival in pancreatic ductal adenocarcinoma. *Bioscience reports,* 39**,** BSR20182306.

EIFLER, K., CUIJPERS, S. A., WILLEMSTEIN, E., RAAIJMAKERS, J. A., EL ATMIOUI, D., OVAA, H., MEDEMA, R. H. & VERTEGAAL, A. C. 2018. SUMO targets the APC/C to regulate transition from metaphase to anaphase. *Nature communications,* 9**,** 1119.

ELIA, A. E., CANTLEY, L. C. & YAFFE, M. B. 2003a. Proteomic screen finds pSer/pThr-binding domain localizing Plk1 to mitotic substrates. *Science,* 299**,** 1228-1231.

ELIA, A. E., RELLOS, P., HAIRE, L. F., CHAO, J. W., IVINS, F. J., HOEPKER, K., MOHAMMAD, D., CANTLEY, L. C., SMERDON, S. J. & YAFFE, M. B. 2003b. The molecular basis for phosphodependent substrate targeting and regulation of Plks by the Polo-box domain. *Cell,* 115**,** 83-95.

ENGELBERT, D., SCHNERCH, D., BAUMGARTEN, A. & WÄSCH, R. 2008. The ubiquitin ligase APC Cdh1 is required to maintain genome integrity in primary human cells. *Oncogene,* 27**,** 907.

ENSERINK, J. M. & KOLODNER, R. D. 2010. An overview of Cdk1-controlled targets and processes. *Cell division,* 5**,** 11.

FACK, F., HÜGLE-DÖRR, B., SONG, D., QUEITSCH, I., PETERSEN, G. & BAUTZ, E. K. 1997. Epitope mapping by phage display: random versus gene-fragment libraries. *Journal of immunological methods,* 206**,** 43-52.

FANG, G. 2002. Checkpoint protein BubR1 acts synergistically with Mad2 to inhibit anaphase-promoting complex. *Molecular biology of the cell,* 13**,** 755-766.

FARAGHER, A. J. & FRY, A. M. 2003. Nek2A kinase stimulates centrosome disjunction and is required for formation of bipolar mitotic spindles. *Molecular biology of the cell,* 14**,** 2876-2889.

FLOYD, S., PINES, J. & LINDON, C. 2008. APC/CCdh1 targets aurora kinase to control reorganization of the mitotic spindle at anaphase. *Current Biology,* 18**,** 1649-1658.

FOSTER, S. A. & MORGAN, D. O. 2012. The APC/C subunit Mnd2/Apc15 promotes Cdc20 autoubiquitination and spindle assembly checkpoint inactivation. *Molecular cell,* 47**,** 921-932.

FOUREST-LIEUVIN, A., PERIS, L., GACHE, V., GARCIA-SAEZ, I., JUILLAN-BINARD, C., LANTEZ, V. & JOB, D. 2006. Microtubule regulation in mitosis: tubulin phosphorylation by the cyclin-dependent kinase Cdk1. *Molecular biology of the cell,* 17**,** 1041-1050.

FRYE, J. J., BROWN, N. G., PETZOLD, G., WATSON, E. R., GRACE, C. R., NOURSE, A., JARVIS, M. A., KRIWACKI, R. W., PETERS, J.-M. & STARK, H. 2013. Electron microscopy structure of human APC/C CDH1–EMI1 reveals multimodal mechanism of E3 ligase shutdown. *Nature structural & molecular biology,* 20**,** 827.

FUJIMITSU, K., GRIMALDI, M. & YAMANO, H. 2016. Cyclin-dependent kinase 1-dependent activation of APC/C ubiquitin ligase. *Science,* 352**,** 1121-4.

FUJITA, T., LIU, W., DOIHARA, H., DATE, H. & WAN, Y. 2008. Dissection of the APCCdh1-Skp2 cascade in breast cancer. *Clinical Cancer Research,* 14**,** 1966-1975.

GARCÍA-HIGUERA, I., MANCHADO, E., DUBUS, P., CAÑAMERO, M., MÉNDEZ, J., MORENO, S. & MALUMBRES, M. 2008. Genomic stability and tumour suppression by the APC/C cofactor Cdh1. *Nature cell biology,* 10**,** 802.

GARNETT, M. J., MANSFELD, J., GODWIN, C., MATSUSAKA, T., WU, J., RUSSELL, P., PINES, J. & VENKITARAMAN, A. R. 2009. UBE2S elongates ubiquitin chains on APC/C substrates to promote mitotic exit. *Nature cell biology,* 11**,** 1363.

GAVET, O. & PINES, J. 2010. Progressive activation of CyclinB1-Cdk1 coordinates entry to mitosis. *Developmental cell,* 18**,** 533-543.

GLOTZER, M., MURRAY, A. W. & KIRSCHNER, M. W. 1991. Cyclin is degraded by the ubiquitin pathway. *Nature,* 349**,** 132.

GOLAN, A., YUDKOVSKY, Y. & HERSHKO, A. 2002. The cyclin-ubiquitin ligase activity of cyclosome/APC is jointly activated by protein kinases Cdk1-cyclin B and Plk. *Journal of biological chemistry,* 277**,** 15552-15557.

GOLSTEYN, R. M., MUNDT, K. E., FRY, A. M. & NIGG, E. A. 1995. Cell cycle regulation of the activity and subcellular localization of Plk1, a human protein kinase implicated in mitotic spindle function. *The Journal of cell biology,* 129**,** 1617-1628.

GOTO, H., KIYONO, T., TOMONO, Y., KAWAJIRI, A., URANO, T., FURUKAWA, K., NIGG, E. A. & INAGAKI, M. 2006. Complex formation of Plk1 and INCENP required for metaphase–anaphase transition. *Nature cell biology,* 8**,** 180.

HAGTING, A., DEN ELZEN, N., VODERMAIER, H. C., WAIZENEGGER, I. C., PETERS, J.-M. & PINES, J. 2002. Human securin proteolysis is controlled by the spindle checkpoint and reveals when the APC/C switches from activation by Cdc20 to Cdh1. *The Journal of cell biology,* 157**,** 1125-1137.

HANSEN, D. V., LOKTEV, A. V., BAN, K. H. & JACKSON, P. K. 2004. Plk1 regulates activation of the anaphase promoting complex by phosphorylating and triggering SCFβTrCP-dependent destruction of the APC inhibitor Emi1. *Molecular biology of the cell,* 15**,** 5623-5634.

HARTWELL, L. H., MORTIMER, R. K., CULOTTI, J. & CULOTTI, M. 1973. Genetic control of the cell division cycle in yeast: V. Genetic analysis of cdc mutants. *Genetics,* 74**,** 267-286.

HAUF, S., COLE, R. W., LATERRA, S., ZIMMER, C., SCHNAPP, G., WALTER, R., HECKEL, A., VAN MEEL, J., RIEDER, C. L. & PETERS, J.-M. 2003. The small molecule Hesperadin reveals a role for Aurora B in correcting kinetochore–microtubule attachment and in maintaining the spindle assembly checkpoint. *J Cell Biol,* 161**,** 281-294.

HE, J., CHAO, W. C., ZHANG, Z., YANG, J., CRONIN, N. & BARFORD, D. 2013. Insights into degron recognition by APC/C coactivators from the structure of an Acm1-Cdh1 complex. *Molecular cell,* 50**,** 649-660.

HEGEMANN, B., HUTCHINS, J. R., HUDECZ, O., NOVATCHKOVA, M., RAMESEDER, J., SYKORA, M. M., LIU, S., MAZANEK, M., LENART, P. & HERICHE, J.-K. 2011. Systematic phosphorylation analysis of human mitotic protein complexes. *Sci. Signal.,* 4**,** rs12-rs12.

HERSHKO, A. 1998. Ciechanover, The ubiquitin system. *Annu Rev Biochem,* 67**,** 425-479.

HERZOG, F., MECHTLER, K. & PETERS, J. M. 2005. Identification of Cell Cycle-Dependent Phosphorylation Sites on the Anaphase-Promoting Complex/Cyclosome by Mass Spectrometry. *Methods in enzymology,* 398**,** 231-245.

HINDRIKSEN, S., LENS, S. & HADDERS, M. A. 2017. The ins and outs of Aurora B inner centromere localization. *Frontiers in cell and developmental biology,* 5**,** 112.

HOLT, L. J., TUCH, B. B., VILLÉN, J., JOHNSON, A. D., GYGI, S. P. & MORGAN, D. O. 2009. Global analysis of Cdk1 substrate phosphorylation sites provides insights into evolution. *Science,* 325**,** 1682-1686.

HUNTER, T. 2012. Why nature chose phosphate to modify proteins. *Philosophical Transactions of the Royal Society B: Biological Sciences,* 367**,** 2513-2516.

JACKMAN, M., LINDON, C., NIGG, E. A. & PINES, J. 2003. Active cyclin B1–Cdk1 first appears on centrosomes in prophase. *Nature cell biology,* 5**,** 143.

JANG, Y.-J., LIN, C.-Y., MA, S. & ERIKSON, R. L. 2002. Functional studies on the role of the C-terminal domain of mammalian polo-like kinase. *Proceedings of the National Academy of Sciences,* 99**,** 1984-1989.

JIN, L., WILLIAMSON, A., BANERJEE, S., PHILIPP, I. & RAPE, M. 2008. Mechanism of ubiquitin-chain formation by the human anaphase-promoting complex. *Cell,* 133**,** 653-665.

JORDAN, M. A. & WILSON, L. 2004. Microtubules as a target for anticancer drugs. *Nature Reviews Cancer,* 4**,** 253.

KAISARI, S., SHOMER, P., ZIV, T., SITRY-SHEVAH, D., MINIOWITZ-SHEMTOV, S., TEICHNER, A. & HERSHKO, A. 2019. Role of Polo-like kinase 1 in the regulation of the action of p31comet in the disassembly of mitotic checkpoint complexes. *Proceedings of the National Academy of Sciences,* 116**,** 11725-11730.

KANG, Y., KIM, J. H., LEE, T. H., KIM, T. S., JUNG, W. H., CHUNG, H. C., PARK, B. W., SHEEN, S. S. & HAN, J. H. 2009. Expression of anaphase-promoting complex7 in fibroadenomas and phyllodes tumors of breast. *Human pathology,* 40**,** 98-107.

KANG, Y. H., PARK, J.-E., YU, L.-R., SOUNG, N.-K., YUN, S.-M., BANG, J. K., SEONG, Y.-S., YU, H., GARFIELD, S. & VEENSTRA, T. D. 2006. Self-regulated Plk1 recruitment to kinetochores by the Plk1-PBIP1 interaction is critical for proper chromosome segregation. *Molecular cell,* 24**,** 409-422.

KATARIA, M. & YAMANO, H. 2019. Interplay between Phosphatases and the Anaphase-Promoting Complex/Cyclosome in Mitosis. *Cells,* 8**,** 814.

KATO, T., DAIGO, Y., ARAGAKI, M., ISHIKAWA, K., SATO, M. & KAJI, M. 2012. Overexpression of CDC20 predicts poor prognosis in primary non-small cell lung cancer patients. *Journal of surgical oncology,* 106**,** 423-430.

KELLY, A. E. & FUNABIKI, H. 2009. Correcting aberrant kinetochore microtubule attachments: an Aurora B-centric view. *Current opinion in cell biology,* 21**,** 51-58.

KIM, J.-M., SOHN, H.-Y., YOON, S. Y., OH, J.-H., YANG, J. O., KIM, J. H., SONG, K. S., RHO, S.-M., YOO, H. S. & KIM, Y. S. 2005. Identification of gastric cancer–related genes using a cDNA microarray containing novel expressed sequence tags expressed in gastric cancer cells. *Clinical Cancer Research,* 11**,** 473-482.

KIMATA, Y., BAXTER, J. E., FRY, A. M. & YAMANO, H. 2008. A role for the Fizzy/Cdc20 family of proteins in activation of the APC/C distinct from substrate recruitment. *Molecular cell,* 32**,** 576-583.

KIMURA, M., KOTANI, S., HATTORI, T., SUMI, N., YOSHIOKA, T., TODOKORO, K. & OKANO, Y. 1997. Cell cycle-dependent expression and spindle pole localization of a novel human protein kinase, Aik, related to Aurora of Drosophila and yeast Ipl1. *Journal of Biological Chemistry,* 272**,** 13766-13771.

KING, R. W., PETERS, J.-M., TUGENDREICH, S., ROLFE, M., HIETER, P. & KIRSCHNER, M. W. 1995. A 20S complex containing CDC27 and CDC16 catalyzes the mitosis-specific conjugation of ubiquitin to cyclin B. *Cell,* 81**,** 279-288.

KOLOTEVA-LEVINE, N., PINCHASI, D., PEREMAN, I., ZUR, A., BRANDEIS, M. & ELROY-STEIN, O. 2004. The Apc5 subunit of the anaphase-promoting complex/cyclosome interacts with poly(A) binding protein and represses internal ribosome entry site-mediated translation. *Mol Cell Biol,* 24**,** 3577-87.

KOMANDER, D. & RAPE, M. 2012. The ubiquitin code. *Annual review of biochemistry,* 81**,** 203-229.

KOPS, G. J., WEAVER, B. A. & CLEVELAND, D. W. 2005. On the road to cancer: aneuploidy and the mitotic checkpoint. *Nat Rev Cancer,* 5**,** 773-85.

KRAFT, C., HERZOG, F., GIEFFERS, C., MECHTLER, K., HAGTING, A., PINES, J. & PETERS, J. M. 2003. Mitotic regulation of the human anaphase-promoting complex by phosphorylation. *Embo j,* 22**,** 6598-609.

KRAMER, E. R., SCHEURINGER, N., PODTELEJNIKOV, A. V., MANN, M. & PETERS, J.-M. 2000. Mitotic regulation of the APC activator proteins CDC20 and CDH1. *Molecular biology of the cell,* 11**,** 1555-1569.

KRENN, V. & MUSACCHIO, A. 2015. The Aurora B kinase in chromosome bi-orientation and spindle checkpoint signaling. *Frontiers in oncology,* 5**,** 225.

KUCHARSKI, T. J., MINSHALL, P. E., MOUSTAFA-KAMAL, M., TURNELL, A. S. & TEODORO, J. G. 2017. Reciprocal regulation between 53BP1 and the anaphase-promoting complex/cyclosome is required for genomic stability during mitotic stress. *Cell reports,* 18**,** 1982-1995.

KULUKIAN, A., HAN, J. S. & CLEVELAND, D. W. 2009. Unattached kinetochores catalyze production of an anaphase inhibitor that requires a Mad2 template to prime Cdc20 for BubR1 binding. *Developmental cell,* 16**,** 105-117.

LARA-GONZALEZ, P., WESTHORPE, F. G. & TAYLOR, S. S. 2012. The spindle assembly checkpoint. *Current biology,* 22**,** R966-R980.

LEE, K. S., OH, D.-Y., KANG, Y. H. & PARK, J.-E. 2008. Self-regulated mechanism of Plk1 localization to kinetochores: lessons from the Plk1-PBIP1 interaction. *Cell division,* 3**,** 4.

LEHMAN, N. L., TIBSHIRANI, R., HSU, J. Y., NATKUNAM, Y., HARRIS, B. T., WEST, R. B., MASEK, M. A., MONTGOMERY, K., VAN DE RIJN, M. & JACKSON, P. K. 2007. Oncogenic regulators and substrates of the anaphase promoting complex/cyclosome are frequently overexpressed in malignant tumors. *The American journal of pathology,* 170**,** 1793-1805.

LÉNÁRT, P., PETRONCZKI, M., STEEGMAIER, M., DI FIORE, B., LIPP, J. J., HOFFMANN, M., RETTIG, W. J., KRAUT, N. & PETERS, J.-M. 2007. The small-molecule inhibitor BI 2536 reveals novel insights into mitotic roles of polo-like kinase 1. *Current biology,* 17**,** 304-315.

LI, D., ZHU, J., FIROZI, P. F., ABBRUZZESE, J. L., EVANS, D. B., CLEARY, K., FRIESS, H. & SEN, S. 2003. Overexpression of oncogenic STK15/BTAK/Aurora A kinase in human pancreatic cancer. *Clinical cancer research,* 9**,** 991-997.

LI, M., FANG, X., WEI, Z., YORK, J. P. & ZHANG, P. 2009. Loss of spindle assembly checkpoint–mediated inhibition of Cdc20 promotes tumorigenesis in mice. *The Journal of cell biology,* 185**,** 983-994.

LI, M., SHIN, Y.-H., HOU, L., HUANG, X., WEI, Z., KLANN, E. & ZHANG, P. 2008. The adaptor protein of the anaphase promoting complex Cdh1 is essential in maintaining replicative lifespan and in learning and memory. *Nature cell biology,* 10**,** 1083.

LINDON, C. 2008. Control of mitotic exit and cytokinesis by the APC/C. Portland Press Limited.

LINDON, C. & PINES, J. 2004. Ordered proteolysis in anaphase inactivates Plk1 to contribute to proper mitotic exit in human cells. *The Journal of cell biology,* 164**,** 233-241.

LINDQVIST, A., KÄLLSTRÖM, H., LUNDGREN, A., BARSOUM, E. & ROSENTHAL, C. K. 2005. Cdc25B cooperates with Cdc25A to induce mitosis but has a unique role in activating cyclin B1–Cdk1 at the centrosome. *J Cell Biol,* 171**,** 35-45.

LISCHETTI, T., ZHANG, G., SEDGWICK, G. G., BOLANOS-GARCIA, V. M. & NILSSON, J. 2014. The internal Cdc20 binding site in BubR1 facilitates both spindle assembly checkpoint signalling and silencing. *Nature communications,* 5**,** 5563.

LITVAK, V., ARGOV, R., DAHAN, N., RAMACHANDRAN, S., AMARILIO, R., SHAINSKAYA, A. & LEV, S. 2004. Mitotic phosphorylation of the peripheral Golgi protein Nir2 by Cdk1 provides a docking mechanism for Plk1 and affects cytokinesis completion. *Molecular cell,* 14**,** 319-330.

LIU, D., VADER, G., VROMANS, M. J., LAMPSON, M. A. & LENS, S. M. 2009. Sensing chromosome bi-orientation by spatial separation of aurora B kinase from kinetochore substrates. *Science,* 323**,** 1350-1353.

LIU, Z., YUAN, F., REN, J., CAO, J., ZHOU, Y., YANG, Q. & XUE, Y. 2012. GPS-ARM: computational analysis of the APC/C recognition motif by predicting D-boxes and KEN-boxes. *PloS one,* 7**,** e34370.

LU, D., GIRARD, J. R., LI, W., MIZRAK, A. & MORGAN, D. O. 2015. Quantitative framework for ordered degradation of APC/C substrates. *BMC biology,* 13**,** 96.

LU, D., HSIAO, J. Y., DAVEY, N. E., VAN VOORHIS, V. A., FOSTER, S. A., TANG, C. & MORGAN, D. O. 2014. Multiple mechanisms determine the order of APC/C substrate degradation in mitosis. *J Cell Biol,* 207**,** 23-39.

LUNDBY, A., LAGE, K., WEINERT, B. T., BEKKER-JENSEN, D. B., SECHER, A., SKOVGAARD, T., KELSTRUP, C. D., DMYTRIYEV, A., CHOUDHARY, C. & LUNDBY, C. 2012. Proteomic analysis of lysine acetylation sites in rat tissues reveals organ specificity and subcellular patterns. *Cell reports,* 2**,** 419-431.

MA, H. T. & POON, R. Y. 2011. How protein kinases co-ordinate mitosis in animal cells. *Biochemical Journal,* 435**,** 17-31.

MACŮREK, L., LINDQVIST, A., LIM, D., LAMPSON, M. A., KLOMPMAKER, R., FREIRE, R., CLOUIN, C., TAYLOR, S. S., YAFFE, M. B. & MEDEMA, R. H. 2008. Polo-like kinase-1 is activated by aurora A to promote checkpoint recovery. *Nature,* 455**,** 119.

MAIATO, H., AFONSO, O., CHEESEMAN, L., FERREIRA, L. & MORAIS-DE-SA, E. 2019. Mitotic exit is controlled during anaphase by an Aurora B-Cyclin B1/Cdk1 crosstalk. *bioRxiv***,** 606517.

MAILAND, N., PODTELEJNIKOV, A. V., GROTH, A., MANN, M., BARTEK, J. & LUKAS, J. 2002. Regulation of G2/M events by Cdc25A through phosphorylation-dependent modulation of its stability. *The EMBO journal,* 21**,** 5911-5920.

MALUMBRES, M. & BARBACID, M. 2005. Mammalian cyclin-dependent kinases. *Trends in biochemical sciences,* 30**,** 630-641.

MALUMBRES, M. & BARBACID, M. 2007. Cell cycle kinases in cancer. *Current opinion in genetics & development,* 17**,** 60-65.

MANSFELD, J., COLLIN, P., COLLINS, M. O., CHOUDHARY, J. S. & PINES, J. 2011. APC15 drives the turnover of MCC-CDC20 to make the spindle assembly checkpoint responsive to kinetochore attachment. *Nature cell biology,* 13**,** 1234.

MARGOTTIN-GOGUET, F., HSU, J. Y., LOKTEV, A., HSIEH, H.-M., REIMANN, J. D. & JACKSON, P. K. 2003. Prophase destruction of Emi1 by the SCFβTrCP/Slimb ubiquitin ligase activates the anaphase promoting complex to allow progression beyond prometaphase. *Developmental cell,* 4**,** 813-826.

MATYSKIELA, M. E. & MORGAN, D. O. 2009. Analysis of activator-binding sites on the APC/C supports a cooperative substrate-binding mechanism. *Molecular cell,* 34**,** 68-80.

MAY, K. M., REYNOLDS, N., CULLEN, C. F., YANAGIDA, M. & OHKURA, H. 2002. Polo boxes and Cut23 (Apc8) mediate an interaction between polo kinase and the anaphase-promoting complex for fission yeast mitosis. *J Cell Biol,* 156**,** 23-28.

MCGARRY, T. J. & KIRSCHNER, M. W. 1998. Geminin, an inhibitor of DNA replication, is degraded during mitosis. *Cell,* 93**,** 1043-1053.

METZGER, M. B., HRISTOVA, V. A. & WEISSMAN, A. M. 2012. HECT and RING finger families of E3 ubiquitin ligases at a glance. *J Cell Sci,* 125**,** 531-537.

MEYER, H.-J. & RAPE, M. Processive ubiquitin chain formation by the anaphase-promoting complex. Seminars in cell & developmental biology, 2011. Elsevier, 544-550.

MIN, M., MAYOR, U. & LINDON, C. 2013. Ubiquitination site preferences in anaphase promoting complex/cyclosome (APC/C) substrates. *Open biology,* 3**,** 130097.

MINOSHIMA, Y., KAWASHIMA, T., HIROSE, K., TONOZUKA, Y., KAWAJIRI, A., BAO, Y. C., DENG, X., TATSUKA, M., NARUMIYA, S. & MAY JR, W. S. 2003. Phosphorylation by aurora B converts MgcRacGAP to a RhoGAP during cytokinesis. *Developmental cell,* 4**,** 549-560.

MOCCIARO, A. & RAPE, M. 2012. Emerging regulatory mechanisms in ubiquitin-dependent cell cycle control. *J Cell Sci,* 125**,** 255-263.

MOLLINARI, C., KLEMAN, J.-P., JIANG, W., SCHOEHN, G., HUNTER, T. & MARGOLIS, R. L. 2002. PRC1 is a microtubule binding and bundling protein essential to maintain the mitotic spindle midzone. *The Journal of cell biology,* 157**,** 1175-1186.

MOSHE, Y., BOULAIRE, J., PAGANO, M. & HERSHKO, A. 2004. Role of Polo-like kinase in the degradation of early mitotic inhibitor 1, a regulator of the anaphase promoting complex/cyclosome. *Proceedings of the National Academy of Sciences,* 101**,** 7937-7942.

MUR, P., DE VOER, R. M., OLIVERA-SALGUERO, R., RODRÍGUEZ-PERALES, S., PONS, T., SETIÉN, F., AIZA, G., VALDÉS-MAS, R., BERTINI, A. & PINEDA, M. 2018. Germline mutations in the spindle assembly checkpoint genes BUB1 and BUB3 are infrequent in familial colorectal cancer and polyposis. *Molecular cancer,* 17**,** 23.

MUSACCHIO, A. 2011. Spindle assembly checkpoint: the third decade. *Philosophical Transactions of the Royal Society B: Biological Sciences,* 366**,** 3595-3604.

MUSACCHIO, A. 2015. The molecular biology of spindle assembly checkpoint signaling dynamics. *Current biology,* 25**,** R1002-R1018.

MUSACCHIO, A. & SALMON, E. D. 2007. The spindle-assembly checkpoint in space and time. *Nature reviews Molecular cell biology,* 8**,** 379.

NAKAJIMA, H., TOYOSHIMA-MORIMOTO, F., TANIGUCHI, E. & NISHIDA, E. 2003. Identification of a consensus motif for Plk (Polo-like kinase) phosphorylation reveals Myt1 as a Plk1 substrate. *Journal of Biological Chemistry,* 278**,** 25277-25280.

NATH, S., BANERJEE, T., SEN, D., DAS, T. & ROYCHOUDHURY, S. 2011. Spindle assembly checkpoint protein Cdc20 transcriptionally activates expression of ubiquitin carrier protein UbcH10. *Journal of Biological Chemistry,* 286**,** 15666-15677.

NEEF, R., GRUNEBERG, U., KOPAJTICH, R., LI, X., NIGG, E. A., SILLJE, H. & BARR, F. A. 2007. Choice of Plk1 docking partners during mitosis and cytokinesis is controlled by the activation state of Cdk1. *Nature cell biology,* 9**,** 436.

NEEF, R., PREISINGER, C., SUTCLIFFE, J., KOPAJTICH, R., NIGG, E. A., MAYER, T. U. & BARR, F. A. 2003. Phosphorylation of mitotic kinesin-like protein 2 by polo-like kinase 1 is required for cytokinesis. *The Journal of cell biology,* 162**,** 863-876.

NEUMANN, B., HELD, M., LIEBEL, U., ERFLE, H., ROGERS, P., PEPPERKOK, R. & ELLENBERG, J. 2006. High-throughput RNAi screening by time-lapse imaging of live human cells. *Nature methods,* 3**,** 385.

NEUMANN, B., WALTER, T., HÉRICHÉ, J.-K., BULKESCHER, J., ERFLE, H., CONRAD, C., ROGERS, P., POSER, I., HELD, M. & LIEBEL, U. 2010. Phenotypic profiling of the human genome by time-lapse microscopy reveals cell division genes. *Nature,* 464**,** 721.

NEZI, L. & MUSACCHIO, A. 2009. Sister chromatid tension and the spindle assembly checkpoint. *Current opinion in cell biology,* 21**,** 785-795.

NIGG, E. A. 2001. Cell division: mitotic kinases as regulators of cell division and its checkpoints. *Nature reviews Molecular cell biology,* 2**,** 21.

O'CONNELL, M. J., WALWORTH, N. C. & CARR, A. M. 2000. The G2-phase DNA-damage checkpoint. *Trends in cell biology,* 10**,** 296-303.

OTTO, N. M., MCDOWELL, W. G., DICKEY, D. M. & POTTER, L. R. 2017. A glutamate-substituted mutant mimics the phosphorylated and active form of guanylyl cyclase-A. *Molecular pharmacology,* 92**,** 67-74.

PACHIS, S. T., HIRUMA, Y., TROMER, E. C., PERRAKIS, A. & KOPS, G. J. 2019. Interactions between N-terminal modules in MPS1 enable spindle checkpoint silencing. *Cell reports,* 26**,** 2101-2112. e6.

PALEOLOGOU, K. E., SCHMID, A. W., ROSPIGLIOSI, C. C., KIM, H.-Y., LAMBERTO, G. R., FREDENBURG, R. A., LANSBURY, P. T., FERNANDEZ, C. O., ELIEZER, D. & ZWECKSTETTER, M. 2008. Phosphorylation at Ser-129 but not the phosphomimics S129E/D inhibits the fibrillation of α-synuclein. *Journal of Biological Chemistry,* 283**,** 16895-16905.

PALLANTE, P., BERLINGIERI, M., TRONCONE, G., KRUHOFFER, M., ORNTOFT, T., VIGLIETTO, G., CALEO, A., MIGLIACCIO, I., DECAUSSIN-PETRUCCI, M. & SANTORO, M. 2005.

UbcH10 overexpression may represent a marker of anaplastic thyroid carcinomas. *British journal of cancer,* 93**,** 464.
PEARLMAN, S. M., SERBER, Z. & FERRELL JR, J. E. 2011. A mechanism for the evolution of phosphorylation sites. *Cell,* 147**,** 934-946.
PENAS, C., RAMACHANDRAN, V. & AYAD, N. G. 2012. The APC/C ubiquitin ligase: from cell biology to tumorigenesis. *Frontiers in oncology,* 1**,** 60.
PETERS, J.-M. 2006. The anaphase promoting complex/cyclosome: a machine designed to destroy. *Nature reviews Molecular cell biology,* 7**,** 644.
PETRONCZKI, M., GLOTZER, M., KRAUT, N. & PETERS, J.-M. 2007. Polo-like kinase 1 triggers the initiation of cytokinesis in human cells by promoting recruitment of the RhoGEF Ect2 to the central spindle. *Developmental cell,* 12**,** 713-725.
PETRONCZKI, M., LÉNÁRT, P. & PETERS, J.-M. 2008. Polo on the rise—from mitotic entry to cytokinesis with Plk1. *Developmental cell,* 14**,** 646-659.
PFLEGER, C. M. & KIRSCHNER, M. W. 2000. The KEN box: an APC recognition signal distinct from the D box targeted by Cdh1. *Genes & development,* 14**,** 655-665.
PHOSPHOSITEPLUS. 2019. Available: https://www.phosphosite.org/homeAction.action [Accessed].
PICKART, C. M. & EDDINS, M. J. 2004. Ubiquitin: structures, functions, mechanisms. *Biochimica et Biophysica Acta (BBA)-Molecular Cell Research,* 1695**,** 55-72.
PINES, J. 2011. Cubism and the cell cycle: the many faces of the APC/C. *Nat Rev Mol Cell Biol,* 12**,** 427-38.
POTAPOVA, T. A., DAUM, J. R., PITTMAN, B. D., HUDSON, J. R., JONES, T. N., SATINOVER, D. L., STUKENBERG, P. T. & GORBSKY, G. J. 2006. The reversibility of mitotic exit in vertebrate cells. *Nature,* 440**,** 954.
PRAY, T. R., PARLATI, F., HUANG, J., WONG, B. R., PAYAN, D. G., BENNETT, M. K., ISSAKANI, S. D., MOLINEAUX, S. & DEMO, S. D. 2002. Cell cycle regulatory E3 ubiquitin ligases as anticancer targets. *Drug Resist Updat,* 5**,** 249-58.
PRIMORAC, I. & MUSACCHIO, A. 2013. Panta rhei: the APC/C at steady state. *J Cell Biol,* 201**,** 177-189.
QI, W., TANG, Z. & YU, H. 2006. Phosphorylation-and polo-box–dependent binding of Plk1 to Bub1 is required for the kinetochore localization of Plk1. *Molecular biology of the cell,* 17**,** 3705-3716.
QIAN, J., BEULLENS, M., HUANG, J., DE MUNTER, S., LESAGE, B. & BOLLEN, M. 2015. Cdk1 orders mitotic events through coordination of a chromosome-associated phosphatase switch. *Nature communications,* 6**,** 10215.
QIAO, R., WEISSMANN, F., YAMAGUCHI, M., BROWN, N. G., VANDERLINDEN, R., IMRE, R., JARVIS, M. A., BRUNNER, M. R., DAVIDSON, I. F. & LITOS, G. 2016. Mechanism of APC/CCDC20 activation by mitotic phosphorylation. *Proceedings of the National Academy of Sciences,* 113**,** E2570-E2578.
QIU, L., TAN, X., LIN, J., LIU, R.-Y., CHEN, S., GENG, R., WU, J. & HUANG, W. 2017. CDC27 Induces Metastasis and Invasion in Colorectal Cancer via the Promotion of Epithelial-To-Mesenchymal Transition. *Journal of Cancer,* 8**,** 2626.
QIU, L., WU, J., PAN, C., TAN, X., LIN, J., LIU, R., CHEN, S., GENG, R. & HUANG, W. 2016. Downregulation of CDC27 inhibits the proliferation of colorectal cancer cells via the accumulation of p21 Cip1/Waf1. *Cell death & disease,* 7**,** e2074.

RAHIMI, H., AHMADZADEH, A., YOUSEF-AMOLI, S., KOKABEE, L., SHOKRGOZAR, M.-A., MAHDIAN, R. & KARIMIPOOR, M. 2015. The expression pattern of APC2 and APC7 in various cancer cell lines and AML patients. *Advances in medical sciences,* 60**,** 259-263.

REDDY, S., RAPE, M., MARGANSKY, W. & KIRSCHNER, M. 2007. Ubiquitination by the anaphase-promoting complex drives spindle checkpoint inactivation. *Nature,* 446**,** 921.

REED, S. I. 2008. Deathproof: new insights on the role of skp2 in tumorigenesis. *Cancer cell,* 13**,** 88-89.

REIMANN, J. D., FREED, E., HSU, J. Y., KRAMER, E. R., PETERS, J.-M. & JACKSON, P. K. 2001. Emi1 is a mitotic regulator that interacts with Cdc20 and inhibits the anaphase promoting complex. *Cell,* 105**,** 645-655.

RIO FRIO, T., LAVOIE, J., HAMEL, N., GEYER, F. C., KUSHNER, Y. B., NOVAK, D. J., WARK, L., CAPELLI, C., REIS-FILHO, J. S. & MAI, S. 2010. Homozygous BUB1B mutation and susceptibility to gastrointestinal neoplasia. *New England Journal of Medicine,* 363**,** 2628-2637.

RITTER, A., KREIS, N. N., LOUWEN, F., WORDEMAN, L. & YUAN, J. 2015. Molecular insight into the regulation and function of MCAK. *Crit Rev Biochem Mol Biol,* 51**,** 228-45.

RODIER, G., COULOMBE, P., TANGUAY, P. L., BOUTONNET, C. & MELOCHE, S. 2008. Phosphorylation of Skp2 regulated by CDK2 and Cdc14B protects it from degradation by APCCdh1 in G1 phase. *The EMBO journal,* 27**,** 679-691.

ROSASCO-NITCHER, S. E., LAN, W., KHORASANIZADEH, S. & STUKENBERG, P. T. 2008. Centromeric Aurora-B activation requires TD-60, microtubules, and substrate priming phosphorylation. *Science,* 319**,** 469-472.

RUDOLPH, D., STEEGMAIER, M., HOFFMANN, M., GRAUERT, M., BAUM, A., QUANT, J., HASLINGER, C., GARIN-CHESA, P. & ADOLF, G. R. 2009. BI 6727, a Polo-like kinase inhibitor with improved pharmacokinetic profile and broad antitumor activity. *Clinical cancer research,* 15**,** 3094-3102.

SACKTON, K. L., DIMOVA, N., ZENG, X., TIAN, W., ZHANG, M., SACKTON, T. B., MEADERS, J., PFAFF, K. L., SIGOILLOT, F. & YU, H. 2014. Synergistic blockade of mitotic exit by two chemical inhibitors of the APC/C. *Nature,* 514**,** 646.

SANSREGRET, L., PATTERSON, J. O., DEWHURST, S., LÓPEZ-GARCÍA, C., KOCH, A., MCGRANAHAN, N., CHAO, W. C. H., BARRY, D. J., ROWAN, A. & INSTRELL, R. 2017. APC/C dysfunction limits excessive cancer chromosomal instability. *Cancer discovery,* 7**,** 218-233.

SANTAGUIDA, S., TIGHE, A., D'ALISE, A. M., TAYLOR, S. S. & MUSACCHIO, A. 2010. Dissecting the role of MPS1 in chromosome biorientation and the spindle checkpoint through the small molecule inhibitor reversine. *The Journal of cell biology,* 190**,** 73-87.

SANTAMARIA, A., NEEF, R., EBERSPÄCHER, U., EIS, K., HUSEMANN, M., MUMBERG, D., PRECHTL, S., SCHULZE, V., SIEMEISTER, G. & WORTMANN, L. 2007. Use of the novel Plk1 inhibitor ZK-thiazolidinone to elucidate functions of Plk1 in early and late stages of mitosis. *Molecular biology of the cell,* 18**,** 4024-4036.

SCHINDELIN, J., ARGANDA-CARRERAS, I., FRISE, E., KAYNIG, V., LONGAIR, M., PIETZSCH, T., PREIBISCH, S., RUEDEN, C., SAALFELD, S. & SCHMID, B. 2012. Fiji: an open-source platform for biological-image analysis. *Nature methods,* 9**,** 676.

SCHULZE, W. X. & MANN, M. 2004. A novel proteomic screen for peptide-protein interactions. *Journal of Biological Chemistry,* 279**,** 10756-10764.

SEDGWICK, G. G., TOWNSEND, K., MARTIN, A., SHIMWELL, N. J., GRAND, R. J., STEWART, G. S., NILSSON, J. & TURNELL, A. S. 2013. Transcriptional intermediary factor 1γ binds to the anaphase-promoting complex/cyclosome and promotes mitosis. *Oncogene,* 32**,** 4622.

SINGHAL, S., AMIN, K., KRUKLITIS, R., DELONG, P., FRISCIA, M. E., LITZKY, L. A., PUTT, M. E., KAISER, L. R. & ALBELDA, S. M. 2003. Alterations in cell cycle genes in early stage lung adenocarcinoma identified by expression profiling. *Cancer biology & therapy,* 2**,** 291-298.

SIVAKUMAR, S. & GORBSKY, G. J. 2015. Spatiotemporal regulation of the anaphase-promoting complex in mitosis. *Nature Reviews Molecular Cell Biology,* 16**,** 82.

STEEN, J. A., STEEN, H., GEORGI, A., PARKER, K., SPRINGER, M., KIRCHNER, M., HAMPRECHT, F. & KIRSCHNER, M. W. 2008. Different phosphorylation states of the anaphase promoting complex in response to antimitotic drugs: a quantitative proteomic analysis. *Proceedings of the National Academy of Sciences,* 105**,** 6069-6074.

STEIGEMANN, P., WURZENBERGER, C., SCHMITZ, M. H., HELD, M., GUIZETTI, J., MAAR, S. & GERLICH, D. W. 2009. Aurora B-mediated abscission checkpoint protects against tetraploidization. *Cell,* 136**,** 473-484.

STEWART, S. & FANG, G. 2005. Destruction box–dependent degradation of Aurora B is mediated by the anaphase-promoting complex/cyclosome and Cdh1. *Cancer research,* 65**,** 8730-8735.

STRACKER, T. H., USUI, T. & PETRINI, J. H. 2009. Taking the time to make important decisions: the checkpoint effector kinases Chk1 and Chk2 and the DNA damage response. *DNA repair,* 8**,** 1047-1054.

SUDAKIN, V., CHAN, G. K. & YEN, T. J. 2001. Checkpoint inhibition of the APC/C in HeLa cells is mediated by a complex of BUBR1, BUB3, CDC20, and MAD2. *The Journal of cell biology,* 154**,** 925-936.

SUMMERS, M. K., PAN, B., MUKHYALA, K. & JACKSON, P. K. 2008. The unique N terminus of the UbcH10 E2 enzyme controls the threshold for APC activation and enhances checkpoint regulation of the APC. *Molecular cell,* 31**,** 544-556.

SUNKEL, C. E. & GLOVER, D. M. 1988. polo, a mitotic mutant of Drosophila displaying abnormal spindle poles. *Journal of cell science,* 89**,** 25-38.

TAKIZAWA, C. G. & MORGAN, D. O. 2000. Control of mitosis by changes in the subcellular location of cyclin-B1–Cdk1 and Cdc25C. *Current opinion in cell biology,* 12**,** 658-665.

TANAKA, T. U. 2005. Chromosome bi-orientation on the mitotic spindle. *Philosophical Transactions of the Royal Society B: Biological Sciences,* 360**,** 581-589.

TANAKA, T. U., RACHIDI, N., JANKE, C., PEREIRA, G., GALOVA, M., SCHIEBEL, E., STARK, M. J. & NASMYTH, K. 2002. Evidence that the Ipl1-Sli15 (Aurora kinase-INCENP) complex promotes chromosome bi-orientation by altering kinetochore-spindle pole connections. *Cell,* 108**,** 317-329.

TAYLOR, S. & PETERS, J.-M. 2008. Polo and Aurora kinases—lessons derived from chemical biology. *Current opinion in cell biology,* 20**,** 77-84.

TINTI, M., KIEMER, L., COSTA, S., MILLER, M. L., SACCO, F., OLSEN, J. V., CARDUCCI, M., PAOLUZI, S., LANGONE, F. & WORKMAN, C. T. 2013. The SH2 domain interaction landscape. *Cell reports,* 3**,** 1293-1305.

TOWNSEND, K., MASON, H., BLACKFORD, A. N., MILLER, E. S., CHAPMAN, J. R., SEDGWICK, G. G., BARONE, G., TURNELL, A. S. & STEWART, G. S. 2009. Mediator of DNA damage checkpoint 1 (MDC1) regulates mitotic progression. *Journal of Biological Chemistry,* 284**,** 33939-33948.

TSUNEMATSU, T., TAKIHARA, Y., ISHIMARU, N., PAGANO, M., TAKATA, T. & KUDO, Y. 2013. Aurora-A controls pre-replicative complex assembly and DNA replication by stabilizing geminin in mitosis. *Nature communications,* 4**,** 1885.

TURNELL, A. S., STEWART, G. S., GRAND, R. J., ROOKES, S. M., MARTIN, A., YAMANO, H., ELLEDGE, S. J. & GALLIMORE, P. H. 2005. The APC/C and CBP/p300 cooperate to regulate transcription and cell-cycle progression. *Nature,* 438**,** 690.

UZUNOVA, K., DYE, B. T., SCHUTZ, H., LADURNER, R., PETZOLD, G., TOYODA, Y., JARVIS, M. A., BROWN, N. G., POSER, I. & NOVATCHKOVA, M. 2012. APC15 mediates CDC20 autoubiquitylation by APC/C MCC and disassembly of the mitotic checkpoint complex. *Nature structural & molecular biology,* 19**,** 1116.

VAN LEUKEN, R., CLIJSTERS, L., VAN ZON, W., LIM, D., YAO, X., WOLTHUIS, R. M., YAFFE, M. B., MEDEMA, R. H. & VAN VUGT, M. A. 2009. Polo-like kinase-1 controls Aurora A destruction by activating APC/C-Cdh1. *PLoS One,* 4**,** e5282.

VAN REE, J. H., JEGANATHAN, K. B., MALUREANU, L. & VAN DEURSEN, J. M. 2010. Overexpression of the E2 ubiquitin–conjugating enzyme UbcH10 causes chromosome missegregation and tumor formation. *The Journal of cell biology,* 188**,** 83-100.

VAN VOORHIS, V. A. & MORGAN, D. O. 2014. Activation of the APC/C ubiquitin ligase by enhanced E2 efficiency. *Current Biology,* 24**,** 1556-1562.

VAN VUGT, M. A., BRÁS, A. & MEDEMA, R. H. 2004. Polo-like kinase-1 controls recovery from a G2 DNA damage-induced arrest in mammalian cells. *Molecular cell,* 15**,** 799-811.

VAN ZON, W. & WOLTHUIS, R. M. 2010. Cyclin A and Nek2A: APC/C–Cdc20 substrates invisible to the mitotic spindle checkpoint. Portland Press Limited.

VASSILEV, L. T. 2006. Cell cycle synchronization at the G2/M phase border by reversible inhibition of CDK1. *Cell cycle,* 5**,** 2555-2556.

VISINTIN, R., PRINZ, S. & AMON, A. 1997. CDC20 and CDH1: a family of substrate-specific activators of APC-dependent proteolysis. *Science,* 278**,** 460-463.

VODERMAIER, H. C., GIEFFERS, C., MAURER-STROH, S., EISENHABER, F. & PETERS, J.-M. 2003. TPR subunits of the anaphase-promoting complex mediate binding to the activator protein CDH1. *Current Biology,* 13**,** 1459-1468.

WAGNER, K. W., SAPINOSO, L. M., FRIERSON JR, H. F., BUTZ, N., MESTAN, J., HOFMANN, F., DEVERAUX, Q. L. & HAMPTON, G. M. 2004. Overexpression, genomic amplification and therapeutic potential of inhibiting the UbcH10 ubiquitin conjugase in human carcinomas of diverse anatomic origin. *Oncogene,* 23**,** 6621.

WAIZENEGGER, I. C., GIMÉNEZ-ABIÁN, J. F., WERNIC, D. & PETERS, J.-M. 2002. Regulation of human separase by securin binding and autocleavage. *Current biology,* 12**,** 1368-1378.

WANG, C.-X., FISK, B. C., WADEHRA, M., SU, H. & BRAUN, J. 2000a. Overexpression of murine fizzy-related (fzr) increases natural killer cell–mediated cell death and suppresses tumor growth. *Blood,* 96**,** 259-263.

WANG, F., DAI, J., DAUM, J. R., NIEDZIALKOWSKA, E., BANERJEE, B., STUKENBERG, P. T., GORBSKY, G. J. & HIGGINS, J. M. 2010. Histone H3 Thr-3 phosphorylation by Haspin positions Aurora B at centromeres in mitosis. *Science,* 330**,** 231-235.

WANG, Q., MOYRET-LALLE, C., COUZON, F., SURBIGUET-CLIPPE, C., SAURIN, J.-C., LORCA, T., NAVARRO, C. & PUISIEUX, A. 2003. Alterations of anaphase-promoting complex genes in human colon cancer cells. *Oncogene,* 22**,** 1486-1490.

WANG, S., CHEN, B., ZHU, Z., ZHANG, L., ZENG, J., XU, G., LIU, G., XIONG, D., LUO, Q. & HUANG, Z. 2018. CDC20 overexpression leads to poor prognosis in solid tumors: a system review and meta-analysis. *Medicine,* 97.

WANG, T. H., WANG, H. S. & SOONG, Y. K. 2000b. Paclitaxel-induced cell death: where the cell cycle and apoptosis come together. *Cancer: Interdisciplinary International Journal of the American Cancer Society,* 88**,** 2619-2628.

WANG, Z., KATSAROS, D., SHEN, Y., FU, Y., CANUTO, E. M., BENEDETTO, C., LU, L., CHU, W.-M., RISCH, H. A. & YU, H. 2015. Biological and clinical significance of MAD2L1 and BUB1, genes frequently appearing in expression signatures for breast cancer prognosis. *PloS one,* 10**,** e0136246.

WATSON, E. R., BROWN, N. G., PETERS, J.-M., STARK, H. & SCHULMAN, B. A. 2018. Posing the APC/C E3 ubiquitin ligase to orchestrate cell division. *Trends in cell biology*.

WEI, W., AYAD, N. G., WAN, Y., ZHANG, G.-J., KIRSCHNER, M. W. & KAELIN JR, W. G. 2004. Degradation of the SCF component Skp2 in cell-cycle phase G1 by the anaphase-promoting complex. *Nature,* 428**,** 194.

WEIDERHOLD, K. N., FADRI-MOSKWIK, M., PAN, J., NISHINO, M., CHUANG, C., DEERAKSA, A., LIN, S.-H. & YU-LEE, L.-Y. 2016. Dynamic phosphorylation of NudC by Aurora B in cytokinesis. *PloS one,* 11**,** e0153455.

WILLIAMSON, A., WICKLIFFE, K. E., MELLONE, B. G., SONG, L., KARPEN, G. H. & RAPE, M. 2009. Identification of a physiological E2 module for the human anaphase-promoting complex. *Proceedings of the National Academy of Sciences,* 106**,** 18213-18218.

WIRTH, K. G., RICCI, R., GIMÉNEZ-ABIÁN, J. F., TAGHYBEEGLU, S., KUDO, N. R., JOCHUM, W., VASSEUR-COGNET, M. & NASMYTH, K. 2004. Loss of the anaphase-promoting complex in quiescent cells causes unscheduled hepatocyte proliferation. *Genes & development,* 18**,** 88-98.

WU, M.-S., MA, Q.-Y., LIU, D.-D., LI, X.-J., DENG, L.-J., LI, N., SHEN, J., ZHAO, Z. & CHEN, J.-X. 2019. CDC20 and its downstream genes: potential prognosis factors of osteosarcoma. *International journal of clinical oncology***,** 1-11.

WU, W.-J., HU, K.-S., WANG, D.-S., ZENG, Z.-L., ZHANG, D.-S., CHEN, D.-L., BAI, L. & XU, R.-H. 2013. CDC20 overexpression predicts a poor prognosis for patients with colorectal cancer. *Journal of translational medicine,* 11**,** 142.

XIE, C., POWELL, C., YAO, M., WU, J. & DONG, Q. 2014. Ubiquitin-conjugating enzyme E2C: a potential cancer biomarker. *The international journal of biochemistry & cell biology,* 47**,** 113-117.

XIN, Y., NING, S., ZHANG, L. & CUI, M. 2018. CDC27 facilitates gastric cancer cell proliferation, invasion and metastasis via twist-induced epithelial-mesenchymal transition. *Cellular Physiology and Biochemistry,* 50**,** 501-511.

YAM, C., FUNG, T. & POON, R. 2002. Cyclin A in cell cycle control and cancer. *Cellular and Molecular Life Sciences CMLS,* 59**,** 1317-1326.

YAMANO, H. 2019. APC/C: current understanding and future perspectives. *F1000Research,* 8.

YU, Y. & MUNGER, K., 2013. Human papillomavirus type 16 E7 oncoprotein inhibits the anaphase promoting complex/cyclosome activity by dysregulating EMI1 expression in mitosis. *Virology*, *446*(1-2), pp.251-259.

YU, H., PETERS, J.-M., KING, R. W., PAGE, A. M., HIETER, P. & KIRSCHNER, M. W. 1998. Identification of a cullin homology region in a subunit of the anaphase-promoting complex. *Science,* 279**,** 1219-1222.

YÜCE, Ö., PIEKNY, A. & GLOTZER, M. 2005. An ECT2–centralspindlin complex regulates the localization and function of RhoA. *The Journal of cell biology,* 170**,** 571-582.

ZHANG, S., CHANG, L., ALFIERI, C., ZHANG, Z., YANG, J., MASLEN, S., SKEHEL, M. & BARFORD, D. 2016. Molecular mechanism of APC/C activation by mitotic phosphorylation. *Nature,* 533**,** 260.

ZHAO, W.-M. & FANG, G. 2005. Anillin is a substrate of anaphase-promoting complex/cyclosome (APC/C) that controls spatial contractility of myosin during late cytokinesis. *Journal of Biological Chemistry,* 280**,** 33516-33524.

ZHOU, Z., HE, M., SHAH, A. A. & WAN, Y. 2016. Insights into APC/C: from cellular function to diseases and therapeutics. *Cell Div,* 11**,** 9.

ZHU, C. & JIANG, W. 2005. Cell cycle-dependent translocation of PRC1 on the spindle by Kif4 is essential for midzone formation and cytokinesis. *Proceedings of the National Academy of Sciences,* 102**,** 343-348.

ZUR, A. & BRANDEIS, M. 2001. Securin degradation is mediated by fzy and fzr, and is required for complete chromatid separation but not for cytokinesis. *The EMBO journal,* 20**,** 792-801.